REGULATION OF LYMPHOCYTE TRANSMIGRATION BY ADAM10 AND TSPANC8 TETRASPANINS

By

JASMEET SINGH REYAT

A thesis submitted to the University of Birmingham for the degree of DOCTOR OF PHILOSOPHY

School of Biosciences
College of Life and Environmental Sciences
University of Birmingham
January 2016

DEDICATIONS

This thesis is dedicated to my grandparents Santokh Singh and Jagdish Kaur Phull whose love, respect, and guidance have moulded my life choices to date and will continue to do so evermore.

ਜੋ ਮਾਗਹਿ ਠਾਕੁਰ ਅਪੁਨੇ ਤੇ ਸੋਈ ਸੋਈ ਦੇਵੈ ॥

Whatever I ask for from my Lord and Master, he gives that to me.

ਨਾਨਕ ਦਾਸੁ ਮੁਖ ਤੇ ਜੋ ਬੋਲੈ ਈਹਾ ਊਹਾ ਸਚੁ ਹੋਵੈ ॥੨॥੧੪॥੪੫॥

Whatever the Lord's slave Nanak utters with his mouth proves to be true, here and hereafter. [SGGS ||2||14||45||]

ACKNOWLEDGEMENTS

At this point, I would like to thank all the individuals without whom this PhD thesis would not have been possible:

Firstly, I would like to thank my supervisor Dr Mike Tomlinson for giving me the opportunity to join his group and to work on this important, novel, and exciting project. I also want to thank him for his time, help, and extraordinary support. His excellent teaching and guidance helped me to achieve so much. I would also like to thank all the members of the Vascular Tetraspanin group for their constructive scientific support and advice. In particular, I would like to thank Jing for teaching me all things 'molly-bolly', and Lizzie and Beccy for always having time to help me out. Many thanks also go to Pete for being an amazing all-round scientist and friend and for putting up with by constant gibberish! I would also like to thank all the project students that have passed through the lab during my time – you made the lab an eventful place…especially Justyna. My gratitude also goes to the 820-lunch time crew – Abs, Alex, Jeremy, Sue – for making lunches hilarious. In particular, I would like to thank Abs for being an amazing friend. My gratitude also goes to the various people on the eighth floor in Biosciences for creating such a good atmosphere to work in, their encouragement and support, and their friendship throughout the duration of my PhD. A big "thank you" also goes to the Friday lunchtime lab meetings in Biosciences and the cardiovascular community in the IBR who have offered help and guidance when I need it.

Furthermore, I wish to thank my co-supervisor Prof. Ed Rainger for his enthusiastic input in the project, for many valuable discussions, advice and all his help and time. Many thanks also go to the whole Leukocyte Trafficking group for all the help and support and for creating a very nice working atmosphere. Special thanks go to Bonita, Hafsa, Myriam, Matt, Phil, and Stacey for their assistance with flow assays and primary cell culture and most of all, for making my time in the IBR a barrel of fun. Furthermore, I would like to thank Professor Gerard Nash for his support and feedback in lab meetings.

I would like to also thank my family who have supported me so much over the past three years. In particular, I would like to thank my Mum and Brother who always encouraged me to be strong and determined and for always offering reassurance and for being understanding – this could not have been done without you.

Finally, I would like to thank the British Heart Foundation for funding my studentship.

ABSTRACT

The passage of leukocytes across blood vessel walls plays a key role in the immune response to infection in inflammatory conditions. ADAM10 is a ubiquitously expressed molecular scissor that proteolytically cleaves key cell surface proteins including vascular endothelial (VE)-cadherin and transmembrane chemokines. Their shedding by ADAM10 promotes leukocyte transmigration in cell line models, however the precise mechanism behind ADAM10's involvement is unknown. ADAM10 associates with six different membrane organising tetraspanins (Tspan5/10/14/15/17/33) termed the TspanC8s. These tetraspanins regulate ADAM10 enzymatic maturation and trafficking to the cell surface and emerging evidence indicates that different TspanC8s can promote ADAM10 cleavage of specific substrates.

It was hypothesised that ADAM10 promotes leukocyte transmigration by cleaving one of its endothelial substrates and one or more of the TspanC8s could facilitate this process. The aim of this thesis was to test this hypothesis using *in vitro* leukocyte adhesion assays with primary human leukocytes and human umbilical vein endothelial cells (HUVECs). siRNA knockdown or pharmacological inhibition of ADAM10 on HUVECs impaired the transmigration of lymphocytes, but not neutrophils or monocytes. ADAM10 knockdown/inhibition caused a reduction in VE-cadherin shedding and an increase in VE-cadherin surface expression. Partial knockdown of VE-cadherin, in the presence of ADAM10 knockdown/inhibition, reduced VE-cadherin levels to normal and restored basal lymphocyte transmigration.

Systematic knockdown of TspanC8s in HUVECs revealed that the presence of either Tspan5 or Tspan17 was sufficient to maintain basal lymphocyte transmigration and reduced VE-cadherin surface levels. Tspan5 and Tspan17 are functionally uncharacterised, but they are the most highly related TspanC8s by sequence (78% amino acid identity) and may share a common role in lymphocyte transmigration by regulation of ADAM10 and VE-cadherin.

TABLE OF CONTENTS

LIST OF FIGURES

LIST OF TABLES

ABBREVIATIONS

ADAM	A disintegrin and metalloprotease
ADAMTS	A disintegrin and metalloprotease with thrombospondin motifs
ANOVA	Analysis of variance
AP-2	Adapter protein-2
APC	Allophycocyanin
APP	Amyloid precursor protein
APS	Ammonium persulfate
BiFC	Bimolecular fluorescence complementation
BSA	Bovine serum albumin
Ca^{2+}	Calcium ion
CAM	Cellular adhesion molecule
CX3CL1	Chemokine: Fractalkine
CX3CR1	Chemokine receptor: CX3C-motif Receptor 1
CXCL16	Chemokine: Bonzo
CXCR6	Chemokine receptor: CXC-motif Receptor 6
DAMP	Damage-associated molecular pattern
DAPT	N-[N-(3,5-difluorophenaceyl)-L-alanyl]-S-phenylglycine t-butyl ester
DC	Dendritic cell
DMEM	Dulbecco's modified eagle's medium
DMSO	Dimethyl sulfoxide
EDTA	Ethylele diamine tetraacetic acid
EGF	Epidermal growth factor
EGFR	Epidermal growth factor receptor
ESAM	Endothelial cell-selective adhesion molecule
ESL-1	E-selectin ligand-1
FBS	Fetal bovine serum
FITC	Fluorescein
fMLP	Formyl-Methionyl-Leucyl-Phenylalanine
g	Gram
GAG	Glycosaminoglycan

GPCR	G-protein coupled receptor
GPVI	Glycoprotein VI
HUVEC	Human umbilical vein endothelial cell
I/R	Ischemia reperfusion
ICAM-1	Intercellular adhesion molecule-1
ICAM-2	Intercellular adhesion molecule-2
IFNγ	Interferon-γ
IgSF	Immunoglobulin superfamily
IL-1R	Interleukin-1 receptor
IL-1β	Interleukin-1β
IL-8	Interleukin-8
JAM	Junctional adhesion molecule
kDa	Killodalton
L	Litre
LFA-1	Lymphocyte function-associated antigen-1
LTB_4	Leukotreine-B_4
M	Molar
mAb	Monoclonal antibody
Mac-1	Macrophage antigen-1
MAPK	Mitogen-activated protein kinase
MCP-1	Macrophage chemotactic protein-1 (CCL2)
MFI	Mean fluorescence intensity
mg	Milligram
MIP-2	Macrophage inflammatory protein-2
µm	Micron
ml	Millilitre
mM	Millimolar
MMP	Matrix metalloprotease
MT-MMP	Matrix metalloprotease with transmembrane spanning regions
NaCl	Sodium chloride
NaN_3	Sodium azide
NFκB	Nuclear factor κ-B

nm	Nanometer
NMR	Nuclear magnetic resonance
PAMP	Pathogen-associated molecular pattern
PB	Pacific blue
PBL	Peripheral blood lymphocyte
PBMC	Peripheral blood mononuclear cell
PBS	Phosphate buffered saline
PBSA	Phosphate buffered saline with bovine serum albumin
PE	Phycoerythrin
PECAM-1	Platelet endothelial cell adhesion molecule-1
PEI	Polyethylenimine
PGD_2	Prostaglandin-D_2
PHA	Phytohaemagglutinin
PI3Kγ	Phosphoinositide 3-kinase-γ
PRR	Pathogen recognition receptor
PSGL-1	P-selectin glycoprotein ligand-1
PVDF	Polyvinylidene fluoride
RGD	Arg-Gly-Asp motif
RIP	Regulated intramembrane proteolysis
ROS	Reactive oxygen species
RT-PCR	Real-time quantitative PCR
SAGE	Serial analysis of gene expression
SDS	Sodium dodecyl sulfate
SHP	Src homology-2 domain containing tyrosine phosphatase
siRNA	Small interfering ribonucleic acid
STED	Stimulated emission deletion microscopy
STORM	Stochastic optical reconstruction microscopy
SVMP	Snake-venom metalloprotease
TBS	Tris-buffered saline
TBST	Tris-buffered saline and tween
TEMED	N,N,N’,N’-Tetramethylethylenediamine
THP-1	Human monocytic cell line

TLR	Toll-like receptor
TNFR	Tumour necrosis factor receptor
TNFα	Tumour necrosis factor-α
UP	Uroplakin
VAM-1	Vascular cell adhesion molecule-1
VEGF	Vascular endothelial growth factor
VE-PTP	Vascular endothelial protein-tyrosine phosphatase
VVO	Vesiculo-vacuolar organelle
Zn^{2+}	Zinc ion

PUBLICATIONS ARRISING FROM THIS WORK

Noy PJ, Yang J, Reyat JS, Matthews AL, Charlton AE, Furmston J, Rogers DA, Rainger GE & Tomlinson MG (2016) **TspanC8 tetraspanins and ADAM10 interact via their extracellular regions: evidence for distinct binding mechanisms for different TspanC8s.** Manuscript accepted with Journal of Biological Chemistry ahead of print.

Matthews AL, Noy PJ, Reyat JS & Tomlinson MG (2016) **Regulation of A Disintegrin and Metalloprotease (ADAM) family sheddases ADAM10 and ADAM17: the emerging role of tetraspanins and rhomboids.** Review article submitted to Platelets.

Reyat JS, Noy PJ, Rainger GE & Tomlinson MG (2016) **Endothelial tetraspanins Tspan5 and Tspan17 regulate the transmigration of lymphocytes by regulating ADAM10 and VE-cadherin.** Manuscript in preparation for Journal of Immunology.

LIST OF PRESENTATIONS

Reyat J.S., Rainger G.E. & Tomlinson M.G. (2013) **The metalloprotease ADAM10 plays no role in the adhesion and transmigration of neutrophils *in vitro*.** 25th UK Adhesion Society Meeting (Birmingham, UK September 2013). *Poster presentation.*

Reyat J.S., Rainger G.E. & Tomlinson M.G. (2014) **Endothelial cell ADAM10 promotes lymphocyte transmigration *in vitro*.** 6th European Conference on Tetrapsanins (Lille, France June 2014). *Oral presentation.*

Reyat J.S., Rainger G.E. & Tomlinson M.G. (2014) **Endothelial cell ADAM10 promotes lymphocyte transmigration *in vitro*.** 16th Imperial College Symposium on Vascular Endothelium (London, UK November 2014). *Poster presentation.*

Reyat J.S., Rainger G.E. & Tomlinson M.G. (2014) **Endothelial cell ADAM10 promotes lymphocyte transmigration *in vitro*.** 26th UK Adhesion Society Meeting (London, UK November 2014). *Oral presentation.*

Reyat J.S., Rainger G.E. & Tomlinson M.G. (2015) **Endothelial cell ADAM10 promotes lymphocyte transmigration *in vitro*.** 2nd British Immunology Society Leukocyte Migration Affinity Group Meeting (Birmingham, UK February 2015). *Oral presentation.*

Reyat J.S., Rainger G.E. & Tomlinson M.G. (2015) **ADAM10-dependent shedding of vascular endothelial (VE)-cadherin regulates lymphocyte transmigration *in vitro*.** 8th

International Summer Conference on Tetraspanins & other Membrane Scaffolds (Nashville, USA June 2015). *Oral presentation.*

Reyat J.S., Noy P.J., Rainger G.E. & Tomlinson M.G. (2015) **Endothelial tetraspanins Tspan5 and Tspan17 enhance lymphocyte transmigration by promoting ADAM10-dependent cleavage of VE-cadherin.** 27th UK Adhesion Society Meeting (Birmingham, UK September 2015). *Poster presentation. First prize winner for outstanding poster presentation.*

Reyat J.S., Noy P.J., Rainger G.E. & Tomlinson M.G. (2015) **Endothelial tetraspanins Tspan5 and Tspan17 enhance lymphocyte transmigration by promoting ADAM10-dependent cleavage of VE-cadherin.** 4th British Heart Foundation Fellows Meeting (Cambridge, UK September 2015). *Poster presentation.*

CHAPTER 1

GENERAL INTRODUCTION

1.1 INFLAMMATION AND IMMUNITY

1.1.1 Inflammation and immunity are protective following injury and infection

Inflammation is a complex response characterised by the host's reaction to invading pathogens, such as viruses, bacteria, fungi, or parasites, but also in response to tissue or cell damage. It serves as a protective mechanism to overcome the initial cause of infection or injury with the principle aim in eliminating the harmful stimuli and contributing to tissue repair thereby resolving the inflammatory insult (Serhan et al., 2008). A principle component of this response is the ability of circulating blood leukocytes to undergo activation and transmigrate to the site of infection or injury in vascularised tissues. This process is regulated by a precisely coordinated sequence of adhesive interactions and signalling events that occur between the inflamed vessel wall and leukocytes (Ley et al., 2007). In addition, leukocytes have been shown to breach the endothelial barrier rapidly with the whole process taking roughly 10 minutes. Inflammation is characterised by five classical symptoms: *dolor* (pain), *calor* (heat), *rubor* (redness), *tumor* (swelling) and *function laesa* (loss of function) (Majno and Joris, 2008). A principle component of these symptoms is induced by the localised effects of inflammatory mediators on the blood vessels surrounding the site of inflammation. Vasodilatory factors, such as histamine and bradykinin, act on the inflamed vasculature to increase blood flow that is characterised by redness and heat; an increase in vascular permeability leading to the leakage of plasma fluids (exudates) causes increased swelling whilst pain is associated with the localised release of chemical stimuli that act upon nerve endings. If all these systems persist or become uncontrollable, this can lead to the eventual loss of organ/tissue function.

Immunity refers to the host defence, which in higher developed organisms consist of two branches, non-specific (innate immunity) or specific (adaptive immunity). The first line of defence, also referred to as the innate immune response, involves a natural resistance

defence mechanism that primes the adaptive immune response (Abbas, Abdul K; Lichtmann, 2011). This initial immune response consists of physical and chemical components (such as the endothelial cells that line the blood vessel walls), phagocytic leukocytes (such as neutrophils, monocytes, and macrophages), and soluble mediators (e.g. components of the complement system, chemokines and cytokines). Tissue resident or sentinel cells such as mast cells, macrophages and dendritic cells (DCs) mediate the initial stages of leukocyte recruitment during an inflammatory response. These cells express surface and intracellular pattern recognition receptors (PRR) such as toll-like receptors (TLRs) (Takeuchi and Akira, 2010) through which they are able to recognise broad structures of potentially harmful material released by invading microorganisms (pathogen-associated molecular patterns; PAMPs) or damaged and/or dead cells (damage-associated molecular patterns; DAMPs) in response to tissue and/or cellular stress (Medzhitov, 2008). These cells can then act upon the danger signals by releasing a wide range of pro-inflammatory mediators such as cytokines (e.g. tumour necrosis factor-α (TNFα) and interleukin-1β (IL-1β)), chemokines (e.g. macrophage chemotactic protein-1 (MCP-1/CCL2) and macrophage inflammatory protein-2 (MIP-2/CXCL12) and other chemoattractants (e.g. leukotriene B_4 (LTB_4) and prostaglandin-D_2 (PGD_2) thereby indicating the site of infection or tissue damage (Bianchi, 2007; McDonald et al., 2010; Sadik et al., 2011; Ahmed et al., 2011). The release of these mediators triggers a cascade of events that leads to an increase in blood flow and permeability of the microvasculature allowing circulating leukocytes to transmigrate out of the peripheral vasculature and into the site of inflammation. The nature of the inflammatory insult will dictate the ability of specific leukocyte subsets to undergo recruitment via the local synthesis of chemokines, cytokines, and chemoattractants by both the host and invading pathogen. In addition, vasodilation of the blood vessel wall allows the passage of protein-rich plasma. Collectively, these events lead to the resolution of inflammation by clearing the infection or further confine the infection to mount a more specific secondary immune response.

One of the most abundant leukocyte subsets in the circulation is neutrophils. Neutrophils account for around 40-60% or all circulating leukocytes and undergo rapid recruitment from the circulation into the extravascular space during an inflammatory response. Their principle function is in pathogen detection and subsequent pathogen destruction by a process of phagocytosis. Much like macrophages, neutrophils express major surface receptors to common bacterial components, which upon interaction lead to the microorganism or cell debris being engulfed (Finlay and Hancock, 2004). Upon activation, neutrophils release numerous factors, such as granular antimicrobial substances and degrading proteases along with oxygen-derived free radicals thereby rapidly destroying pathogens. However, uncontrolled activation of neutrophils can lead to the aberrant release of these cytotoxic factors, which can also injure host cells and lead to vascular and/or tissue damage (Finlay and Hancock, 2004).

In addition, neutrophils also assist the secondary recruitment of other leukocytes and their subsets by generating and releasing pro-inflammatory cytokines and chemokines, thereby further amplifying the inflammatory response. During an acute inflammatory response, the recruitment of neutrophils into the tissue parenchyma is closely followed by the influx of monocytes which then differentiate into macrophages that help to clear infections via their ability to phagocytose pathogens (Finlay and Hancock, 2004). Indeed, the innate immune response is sometimes not sufficient in resolving the pathogen-associated inflammation. Under these conditions, the priming of the adaptive immune response, which initiates a slower but highly specific response, is critical (Abbas, Abdul K; Lichtmann, 2011). In contrast to cells of the innate immune response, cells of the adaptive immunity (B- and T-lymphocytes) target highly specific structures of microbial molecules (antigens) and can develop a memory to specific pathogens. The final resolving phase of inflammation following pathogen elimination requires the activation of tissue repair mechanisms (e.g. promoting fibroblast growth and adherence) (Finlay and Hancock, 2004).

Inflammation can be acute, lasting for a short period of time (minutes to days), or chronic (lasting days to years). Whereas acute inflammatory responses are transient and generally involve neutrophils and plasma exudation, chronic inflammation occurs when the inflammatory insult/trigger is persistent (e.g. during autoimmune diseases) and involves primarily macrophages/monocytes and lymphocytes. Collectively, immunity is a highly regulated and carefully balanced process. Disruption of regulatory mechanisms can lead to chronic inflammation that is commonly seen in severe pathological conditions, such as rheumatoid arthritis, atherosclerosis, and cancer. Therefore understanding the intricacies of the immune system, especially the mechanisms mediating leukocyte recruitment, is key to the development of novel anti-inflammatory therapies.

1.1.2 The Leukocyte Adhesion Cascade

1.1.2.1 Overview

During inflammation, leukocytes have to breach the vessel wall, which forms a complex physical barrier composed of cellular (the endothelium and pericyte sheath) and non-cellular (vascular basement membrane) components between the circulation and extravascular tissue (Nourshargh et al., 2010). The use of advanced imaging modalities and intravital microscopy have allowed the visualisation of leukocyte transmigration *in vivo* thereby advancing our knowledge of mechanisms that underpin this process. In particular, leukocyte transmigration occurs in small vessels such as the post-capillary venules and involves overcoming the primary barrier of endothelial cells on the luminal surface. Endothelial cells form a cobblestone-like appearance (10-15µm wide and 25-40 µm long) once confluent, that line the outermost layer of the vascular lumen. It is now well established that leukocyte transendothelial migration requires a cross talk of precisely coordinated adhesive interactions and signalling events between adhesion molecules expressed on leukocytes and endothelial cells (Ley et al., 2007) (Figure 1.1). The specific

cellular and molecular interactions involved in this process are more commonly known as the leukocyte adhesion cascade, which involves multifactorial and distinct steps: capture of leukocytes from the circulation, rolling of these cells on the luminal side of the endothelium, activation-induced arrest, adhesion strengthening, shape change and intraluminal crawling and paracellular or transcellular migration through the endothelium.

1.1.2.2 Leukocyte capture and rolling

Proinflammatory mediators released by sentinel tissue resident cells act transiently by binding to specific high-affinity receptors expressed on their target cells such as leukocytes and endothelial cells. Activation of the endothelium results in the upregulation and/or redistribution of adhesion molecules (Nourshargh et al., 2010). Selectins are a class of proteins that are involved in initiating the capture of circulating leukocytes. Upregulation of selectin expression (E-selectin and P-selectin) on endothelial cells allows leukocytes to undergo capture (also known as tethering) through forming an interaction with the respective selectin ligands P-selectin glycoprotein ligand-1 (PSGL-1), E-selectin ligand-1 (ESL-1), CD44 and other glycosylated ligands expressed on leukocytes (Zarbock et al., 2011; Vestweber and Blanks, 1999). To date, the selectin family comprises of three characterised members: E-selectin, which is expressed on inflamed endothelial cells, L-selectin, which is expressed on most leukocytes, and P-selectin, which is expressed on inflamed endothelial cells and on activated platelets (Ley et al., 2007). Certain leukocyte subsets, such as mononuclear cells, have also been shown to roll using $\alpha_4\beta_7$ integrin (Johnston, 1996). Selectin ligands are all fucosylated carbohydrate structures containing sulphated-sialyl-Lewis^x and are expressed mainly on leukocytes (McEver and Zhu, 2010). The sulphated-sialy-Lewis^X are tetrasaccharide carbohydrates which are recognised by the lectin domain of selectins (McEver, 2002). The binding of leukocytes to selectins expressed on endothelial cells can also facilitate secondary leukocyte tethering, allowing other leukocytes to interact with attached leukocytes through binding of leukocyte L-

selectin with PSGL-1, thereby further recruiting leukocytes to the sites of inflammation (Sperandio et al., 2003; Walcheck et al., 1996).

Following the capture of leukocytes from the circulation, leukocytes then undergo a period of rolling on the endothelial surface. This process is enabled by high on- and off-rate of selectin/selectin receptor bonds that leads to detachment of leukocytes from the endothelium and the formation of new adhesive interactions (Alon et al., 1995). These specific interactions between selectins and their respective ligands are also known as catch bonds, which strengthen in increased areas of shear stress thereby causing leukocyte rolling along the vessel wall (Finger et al., 1996; Lawrence et al., 1997). More recently, the formation of long membrane tethers containing PSGL-1, so-called “slings”, has been shown to allow efficient leukocyte rolling under conditions of high shear stress (Sundd et al., 2012). The “slings” form at the rear of leukocytes, such as neutrophils, and are rapidly mobilised to the front of the cell as it rolls, whereby it re-attaches to the underlying endothelium thereby increasing the chances of leukocyte-chemokine interactions. Leukocyte rolling along the luminal side of the vessel wall is pertinent in initiating the subsequent steps of the leukocyte adhesion cascade, as exemplified by studies using blocking antibodies to the selectins that were found to completely abolish leukocyte adhesion and transmigration (Kanwar et al., 1997). As well as forming extracellular interactions with their respective ligands, selectins have functional signalling properties. Upon binding of selectins with their respective ligands, downstream signalling events in both endothelial cells and leukocytes induce activation and subsequent integrin-mediated firm adhesion (Simon et al., 2000; Schmidt et al., 2013). The majority of the known signalling pathways involve changes in kinase activity such as triggering of p38 mitogen-activated protein kinase (MAPK)-signalling pathways and phosphoinositide 3-kinase-γ (PI3Kγ) (Simon et al., 2000; Puri et al., 2005; Schmidt et al., 2013). However, the intricacies of these signalling pathways and the precise mechanisms remain unclear.

A

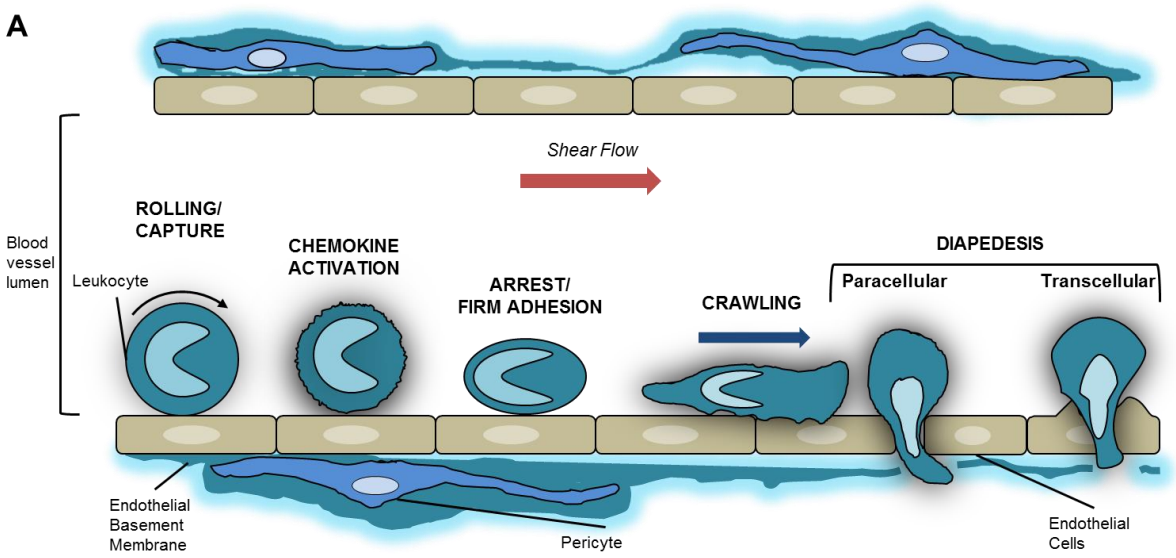

B

	Rolling/ capture	Chemokine activation	Arrest/ Firm adhesion	Crawling	Paracellular transmigration	Transcellular transmigration
Endothelium	P-selectin E-selectin	CXCL1 CXCL2 CCL2 LTB_4 PAF	ICAM-1 VCAM-1	ICAM-1 ICAM-2	JAM-A JAM-B JAM-C ESAM PECAM-1 CD99 ICAM-2 VE-cadherin	VVOs ICAM-1
Leukocytes	PSGL-1 ESL-1 L-selectin	G-protein coupled receptors	LFA-1 VLA-4 $\alpha_4\beta_7$	LFA-1 VLA-4	LFA-1 VLA-4	LFA-1

Figure 1.1 Leukocyte vessel wall interactions during leukocyte adhesion and transmigration. (A) In response to a diverse array of pro-inflammatory mediators, stimulation of vascular endothelial cells upregulates leukocyte cellular adhesion molecules that support the recruitment and subsequent adhesion of leukocytes to the luminal vessel wall. Upon activation, leukocytes undergo rapid firm adhesion and intravascular crawling that is supported by leukocyte selectin and integrin interactions with cellular adhesion molecules. Integrin-ligand clustering increases adhesive interactions between leukocytes and endothelial cells under conditions of hydrodynamic shear forces. Subsequent dissociation of endothelial junctional molecules or endothelial cell cytoskeletal rearrangement dictates the mode by which leukocytes breach the endothelial barrier and enter the extravascular tissue. (B) A table detailing some of the key adhesion molecules and structures expressed on leukocytes and endothelial cells involved in the distinct stages of leukocyte recruitment, activation-induced arrest, and transmigration (Ley et al., 2007; Nourshargh et al., 2010; Nourshargh and Alon, 2014).

1.1.2.3 Leukocyte activation-induced arrest and intraluminal crawling

A reduction in rolling velocity allows leukocytes to undergo activation and subsequent arrest that is triggered by immobilised chemokines (e.g. CXCL1 and CXCL2) that are expressed on the apical surface of endothelial cells anchored by glycosaminoglycans (GAGs) (Rot, 2010). This leads to the formation of a chemotactic gradient which guides leukocytes through the vasculature to the sites of injury (Phillipson and Kubes, 2011). Chemokines and chemoattractants act on leukocytes via G-protein coupled receptors (GPCRs). Upon binding of chemokines or chemoattractants to GPCRs, a complex intracellular signalling cascade is triggered that leads to changes in integrin affinity by transforming integrins into their high-affinity conformation in a mechanism referred to as inside-out signalling (Ley et al., 2007).

Integrins constitute a family of 30 members that are heterodimeric proteins consisting of α- and β-subunits found expressed on the surface of leukocytes and other cells (Herter and Zarbock, 2013). Under quiescent conditions, and with the exception of effector lymphocytes and certain monocyte subsets (Carlin et al., 2013; San Lek et al., 2013; Shulman et al., 2012), integrins exhibit a non-active conformation that is associated with a low binding affinity (Kinashi, 2005). Chemokine-induced activation of leukocytes rapidly changes the affinity of integrins from a low-affinity state to an intermediate affinity and finally high-affinity state that promotes their ability to form firm shear-resistant interactions with cellular adhesion molecules (CAMs) expressed on endothelial cells (Alon and Dustin, 2007; Carman and Springer, 2003; Ley et al., 2007). This is mediated through the opening of the ligand binding pocket, increased ligand-binding and decreased ligand dissociation of the integrin (Kinashi, 2005). Moreover, intracellular signals, driven by cytoskeletal focal adhesion proteins talin-1 and kindlin-3, further drive integrins into their active high-affinity conformations (Lefort et al., 2012; Moser et al., 2009; Ye et al., 2013). An important feature of integrin binding stability is the ability of integrins to undergo lateral clustering on the leukocyte cell surface that increases the avidity of integrin binding to

clustered CAMs expressed on endothelial cells through the formation of multivalent interactions. Upon activation, leukocyte-specific integrins (mainly β_1 and β_2 integrins) readily bind to endothelial cell CAMs (e.g. intercellular adhesion molecule 1 (ICAM-1) and vascular cell adhesion molecule 1 (VCAM-1)) (Campbell et al., 1996; Shamri et al., 2005). On leukocytes, the major integrins involved in adhesion strengthening and consequently leukocyte arrest are lymphocyte function-associated antigen 1 (LFA-1; also known as $\alpha_L\beta_2$ integrin) and macrophage antigen-1 (Mac-1; $\alpha_M\beta_2$), which bind with high affinity to ICAM-1, and very late antigen 4 (VLA-4; $\alpha_4\beta_1$) which binds to VCAM-1. This process represents the transition between selectin-mediated rolling to integrin-mediated firm adhesion/arrest.

Upon arrest to the endothelium, leukocytes undergo morphological changes from a spherical, rolling phenotype to a flattened and polarised morphology. These changes are dependent on outside-in signalling events that result in the reorganisation of the leukocyte cytoskeleton and characteristic presence of lamellipodia and uropod regions at the leading and trailing edges, respectively (Nourshargh et al., 2010; Hyun et al., 2012). This allows the adhered leukocytes to undergo cell spreading and intraluminal crawling that is mediated by F-actin polymerization at the front of the leukocyte and actin-myosin contraction and retraction at the back of the cell. Leukocytes then crawl to a favoured site of transmigration that is transitioned by the presence of a haptotactic gradient of chemoattractants (Phillipson et al., 2006; Schenkel et al., 2004). Leukocytic integrin binding to CAMs, in particular, Mac-1 binding to ICAM-1, allows leukocytes to form protrusions into endothelial cells and endothelial cell-junctions, which is further associated with endothelial cell contraction and the opening of inter-endothelial contacts. This process of directional crawling and sensing of migratory ‘hotspots’ might be important in facilitating efficient leukocyte motility to endothelial cell-junctions to facilitate subsequent leukocyte transmigration through the endothelial layer (Phillipson et al., 2006; Schenkel et al., 2004).

1.1.2.4 Leukocyte transmigration through the endothelial barrier

The migration of leukocytes through the endothelial barrier can occur via both paracellular (through endothelial junctions) or transcellular routes (through the body of the endothelial cell), although the former is the preferred route of leukocyte transmigration (Ley et al., 2007). One important feature of leukocyte transmigration is that it must maintain vessel wall integrity by causing minimal disruption to the endothelium. Recent *in vitro* studies have suggested that endothelial cells are able to support leukocyte transmigration through the formation of docking structures or transmigratory cups around the penetrating leukocyte that function as endothelial adhesive platforms (Barreiro et al., 2008, 2004; Ley and Zhang, 2008; Petri et al., 2011; Carman and Springer, 2004). It is proposed that these transmigratory cups, which are enriched with ICAM-1 and VCAM-1, might form a seal around the adherent leukocyte, thereby maintaining endothelial barrier integrity (Phillipson et al., 2008). It is proposed that ligand clustering of ICAM-1 and VCAM-1 is induced by tetraspanin or pentaspanin partners CD9, CD151 and CD47 (Barreiro et al., 2008; Azcutia et al., 2012). Engagement of leukocytes to these enriched areas of CAMs may act as optimal adhesion platforms, which facilitate the opening of endothelial junctions and subsequent priming of leukocyte transmigration. In endothelial cells, this is associated with increased intracellular Ca^{2+} (Huang et al., 1993; Pfau et al., 1995), initiation of intracellular signalling pathways such as the MAPK pathway (Hu et al., 2000) and generation of reactive oxygen species (ROS) (Deem et al., 2007; Martinelli et al., 2009). Altogether, this sequestering of leukocytes might prime the leukocyte for efficient transmigration. Various junctional adhesion molecules, including PECAM-1, ICAM-1, JAM-A, JAM-B, JAM-C, ICAM-2, CD99, PVR/CD155, endothelial cell-selective adhesion molecule (ESAM) and vascular endothelial cadherin (VE-cadherin), have been implicated in facilitating the transendothelial migration of leukocytes (Thompson et al., 2001; Dejana, 2004; Wegmann et al., 2006; Woodfin et al., 2007; Muller, 2011; Vestweber, 2012b; Wessel et al., 2014; Nourshargh and Alon, 2014) (Figure 1.2). However, the specific

adhesion molecules involved in leukocyte diapedesis vary depending on the type of leukocyte, the phase of transmigration, the inflammatory stimulus and the vessel wall niche (Ley et al., 2007; Muller, 2011; Nourshargh et al., 2010; Vestweber, 2012b; Voisin and Nourshargh, 2013).

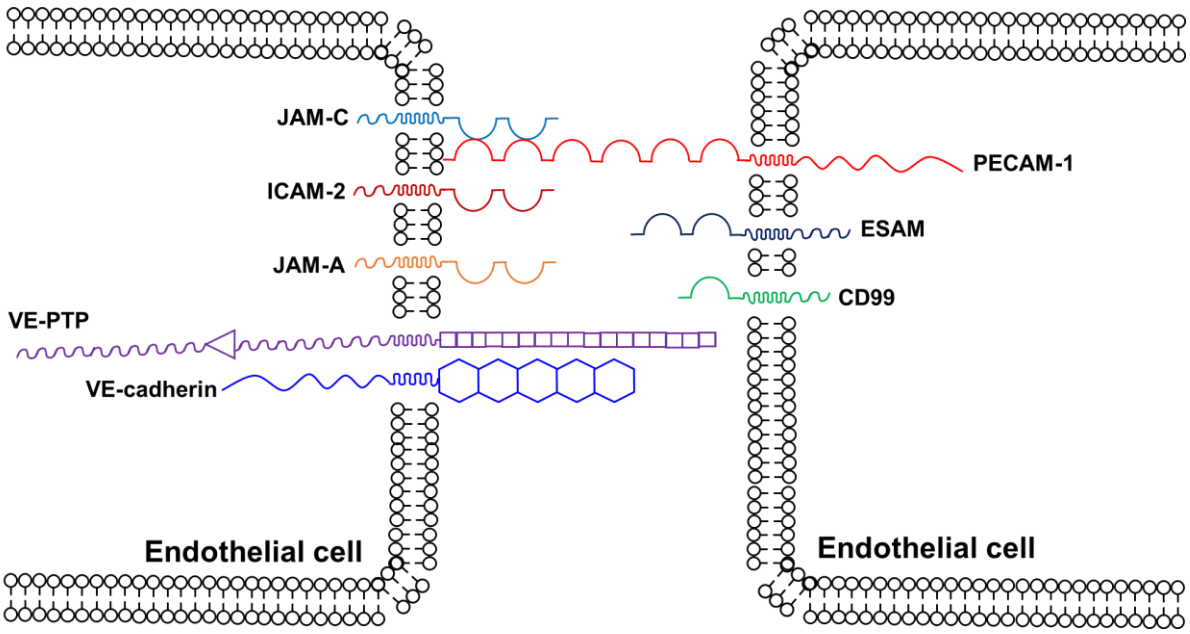

Figure 1.2 Key adhesion proteins at endothelial cell junctions that are important in facilitating paracellular leukocyte transmigration. Transmigration of leukocytes at endothelial cell junctions requires the dissociation of key junction proteins. Cell-cell contacts between adjacent endothelial cells are maintained by members of the junctional adhesion molecule family (JAMs), endothelial cell-selective adhesion molecule (ESAM) and CD99. In addition, endothelial cells contain adherence junctional proteins vascular endothelial cadherin (VE-cadherin) and its associated tyrosine phosphatase (VE-PTP). Moreover, platelet-endothelial cellular adhesion molecule-1 (PECAM-1) and ICAM-2 are also found at endothelial cell junctions, contributing to endothelial-cell adhesion (adapted from (Nourshargh and Alon, 2014)).

It is now regarded that the most preferred route of leukocyte diapedesis is through paracellular means – migration of leukocytes through endothelial cell junctions (Ley et al., 2007; Muller, 2011; Woodfin et al., 2011; Nourshargh and Alon, 2014). Endothelial cells exhibit highly organised molecular junctional complexes that form between adjacent cells. These intercellular junctions are comprised of tight junction (e.g. JAMs and claudins) and adherens junction (such as VE-cadherin) proteins. Junctional proteins usually are

transmembrane proteins linked to the intracellular cytoskeleton with intracellular signalling abilities. They function as important regulators of vascular permeability controlling the passage of circulating cells and plasma proteins into the tissue by providing vascular stability (Vestweber, 2012b).

The use of genetically modified *in vivo* models of inflammation with highly stabilised endothelial junctions has highlighted paracellular transmigration to be the dominant route of leukocyte diapedesis (Schulte et al., 2011). Under physiological conditions of leukocyte transmigration, certain junctional proteins (such as VE-cadherin) undergo transient dissociation from the endothelial cell junctions and are recycled back to the border or undergo proteolytic cleavage (Ley et al., 2007; Muller, 2011; Vestweber, 2012b; Voisin and Nourshargh, 2013). The introduction of a non-internalising stable mutant of VE-cadherin in mice led to resistance to vascular permeability upon challenge with permeability inducing agents such as histamine and VEGF, that correlated with an inhibition in junctional dissociation of VE-cadherin (Schulte et al., 2011).

Separately, stimulus-specific recruitment of neutrophils in various *in vivo* inflammatory models (IL-1β challenge, formyl-methionyl-leucyl-phenylalanine (fMLP) challenge and pathological ischemia-reperfusion (I/R) injury) showed that neutrophils preferentially transmigrated at endothelial cell junctions (Woodfin et al., 2011). Paracellular transmigration relies on a well-orchestrated interplay between endothelial cells and leukocyte adhesion molecules. The presence of adhesion molecules at distinct regions of endothelial cell junctions may differentially facilitate the leukocyte's ability to breach the endothelial barrier (Muller, 2011). Particularly, this has been shown to be true for the transmigration of neutrophils in a cytokine-dependent manner. Stimulation of mouse cremasteric tissue with IL-1β, but not TNFα or LTB_4, caused neutrophils to rapidly mobilise on ICAM-2 which guided them to endothelial cell junctions, followed by JAM-A which mediated neutrophil transmigration through the endothelial cell junction and finally PECAM-1 which supported penetration of neutrophils through the venular basement

membrane layer (Woodfin et al., 2007). Notably, many junctional endothelial cell adhesion molecules undergo recycling forming intracellular compartments, such as the lateral border recycling compartment, or get integrated into endosomes (Ley et al., 2007; Muller, 2011; Vestweber, 2012b).

The other mode of transmigration, known as transcellular migration, relies on leukocytes migrating through the body of the endothelial cell (Feng et al., 1998; Millán et al., 2006; Carman et al., 2007; Marmon et al., 2009; Martinelli et al., 2014). Much less is understood about the distinctive mechanisms that mediate this pathway. This process is thought to be mediated by leukocyte protrusions which extend into the endothelial cell body searching for permissive sites of migration (Ley et al., 2007). Binding of leukocyte protrusions to endothelial cell ICAM-1 have thought to translocate apical ICAM-1 into vesiculo-vacuolar organelles (VVOs), thereby facilitating bound leukocytes to follow a migratory pathway through endothelial cells (Millán et al., 2006; Carman et al., 2007). However, the physiological relevance of this pathway remains unclear. Mice lacking CD11b (Mac-1) on leukocytes have reduced leukocyte crawling and have a higher incidence of transmigration through transcellular means rather than at junctions (Phillipson et al., 2006). More recently, Martinelli et al. showed how lymphocyte transmigration could be strongly dictated by the pathway that has the least resistance. Using *in vitro* adhesion assays and transmission electron microscopy the authors describe how under conditions of high junctional resistance, lymphocytes make 'invadosome' like protrusions through endothelial cells thereby disrupting actin filaments to reduce F-actin density and associated stiffness, thereby allowing lymphocytes to follow transcellular migration – a process the authors term 'tenertaxis' (Martinelli et al., 2014). Indeed, in vascular beds that have high barrier function such as in the central nervous system, transcellular migration of leukocytes seems to be the predominant means of migration (Engelhardt and Ransohoff, 2012). These findings suggest that the mode of leukocyte transmigration can be dictated by inter-endothelial adhesive strength.

1.2 A DISINTEGRIN AND METALLOPROTEASE 10 (ADAM10)

1.2.1 ADAM proteases: molecular scissors with important roles in physiology and pathology

Chronic inflammatory conditions such as cancer, atherosclerosis, stroke and asthma are characterised by the excessive infiltration of leukocytes into the site of inflammation (Nourshargh and Alon, 2014; Nourshargh et al., 2010). Many therapeutic strategies against chronic inflammatory conditions have relied on targeting the immune response by focusing on the molecular pathways including localised cytokines, growth factors, receptors, and adhesion molecules expressed either on leukocytes or on endothelial cells that mediate the inappropriate triggering of the immune response. The identification of molecular proteases, that govern the shedding or proteolytic cleavage of many of the molecules mentioned, offers a mechanism by which chronic inflammatory conditions could be controlled by functionally altering the repertoire of cell surface proteins that are expressed on the localised cells at the inflammatory interface. These metalloproteases, which can be sub-classified into matrix metalloproteases (MMPs), MMPs with transmembrane-spanning regions (MT-MMPs), snake venom metalloproteases (SVMPs), members of the a disintegrin and metalloproteases (ADAMs) and ADAMs with thrombospondin motifs (ADAMTS) (Figure 1.3), has highlighted a fundamental role of proteolytic shedding in inflammation (Dreymueller et al., 2015). Although previous studies utilising broad-spectrum inhibitors in clinical trials has proven unrewarding (Khokha et al., 2013; Vandenbroucke et al., 2011), the recent emergence of ADAMs as key regulators of

proteolytic shedding offers a potential molecular mechanism which could govern cell function during inflammation.

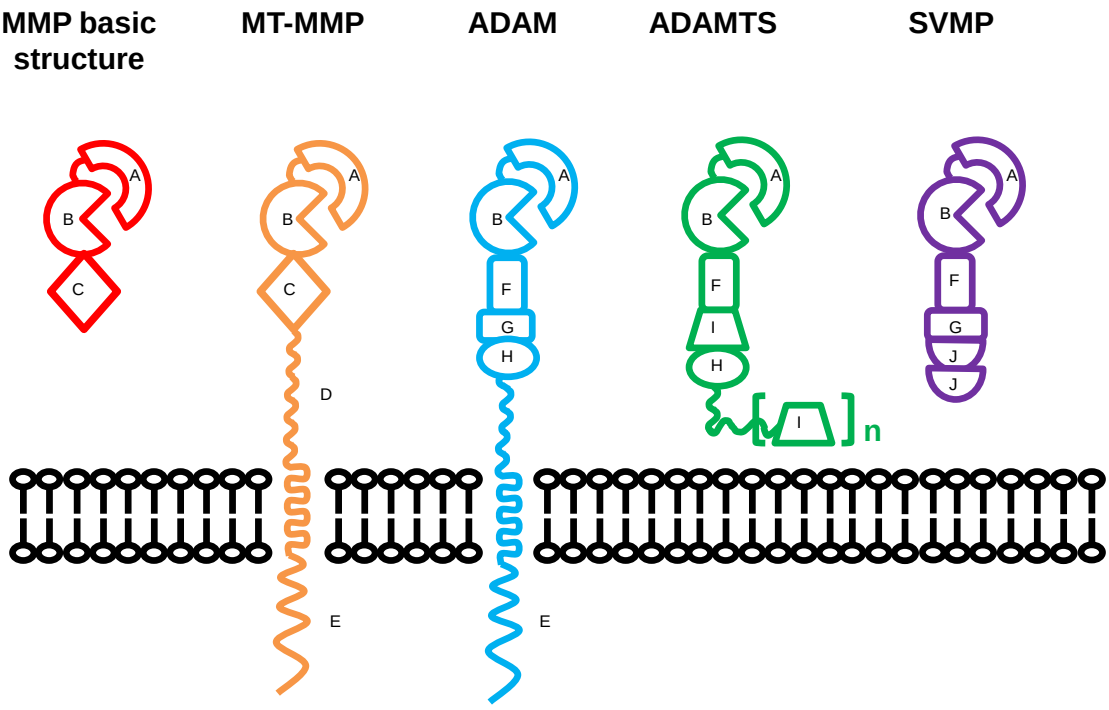

Figure 1.3 Schematic representation of the domain structure of metalloproteases. The family members consist of a common propeptide (A) and catalytic metalloprotease domain (B). In addition, matrix metalloproteases (MMPs) and transmembrane MMPs (MT-MMP) contain a hemopexin-like domain (C). A disintegrin and metalloproteases (ADAM) and MT-MMPs contain a stalk region (D), a transmembrane region, and a cytoplasmic tail (E). ADAMs and ADAMs with thrombospondin motifs (ADAMTS) contain a disintegrin domain (F), a cysteine region (G), an EGF-like domain (H) and ADAMTSs contain addition thrombospondin motifs (I). Snake-venom metalloproteases (SVMP) contain additional C-type lectin domains (J).

1.2.1.1 Overview of ADAMs

To date, the ADAM family comprises of ~34 members of which 22 have been identified in humans (Edwards et al., 2008). In terms of their structure, ADAMs are expressed as transmembrane proteins consisting of an N-terminal pro-domain followed by a

metalloprotease domain, a disintegrin domain, a cysteine-rich region, an EGF-like domain (only present in certain ADAMs), a transmembrane region and finally a cytoplasmic tail (Klein and Bischoff, 2011) (Figure 1.3). In terms of their function, ADAMs exhibit proteolytic or non-proteolytic activity (by interacting with other proteins) or combining both functions (Reiss and Saftig, 2009). The proteolytic activity of ADAMs seems to be the dominant characterised function of ADAM. In this regard, ADAMs can be thought of as "molecular scissors," which proteolytically cleave or "shed" the extracellular regions of other transmembrane proteins.

As the name suggests, the metalloprotease domain facilitates ADAM proteolytic activity. A classical component that dictates ADAMs proteolytic activity is the presence of a Zn^{2+} ion in the active metalloprotease domain. This has shown to be governed by a zinc-binding motif containing three histidine residues (HEXGHXXGXXHD) and a highly conserved methionine-turn in the active site helix (Bode et al., 1993; Orth et al., 2004). Based on the presence of this component and through the use of predicted structures of the zinc-binding site, ADAM8, 9, 10, 12, 15, 17, 19, 20, 21, 28, 30, 33 and DEC1 have been shown to have proteolytic activity in humans and mice (Andreini et al., 2005) (Figure 1.4). Crystal structures of the ADAM metalloprotease-disintegrin-cysteine rich domains have shown that this region of the ADAM protease forms an arm-like structure, with the active metalloprotease domain and cysteine-rich domain interacting with the substrate of interest (Igarashi et al., 2007; Takeda et al., 2006) (Figure 1.5). In addition, the cytoplasmic tails of ADAMs have been shown to be important regulators of proteolytic activity, signalling, and membrane localisation. In particular, recent studies have been shown that deletion of the cytoplasmic domain from ADAM10 results in reduced constitutive shedding activity, possibly because the tail has an endoplasmic retention motif that is important for ADAM10 trafficking (Maretzky et al., 2015). Moreover, inducible shedding through treatment of ADAM10-deficient mouse embryonic fibroblasts with ionomycin that causes enhanced influx of extracellular Ca^{2+} did not alter the shedding

abilities of the ADAM10 substrate betacellulin in the cytoplasmic tail-mutated ADAM10-overexpressing cells. This suggests that the cytoplasmic tail is indispensable for ADAM10 inducible activity (Maretzky et al., 2015). Similar observations have been concluded in studies looking at ADAM17 inducible activity, highlighting a dispensable role of the cytoplasmic domain for ADAM17 in regulating its activation (Hall and Blobel, 2012). In addition, the majority of ADAMs contain potential sites of phosphorylation and proline-rich regions, which can bind to SH2/3 domain-containing proteins potentially regulating ADAM activity (Edwards et al., 2008; Ebsen et al., 2014). Separate studies have also highlighted a role of ADAMs in forming homodimers at the plasma membrane (Xu et al., 2012; Deng et al., 2014), although the physiological implications of this structural modification to ADAMs is less well understood.

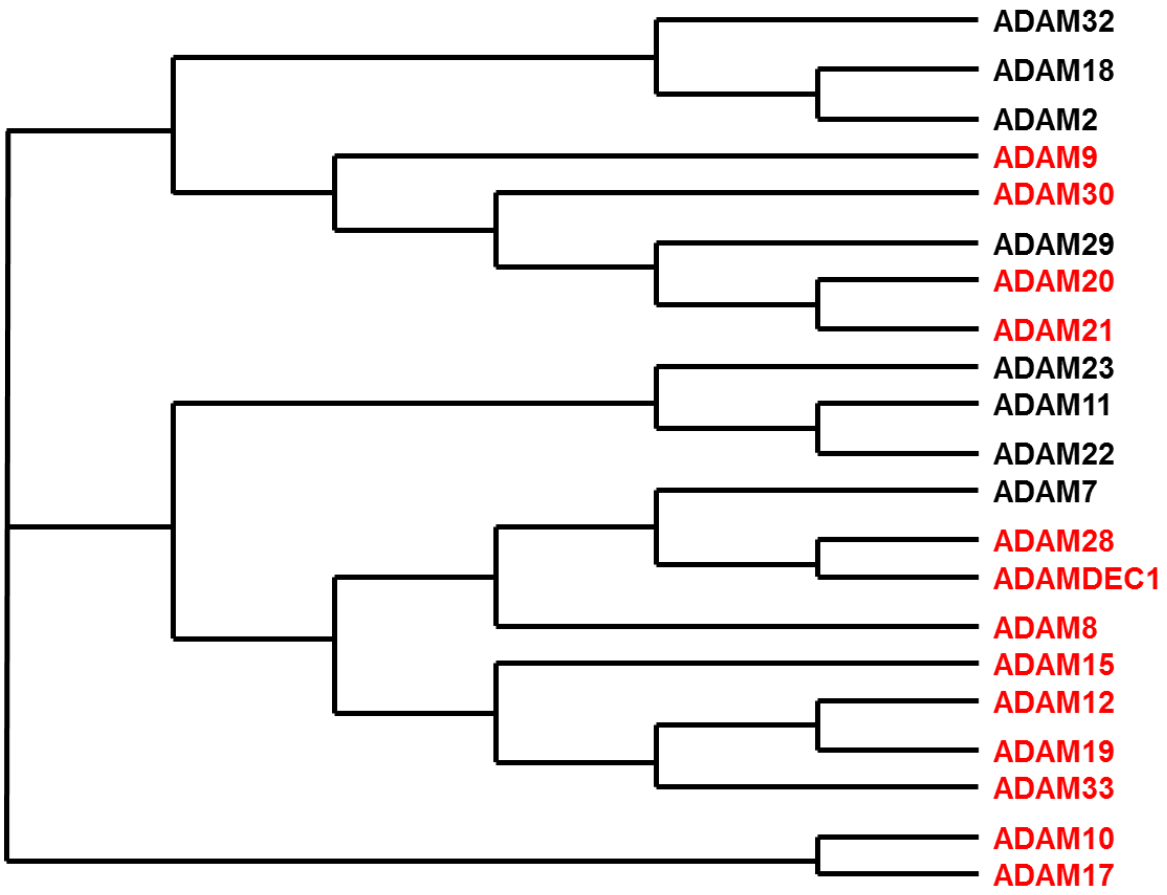

Figure 1.4 Phylogenetic tree of ADAM proteases. ADAM proteases expressed in humans were analysed for sequence similarity using Clustal OMEGA protein sequence alignment software based on the sequence of their metalloproteinase domains. Proteolytically active ADAMs are shown in red (adapted from Edwards et al., 2008).

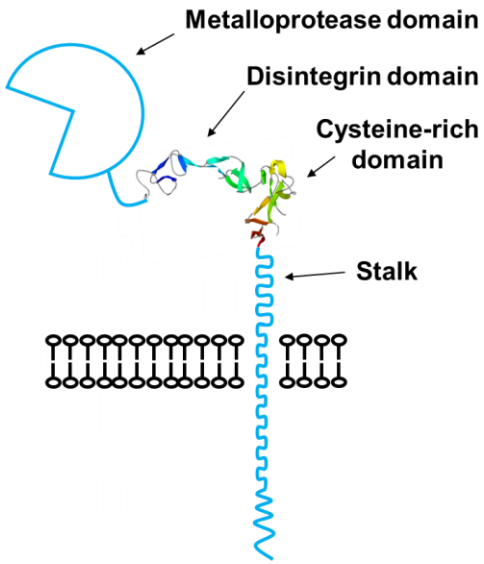

Figure 1.5 Predicted ADAM10 structure based on its characterised domains. Predicted ADAM10 structure based on the known ADAM10 crystal structure of the disintegrin and cysteine-rich domains which forms an arm-like structure (Janes et al., 2005).

As mentioned above, certain ADAMs also exhibit non-proteolytic activity such as in regulating adhesion. In particular the disintegrin domain has been shown to mediate interactions with integrins or with extracellular matrix components (Bridges and Bowditch, 2005). For example, the disintegrin domain of ADAM15 contains an RGD motif (Arg-Gly-Asp) that facilitates non-proteolytic interactions with the integrins $\alpha_v\beta_3$ and $\alpha_5\beta_1$ on hematopoietic cell lines (Nath et al., 1999, 2000). The physiological implications of ADAM association on integrin function require further investigations.

In terms of their synthesis, ADAMs are produced as inactive proenzymes with the prodomain functioning as an intramolecular chaperone. The prodomain is particularly important in maintaining the structural integrity of the ADAM through its correct folding whilst keeping the protease as an inactive zymogen. Following ADAM biosynthesis in the endoplasmic reticulum, ADAMs are transported to the Golgi, where they undergo maturation. During this maturation process, furin or proprotein convertase 7 cleave the prodomain of the ADAM protease (Gonzales et al., 2004; Anders et al., 2001), freeing the interaction with the zinc ion in the catalytic site, resulting in the active mature glycosylated

form that is trafficked to the cell surface following packaging and compartmentalisation into endosomes in the Golgi (Schlöndorff et al., 2000). More recently, the shedding of the prodomain of ADAM9, 10 and 17 in a newly identified site within the prodomain sequence, by a yet unidentified protease, was shown to be prerequisite to the canonical shedding of the complete prodomain that promotes maturation of the ADAM sheddases (Wong et al., 2015). Mutation of the newly identified prodomain shedding site resulted in reduced catalytic activity of the sheddases, suggesting that this site is required for optimal maturation of the fully catalytic ADAMs in addition to the previously known separate furin cleavage site (Wong et al., 2015).

Characterised substrates for ADAM proteolysis are generally other cell surface transmembrane proteins (Table 1.1). ADAMs cleave substrates in close proximity to the cell surface. In doing so, proteolytic shedding results in the release of a soluble ectodomain fragment of the substrate into the extracellular space which can exhibit agonist (e.g. Tumour necrosis factor (TNF)) or antagonist (TNFR) properties. As such, the consequences of proteolytic shedding include the removal of chemokines or cytokines from the cell surface, the removal of growth factors, the weakening of cell-cell adhesion or the initiation of intracellular signalling pathways. Subsequently, a cell membrane-bound fragment consisting of the transmembrane region and cytoplasmic tail remains at the plasma membrane. It is considered that proteolytic release of the ectodomain results in exposure of the generated membrane bound fragment, which is further processed by intramembrane proteolysis by the γ-secretase (a process more commonly known as regulated intramembrane proteolysis (RIP)), thereby releasing the intracellular tail which can then regulate downstream signalling or undergo degradation (Tousseyn et al., 2009) (Figure 1.7). In contrast to other proteolytic enzymes that recognise particular signature sequences for their proteolytic activity, ADAMs cleave their substrates with no clearly defined amino acid recognition motif that is common to different substrates. Indeed, some ADAM substrate cleavage sites have been mapped. For example, ADAM10

cleaves amyloid precursor protein (APP) in between Lys687 and Leu688 (Lammich et al., 1999). However, ADAMs require other structural determinants that are somewhat distinct from the cleavage site which facilitate substrate recognition (Stawikowska et al., 2013). ADAMs generate their substrate recognition partially through substrate-binding pockets in the active metalloprotease domain (Caescu et al., 2009). In addition the juxtamembrane domains, namely the disintegrin and cysteine-rich regions along with the transmembrane stalk are required for substrate recognition (Düsterhöft et al., 2014; Janes et al., 2005), at least for a select group of substrates which have had their ADAM proteolytic cleavage site mapped. Proteolytic shedding by ADAMs has been implicated as a critical mediator in embryonic development but also in physiological and pathological processes in the adult. As a result, the role of ADAMs in inflammation and cancer in particular is of increasing interest for potential drug targeting (Pruessmeyer and Ludwig, 2009; Rose-John, 2013; Saftig and Reiss, 2011; Dreymueller et al., 2015).

Protein Name	Alternative Names	Known Substrates
ADAM8	Cell surface antigen MS2, CD156a	cKit ligand, L-selectin, TGFα, CX3CL1, SCF, CD16, TNFα, TNFR1, VCAM-1
ADAM9	KIAA0021, MCMP, MDC9, Metrin γ	ADAM10, cKit Ligand, Delta-like 1, HB-EGF, VCAM-1, VE-cadherin, prion protein
ADAM10	Kuzbanian, MADM, CD156c	CD44, CX3CL1, CXCL16, HB-EGF, IL-6R, Notch, VE-cadherin, VEGFRII, Betacellulin, Corin, TRANCE, TNF, Ephrin, APP, MHC class I, human thyrotropin receptor, GPVI
ADAM12	Meltrin α	Betacellulin, Delta-like 1, HB-EGF, IGFBP 3/5, FGFR2iib, ADAM10, sonic hedgehog, Kilt1, VE-cadherin, Flk-1, Tie-2, VECAM-1
ADAM15	Metargidin for metalloprotease-RGD-disintegrin, MDC-15	IV collagen, gelatine, MCIB, E-cadherin, FGFR-2
ADAM17	CSVP, TACE, CD156b	CD40, CD44, cKit ligand, CX3CL1, Delta-like 1, CD163, EMMPRIN, EPCR, Ephrin B4, FLT3L, HB-EGF, ICAM-1, IGFR-1, IL-1RII, IL-6R, Jagged 1, JAM-A, L1-CAM, L-selectin, Notch, PECAM, Semaphorin 4D, Syndecan 1 and 4, TNFα, TNF receptor p55 (TNFRI), TNF receptor p75 (TNFRII), TGFα, VCAM-1, VEGFR2, TRANCE, CD74, Mac-1, FCγRIIIA, EGF, vasorin, GPVI
ADAM19	Meltrin β, MADDAM	cKit ligand, HB-EGF, α2 macroglobulin, Neuregulins, TNFα, TRANCE
ADAM28	ADAM23, MDCL	IGFBP3
ADAM33	C20orf153	cKit ligand, TRANCE, Insulin B chain

Table 1.1 Catalytically active ADAM proteases and their known substrates in vascular pathology and physiology (adapted from (Dreymueller et al., 2012b)).

The majority of the known shedding on human cells is mediated by two of the most closely related ADAM family members, ADAM10 and ADAM17. The importance of these two sheddases is highlighted through whole-body knockout mice. These show embryonic lethality for ADAM10, with mice dying at embryonic day 9.5 with severe defects in heart and somite development, and death shortly after birth for mice lacking ADAM17 (Hartmann et al., 2002; Peschon et al., 1998). The abnormalities observed in the global ADAM10 knockout mouse phenocopy defects in Notch1 knockout mice (Conlon et al., 1995). It is thought that the defects observed in the ADAM17 knockout mice, such as the increased heart valve development and the open eye phenotype, are a result of perturbed growth factor shedding that is required for epidermal growth factor receptor (EGFR) transactivation (Jackson, 2003). In addition, ADAM10 and ADAM17 are ubiquitously expressed both during development and in adult tissue. As a result, both proteases have been implicated in various acute inflammatory diseases, neurodegenerative diseases and cancer development (Dreymueller et al., 2015). In contrast, much less is known about the other proteolytically active ADAMs (ADAM8, 9, 12, 15, 19, 20, 21, 28, 30, and 33). This is most likely due to relatively weak phenotypes that are observed in the particular knockout mice (Dreymueller et al., 2015).

1.2.1.2 ADAM10 in inflammation

There is now an increasing understanding of the involvement of ADAM10 in inflammation, particularly in inflammation associated with the lung (Dreymueller et al., 2015). ADAM10 has at least 40 reported targets and is responsible for a substantial proportion of shedding on human cells (Saftig and Reiss, 2011). ADAM10 is known for its shedding of Notch and APP (Hartmann et al., 2002) (Figure 1.6). The former shedding event is triggered when Notch ligands (for example, Delta like ligands or Jagged) bind to the Notch receptor, allowing ADAM10 to then cleave within the membrane proximal region of Notch, releasing

the ectodomain fragment. Activated ADAM17 has also been shown to regulate the shedding of Notch, although this appears to be independent of engagement of Notch ligands (Bozkulak and Weinmaster, 2009). Regulated ADAM10-dependent shedding of Notch seems to explain the developmental defects that are observed in the ADAM10 knockout mice (Hartmann et al., 2002). Notch shedding by ADAM10 is crucial for many processes in the adult, including tissue regeneration (Weber et al., 2011) and myeloid development (Weber et al., 2011; Yoda et al., 2011). In addition to Notch shedding, ADAM10 is also known for its processing of APP. APP is processed by extracellular α- and β-sheddases along with γ-secretase (Prox et al., 2012a). As a result, a variety of different ectodomains are generated upon engagement of the various sheddases. ADAM10 is regarded as an α-sheddase and cleaves APP between the β- and γ-shedding sites, thereby preventing the production of the amyloidβ peptide that is associated with promoting Alzheimer's disease (Saftig and Lichtenthaler, 2015). Overexpression of ADAM10 in mouse brains has been shown to protect against Alzheimer's disease (Postina et al., 2004) and as a result, ADAM10 activity in Alzheimer's is of key therapeutic interest (Saftig and Lichtenthaler, 2015).

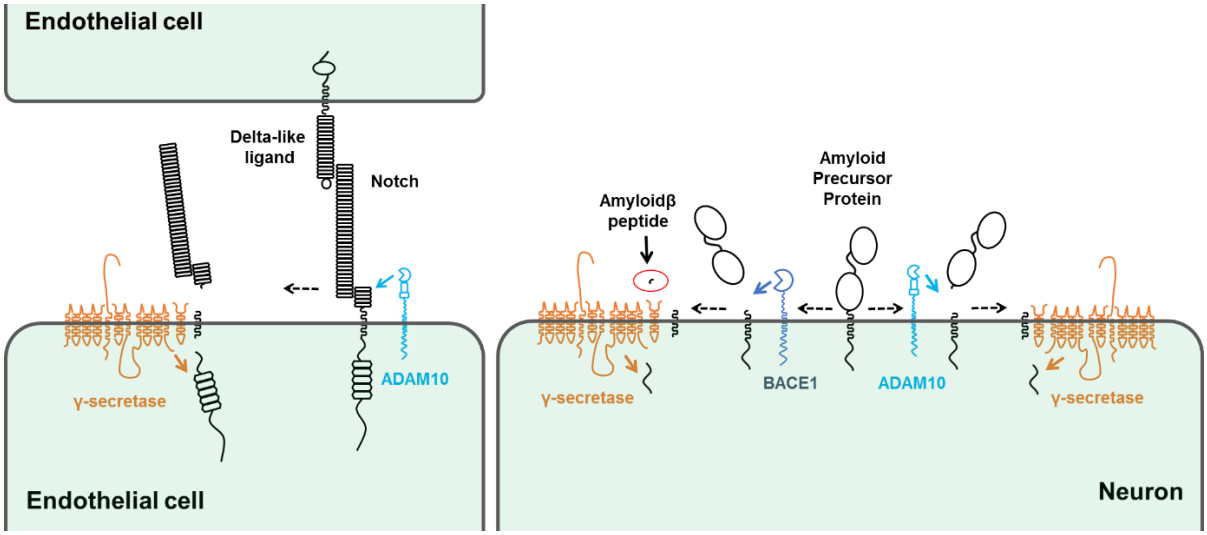

Figure 1.6 ADAM10 is the principle sheddase for Notch and amyloid precursor protein (APP). Engagement of Notch ligands to Notch leads to conformational changes in Notch that allow ADAM10 to cleave the extracellular fragment. This then allows the γ-secretase complex to further process the membrane bound stump of Notch, which leads to the production of a transcriptionally active intracellular domain, which can be trafficked to the nucleus and control cell fate decisions (left). ADAM10-dependent shedding of APP prevents the production of the amyloidβ peptide (inside red oval) that is responsible for Alzheimer's disease by cleaving APP between its BACE1 shedding site and γ-secretase shedding site (right).

In inflammation, ADAM10 seems to cleave an array of substrates that are expressed in various vascular beds (Figure 1.7). In particular, ADAM10 has been shown to shed the low affinity IgE receptor CD23 which is implicated in initiating the allergic immune response (Weskamp et al., 2006), VE- and E-cadherin that mediate cell adhesion and vascular permeability (Schulz et al., 2008; Maretzky et al., 2005), EGF that regulates transactivation of its receptor(s) thereby controlling cell proliferation and differentiation (Yan et al., 2002), the two transmembrane chemokines, CX3CL1 and CXCL16 that mediate leukocyte adhesion (Abel et al., 2004; Hundhausen et al., 2003), and the receptor for advanced glycation endproducts (Raucci et al., 2008) (Figure 1.7). Many of these substrates have been identified through the use of *in vitro* shedding assays and a limited amount of *in vivo* data exists through the use of ADAM10 cell-specific knockout-mice.

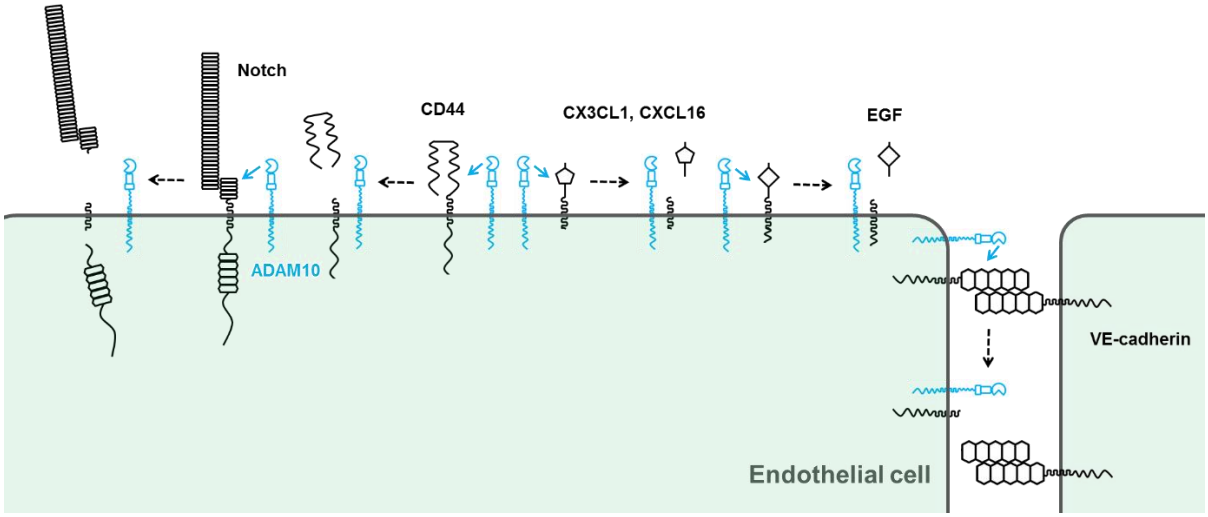

Figure 1.7 Key endothelial ADAM10 substrates implicated in inflammation. Engagement of ADAM10 regulates the shedding of various endothelial cell substrates, such as Notch, CD44, CX3CL1, CXCL16, EGF, and VE-cadherin.

In addition to ADAM10, ADAM17 has been shown to have a dominant role in inflammation, by acting on its endothelial and leukocytic substrates, such as ICAM-1 and L-selectin. Rapid shedding of L-selectin from the surface of leukocytes, such as neutrophils, has been shown to cause reduced leukocyte rolling and a subsequent decrease in leukocyte-endothelial adhesive interactions under *in vitro* flow conditions (Smalley and Ley, 2005). In addition, generation of mice expressing a mutant shedding resistant form of L-selectin in the T-cell lineage revealed that L-selectin shedding is required for optimal re-entry of antigen-activated T-cells into the peripheral lymph nodes (Galkina et al., 2003). *In vivo* models of acute inflammation using ADAM17 deficient neutrophils have revealed through models of thioglycollate or *Escherichia coli*-induced peritonitis that L-selectin mediates the early recruitment of neutrophils into the peritoneum (Long et al., 2010; Tang et al., 2011). In addition to shedding of L-selectin, ADAM17 has also been implicated in *in vitro* studies as the primary sheddase that cleaves endothelial CAMs, ICAM-1 and VCAM-1 under protein kinase C-induced conditions (Singh et al., 2005; Tsakadze et al., 2006). The shedding of these two CAMs may prime leukocytes to

locomote along the apical surface of endothelial cells in search for exit points for transmigration as well as regulating leukocyte transmigration by inducing intracellular signalling pathways within the endothelial cells.

1.2.1.2.1 ADAM10-dependent shedding of endothelial substrates

Endothelial cells play a critical role in inflammation by facilitating efficient leukocyte recruitment and subsequent transmigration of leukocytes as well as regulating vascular permeability (Vestweber, 2015). Indeed, endothelial ADAM10 has been implicated in regulating inflammation by promoting neovascularisation and facilitating the inflammatory responses of endothelial cells, in addition to ADAM10's established role in the early development of vascular structures (van der Vorst et al., 2012).

The generation of the ADAM10 endothelial-specific knockout mice (driven by Tie2-Cre) highlighted an important role of ADAM10 in vascular development (Glomski et al., 2011). These conditional endothelial ADAM10 knockout mice are largely viable displaying mild abnormalities in the retinal vasculature with enhanced vessel branching (Glomski et al., 2011) and shorter femurs, tibiae and humeri attributed to defects in osteoclastogenesis at the chondro-osseus junction (Zhao et al., 2014). These defects in endothelial cells seem to be driven by Notch-dependent cell fate decisions that require Notch shedding by ADAM10. Indeed, downstream Notch signalling target genes such as Snail and Brmp2 have impaired expression in ADAM10 deficient endothelial cells, suggesting a critical role of ADAM10 in Notch signalling and cardiac development (Zhang et al., 2010).

To date, characterised ADAM10 endothelial substrates involved in inflammation have largely been discovered through the use of *in vitro* models. One of the initial endothelial ADAM10 substrates discovered to play a role in guiding leukocytes during inflammation, were the two transmembrane chemokines, CX3CL1 and CXCL16 (Hundhausen et al., 2007). These chemokines have been shown to be important in mediating leukocyte

adhesion by binding to their respective ligands expressed on leukocytes, namely CX3CR1 and CXCR6 (Ludwig and Weber, 2007). Through the utilisation of cell lines made to overexpress either of the two transmembrane chemokines, Hundhausen et al. showed that ADAM10 was required to provide a chemokine-shedding event that then allowed the bound leukocytes to locomote along the endothelium and undergo subsequent transmigration, a term the authors called 'de-adhesion' (Hundhausen et al., 2007). The subsequently cleaved ectodomain of the chemokines also act as chemotactic gradients that are required for promoting adhesion of circulating leukocytes (Hundhausen et al., 2007). In addition to ADAM10, ADAM17 has also been shown to cleave CX3CL1 under PMA-induced conditions (Garton et al., 2001). Indeed, ADAM10 is largely regarded as a constitutive sheddase and regulates the homeostatic shedding of CX3CL1, whilst under certain stimulatory conditions, such as PMA treatment, ADAM17 could dominate the proteolytic shedding event (Garton et al., 2001; Hundhausen et al., 2003). More recently, the membrane dynamics surrounding CX3CL1 shedding by ADAM10 have been explored using single-particle tracking methodologies. In this study, Wong et al. showed that CX3CL1 is confined at the plasma membrane via its intracellular tail that forms an interaction with the cortical actin cytoskeleton. Disruption of the cortical actin cytoskeleton resulted in increased CX3CL1-ADAM10 interactions and subsequent enhanced shedding of the transmembrane chemokine (Wong et al., 2014).

ADAM10 has also been shown to regulate vascular permeability (Ponnuchamy and Khalil, 2008). VE-cadherin, a junctional adhesion molecule that acts as a gateway for the passage of leukocytes or macromolecules (Vestweber, 2015), has been shown to be proteolytically cleaved by ADAM10 (Schulz et al., 2008). In this study, Schulz et al. demonstrated that inhibition of ADAM10 on endothelial cells using siRNA or pharmacological inhibitors resulted in reduced VE-cadherin shedding. This shedding capability of ADAM10 was enhanced following stimulation of endothelial cells with the calcium ionophore, ionomycin, and was associated with increased endothelial barrier

permeability as assessed using a FITC-dextran permeability dye (Schulz et al., 2008). The authors also went on to show that thrombin induced vascular permeability was reduced following endothelial ADAM10 inhibition (Schulz et al., 2008). In addition, the transmigration of THP-1 immortalised monocytic cells across ADAM10 inhibited or knocked down endothelial cells was compromised (Schulz et al., 2008). However, the authors did not definitively show if the reduction in THP-1 cell migration was due to increased VE-cadherin at the endothelial cell junctions. In addition to VE-cadherin, endothelial ADAM10 also regulates the shedding of the Ephrin guidance molecule, Ephrin-A (Janes et al., 2005). Ephrin-A mediates cell-cell adhesion by binding to its respective receptor EphA. ADAM10 mediated shedding of Ephrin-A disrupts this complex leading to cell detachment (Coulthard et al., 2012). Moreover, soluble Ephrin-A has been shown to induce vascular permeability, a process that is mediated through direct interaction with its receptor EphA and is dependent on downstream intracellular NFκB mediated responses (Coulthard et al., 2012).

1.2.1.2.2 ADAM10-dependent shedding of leukocytic substrates

The most characterised role of ADAM10 in leukocyte adhesion and transmigration has been shown with the use of leukocytic cell lines and more recently through the use of *in vivo* conditional ADAM10 knockout mice with deletions of ADAM10 in the myeloid and hematopoietic lineages. Initial *in vitro* studies highlighted that ADAM10 was important in the chemotactic migration of neutrophils and monocytes across immortalised endothelial cell monolayers (ECV-304 cells) (Pruessmeyer et al., 2014). Pharmacological inhibition of ADAM10 expressed on human neutrophils or on the monocytic derived cell line THP-1 cells resulted in reduced migration of these cells towards the chemokines IL-8 and CCL2, respectively (Pruessmeyer et al., 2014). Furthermore, genetic ablation of ADAM10 on human neutrophils or THP-1 cells revealed a similar phenotype to that observed following pharmacological inhibition of ADAM10 (Pruessmeyer et al., 2014). The reduced migration

of neutrophils and THP-1 cells was attributed to various intracellular signalling and adhesive events that are required for leukocyte transmigration. Pharmacological inhibition or genetic silencing of ADAM10 on neutrophils or THP-1 cells caused a reduction in p38 phosphorylation, reduced Rho GTPase activation, diminished F-actin polymerisation and reduced adhesion to fibronectin attributed to the improper activation of α_5-integrin (Pruessmeyer et al., 2014). Furthermore, Pruessmeyer et al. confirmed the relevance of these findings by using *in vivo* conditional ADAM10 knockout mice, lacking ADAM10 in the myeloid lineage and hematopoietic lineage. Deletion of ADAM10 on myeloid cells, as driven by a LysM-Cre promoter, resulted in reduced recruitment of neutrophils and monocytes into the lung and reduced inflammation-induced oedema formation (Pruessmeyer et al., 2014). In addition, ADAM10 deletion in the hematopoietic lineage (as driven by a Vav-Cre promoter) impaired the recruitment of neutrophils and monocytes into the lung alveoli following intranasal administration of LPS (Pruessmeyer et al., 2014). However, the precise mechanisms surrounding ADAM10's role in leukocyte transmigration remain unknown.

Due to the importance of these and other substrates in a variety of processes, ADAM10 is of major research interest in developmental biology, the cardiovascular system, immunology, cancer, and Alzheimer's disease. However, the regulation of this ubiquitously expressed metalloprotease, in terms of activation and localisation to substrates during inflammation, is poorly understood.

1.3 TETRASPANINS

1.3.1 Introduction to tetraspanins

Tetraspanin superfamily proteins are composed of four transmembrane regions, two extracellular loops of unequal size, one intracellular loop and short intracellular N- and C-

terminal tails (Figure 1.8) (Hemler, 2014). The tetraspanins are further characterised by a conserved gene structure and conserved cysteine residues that are important for the structure of the main extracellular loop. Tetraspanins function by interacting with other transmembrane 'partner proteins', which include integrins, immunoglobulin superfamily (IgSF) member proteins and others such as ADAM10 (Charrin et al., 2014; Hemler, 2014). Tetraspanins regulate various aspects of partner protein function, namely biosynthesis, intracellular trafficking, and lateral mobility and clustering at the cell surface (Charrin et al., 2014; Hemler, 2014). There are 33 tetraspanins in mammals and the superfamily extends to other animals, plants, and multicellular fungi (Huang et al., 2005). Human cells typically express approximately 20 different tetraspanins, and tetraspanin mutations cause diseases that are consistent with impaired function of their respective partner proteins.

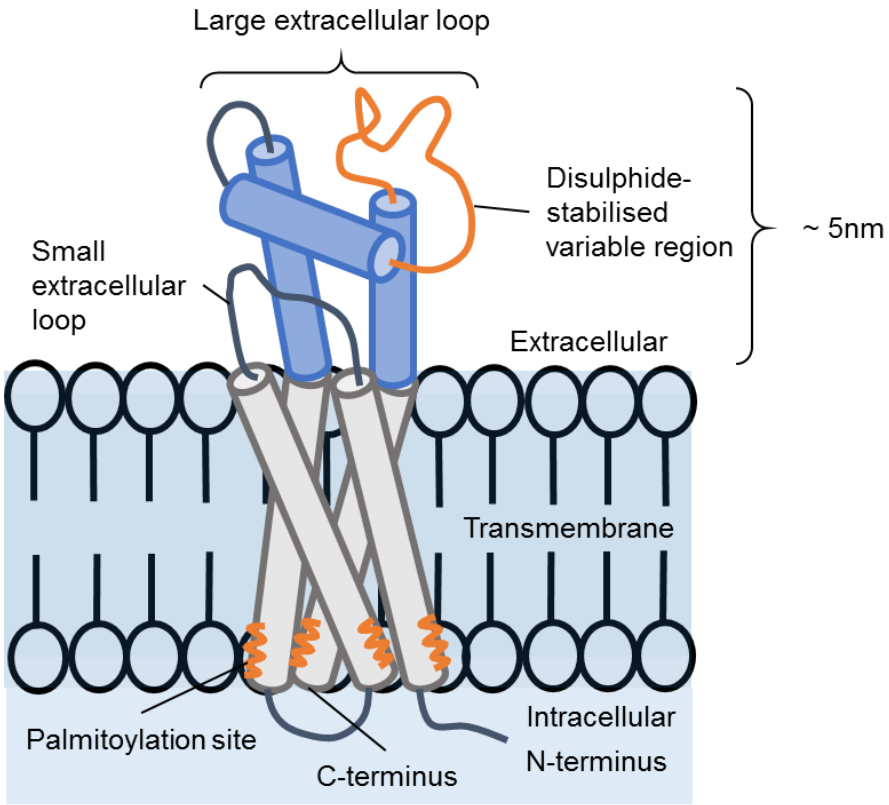

Figure 1.8 The conserved structure of tetraspanin proteins. (adapted from (Hemler, 2014)).

1.3.2 Structure of tetraspanins

The use of cryo-electron microscopy has helped to reveal the low resolution structure of uroplakin tetraspanins UPIa and UPIb, detailing a compact, rod-like structure, composed of four transmembrane helices along with two extracellular regions (namely, EC1 and EC2) in which the extracellular regions protrudes 3.5-5 nm above the plasma membrane (Min et al., 2006) (Figure 1.9).

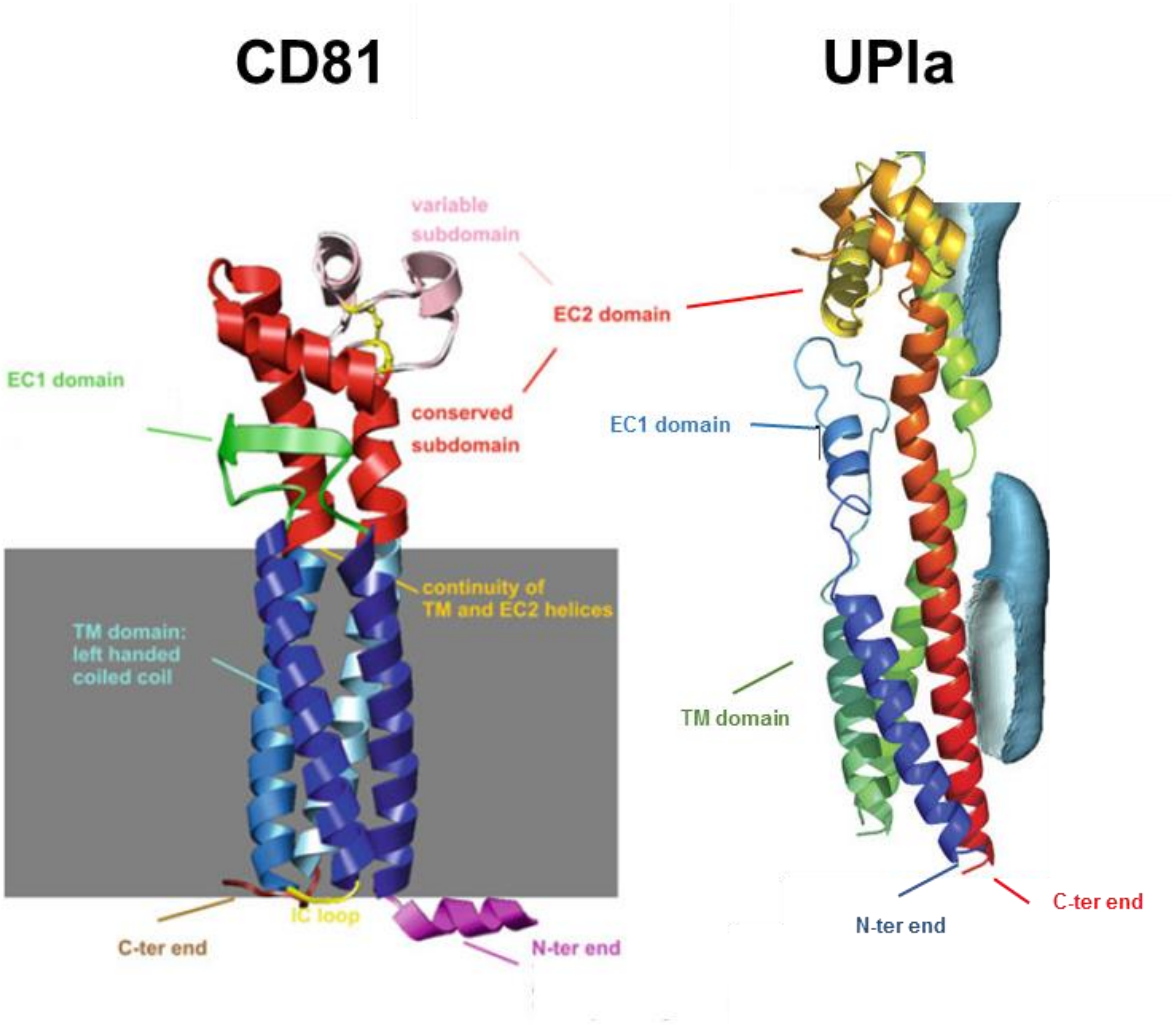

Figure 1.9 Ribbon schematics of the low resolution cryo-EM and predicted 3D structure of CD81. (adapted from (Seigneuret, 2006; Min et al., 2006).

The use of crystallography (Kitadokoro et al., 2001) and nuclear magnetic resonance (NMR) (Rajesh et al., 2012) resolved the structure of the EC2 domain of CD81, revealing a hydrophobic patch that was shown not to mediate tetraspanin-tetraspanin interactions. Combining this with computational methods resulted in the complete modelling of the predicted structure of the tetraspanin CD81 (Figure 1.9) (Seigneuret et al., 2001; Seigneuret, 2006).

Tetraspanins also undergo post-translational modifications that include palmitoylation at cysteine residues within the cytoplasmic tails at membrane proximal regions, N-linked glycosylation within the large extracellular loop and ubiquitination of the cytoplasmic tails (Charrin et al., 2009a). Palmitoylation of membrane proximal cysteines facilitates the association of tetraspanins with other tetraspanins and has shown to promote clustering of tetraspanin-tetraspanin interactions at the plasma membrane (Israels and McMillan-Ward, 2010; Delandre et al., 2009; Zhu et al., 2012). This palmitoylation process occurs during trafficking of the tetraspanin through the Golgi and is mediated by palmitoyltranferases (for example, DHHC2 which palmitoylates tetraspanins CD9 and CD151) (Sharma et al., 2008) and disruption of this process results in loss of tetraspanin function and an increase in protein degradation (Sharma et al., 2008). In addition to cysteine palmitoylation, N-linked glycosylation within the large extracellular loop of certain tetraspanins has been shown to be important in tetraspanin functioning. For example, N-linked glycosylation of CD151 is important in mediating the adhesive strengthening of the α_3 integrin subunit that it associates with (Baldwin et al., 2008). Tetraspanins also share varying levels of protein sequence homology amongst other members of the superfamily with certain tetraspanins (e.g. Tspan5 and Tspan17) sharing high levels (~78%) sequence homology in humans and others sharing less protein sequence homology (e.g. 26% sequence homology for the distantly related Tspan15 and Tspan10). Nevertheless,

tetraspanins seem to have arisen from a common ancestor since several intron/exon sites are conserved within tetraspanin genes (Garcia-España et al., 2008).

1.3.2 Tetraspanins as membrane organisers

Tetraspanins form dynamic interactions with specific partner proteins and with other tetraspanins (Charrin et al., 2014; Hemler, 2014). By doing this, tetraspanins are able to promote the trafficking, clustering and lateral mobility of their respective partner proteins (Charrin et al., 2014; Hemler, 2014). Some of the best characterised tetraspanin-partner protein interactions include integrins (e.g. $\alpha_3\beta_1$, $\alpha_6\beta_1$, $\alpha_6\beta_4$ which all associate with CD151, IgSF members (EWI-F, EWI-2, CD19, ICAM-1, VCAM-1 which associate with CD81, CD9, CD81, CD9 and CD151, respectively), proteases (ADAM10 and MT-MMP1 which associate with the TspanC8 subgroup of tetraspanins and CD151, respectively) and intracellular signalling proteins (protein kinase C enzymes associate with CD151) (Charrin et al., 2014). Previous studies highlighted that tetraspanins were able to recruit specific partner proteins and other tetraspanins into larger membrane microdomains (typically consisting of three or more different tetraspanins) which acted as optimal platforms for adhesion and cell signalling (Barreiro et al., 2008; Espenel et al., 2008). However, recent studies of tetraspanins using advanced microscopy, such as super resolution microscopy and single particle tracking analysis, have highlighted that tetraspanins are more dynamic at the plasma membrane, shuttling from regions of high tetraspanin density and the rest of the membrane and forming tetraspanin-tetraspanin interactions in both of these distinct areas (Espenel et al., 2008)

.

1.3.2.1 Tetraspanins regulate membrane protein compartmentalisation

The tetraspanin association with their respective partner proteins has largely been deduced through the use of different detergents and subsequent co-immunoprecipitation experiments. Many of these biochemical experiments have relied on the use of detergents with varying stringency and the levels of interaction with other tetraspanins and specific partner proteins, especially weak interactions, can be misinterpreted as artefacts of the lysis conditions. Therefore caution has to be taken when solely considering biochemical assays to decipher tetraspanin-protein interactions. Primary tetraspanin interactions are thought to be strong interactions between tetraspanins and specific partner proteins that are maintained under stringent lysis conditions, such as Triton X-100 or Digitonin (Serru et al., 1999; Yauch et al., 1998). Examples of primary tetraspanin-partner protein interactions include CD151 with the laminin binding integrin $\alpha_3\beta_{1,,}$ and CD9 with the IgSF member EWI-F (Charrin et al., 2001; Serru et al., 1999). Secondary tetraspanin interactions are maintained under less stringent conditions (e.g. Brij97). These tetraspanin-partner interactions are not direct, but are maintained by tetraspanin-tetraspanin interactions in Brij97 that would be disrupted in more stringent detergents (Berditchevski et al., 1996). In addition, these tetraspanin-tetraspanin interactions are regulated by cholesterol and gangliosides (Charrin et al., 2003; Odintsova et al., 2006) along with intracellular palmitoylation of cysteine residues (Charrin et al., 2002), which regulate tetraspanin membrane dynamics and subsequent clustering (Espenel et al., 2008; Termini et al., 2014).

The use of chimeric protein constructs to map tetraspanin-partner protein interactions have proven invaluable. Chimeric tetraspanin proteins are made by swapping various regions of the tetraspanin with regions of a tetraspanin that does not interact with the partner protein. By utilising this approach, many tetraspanin partner protein interactions have been deciphered. For example, CD81 interacts with the fourth IgSF domain of EWI-2 along with a glycine-zipper motif located in the transmembrane region (Montpellier et

al., 2011). On CD81, the larger extracellular loop and transmembrane regions 3 and 4 are required for its interaction with EWI-2 (Montpellier et al., 2011). CD9 also interacts via its fourth transmembrane region to the transmembrane region with the second EWI member, EWI-F (Charrin et al., 2009b). More recently, the Tomlinson group have mapped the interacting regions of six tetraspanins (Tspan5, 10, 14, 15, 17 and 33; collectively referred to at the TspanC8 subgroup of tetraspanins) and their partner protein ADAM10, using a similar approach to that explained previously (Noy et al., 2016) (see Section 1.3.3). However, these biochemical assays are limited by the fact that the dynamics of specific tetraspanin-partner protein interactions cannot be investigated.

Tetraspanins are now thought of as proteins that dynamically patrol the plasma membrane forming interactions with specific partner proteins. Single particle tracking analysis of fluorescent tagged CD9 molecules revealed that CD9 molecules preferentially followed a Brownian motion, moving to and from small clusters of CD9 (Espenel et al., 2008). More recently, the use of dual colour stimulated emission depletion (STED) microscopy has highlighted the nanoscale organisation of these tetraspanin enriched domains (Zuidscherwoude et al., 2015). This study showed that endogenous tetraspanin nanoclusters on B cells are smaller than 120 nm in size and revealed that these clusters contain less than 10 CD53 molecules, which prefer to form homodimeric interactions with one another (Zuidscherwoude et al., 2015). These nanoclusters seem to be specific to a single tetraspanin and respective tetraspanin partner proteins seem to form separate clusters that are in close proximity to their tetraspanin partners (Zuidscherwoude et al., 2015). An individual tetraspanin enriched cluster contained, on average, 3.5 molecules of CD53 and where multiple tetraspanins could interact with a single partner protein (e.g. MHC class II and tetraspanins CD53 and CD37) the tetraspanin clusters overlapped with the partner protein in which the tetraspanins were adjacently positioned at the plasma membrane (Zuidscherwoude et al., 2015). Similar observations were made in a study looking at CD82 distribution in KG1a cells, which revealed a nanocluster size of 90 nm

using stochastic optical reconstruction microscopy (STORM) (Termini et al., 2014). These data suggest that tetraspanin clusters are organised into smaller nanoclusters that form distinct distribution patterns at the plasma membrane with their respective partner proteins (Zuidscherwoude et al., 2015).

1.3.2.2 Tetraspanins mediate partner protein function via their trafficking, lateral mobility and clustering

One function of tetraspanins is their ability to regulate the biosynthesis and maturation of their specific partner proteins. A well-characterised example of this is the association of the tetraspanin CD81 and its partner protein CD19. CD19 is an IgSF member that is expressed on B cells and forms a complex with CD81 and CD21 (Bradbury et al., 1992; Matsumoto et al., 1993). Mice deficient in CD81 displayed a 50% reduction in cell surface CD19 compared to wild-type mice. This phenotype was due to impaired trafficking of CD19 from the endoplasmic reticulum to the Golgi (Shoham et al., 2003). Furthermore, CD19 expression in a CD81 deficient human patient showed abrogated CD19 expression at the surface of B cells due to impaired trafficking of CD19 by CD81 (Van Zelm et al., 2010). Both the mouse study and the human patient study showed impaired B cell antibody responses upon challenge (Levy and Shoham, 2005; Van Zelm et al., 2010).

Another function of tetraspanins is their ability to promote clustering of their partner proteins at the plasma membrane, which then promotes partner protein function such as signalling and adhesion. Tetraspanins have been shown to enhance the adhesive capacity of their partner proteins by promoting clustering during the process of leukocyte extravasation. This has been demonstrated on endothelial cells under pro-inflammatory cytokine conditions. Endothelial tetraspanins CD9, CD63 and CD151 have been shown to form essential interactions with their partner proteins, ICAM-1, P-selectin and VCAM-1, respectively (Barreiro et al., 2008; Doyle et al., 2011) (also see Section 1.1.3) (Figure

1.10). Doyle et al. (2011) were able to show that CD63 knockdown using siRNA and the knockout of CD63 in mice resulted in a reduction in P-selectin expression and subsequent loss of P-selectin specific recruitment of monocytes, thereby mimicking phenotypes observed in P-selectin knockout mice. Image analysis using scanning electron microscopy showed that CD63 co-localises with P-selectin on endothelial cells to form part of larger tetraspanin adhesion microdomains by mediating CD63 dependent clustering of P-selectin. Moreover, CD63 and P-selectin localised to intracellular organelles such as lysosomes and Weibel-Palade bodies and upon activation of the endothelium were rapidly trafficked to the cell surface to support leukocyte capture (Doyle et al., 2011). In addition to this study, another two endothelial tetraspanins, CD9 and CD151, have been shown to interact with the CAMs ICAM-1 and VCAM-1, respectively (Barreiro et al., 2008, 2005). Initial experiments showed how ICAM-1 and VCAM-1 were recruited into docking structures upon co-incubation of endothelial cells with leukocytes (Barreiro et al., 2005). The same authors also published that ICAM-1 and VCAM-1 associated with tetraspanins CD9 and CD151 in tetraspanin-enriched microdomains. Upon adhesion of leukocytes to cytokine-stimulated endothelial cells, CD9 and CD151 clustered ICAM-1 and VCAM-1 forming endothelial adhesive platforms and subsequently increasing the formation of microvilli that encapsulate the leukocyte and prime it for transmigration (Barreiro et al., 2008). In addition to this, leukocyte tetraspanins CD81 and CD9 are important in inducing adhesion strengthening by clustering leukocyte integrins VLA-4 and LFA-1, respectively (Feigelson et al., 2003; Reyes et al., 2015). The tetraspanin CD151 interacts with and regulates the avidity of laminin binding integrins $\alpha_3\beta_1$, $\alpha_6\beta_1$, and $\alpha_6\beta_4$ (Sterk et al., 2002). CD151 associates with the α-subunit of these integrins (Hemler, 2014) and its implicated roles include decreased diffusion of the α_6 subunit, thereby making the integrin stable for adhesive functioning (Yang et al., 2012) along with affecting distribution and recycling of α_3 and α_6 subunits during cell migration (Winterwood et al., 2006; Yang et al., 2008). The role of CD151 in regulating integrin

function has resulted in interest in the role of this tetraspanin in pathological angiogenesis and tumour cell growth, invasion and metastasis (Bailey et al., 2011; Hemler, 2014).

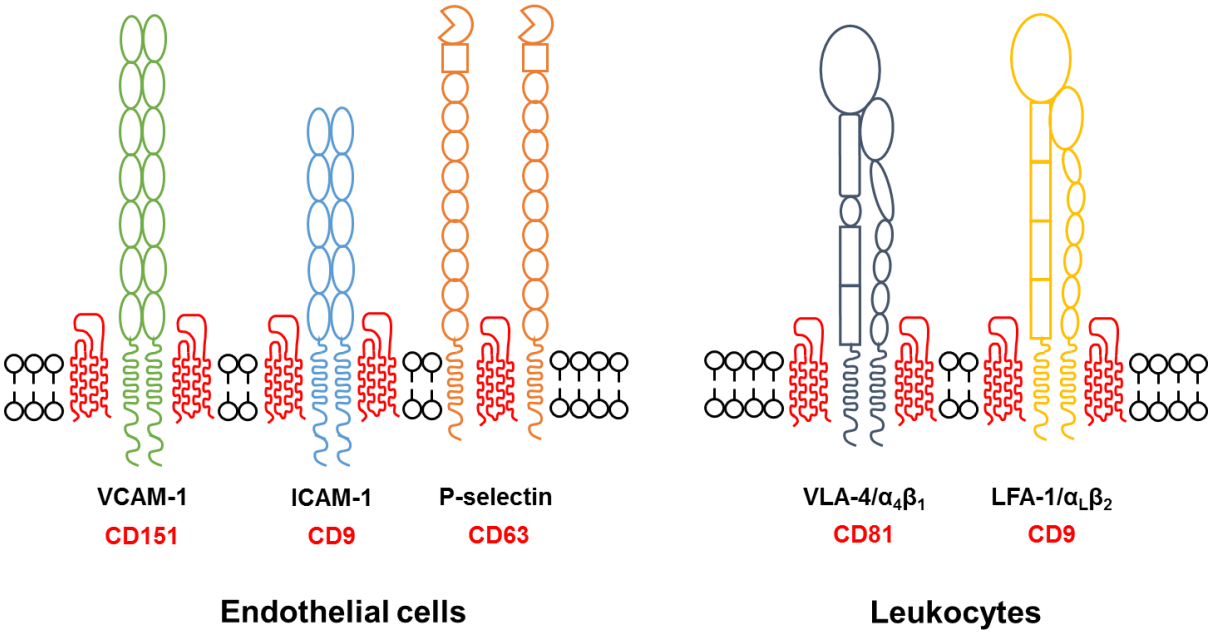

Figure 1.10 Tetraspanin-associated partner proteins on endothelial cells and leukocytes involved in leukocyte adhesion and transmigration. Endothelial tetraspanins CD151, CD9, and CD63 associate with the CAMs VCAM-1, ICAM-1 and P-selectin, respectively. In addition, leukocyte tetraspanins CD81 and CD9 associate with leukocyte integrins VLA-4 and LFA-1, respectively (Barreiro et al., 2008; Doyle et al., 2011; Feigelson et al., 2003; Reyes et al., 2015).

In addition to trafficking and clustering of partner proteins, tetraspanins also regulate efficient partner protein signalling. One of the most characterised examples of tetraspanin dependent partner protein signalling is the regulation of Frizzled 4 signalling in response to its ligand Norrin by the tetraspanin Tspan12 (Junge et al., 2009). Frizzled 4 belongs to the Wnt receptor family and it associates with its co-receptors Lrp5 and Lrp6. Binding of Norrin to Frizzled 4 stabilises β-catenin that exhibits transcriptional activity in the nucleus. Knockout of Tspan12 in mice phenocopied mice deficient in Frizzled 4, Lrp5 or Norrin exhibiting vascular abnormalities in the retina (Junge et al., 2009). In *in vitro* studies, overexpression of Tspan12 promoted Norrin-induced Frizzled 4 signalling and this

pathway was compromised when Tspan12 was knocked down. This interaction was specific to Tspan12 and Norrin/Frizzled 4 since when different tetraspanins were investigated or the introduction of Wnt (another Frizzled 4 ligand) was used, the signalling downstream of Frizzled 4 was unaffected, suggesting the Tspan12 interaction with Frizzled 4/Norrin is specific. Co-immunoprecipitation assays revealed that Tspan12 associated with Frizzled 4 and was required for clustering of Frizzled 4 (Junge et al., 2009). Furthermore, mutations of Tspan12 causes familial exudative vitreoretinopathy, an inherited blinding disorder characterised by abnormal retinal vascular system development (Nikopoulos et al., 2010; Poulter et al., 2010).

1.3.3 ADAM10 associates with the TspanC8 subgroup of tetraspanins

In addition to the functions highlighted above, tetraspanins have been also shown to associate with ADAM proteases. ADAM10 was initially described to be tetraspanin-associated under mild detergent lysis conditions with several tetraspanins including CD9, CD81 and CD82 (Arduise et al., 2008). This study showed incubation of Raji cells with mAb antibodies to the respective tetraspanins enhanced the shedding of ADAM10 substrates EGF and TNFα by altering ADAM10 localisation at the plasma membrane (Arduise et al., 2008). In addition to this study, ADAM10 was also shown to interact with Tspan12 which promoted ADAM10 maturation and subsequent shedding of APP (Xu et al., 2009). However, this was later confirmed not to be a direct tetraspanin-partner protein interaction through the use of more stringent lysis detergents (Dornier et al., 2012; Haining et al., 2012). ADAM10 was subsequently shown by the Tomlinson group and two other independent research groups to associate with six, largely understudied but related tetraspanins (Dornier et al., 2012; Haining et al., 2012; Prox et al., 2012b). These tetraspanins included Tspan5, 10, 14, 15, 17 and 33 which all belong to the TspanC8 subgroup of tetraspanins, as characterised by the presence of eight cysteine residues

within their large extracellular loop (Dornier et al., 2012; Haining et al., 2012; Prox et al., 2012b). The TspanC8s were shown to promote ADAM10 exit from the endoplasmic reticulum, enzymatic maturation (during which the inhibitory prodomain is removed), and trafficking to the cell surface (Dornier et al., 2012; Haining et al., 2012; Prox et al., 2012b) (Figure 1.11). Indeed, this mechanism of trafficking has been shown to hold true in human endothelial cells (Haining et al., 2012), mice (Haining et al., 2012) and *Drosophila* (Dornier et al., 2012) indicating that TspanC8s are fundamental to ADAM10 function. This interaction was characterised through the use of co-immunoprecipitation assays which revealed that the TspanC8s specifically immunoprecipitated with ADAM10 under stringent lysis conditions (Dornier et al., 2012; Haining et al., 2012; Prox et al., 2012b). Overexpression of the TspanC8s in various cell line-models promoted the maturation and trafficking of ADAM10 to the cell surface and the large extracellular loop of the TspanC8s was required for ADAM10 maturation (Dornier et al., 2012; Haining et al., 2012; Noy et al., 2016). In addition, knockdown of TspanC8s affected ADAM10 surface expression. Haining et al. showed that HUVECs express at least five of the TspanC8s at the mRNA level, and siRNA-mediated knockdown of the most highly expressed HUVEC TspanC8, Tspan14, lead to a 50% reduction in the surface expression of ADAM10 and decreased the shedding of the endothelial ADAM10 substrate VE-cadherin (Haining et al., 2012). In addition Tspan33 knockout erythrocytes showed reduced cell surface expression of ADAM10 (~90% compared to wild type erythrocytes) (Haining et al., 2012). Dornier et al. showed ADAM10 trafficking becomes compromised following deletion of TspanC8s in the HeLa cell line. Deletion of *Drosophila* orthologs of Tspan5, 10 and 14 resulted in an increase in the number of sensory organ precursor cells and a dramatic bristle loss phenotype as a result of impaired ADAM10 and Notch activity (Dornier et al., 2012).

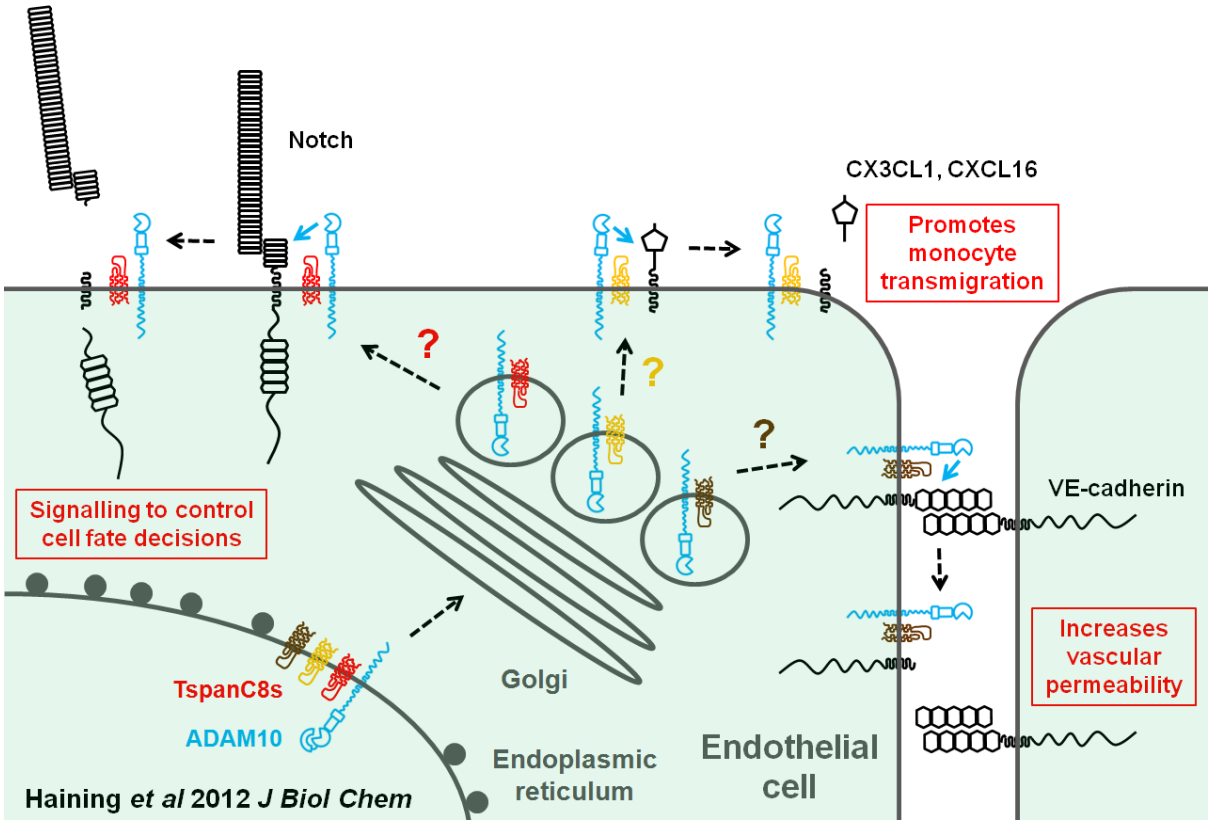

Figure 1.11 Tetraspanin regulation of ADAM10 trafficking to the cell surface. Schematic shows a proposed mechanism by which TspanC8s promote ADAM10s trafficking to the cell surface where ADAM10 can then interact with its various endothelial-specific substrates such as CX3CL1, CXCL16, VE-cadherin and Notch. The consequences of ADAM10-dependent shedding are shown in red boxes.

It could be regarded that ADAM10 exists as six distinct proteases depending on which TspanC8 tetraspanin it forms an interaction with and these individual TspanC8/ADAM10 complexes could differentially traffic ADAM10 to distinct substrates. Such evidence exists in cell line models whereby the shedding of key ADAM10 substrates has been assessed by co-transfecting the various TspanC8s with a particular ADAM10 substrate. These experiments showed that Tspan5 and Tspan14, but not Tspan15, promoted Notch cleavage (Dornier et al., 2012). In U20S-N1 cells (U20S stably expressing Notch 1) stably expressing Tspan15, a 60% decrease in OP9-DLL1 (OP9 cells stably expressing Delta-like ligand 1)-induced Notch activity was observed when compared to control cells.

Silencing of Tspan15 in U2OS-N1/Tspan15 cells restored Notch activity (Jouannet et al., 2016). Furthermore, Tspan15 suppressed ADAM10-mediated APP shedding in U2OS-N1 and PC3 cells (Jouannet et al., 2016) but promoted shedding of APP in HEK and N2A cells (Dornier et al., 2012). Moreover, the Tomlinson group have recently shown using a similar co-transfection model that Tspan15 promotes cleavage of N-cadherin, while Tspan14 protects shedding of the platelet collagen receptor GPVI in HEK293T cells (Noy et al., 2016). These distinct TspanC8/ADAM10 complexes have been shown to have distinct TspanC8 subcellular localisation patterns in cell lines (Dornier et al., 2012). For example, Tspan10 and Tspan17 were shown to re-localise ADAM10 into intracellular compartments that co-localised with the late endosome marker, CD63. In contrast, Tspan5, 14, 15 and 33 all promoted ADAM10 membrane localisation in a HeLa cell line model (Dornier et al., 2012). Tspan5 and Tspan15 were shown to localise ADAM10 differently, with Tspan5 being predominantly membrane localised and Tspan15 being more localised in the late endocytic compartment (Jouannet et al., 2016). The mapping of the binding regions of TspanC8s to ADAM10 has revealed distinct binding abilities of the TspanC8s to ADAM10. By using a chimeric approach, Noy et al. showed that a membrane-proximal region of ADAM10, encompassing the stalk, cysteine-rich and disintegrin domains, mediated its co-immunoprecipitation with Tspan14 (Noy et al., 2016). Truncated ADAM10 constructs revealed differential TspanC8 binding requirements: Tspan15 interacted with the ADAM10 stalk alone, all other TspanC8s required the stalk plus cysteine-rich region, and Tspan17 interaction was impaired by inclusion of the disintegrin domain (Noy et al., 2016). Since ADAM10 shedding of its substrates appears to be not defined by a specific amino acid motif, the data outlined by Noy et al. strongly suggests that ADAM10 may adopt distinct conformations in complex with different TspanC8s, which could impact on substrate selectivity and ADAM10 activity.

1.4 HYPOTHESIS & AIMS

Hypothesis:

ADAM10 on primary endothelial cells is essential for primary human leukocyte transmigration under flow conditions, due to its cleavage of VE-cadherin and/or the transmembrane chemokines CX3CL1 and CXCL16. Furthermore, one or more TspanC8 tetraspanins may regulate this function of ADAM10 by specifically affecting the cleavage of one of these substrates.

Aims:

1. To elucidate the effects of endothelial ADAM10 knockdown on the adhesion and transmigration of different leukocyte subsets *in vitro*.

An *in vitro* flow-based adhesion assay in combination with static adhesion assays were utilized in which endothelial ADAM10 was targeted using siRNA knockdown or inhibited using a pharmacological inhibitor prior to assessing the recruitment and transmigration of neutrophils, peripheral blood lymphocytes (PBLs) or monocytes.

2. To determine the mechanism by which endothelial ADAM10 exerts its effect by identifying the key substrate(s) involved.

HUVECs were screened for their expression of CX3CL1, CXCL16 and VE-cadherin using flow cytometry and Western blotting approaches under pro-inflammatory conditions. Manipulation of VE-cadherin surface levels in the presence of ADAM10 knockdown or inhibition were assessed to elucidate the function of VE-cadherin in PBL transmigration.

3. To investigate the role of specific endothelial TspanC8 tetraspanins that are required for ADAM10's role in PBL transmigration.

Lentiviral overexpression and siRNA knockdown of endothelial TspanC8s were used to deduce a function of TspanC8s in PBL transmigration.

CHAPTER 2

MATERIALS AND METHODS

2.1 LIST OF REAGENTS

2.1.1 General reagents

Cell culture reagents

Reagent	Details and source
Amphotericin B	Life Technologies Invitrogen Compounds (Paisley, UK)
Bovine brain extract	First Link (UK) Ltd. (Wolverhampton, UK)
Dimethyl sulfoxide (DMSO)	Sigma-Aldrich (Poole, Dorset, UK)
Dulbecco's Modified Eagles Medium (DMEM)	1000 mg/L glucose, Sigma-Aldrich (Poole, Dorset, UK)
Epidermal growth factor (EGF)	Sigma-Aldrich (Poole, Dorset, UK)
Ethylene diamine tetraacetic acid (EDTA)	0.02%, Sigma-Aldrich (Poole, Dorset, UK)
Fetal bovine serum (FBS)	Gibco (Paisley, UK)
Heparin	Sigma-Aldrich (Poole, Dorset, UK)
Hydrocortisone	Sigma-Aldrich (Poole, Dorset, UK)
L-Glutamine	200mM, Gibco (Paisley, UK)
M119 medium	Earls salts, Sigma-Aldrich (Poole, Dorset, UK)
Penicillin/Streptomycin	Sigma-Aldrich (Poole, Dorset, UK)
Phosphate Buffer Saline (PBS)	1X PBS with calcium and magnesium, Sigma-Aldrich (Poole, Dorset, UK) 1X PBS without calcium and magnesium, Sigma-Aldrich (Poole, Dorset, UK)
Trypsin-EDTA solution	Diluted from 10X to 2X in PBS, Sigma-Aldrich (Poole, Dorset, UK)

Human leukocyte isolation reagents

Reagent	Details and source
Bovine serum albumin (BSA)	7.5% V, Gibco (Paisley, UK)
Histopaque-1077	Sigma-Aldrich (Poole, Dorset, UK)

Histopaque-1119	Sigma-Aldrich (Poole, Dorset, UK)

Cytokines and inhibitors

Reagent	Details and source
GI254023X	Cat No.: SML0789, Sigma-Aldrich (Poole, Dorset, UK)
N-[N-(3,5-difluorophenacetyl)-L-alanyl]-S-phenylglycine t-butyl ester (DAPT)	Cat No.: D5942, Sigma-Aldrich (Poole, Dorset, UK)
Recombinant human Interferon-γ (IFNγ)	Cat No.: 300-02, Preprotech (London, UK)
Recombinant human Interleukin-1-β (IL-1β)	Cat No.: SRP3083, Sigma-Aldrich (Poole, Dorset, UK)
Recombinant human Tumour necrosis factor-α (TNFα)	Cat No.: 210-TA, R&D systems (Abingdon, Cambridge, UK)

Commonly used buffers

Antigen	Details
2X SDS non-reducing sample buffer	20 ml 1 M Tris, pH 6.8 80 ml 10% SDS 40 ml Glycerol 60 ml dH_2O 5 mg Bromophenol blue
Antibody incubation buffer	15 g BSA 0.6 g NaN_3 500 ml TBST
Blocking solution	1 g Marvel 10 ml TBST
FACS buffer	10 g BSA 1ml NaN_3 500 ml PBS
SDS polyacrylamide resolving buffer	30.3 g Tris 2 g SDS pH 8.8 500 ml dH_2O
SDS polyacrylamide stacking buffer	30.3 g Tris 2 g SDS pH 6.8 500 ml dH_2O
SDS-Page running buffer	15 g Tris 72 g Glycine 50 mL 10% SDS 5 L dH_2O

TBS	20 mM Tris 137 mM NaCl pH 7.6 2 L dH_2O
TBST	20 mM Tris 137 mM NaCl 5 ml Tween pH 7.6 5 L dH_2O
TBST high salt wash buffer	500 mM NaCl 2 L TBST
Triton X-100 lysis buffer	250 ml 2% Triton X-100 1 M Tris, pH 7.5 5 M NaCl 0.5 M EDTA, pH 8.0 0.05 g NaN_3 250 ml dH_2O
Western blot stripping buffer	1 M Tris, pH 7.6 50 ml 10% SDS 500 ml dH_2O
Western transfer buffer	15 g Tris 72 g Glycine 1 L Methanol 5 L dH_2O

Other reagents

Reagent	Details and source
Acrylamide	30%, Geneflow (Lichfield, UK)
Ammonium persulfate (APS)	10%, Sigma-Aldrich (Poole, Dorset, UK)
Bromophenol Blue	Bio-Rad (Hemel Hempstead, Hertfordshire, UK)
Collagenase	Type Ia, Stock kept at: 10 mg/ml, Sigma-Aldrich (Poole, Dorset, UK)
Ethanol	70%, Fisher Scientific (Loughborough, Leicestershire, UK)
Ethylenediaminetetraacetic acid (EDTA)	0.02%, Sigma-Aldrich (Poole, Dorset, UK)
Gelatine	0.1% in PBS
Glycerol	Fisher Scientific (Loughborough, Leicestershire, UK)
Glycine	Sigma-Aldrich (Poole, Dorset, UK)
Lipofectamine RNAiMAX	Life Technologies Invitrogen Compounds (Paisley, UK)
Marvel	Premiere Foods (St Albans, Hertfordshire, UK)

Methanol	Fisher Scientific (Loughborough, Leicestershire, UK)
N,N,N',N'-Tetramethylethylenediamine (TEMED)	Sigma-Aldrich (Poole, Dorset, UK)
OptiMEM	Gibco (Paisley, UK)
Paraformaldehyde	36.5%, Sigma-Aldrich (Poole, Dorset, UK)
Polybrene	Sigma Aldrich (Poole, Dorset, UK)
Polyethylenimine	Sigma-Aldrich (Poole, Dorset, UK)
Polyvinylidene fluoride (PVDF) membrane	Immobilon-FL, Merck Millipore (Watford, Hertfordshire, UK)
Protease inhibitor cocktail	Sigma-Aldrich (Poole, Dorset, UK)
Protein marker	BLUEye™, Geneflow (Lichfield, UK)
Puromycin	Sigma-Aldrich (Poole, Dorset, UK)
Sodium azide (NaN_3)	Sigma-Aldrich (Poole, Dorset, UK)
Sodium chloride (NaCl)	150 mM, Sigma-Aldrich (Poole, Dorset, UK)
Sodium dodecyl sulphate (SDS)	Fisher Scientific (Loughborough, Leicestershire, UK)
Tris	Fisher Scientific (Loughborough, Leicestershire, UK)
Triton X-100 lysis buffer	1%, Sigma-Aldrich (Poole, Dorset, UK)
Whatman filter paper	3MM, GE Healthcare (Amersham, Buckinghamshire, UK)
β-mercaptoethanol	Sigma-Aldrich (Poole, Dorset, UK)

2.1.2 List of antibodies

Primary antibodies

Antigen	Details and source
ADAM10	Purified monoclonal mouse anti-human ADAM10 FITC, R&D Systems (Abingdon, UK), working concentration: 10 µg/ml (flow cytometry)
CD3	Purified monoclonal mouse anti-human CD3 PerCPCy$^{5.5}$, clone OKT3, eBiosciences (Hatfield, UK), working concentration: 2 µg/ml (flow cytometry)
CD4	Purified monoclonal mouse anti-human CD4 APCCy7, clone OKT3, eBiosciences (Hatfield, UK), working concentration: 2 µg/ml (flow cytometry)
CD8	Purified monoclonal mouse anti-human CD8 PB, clone SK1, eBiosciences (Hatfield, UK), working concentration: 2 µg/ml (flow cytometry)
CD14	Purified monoclonal mouse anti-human CD14 APC, clone OKT3, eBiosciences (Hatfield, UK), working concentration: 2 µg/ml (flow cytometry)
CD19	Purified monoclonal mouse anti-human CD19 PECy7, clone OKT3, eBiosciences (Hatfield, UK), working concentration: 2 µg/ml (flow

	cytometry)
CD56	Purified monoclonal mouse anti-human CD56 PE, clone CMSSB, eBiosciences (Hatfield, UK), working concentration: 2 µg/ml (flow cytometry)
CX3CL1	Purified monoclonal mouse anti-human CX3CL1/Fractalkine FITC, R&D Systems (Abingdon, UK), working concentration: 2 µg/ml (flow cytometry)
CX3CR1	Purified monoclonal mouse anti-human CX3CR1 FITC, R&D Systems (Abingdon, UK), working concentration: 2 µg/ml (flow cytometry)
CXCL16	Purified monoclonal mouse anti-human CXCL16 APC, R&D Systems (Abingdon, UK), working concentration: 2 µg/ml (flow cytometry)
CXCR6	Purified monoclonal mouse anti-CXCR6 APC, R&D Systems (Abingdon, UK), working concentration: 2 µg/ml (flow cytometry)
FLAG	Purified monoclonal anti-human FLAG M2, clone M2, Sigma-Aldrich (Poole, Dorset, UK), working concentration: 1 µg/ml (Western blotting)
Human BD Fc Block™	Purified recombinant Fc protein, BD Biosciences (Oxford, UK), working concentration: 2.5 µg/ml (flow cytometry)
Rabbit IgG	Purified polyclonal rabbit anti-human Rabbit IgG, Cell Signalling Technology (Danvers, USA), working concentration: 1 µg/ml (Western blotting)
VE-cadherin	Purified monoclonal mouse anti-human VE-cadherin (F-8), Santa Cruz Biotechnology Inc. (Santa Cruz, USA), working concentration: 1 µg/ml (Western blotting) Purified monoclonal mouse anti-human VE-cadherin APC, clone 16B1, eBiosciences (Hatfield, UK), working concentration: 2 µg/ml (flow cytometry)
α-Tubulin	Purified monoclonal mouse anti-human α-Tubulin, clone DM1A, Sigma-Aldrich (Poole, Dorset, UK), working concentration: 1 µg/ml (Western blotting)

Isotype control antibodies

Isotype	Details and source
Mouse IgG_1	FITC-conjugated, clone 51637, R&D Systems (Abingdon, UK)
Mouse IgG_{2B}	APC-conjugated, clone 123413, R&D Systems (Abingdon, UK)
Mouse IgG_{2B}	FITC-conjugated, clone 163003, R&D Systems (Abingdon, UK)
Rat IgG_{2A}	APC-conjugated, clone 256213, R&D Systems (Abingdon, UK)

Secondary antibodies

Antigen	Details and source
Mouse IgG	Goat anti-Mouse IRDye 680RD, LI-COR (Cambridge, UK) Goat anti-Mouse IRDye 800CW, LI-COR (Cambridge, UK)
Rabbit IgG	Goat anti-Rabbit IRDye 800CW, LI-COR (Cambridge, UK)

2.2 CELL CULTURE

All cells were kept in a humidified incubator at 37°C, 5% CO_2.

2.2.1 Cell lines

2.2.1.1 Culture of HEK292T cells

The HEK293T human embryonic kidney cell line was obtained from laboratory stocks and cultured in DMEM media with added supplements: 10% heat inactivated FBS, 4 mM glutamine, 100 U/ml penicillin and 100 µg/ml streptomycin.

2.2.2 Isolation and culture of primary human umbilical vein endothelial cells (HUVECs)

2.2.2.1 Isolation of HUVECs

Human umbilical cords were obtained from the Human Biomaterials Resource Centre (University of Birmingham) (09/H1010/75) which holds ethical approval and collection of fully consented tissue from the Birmingham Women's Hospital NHS Trust. HUVECs were isolated using the collagenase digestion method (Cooke et al., 1993). Briefly, umbilical cords were placed on a tray and sprayed down with 70% ethanol in a tissue culture hood. The vein was identified and cannulated at both ends of the umbilical cord using cable ties. Venous blood was removed from the cord by perfusion of PBS. Residual PBS was then removed by passing air through the cord using an empty syringe. For the digestion of the endothelial cells from the venular wall, collagenase type Ia was diluted to a working concentration of 1 mg/ml in PBS before being passed through the vein. Once both

cannulae were filled with collagenase, the cannulae were clamped at both ends and cord was placed into an incubator for 15 minutes at 37°C and 5% CO_2. The cord was then massaged gently for a minute prior to the contents of the vein being flushed out using PBS into a 50 ml centrifuge tube (Corning, UK). Residual PBS in the cord was removed by passing air through the cord and collected into the same 50 ml centrifuge tube. The 50 mL centrifuge tube was centrifuged at 400g for 5 minutes at room temperature. Following centrifugation, the supernatant was removed and the pellet was resuspended in 1 ml of complete HUVEC growth medium or complete HUVEC medium, depending on what the cells were going to be used for (see Section 2.2.2.2 for media recipes) post cell count.

2.2.2.2 Culture of isolated cells

Depending on the nature of use, HUVECs were cultured under two different conditions. For subculture, HUVECs were cultured in M199 media with added supplements (referred to as complete HUVEC growth medium): 10% heat inactivated FBS, 4 mM glutamine, 0.3% bovine brain extract (provided by Dr Victoria Heath), 90 µg/ml heparin and 100 U/ml penicillin and 100 µg/ml streptomycin. These HUVECs were used up to passage six and grown in 10cm dishes that had previously been treated with 0.1% gelatine. For adhesion assays, passage zero/one HUVECs were used in M199 media with added supplements (referred to as complete HUVEC medium): 20% heat inactivated FBS, 4 mM glutamine, 100U/ml penicillin and 100 µg/ml streptomycin, 10 ng/ml epidermal growth factor, 1 µg/ml hydrocortisone and 2.5 µg/ml amphotericin B. Under both culture conditions, the media was changed every two days. Once confluent, endothelial cells exhibit a cobblestone-like morphology (Figure 2.4).

2.2.3 Determination of cell number

Cell number was determined using an automated cell counter. Briefly, media from cell dishes/flasks was removed and 2 ml trypsin/EDTA was added. For HUVECs, the cell monolayer was washed once with pre-warmed PBS prior to adding trypsin/EDTA. The cells were placed into an incubator at 37°C and 5% CO_2 for 2 minutes. The cells were then viewed under a microscope until the cells became round in shape. The dish/flask was tapped gently to detach the cells and the trypsin was inactivated by adding 8 ml culture medium (dependent on cell type; complete HUVEC medium/complete HUVEC growth medium for HUVEC or DMEM for HEK293T cells) to the culture dish/flask and the cell suspension was transferred into a 15 ml centrifuge tube (Corning, UK). The cell suspension was centrifuged at 400g for 5 minutes at room temperature. Following centrifugation, the supernatant was aspirated and the pellet was resuspended in 1 ml of the respective medium. To determine cell count, the cell suspension was diluted 1:20 by transferring 20 µl of the cell suspension into an Eppendorf containing 380 µl of media. 20 µl of this solution was then transferred into a Cell-o-meter™ cell counting slide and counted using the digital cell counting software (Nexecelom Bioscience, Lawrence, MA, USA). The original cell suspension was then adjusted accordingly based on the cell count.

2.2.4 Cell transfection protocols

2.2.4.1 Transfection of HEK293T using PEI

HEK293T cells were transiently transfected using polyethylenimine (PEI) (Ehrhardt et al., 2006 & Haining et al., 2012). Briefly, HEK293T cells were plated out into 6-well plates at a cell density to reach 60% - 80% confluency 24 hours before transfection in complete DMEM medium. 100 µl Opti-MEM serum-free media was incubated with 1 µg DNA with 4

µl PEI (1 mg/ml stock) for 10 minutes at room temperature to allow DNA/PEI complexes to form. The DNA/PEI mix was then added directly to the HEK293T cells in culture media and cells were used 48 hours after transfection for flow cytometry.

Specific plasmids transiently transfected into HEK293T cells include a pcDNA3.1 mock vector (Invitrogen) or a pcDNA3.1 vector containing either human CX3CL1 or CXCL16 fused with 2Z tags (a kind gift from Andreas Ludwig, Aachen, Germany) which were used to assess expression of these chemokines in HEK293T cells.

2.2.4.2 Transfection of HUVECs with siRNA

HUVECs were transiently transfected using Lipofectamine RNAiMAX (Life Technologies Invitrogen Compounds) and at least two individual siRNA duplexes to ADAM10, VE-cadherin, Tspan5, Tspan10, Tspan14, Tspan15, Tspan17 and Tspan33 (Life Technologies Ambion Compounds) to knockdown proteins of interest during various endothelial functional assays, as previously described (Haining et al., 2012). Briefly, HUVECs were plated out at a cell density to reach 60% - 80% confluency 24 hours before transfection in either complete HUVEC growth medium or in complete HUVEC medium, depending on the nature of the functional assay the HUVEC were going to be used for (see Section 2.2.2.2). A duplex mix, containing siRNA duplex(s) and Opti-MEM serum free media were prepared. For the introduction of individual siRNA duplexes, a final siRNA concentration of 10 nM was used. When assessing combinational knockdowns, a final siRNA total of 30 nM or 25 nM was used. Separately, a Lipofectamine mix containing just Lipofectamine RNAiMAX and Opti-MEM was prepared. The two mixes were kept at room temperature for 5 minutes before being combined and left at room temperature for a further 10 minutes. The HUVECs were prepared by washing twice with PBS, and the respective duplex/Lipofectamine mixes were added to the cells. In addition, further Opti-MEM was added to dilute the duplex/Lipofectamine mix 5-fold. The HUVECs

were incubated for 4 hours at 37°C and 5% CO_2 after which the media was changed to complete HUVEC media without antibiotics or complete HUVEC growth media without antibiotics and the HUVECs were then used for functional assays at the 48-hour time point post siRNA transfection. Typical cell counts and volumes of reagents are listed below (Kaur et al., 2011).

Plate size	Cells plated	siRNA mix		Lipofectamine mix		Final volume
		siRNA (50 µM)	Opti-MEM	RNAiMAX	Optimem	
12 well	8.75 x 10^4	1.25 µl	83.75 µl	1.5 µl	13.5 µl	500 µl
6 well	1.75 x 10^5	2.5 µl	167.5 µl	3 µl	27 µl	1 ml
6 cm	3.6 x 10^5	3.6 µl	241.4 µl	4.3 µl	38.7 µl	2 ml

Table 2.1 Reagents and quantities required for siRNA transfection of HUVECs.

2.2.4.3 Lentiviral transduction of HUVECs

In order to transduce HUVECS to stably express specific proteins of interest, HEK293T cells were used as surrogate cells to produce lentivirus that could then be used to infect HUVECs. Briefly, 5x10^5 HEK293T cells were plated onto six well plates in complete DMEM media. Following 24 hours, a PEI transfection was performed as described in Section 2.2.4.1. In addition, the amount of DNA introduced was reduced since three different vectors were being introduced into the cells: 0.54 µg transfer vector (plasmid containing gene of interest), 0.33 µg packaging vector (PSPAX2) and 0.13 µg envelope vector (PMD2G) per well of the six well plate. For the gene of interest plasmids, mouse TspanC8 tetraspanins with N-terminal FLAG tags were expressed using the pLVX vector, which contains an IRES-driven puromycin resistance cassette (Clontech, Mountain View, CA, USA) (prepared by Dr Jing Yang). The HEK293T cells were incubated at 37°C and CO_2 for 48 hours and the resulting viral media was used to infect HUVECs.

To transduce HUVECs, the HUVECs were initially plated into 0.1% gelatine coated six well plate at a cell density of 1.75x10^5 cells per well in complete HUVEC growth medium.

Following 24 hours, virus containing media was collected from the HEK293T cells and centrifuged for 5 minutes at 195 g to remove cell debris. The viral media was supplemented with 8 µg/ml polybrene, 90 µg/ml heparin and 0.3% bovine brain extract before being passed through a 0.45 µm pore filter (Corning). The media on the HUVECs was aspirated and replaced with the supplemented virus-containing media and the HUVECs were incubated for a further 72 hours at 37°C and 5% CO_2. Following 72 hours, the virus containing media on the HUVECs was aspirated and replaced with complete HUVEC growth medium with 0.5 µg/ml puromycin. The HUVECs were cultured for a further 48 hours or until the mock transfected HUVECs had all died, as confirmed by checking the HUVECs using a microscope. Stably transduced HUVECs were then cultured in complete HUVEC growth media and used in various endothelial function assays.

2.2.5 Measuring trans-endothelial electrical resistance of HUVEC monolayers

The electrical resistance across a monolayer of HUVEC either treated with the ADAM10 inhibitor (GI254023X) or following endothelial ADAM10 knockdown was assessed using the Minicell-ERS resistance according to the manufacturer's instructions (Merck Millipore, USA). HUVECs were plated in complete HUVEC growth medium into 0.1% gelatine-coated 0.4 µm polyester membrane transwell-clear filters (Corning, Flintshire, Cheshire, UK) at a cell density of $4x10^4$ cells/300 µl, a concentration of cells that has previously been shown to form a complete monolayer within 24 hours of seeding (McGettrick et al., 2009). Following 24 hours, the HUVEC media in the filters was changed and replaced with complete HUVEC growth medium either containing 0.02% DMSO or 20 µM GI254023X and resistance readings were taken at 0, 4, 12, 24 and 48 hours after inhibitor treatment. For assessing the effects of ADAM10 knockdown on the trans-endothelial

electrical resistance of HUVECs, HUVECs were cultured as above and transfected separately with two siRNA duplexes to ADAM10 as explained in Section 2.2.4.2. 4 hours after transfection the HUVECs were cultured in complete HUVEC growth medium without antibiotics and resistance readings were taken sequentially at 0, 4, 12, 24 and 48 hours. The 0 hour time point corresponded to 4 hours after endothelial ADAM10 knockdown.

When making the resistance readings, the electrodes were initially calibrated by immersing them in fresh complete HUVEC growth media for 15 minutes and manually adjusting the basal resistance reading to zero. The filters were sequentially placed into the electrode chamber that contained 700 µl complete HUVEC growth medium and the top electrode was placed into the filter so that it was centrally located to ensure maximal reproducibility. The electrical resistance across the HUVEC monolayer was measured and recorded. Between resistance readings, the electrodes were washed in fresh HUVEC growth medium. To calculate the electrical resistance across the complete HUVEC monolayer, the resistance of a blank filter was subtracted from the resistance of a sample filter. This value was then multiplied by the area of the filter, to calculate the resistance in Ωcm^2.

2.2.6 Analysis of cell surface molecules by flow cytometry

For characterisation of surface expression of adhesion molecules and specific ADAM10 substrates on HUVECs or isolated PBLs a cytometric assay was used as described before (Haining et al., 2012). Untreated HUVECs or HUVECs stimulated with different inflammatory cytokines were analysed. HUVECs cultured in 24 well plates were initially washed once with PBS. The cells were then treated with accutase to dissociate adherent cells. The action of accutase was counteracted using an equal volume of HUVEC growth media followed by centrifugation for 5 minutes at 300g at room temperature. The cells were then incubated with primary conjugated antibodies (ADAM10, VE-cadherin,

CX3CL1, CXCL16, and VCAM-1) along with appropriate control antibodies (detailed information about antibodies used are listed in Section 2.1.2). Incubation was performed for 30 minutes on ice in the dark. Subsequently, stained cells were washed twice with FACS buffer by centrifugation for 5 minutes at 300g. As such, the stained cells were diluted in 500 µl FACS buffer before being processed by the flow cytometer. Live cell populations were gated on by adding 1 µl propidium iodide (10 µg/ml) to each sample prior to running it through the flow cytometer. Propidium iodide is a membrane impermeable dye that is only taken up by dead cells, so can be used to distinguish live and dead cell populations (Haining et al., 2012).

For staining of distinct PBL/PBMC subsets for their parental markers and chemokine receptors, $2x10^6$ cells/ml were divided into FACS tubes and centrifuged at 300g for 5 minutes at room temperature prior to being incubated with 5 µg/ml BD Fc Block™ in FACS buffer (see Section 2.1.2) for 30 minutes on ice to block unspecific binding. After the blocking step, 16 µl of primary antibody cocktail in FACS buffer was added. The cocktail of antibodies contained 2 µl of the following PBMC markers: CD3, CD4, CD8, CD56, CD14, CD19 along with either CXCR6 or CX3CR1. PBL/PBMC were also stained for the appropriate control antibodies (detailed information about antibodies used in this study including concentrations are listed in Section 2.1.2). Incubation was performed for 30 minutes on ice in the dark. Subsequently, stained cells were washed twice with FACS buffer by centrifugation for 5 minutes at 300g and the stained cells were diluted in 500 µl FACS buffer before being processed by the flow cytometer. Samples were originally gated on size and granularity before being gated to show the individual PBL populations. Manual compensation was carried out in every experiment to ensure that there was no bleeding of the fluorophores (Figure 2.1).

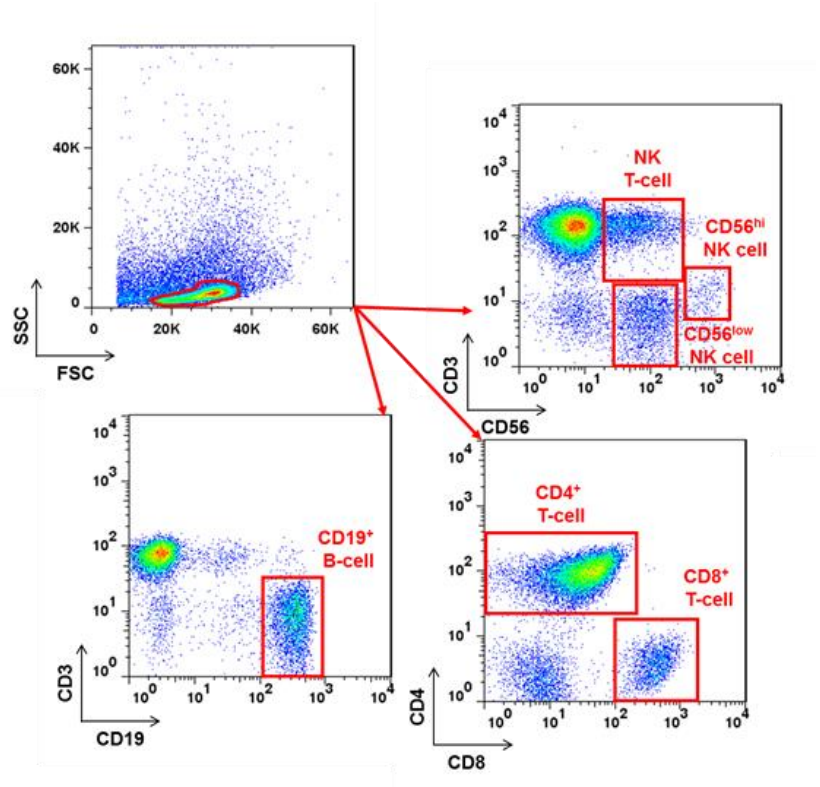

Figure 2.1 Gating strategy for PBL subsets using flow cytometry. A total of 1x10^6 cells were originally gated on size and granularity prior to being gated for specific lymphocyte populations.

Samples were acquired on a Beckman CyAn^{TN} ADP flow cytometer (Beckman Coulter (UK) Ltd., High Wycombe, UK) using Summit acquisition software (Beckman Coulter) and analysed using FlowJo software (Tree Star Inc. Ashland, OR, USA). Flow cytometry data were presented as the percentage surface expression calculated by subtracting isotype control mean fluorescence intensity (MFI) values from the positively stained MFI values. Control cells (DMSO control treated or No siRNA treated) MFI values were normalised to 100% and respective treated cells were expressed relative to this value as a percentage.

2.3 *IN VITRO* ADHESION ASSAYS

Two well characterised *in vitro* models of leukocyte adhesion were utilised in this study; flow-based adhesion assays and static adhesion assays (Munir et al., 2015; Butler et al., 2009)

2.3.1 Cell seeding

For flow-based adhesion assays, HUVECs were seeded in Ibidi µ-slides $VI^{0.4}$ (Ibidi, Maastricht, Germany). Briefly, HUVECs were trypsinised from a confluent 10 cm dish (~$3x10^6$ cells) as explained in Section 2.2.3. The HUVECs were resuspended in 760 µl complete HUVEC media (1x10 cm dish seeded four 6-channel Ibidi microslides (~$1.25x10^5$ cells/channel)). 30 µl of the cell suspension was added to each of the channels (this volume of media had previously been shown to adequately cover the growth area of the channel through capillary action (Munir et al., 2015)). The Ibidi microslide was incubated at 37°C and 5% CO_2 for an hour. After this, 140 µl of fresh pre-warmed complete HUVEC media was added to each of the channels and subsequently aspirated. This was repeated for an additional two times to remove any non-adherent HUVECs. Finally, 140 µl of complete HUVEC medium was added to each of the channels and the Ibidi microslide was cultured for a further 24 hours at 37°C and 5% CO_2. Any remaining cell suspension was resuspended in 10 ml fresh pre-warmed complete HUVEC growth medium and sub-cultured in a 0.1% gelatine coated 10 cm dish at 37°C and 5% CO_2.

For static adhesion assays, HUVECs from a confluent 10cm dish were trypsinised as explained in Section 2.2.3. The HUVECs were resuspended in 1 ml complete HUVEC medium and adjusted to a working concentration of $1.75x10^5$ cells/ml. 1 ml of the cell suspension was added to each well of a 0.1% gelatine coated 12-well plate. In addition, 1

ml of complete HUVEC medium was added to each well and the HUVECs were cultured for 24 hours at 37°C and 5% CO_2.

2.3.2 Cytokine stimulation of endothelial cells

To asses leukocyte recruitment and transmigration to primary HUVECs *in vitro*, a range of different cytokines were used that have previously been shown to support the recruitment and subsequent transmigration of specific leukocyte subsets by upregulating various cellular adhesion molecules (CAMs) and chemokines (Munir et al., 2015; Ahmed et al., 2011; Rainger et al., 2001). For stimulation of HUVECs with tumour necrosis factor-α (TNFα), a stock vial of previously frozen TNFα ($1x10^5$ U/ml) was thawed and diluted 1:1000 in complete HUVEC medium to a final concentration of 100 U/ml (equivalent to ~10 ng/ml). The resuspended TNFα was added to the Ibidi microslide channels or 12-well plates and treated cells were incubated at 37°C and 5% CO_2 for 4 hours prior to the flow adhesion assay. TNFα was also used in combination with interferon-γ (IFNγ). For stimulation of HUVECs with TNFα/IFNγ, a stock vial of previously frozen IFNγ (10 µg/ml) was thawed and diluted 1:1000 in complete HUVEC medium to a final concentration of 10 ng/ml. This was added to complete HUVEC medium containing previously diluted TNFα at 100 U/ml, as explained above. The TNFα/IFNγ media was then added to HUVECs grown in Ibidi microslide channels or to HUVECs grown in 12-well plates and treated cells were incubated at 37°C and 5% CO_2 for 24 hours prior to the adhesion assay. A final cytokine that was used was interleukin-1β (IL-1β). This was prepared by thawing a 500 ng/ml stock IL-1β and diluting 1:100 in complete HUVEC media to a final concentration of 5 ng/ml (~2.5 nM). The HUVECs in the Ibidi microslide channels were treated with IL-1β at 37°C and 5% CO_2 for 4 hours prior to the adhesion assay.

2.3.3 Isolation of leukocyte subsets

Primary human neutrophils, PBLs or monocytes were isolated from venous blood using a two-step density gradient method (Rainger et al., 2001) (Figure 2.2). Blood samples were obtained from healthy donors with written informed consent that had previously been approved from the University of Birmingham Local Ethical Review Committee (ERN_07-058). Venous blood was drawn from donors and aliquoted directly into EDTA tubes (Sarstedt, Nümbrecht, Germany), and gently inverted. 2.5 ml of Histopaque 1077 was layered onto 2.5 ml Histopaque 1119 followed by layering of 5 ml whole blood in a 10 ml round bottomed tube (Appleton Woods Ltd., Birmingham, UK). The tube was centrifuged at 800g for 30 minutes to isolate peripheral blood mononuclear cells (PBMCs) or for 40 minutes to isolate neutrophils at room temperature. PBMCs were harvested by taking the upper band at the interface of human plasma and Histopaque 1077. Neutrophils were harvested by taking the lower band at the interface of Histopaque 1077 and Histopaque 1119 (above the erythrocyte layer) (Figure 2.2). Harvested cells were transferred into 15 ml centrifuge tubes and made up to 10 ml with PBSA. PBSA was prepared by diluting a 7.5% BSA solution 1:50 in 50 ml PBS to a final concentration of 0.15% (w/v; PBSA). The tubes were centrifuged at 400g for 5 minutes at room temperature. The supernatant was aspirated and the pellet was resuspended in 10 ml PBSA and further centrifuged at 400g for 5 minutes. The pellet was resuspended and cell number was counted as explained in Section 2.2.3. For isolating a PBL purified population, PBMCs were panned on culture plastic for 30 minutes at 37°C to remove monocytes. The PBL were washed again using PBSA and centrifuged at 400g for 5 minutes. Following centrifugation, the pellet was resuspended and the cell number was counted as explained in Section 2.2.3. The isolated leukocytes were adjusted to a final concentration of $1x10^6$ cells/ml in PBSA for flow adhesion assays or in M199+BSA for static adhesion assays (M199+BSA was made similarly to how PBSA by swapping PBS with M199). The cells were maintained at room temperature prior to the adhesion assays.

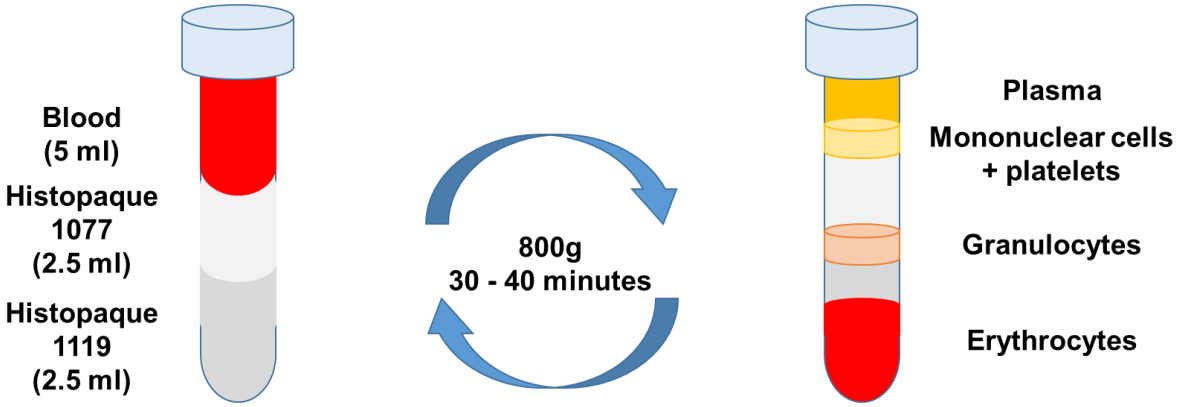

Figure 2.2 Two-step density centrifugation of whole blood to isolate peripheral blood lymphocytes (PBLs), monocytes or neutrophils. Blood (5ml) was layered onto 2.5 ml Histopaque 1077 and 2.5 ml Histopaque 1119. The tube was centrifuged for either 30 minutes to isolate PBLs or monocytes or for 40 minutes to isolate neutrophils at 800g at room temperature. After centrifugation, the specific leukocyte layers were collected and purified (Rainger et al., 2001).

Monocyte isolation for static adhesion assays was carried out slightly differently compared to the isolation of neutrophils or PBLs. Briefly, monocytes were isolated by taking the PBMC layer following centrifugation of whole blood, as explained above. The PBMC fraction was centrifuged twice in room temperature MACS buffer (28.2 ml calcium-free PBS, 8.8 ml 0.2% EDTA and 3.3 ml 7.5% BSA) at 800g for 5 minutes. The PBMCs were then counted, as explained in Section 2.2.3, before undergoing positive selection through the use of MACS columns (Miltenyi Biotec Ltd, Woking, Surrey, UK). The MS column was prepared by initially rinsing the column with ice-cold MACS buffer. The eluate was discarded. Next 500 µl of the washed PBMC fraction was put through the column. The column was then washed three times with 500 µl ice-cold MACS buffer to remove any non-adherent peripheral blood leukocytes. The column was then flushed using 1 ml ice-cold MACS buffer and the plunger and the cells were collected. The monocytes were centrifuged at 800g for 5 minutes at 4°C and subsequently counted, as explained in Section 2.2.3. The final concentration was then adjusted to $1x10^5$ monocytes per ml of M199+BSA and used in the static adhesion assays, similarly to PBLs.

2.3.4 Flow adhesion assays

Flow adhesion assays were set up as shown in Figure 2.3. Prior to the adhesion assay, the heater was turned on and set to 37°C. A 20 ml syringe without its plunger and a 5 ml syringe were attached to a 3-way tap and secured in place within the perspex chamber using micropore tape. Silicon tubing (~2-4 mm thickness) (referred to as thick tubing) was cut to the right distance between the electronic value and the 3 way tap. Roughly 8-10mm silicon tubing (~1-3 mm thickness) (referred to as thin tubing) was cut and inserted to one end of the thick tubing. The thick tubing was attached to the side of the 3 way tap and the other side of the thick tubing (containing the short piece of thin tubing) was connected to the electronic 3-way microvalve corresponding to the 'wash buffer reserviour' connection. A 6-8 mm piece of thick and thin tubing was cut. The thin tubing was inserted into one end of the thick tubing before the thick tubing was inserted onto the end of a 2 ml syringe containing no plunger. The 2 ml syringe was then connected onto a port on the electronic microvalve corresponding to the 'perfused cell reserviour'. Further thin tubing was cut to measure the distance between the electronic valve and the middle of the stage of the microscope. In addtion, a short piece (~8-10 mm) of thick tubing was cut and attached to one end of the thin tubing. An L-shaped connector was placed on the end of the thick tubing and used to connect to the Ibidi microslide channel. The tubing was primed by inititally filling up the wash buffer reserviour with PBSA and flowing through this buffer to remove any air bubbles. On the other end of the flow adhesion assay setup, Manometer tubing (~29 mm) was attached to a 50 ml glass syringe. The glass syringe was primed using PBSA. To the end of the Manometer tubing (Smiths Medical, Ashford, Kent, UK) that was not connected to the glass syringe, a small piece of thick tubing (~10-12 mm) was attached to securely connect an L-shapped connector. The glass syringe was placed into a syringe pump for infusion/withdrawal (Harvard system). The refill flow

rate required to generate the desired wall shear stress of 0.05Pa was calculated (0.4 ml/min) and programmed into the Harvard system.

The Ibidi microslide was placed onto the stage of an inverted phase contrast microscope. The L-shaped connectors were connected to opposing ends of the channel (one in the inlet port and the other in the outlet port). PBSA was initially run through the channel. The syringe pump on the Harvard System was set to refill and 'run' was pressed. The focus of the microscope was adjusted to visualise the HUVEC monolayer.

Two minutes prior to starting the adhesion assay, 2 ml of purified leukocytes (either neutrophils or PBLs) were added to the 'perfused cell reserviour' and allowed to aclimatise to the temperatute. The HUVEC monolayer was washed by perfusing PBSA for 2 minutes. Upon completion of this, the electronic valve was turned ON to perfuse the leukocytes across the HUVEC monolayer. Following perfusion of leukocytes for 4 minutes, the electronic valve was switched OFF and PBSA from the 'wash buffer reserviour' was perfused for the remainder of the experiment.

The recruitment and transmigration of leukocytes under flow conditions was done post-perfusion of leukocytes. All digital recordings were made of at least 5-10 fields of view in the centre plane of the flow channel. The centre was identified by moving the microscope objective to the edge of the channel at the inlet port and identifying the middle of the port. Initial recordings of leukocyte behaviour post-leukocyte perfusion were made 2 minutes after perfusion of the leukocyte bolus. For these videos, 10 second recordings (taking images every second) were made of 5-10 randomised fields of view down the centre of the flow channel. Following these videos, a field of view that contained at least 10 transmigrated leukocytes was selected and a single recording was made for 5 minutes, taking images every 30 seconds. This video was used to calculate the velocity of migrated cells either above or below the HUVEC monolayer. Finally, another series of 10 second videos of 5-10 fields of view (typically 9 minutes post-perfusion of leukocytes) were made to assess prolonged transmigration. Upon completion of this, the syringe

pump connected to the Harvard System was stopped and the tubing connected to the Ibidi microsclide was removed. The perfused cells reservoir was rinsed with PBSA and the system was primed again for subsequent microslide channels.

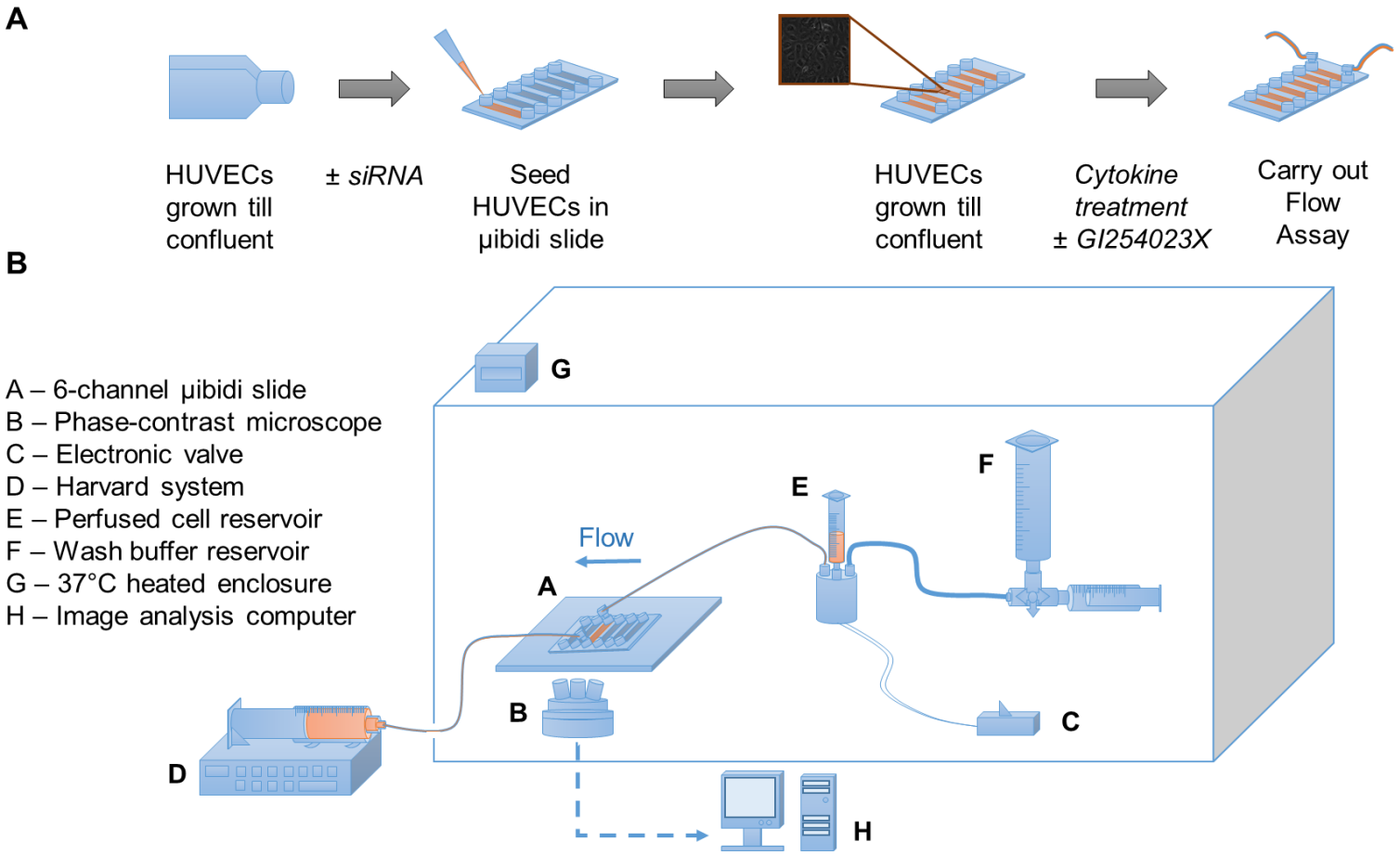

Figure 2.3 ***In vitro*** **flow-based adhesion assay setup.** (A) HUVECs were seeded in µ-Ibidi slides and grown until confluence before being cytokine-stimulated and incorporated into the flow adhesion assay. Endothelial ADAM10 was targeted by either using siRNA to ADAM10 or by using the ADAM10 preferential inhibitor, GI254023X. (B) The µ-Ibidi slide was mounted on the stage of a phase contrast microscope within a 37°C Perspex enclosure. Freshly isolated leukocytes were placed in the perfused cell reservoir which was electronically controlled. Wash buffer was placed in the wash buffer reservoir. All of the various components were connected using silicon piping to a Harvard System to mimic physiological shear stresses. Images were taken via a phase contrast microscope and analysed digitally.

2.3.5 Static adhesion assays

Static adhesion assays were utilised to assess PBL or monocyte transmigration, since it is a more high-throughput method compared to flow adhesion assays (Butler et al., 2009). HUVECs were plated into 12-well plates and treated with pro-inflammatory cytokines as described in Sections 2.3.1 and 2.3.2. Prior to the adhesion assay, the heater on the microsope was turned on and set to 37°C. For these adhesion assays, M199+BSA buffer was used as a wash buffer. Initally, the HUVEC monolayer was rinsed twice with 1 ml M199+BSA to remove any residual cytokines/inhibitors. 1 ml of freshly isolated PBLs (see Section 2.3.3) were added to the HUVEC monolayers and the 12-well plate was placed into the incubator for seven minutes at 37°C and 5% CO_2. This period of time has been shown to be sufficient to visualise adequate numbers of transmigrated PBLs or monocytes (Chimen et al., 2015). Following incubation, the cellular suspension was aspirated and the HUVEC monolayers were subsequently rinsed with two washes of 1 ml M199+BSA. The HUVEC monolayers were then fixed using 2% paraformaldehyde for 5 minutes at room temperature. Excess paraformaldehyde was removed and the wells were washed for a further two times using PBS. A final volume of 1 ml PBS was left in the wells and the HUVEC monolayers were imaged using a phase-contrast microscope.

2.3.6 Quantification of leukocyte behaviours

For flow adhesion assays, leukocyte recruitment and behaviour was analysed using the videos captured during the assays using ImagePro analysis software. Initially the 10-second recordings 2 minutes post-perfusion of leukocytes were analysed for leukocyte behaviour. The number of leukocytes were counted that were present throughout the 10 second recording. From this value the mean number of adherent neutrophils per field was calculated. In order to calculate the total adhesion, the area of a single field was calculated by measuring the length and width of a single frame. This was multiplied by

the mean number of leukocytes that were counted and further multiplied by the amount of leukocytes perfused (e.g. $1x10^6$ cells/ml * refill flow rate (Q) [0.4 ml/min] * 4 minutes) to get a value corresponding to the total adhesion (adherent cells/mm^2/10^6 cells perfused).

Leukocytes were classified based on three distinct behaviours: leukocytes were either rolling, firmly adherent or transmigrated (Figure 2.4). A rolling leukocyte was classified as a phase bright cell moving very slowly along the HUVEC monolayer (1-10 µm/s). A firmly adherent leukocyte was a phase bright cell bound to the surface of the HUVEC monolayer either not moving during the duration of the video or showing evidence of having undergone shape-change and exhibiting migratory properties on the HUVEC monolayer. A transmigrated leukocyte was classified as a cell that appeared phase-dark with altered cell morphology and had migrated underneath the HUVEC monolayer. The percentage of leukocytes exhibiting the various behaviours was calculated. For leukocyte velocity calculations, the rolling velocity of leukocytes was calculated by measuring the distance travelled by a tracked leukocyte over a period of 10 seconds. The distance (measured in microns (µm)) was converted into µm/sec by dividing by the duration of the video (e.g. 10 seconds). The velocity of surface adherent (phase bright) and transmigrated (phase dark) leukocytes was calculated using the 5 minute velocity recording. To do this, an outline was drawn around the migrated leukocytes at the beginning of the sequence and their movement was tracked throughout the duration of the video recording. X and Y coordinates of the centroid were noted at each 30-second interval for each tracked leukocyte. Pythagoras' theorem was applied to the X and Y values to calculate the distance travelled in µm/min. A minimum of 10 migrated leukocytes were tracked and used to calculate a mean velocity of either firmly adherent leukocytes or transmigrated leukocytes.

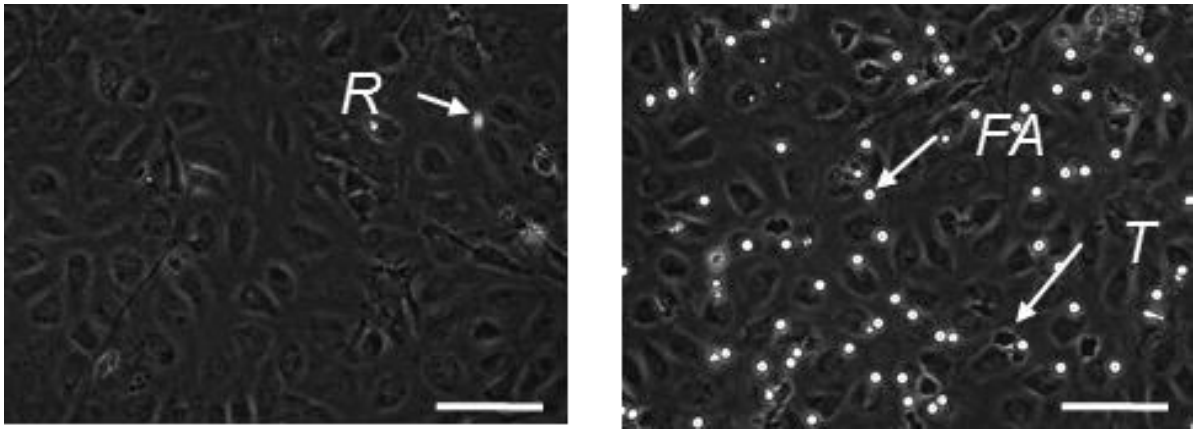

Figure 2.4 Phase contrast images highlighting leukocyte behaviours. HUVECs were grown to confluence and either left unstimulated (left image) or stimulated for 4 hours with 100 U/ml TNFα (right image). Neutrophils were then perfused over the monolayer and representative images are shown. Leukocytes were classified as either rolling (phase bright cell moving very slowly along the HUVEC monolayer (1-10 µm/s)), firmly adherent (leukocyte was a phase bright cell bound to the surface of the HUVEC monolayer either not moving during the duration of the video or showing evidence of having undergone shape-change and exhibiting migratory properties on the HUVEC monolayer), or transmigrated (cell that appeared phase-dark with altered cell morphology and had migrated underneath the HUVEC monolayer). *R* – rolling, *FA* – firmly adherent, *T* – transmigrated leukocyte. Scale bar: 80 µm.

For analysis of static adhesion assays, leukocytes were classified as either firmly adherent (phase bright; on top of the HUVEC monolayer) or transmigrated (phase dark; beneath the HUVEC monolayer). Digital images of the HUVEC monolayers were made immediately after the final wash stage. Images of five randomised fields of view were taken to count adherent cells. Since the HUVEC monolayers were fixed using 2% paraformaldehyde, velocity data could not be calculated from static adhesion assays. Total cell counts were made and results were expressed as percentages of the respective leukocyte behaviour (either firmly adherent or transmigrated). A total adhesion value was also calculated similarly to how the total adhesion was calculated under flow adhesion assay conditions.

2.4 BIOCHEMICAL ASSAYS

2.4.1 Analysis of protein expression by Western blotting

2.4.1.1 Whole cell protein extraction

Whole cell extracts were made from $1x10^6$ HUVEC plated in 6 cm dishes. Initially media from the cells was aspirated and the cell monolayers were washed twice using PBS at room temperature. A volume of 1 ml PBS was added to each well and subsequently the cell monolayer was scraped and transferred into a 1.5 ml Eppendorf tube (Eppendorf, Stevenage, UK) placed on ice and centrifuged at 80g for 3 minutes to pellet the cellular contents. The supernatant was aspirated and the pellet was resuspended in 60 µl 1% Triton X-100 lysis buffer (see Section 2.1.1) containing a protease inhibitor cocktail. Subsequently, the cells were vortexed before being incubated on ice for 30 minutes. The cell suspension was then centrifuged at 2100g for 10 minutes at 4°C to pellet any nuclear debris. The supernatant or cell extract was transferred into a new 1.5 ml Eppendorf tube and incubated at 100°C in a heat block for 5 minutes in an equal volume of 2x SDS non-reducing sample buffer (see Section 2.1.1) prior to being subjected to separation by gel electrophoresis (see Section 2.4.1.2) or stored at -20°C for later use.

2.4.1.2 Separation of proteins by gel electrophoresis

SDS polyacrylamide gels were prepared in gel cassettes (Novex, Life Technologies, Paisley, UK) and a SDS polyacrylamide resolving gel was prepared (see Section 2.1.1) and poured into the plate. After the resolving gel had set, a SDS polyacrylamide stacking gel was prepared and poured onto the set resolving layer. In addition, a 12-well comb was placed into the stacking layer.

Once the gel had set, the comb was removed along with the tape running at the bottom of the cassette and placed into the separation tank as described in the manufacturer's instructions (XCell SureLock^{TM} Mini-Cell Electrophoresis system, Life Technologies,

Paisley, UK). Protein samples prepared in Section 2.4.1.1 were loaded onto the gel along with a protein ladder (BLUEye™) diluted 1:10 in 2x SDS non-reducing sample buffer. The gel separation tank was filled with SDS Page non-gradient gel buffer (see Section 2.1.1). The SDS polyacrylamide gel was then run at 125V (constant voltage) for 90 minutes or until the gel front had reached the bottom of the gel, as detected by the presence of bromophenol blue in the loading dye.

2.4.1.3 Transfer of proteins from SDS-polyacrylamide gel onto polyvinylidene difluoride (PVDF) Immobilon-FL membrane

After running the gel, it was removed from its cassette and the stacking gel was discarded before being soaked in Western transfer buffer (see Section 2.1.1) for 20 minutes prior to assembling the transfer chamber. A PVDF Immobilon-FL membrane (Merck Millipore IPVH00010) was pre-activated in methanol for a second or two, and then soaked in Western transfer buffer for a further 30 minutes. The gel transfer apparatus (XCell II™ Blot Module, Life technologies) along with 3MM whatman filter paper (Amersham, Buckinghamshire, UK) were soaked in Western transfer buffer. To set up the transfer, three blotting pads were initially placed onto the anode side of the transfer casing. Onto this a piece or previously soaked 3MM whatman paper was placed on top of which the PVDF Immobilon-FL membrane was placed followed by a further piece of 3MM whatman paper. At this point, a plastic tube was rolled over the stacked gel and membrane to remove any air bubbles. A further three blotting pads were added and the cathode side of the transfer casing was placed on top before transferring and securing the whole stack into the gel transfer apparatus. The gel tank was then filled with Western transfer buffer and set to run at 30V for 1 hours and 30 minutes.

2.4.1.4 Immune-detection of proteins

Following transfer, membrane was then blocked in a 1x TBST solution containing 5% (w/v) milk (Marvel) on a rotating platform at room temperature for a minimum of 1 hour.

Excess milk was tipped off and discarded and the membrane was washed once with 1x TBST. The membrane was then incubated with antibody buffer (see Section 2.1.1) with the required primary antibody (see Section 2.1.2) for 24 hours at 4°C on a rotating platform. Following primary antibody incubation, the membrane was washed 5 times for 5 minutes in 1x TBST high salt wash buffer (see Section 2.1.1), before a 2 hour incubation at room temperature in antibody buffer with the required secondary antibody (see Section 2.1.2) on a rotating platform. The membrane was then washed for a further 5 times as explained previously.

After the membrane had been probed with the relevant antibodies, the membrane was washed with two swirls of TBS to remove excess tween. The membrane was then imaged using the Odyssey Infrared Imaging System (LI-COR, Cambridge, UK) using the manufacturer's guidance.

For certain experiments, such as detecting loading controls, the membrane was stripped using stripping buffer (see Section 2.1.1). Briefly, the membrane was placed in pre-warmed stripping buffer in a 60°C water bath for 30 minutes. The stripping buffer was then tipped off and the membrane was washed five times for five minutes in 1x TBST high salt wash buffer before being re-probed with the appropriate antibodies and subsequently developed as explained above.

2.4.1.5 Quantitative analysis of Western blots

Following scanning of the membrane, the densities of the bands were analysed using the Odyssey software (LI-COR). Briefly, the background method was selected by using the

drawing panel to select an area of the blot that well represented the background (i.e. contained no bands of interest). Rectangle boxes were then drawn around the bands of interest and relative band intensities were noted. Proteins of interest were compared to loading controls.

2.4.2 Cell-based cleavage assay

To assess the effects of ADAM10-dependent shedding of VE-cadherin, a cleavage-based assay was adopted (Schulz et al., 2008; Haining et al., 2012). In this assay, HUVECs were cultured in complete HUVEC growth medium on 0.1% gelatine coated 6 cm dishes. ADAM10 activity was targeted either through the use of the ADAM10 preferential inhibitor (GI254023X) or through gene silencing of ADAM10 using siRNA. For ADAM10 inhibitor cleavage assays, HUVECs were grown till confluence before being treated with either 0.02% DMSO or 20 µM GI254023X along with 10 µM of the γ-secretase inhibitor, DAPT for 24 hours at 37°C and 5% CO_2. For ADAM10 siRNA knockdown experiments, HUVECs were transfected with one of two siRNA duplexes as explained in Section 2.2.4.2 and grown for 48 hours. 24 hours before harvesting the ADAM10 knockdown HUVECS, 10 µM DAPT was added to prevent further processing of the C-terminal fragments of VE-cadherin. HUVECs were then harvested and subsequently underwent Western blotting as explained in Section 2.4.1. The results were imaged and quantified on the Odyssey Infrared Imaging System. For quantification of protein bands during shedding assays, bands were drawn around known full-length and cleaved fragments of the protein. The percentage cleaved protein was calculated by adding the cleaved band(s) intensity along with the full-length band(s) intensity to get a total protein band intensity value. The cleaved band(s) intensity was then divided by the total protein band intensity value and multiplied by 100 to get the percentage cleaved value.

2.4.3 Analysis of protein knockdown by real time quantitative PCR (qPCR)

2.4.3.1 Extraction of mRNA from HUVECs

Total RNA was extracted from $1x10^6$ HUVECs. Briefly, HUVECs were harvested by dissociation using Trypsin/EDTA solution and centrifuged as explained in Section 2.2.3. Following centrifugation, the pellet was washed twice using PBS to remove excess media. RNA was isolated directly from the cell pellet using the RNeasy mini kit (Qiagen, Manchester, UK), according to the manufacturer's instructions. Initially, the cells were passed through a QIAshredder (Qiagen) to homogenise the cells prior to RNA isolation.

2.4.3.2 Conversion of mRNA to cDNA

The total yield of RNA isolated was detected using a NanoDrop (NanoDrop 1000, Wilmington, DE, USA) and adjusted to 1 µg/µl. This was then reverse-transcribed to a single strand of cDNA using a High Capacity cDNA Reverse Transcription kit (Applied Biosystems, Paisley, UK). 10X reverse transcription buffer along with 25X dNTP mix (100 nM), 10X reverse transcriptase random primers and MultiScribe™ reverse transcriptase were combined with the RNA in a final volume of 20 µl. The reactions were incubated in a thermocycler at the following conditions: 25°C for 10 minutes, 37°C for 120 minutes followed by an 85°C step for 5 minutes.

2.4.3.3 qPCR

Real time PCR was performed using the Taqman® Gene Expression Assay (Applied Biosystems) using the ABI Prism 7000 system (Applied Biosystems). Taqman FAM-TAMRA primers for GAPDH, Tspan5, Tspan10, Tspan14, Tspan15, Tspan17, and

Tspan33 were used. A 20 µl reaction mixture, containing 10 µl 2x Taqman® Master Mix, 1 µl desired gene Taqman® FAM-TAMRA hydrolysis probes along with 50 ng cDNA was amplified using the following thermal cycle parameters: a single cycle at 50°C for 2 minutes followed by a single cycle at 95°C for 10 minutes (denaturation) prior to 44 cycles of 95°C for 15 seconds denaturation and 44 cycles of 60°C for annealing and extension. The data was analysed using the ABI PRISM 7000 SDS Software (Applied Biosystems). A form of the ΔΔCt method was used to calculate the total mRNA levels in the PCR reactions used to assess knockdown efficiency (Pfaffl, 2001). Ct marks the point at which the threshold line meets the amplification curve in the exponential phase of the reaction. A baseline was initially set to remove any background non-specific noise at the initial stages of the reaction. The threshold was manually adjusted so that it crossed the exponential phase of all the PCR reactions in each experiment. From this, Ct values were noted. The Ct values of TspanC8s were compared to CT values of the housekeeping gene GAPDH. From this ΔΔCt values ($2^{-\Delta\Delta Ct}$) were recorded and represented as the relative mRNA expression.

2.5 STATISTICAL ANALYSIS

All data analysis was performed using GraphPad Prism® 5 software. Data were presented as means ± standard error of the mean. Differences between two groups (e.g. untreated versus treated) were analysed using Students *t* test. To analyse differences between multiple groups (e.g. varying concentrations) one-way or two-way analysis of variance (ANOVA) followed by Dunnett's post hoc or Bonferroni multiple comparisons post hoc tests were used. Percentage data underwent arcsine transformation to normally distribute the data prior to statistical analysis. P-values < 0.05 were considered to be statistically significant.

CHAPTER 3

THE ROLE OF ADAM10 IN REGULATING LEUKOCYTE RECRUITMENT AND TRANSMIGRATION

3.1 INTRODUCTION

The recruitment of leukocytes via a process of margination from blood flow, through the vessel wall to sites of inflammation, is a crucial event in host defence during injury and infection. The principle barrier that circulating leukocytes have to overcome first in order to extravasate into the tissue, is the endothelial cell barrier (Nourshargh et al., 2010). This is facilitated by the action of pro-inflammatory stimuli on the endothelial cells that lead to vessel wall leakiness and subsequently allows leukocyte transmigration to occur. This process requires the interaction of adhesion molecules expressed on immune cells as well as the endothelium (Vestweber, 2007). In chronic inflammatory diseases, the process of leukocyte recruitment and transmigration becomes accelerated. An emerging molecular mechanism that can regulate leukocyte recruitment and transmigration is the proteolytic cleavage or 'ectodomain shedding' of key CAMs. Several leukocyte receptors have been documented to undergo ADAM-mediated ectodomain shedding during leukocyte recruitment and transmigration (Dreymueller et al., 2012b, 2015). Some of the major receptors that undergo ectodomain shedding include the endothelial expressed cellular adhesion molecules ICAM-1 and VCAM-1, the two transmembrane chemokines CX3CL1 and CXCL16, the junctional proteins VE-cadherin and JAM-A, and the leukocyte homing receptor L-selectin (Tsakadze et al., 2006; Singh et al., 2005; Hundhausen et al., 2003; Abel et al., 2004; Schulz et al., 2008; Koenen et al., 2009; Hafezi-Moghadam et al., 2001). Many of the molecules involved in leukocyte adhesion and transmigration are shed by ADAM10 (e.g. VE-cadherin), others by ADAM17 (e.g. L-selectin) and some by both proteases (e.g. CX3CL1) (Schulz et al., 2008; Peschon et al., 1998; Garton et al., 2001; Hundhausen et al., 2003).

A role of ADAM10 in leukocyte adhesion and transmigration has previously been shown by regulating the shedding of endothelial transmembrane chemokines, CX3CL1 and CXCL16, and the adherens junction molecule VE-cadherin (Hundhausen et al., 2003, 2007; Schulz et al., 2008). However, most of these studies deciphered a role of ADAM10

using cell lines or transfected cells and the mechanism by which ADAM10 regulates leukocyte transmigration in primary cells and under physiological flow conditions is not clear. Therefore, the principle aim of this study was to determine whether endothelial ADAM10 could differentially regulate the efficient recruitment and transmigration of human leukocytes by shedding key cell surface receptors involved in the distinct stages of leukocyte capture, activation induced arrest and transmigration. To investigate this, endothelial ADAM10 expressed on HUVECs was targeted using gene knockdown techniques or through the use of a preferential ADAM10 pharmacological inhibitor (GI254023X). This pharmacological inhibitor has been shown to have 100-fold more binding specificity for ADAM10 over its most closely related family member, ADAM17 (Ludwig et al., 2005). Separately, leukocyte-expressed ADAM10 was also targeted using the ADAM10 inhibitor. The cells were then incorporated into either an *in vitro* flow-based adhesion assay or a static adhesion assay and characteristic leukocyte behaviours during an inflammatory response were analysed by phase-contrast video microscopy. This forms the basis of investigations undertaken in this chapter.

3.2 RESULTS

3.2.1 Effects of ADAM10 knockdown/inhibition on lymphocyte cell recruitment and transmigration

3.2.1.1 Endothelial ADAM10 regulates the transmigration of lymphocytes

In order to assess the role of endothelial ADAM10 in regulating the recruitment and transmigration of peripheral blood lymphocytes (PBLs) under physiological flow conditions, ADAM10-targetted siRNAs were used to reduce endothelial ADAM10 levels. Low passage (P0 – P1) HUVECs were used because these cells have been extensively characterised for use in leukocyte adhesion assays. In addition, HUVECs upregulate the various selectins/CAMs that support leukocyte adhesion and transmigration similar to the endothelial cells found in the post-capillary venules (Sheikh et al., 2003). For these experiments, HUVECs in wells of a 6-well plate were transfected with either a non-silencing control or with one of two siRNA duplexes to ADAM10. 4 hours post transfection the HUVECs were dissociated and re-plated into a 6-well Ibidi microslide. 24 hours post transfection HUVECs were stimulated for a further 24 hours with 100 U/ml TNFα and 10 ng/ml IFNγ, a cocktail of potent cytokines that when used in combination have been shown to support the adhesion and transmigration of PBLs by upregulating the interferon-inducible chemokines CXCL9-12 (Ahmed et al., 2011). Freshly isolated PBLs were extracted from venous blood following density centrifugation on Histopaque as described in Section 2.3.3 and adjusted to a working concentration of $1x10^6$/ml. The Ibidi microslide was incorporated into a flow adhesion assay to assess PBL recruitment and transmigration by mounting onto the stage of a phase contrast microscope within a 37°C Perspex chamber (as described in Section 2.3.4). Respective videos were recorded for leukocyte behaviours and were subsequently analysed and total adhesion calculated as explained in Section 2.3.6.

As shown in Figure 3.1, knockdown of endothelial ADAM10 reduced the ability of PBLs to transmigrate by 50% (Figure 3.1 A & B). This reduction was accompanied by a subsequent increase in the percentage of adherent PBLs on the surface of the HUVEC monolayer (Figure 3.1 A & B). Interestingly, knockdown of ADAM10 resulted in reduced PBL transmigration that was still apparent at 9 minutes post-perfusion of PBLs when compared to the negative control siRNA control (Figure 3.1 A & B). No differences were observed in PBL rolling behaviour (Figure 3.1 A & B). In addition, no differences in total adhesion were observed following endothelial ADAM10 knockdown (Figure 3.1 B). The knockdown efficiency of endothelial ADAM10 was assessed by flow cytometry. Expression of ADAM10 was significantly reduced in siRNA treated cells (~90% reduced upon quantification) (Figure 3.1 D & E).

In addition to PBL behaviours, PBLs were also analysed for velocity behaviours. For rolling velocities, PBLs classified as rolling were tracked over a 10 second video and the distance was noted in microns. This was then converted to give a value in microns per second. To assess the velocities of firmly adherent or transmigrated PBLs, the locomotion of firmly adherent or transmigrated PBLs was tracked over a period of 5 minutes. The distance of 10-tracked cells in each experiment per treatment condition was converted from microns into microns per minute. Similar tracking velocities were noted for PBLs on cytokine-stimulated HUVECs as previously published (McGettrick et al., 2009). However, knockdown of endothelial ADAM10 had no significant effect on PBL velocities (Table 3.1).

To conclude, knockdown of endothelial ADAM10 reduces the transmigration of PBLs under physiological flow conditions.

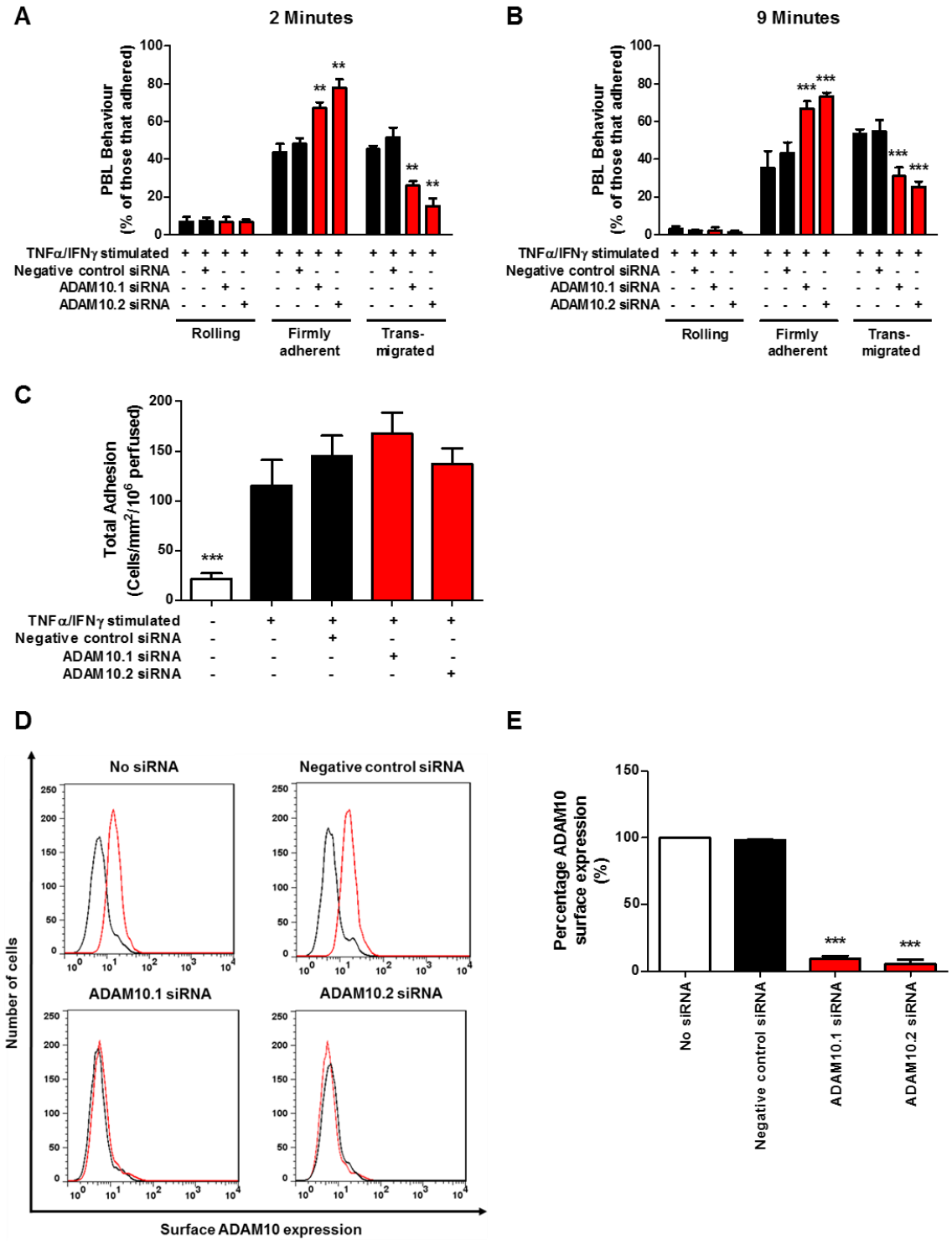
A
2 Minutes
PBL Behaviour (% of those that adhered)
TNFα/IFNγ stimulated
Negative control siRNA
ADAM10.1 siRNA
ADAM10.2 siRNA
Rolling
Firmly adherent
Trans-migrated
B
9 Minutes
C
Total Adhesion (Cells/mm²/10⁶ perfused)
D
No siRNA
Negative control siRNA
ADAM10.1 siRNA
ADAM10.2 siRNA
Number of cells
Surface ADAM10 expression
E
Percentage ADAM10 surface expression (%)

Figure 3.1 Knockdown of endothelial ADAM10 decreases the transmigration of lymphocytes under *in vitro* flow conditions. HUVECs were transfected with two different siRNA duplexes to ADAM10 (red bars) alongside a non-specific siRNA (black bars) at a final concentration of 10 nM prior to being seeded into 6-well Ibidi slides. 24 hours after transfection, the HUVECs were stimulated with 100 U/ml TNFα along with 10 ng/ml IFNγ for an additional 24 hours. Freshly isolated PBLs were then perfused over the pre-activated HUVEC monolayer at 0.05 Pa in PBSA for 4 minutes. Video-recordings of five different fields of view of the endothelial monolayer were made using time-lapse video microscopy at two-minutes (A) or nine-minutes (B) post perfusion of PBLs, respectively. PBLs were classified as rolling, firmly adherent or transmigrated. The total number of cells classified for each of the behaviours were combined to give a total adhesion count (C). HUVECs transfected with siRNA were analysed by flow cytometry to measure surface ADAM10 expression. The red line represents ADAM10 staining and the black line isotype control staining (D). Surface ADAM10 levels from panel D were quantitated and normalised to the "No siRNA" treated condition (E). Error bars represent the standard error of the mean from five independent experiments. Data were normalised by arcsine transformation and statistically analysed by a one-way ANOVA and Dunnett's post-hoc comparisons test for total adhesion or knockdown confirmation (***$p < 0.001$ compared to negative control siRNA transfected data) or by a two-way ANOVA and Bonferroni post-hoc comparisons test for cell behaviours (**$p < 0.01$, ***$p < 0.001$ compared to the negative control siRNA transfected data).

Condition	Rolling velocity ($\mu m\ sec^{-1}$)	Firmly adherent velocity ($\mu m\ min^{-1}$)	Transmigrated velocity ($\mu m\ min^{-1}$)
No siRNA	6.17 ± 0.24	5.25 ± 0.56	15.21 ± 1.20
Negative control siRNA	6.15 ± 0.60	5.67 ± 1.15	13.56 ± 1.11
ADAM10.1 siRNA	6.39 ± 0.36	4.26 ± 0.78	16.29 ± 0.73
ADAM10.2 siRNA	6.44 ± 0.54	4.87 ± 0.98	15.92 ± 0.84

Table 3.1 Knockdown of endothelial ADAM10 has no effect on PBL velocities. PBL velocities were tracked using ImagePro cell tracking software. For PBL rolling velocities, PBLs classified as rolling were tracked over a 10-second video of a single frame and the total distance travelled was converted to $\mu m\ sec^{-1}$. For firmly adherent or transmigrated PBL velocities, firmly adherent or transmigrated PBLs were drawn around and tracked over a 5-minute video of a single frame. The distance travelled was calculated by applying Pythagoras theorem for calculated 'x' and 'y' distances of tracked PBLs and converted to $\mu m\ min^{-1}$. Values represented are mean ± standard error of 20, 30, or 50 tracked cells for rolling, firmly adherent or transmigrated conditions from three to five different experiments, respectively.

To establish a more high-throughput assay of transmigration to facilitate future mechanistic studies, PBL transmigration was assessed under static conditions. HUVECs were transfected with siRNA duplexes targeting ADAM10 or a negative control non-specific siRNA duplex before stimulation with 100 U/ml TNFα and 10 ng/ml IFNγ, as described previously. PBL were then isolated, purified and adjusted to a working concentration at $1x10^6$/ml. The PBL were allowed to adhere and undergo transmigration by incubating the plate at 37°C for 7 minutes, an optimal time-point to see differences in PBL adhesion and transmigration under static conditions (Chimen et al., 2015). Non-adherent PBLs were washed off and the HUVEC monolayers were fixed with 2% formaldehyde before being imaged using phase-contrast microscopy. PBL behaviours and total adhesion were calculated from the captured images. Consistent with studies under flow (Figure 3.1), knockdown of endothelial ADAM10 reduced PBL transmigration by approximately 45% with a consequent increase in the percentage of firmly adherent cells that had not transmigrated (Figure 3.2 A). Similar observations were also seen when looking at PBL total adhesion, with knockdown of endothelial ADAM10 having no effect on this parameter (Figure 3.2 B). Knockdown of ADAM10 expression in endothelial cells was confirmed as previously described by flow cytometry and found to be at least 85% reduced (Figure 3.2 C & D).

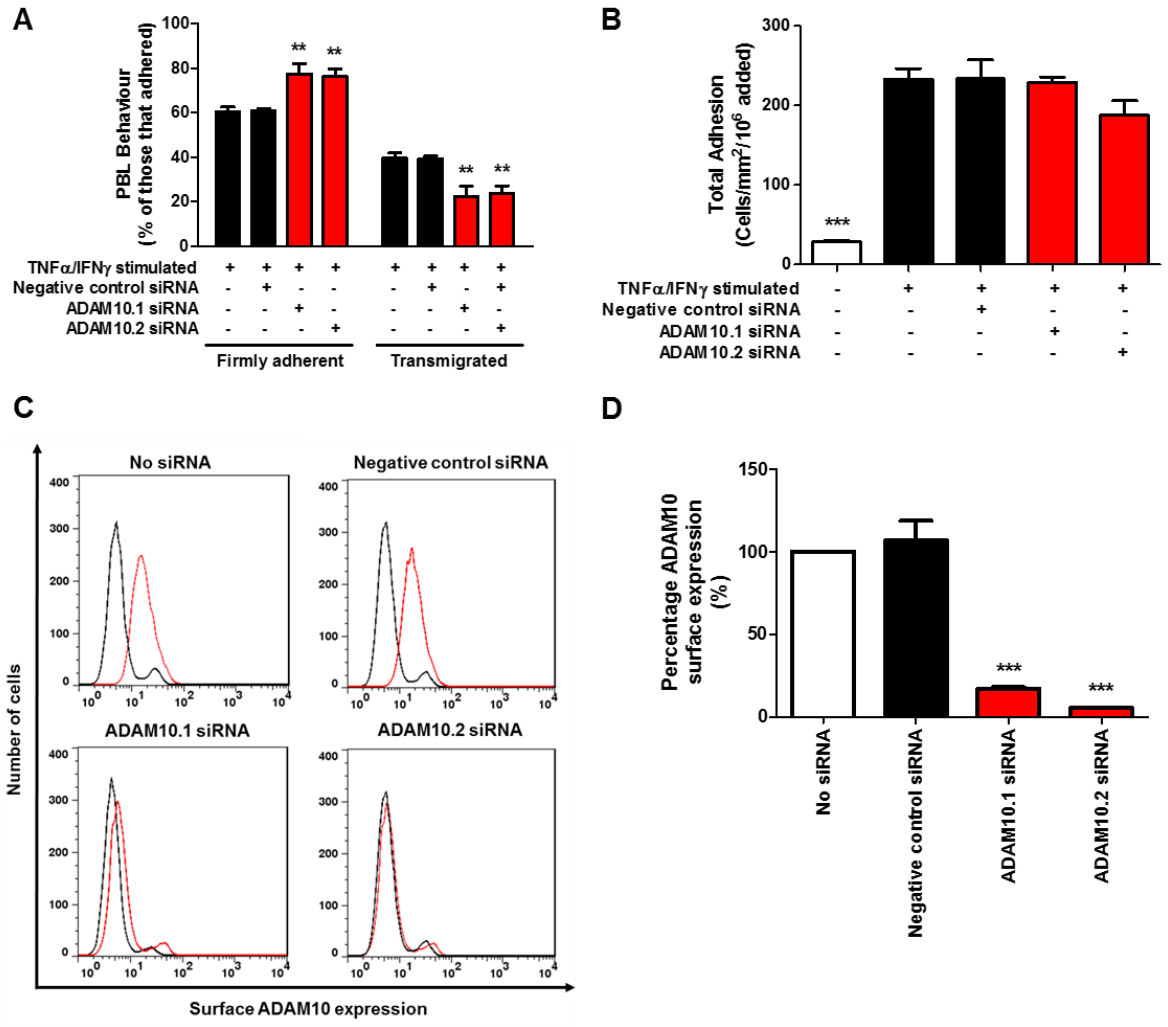

Figure 3.*2* Knockdown of endothelial ADAM10 decreases the transmigration of lymphocytes under *in vitro* static conditions. HUVECs were transfected with two different siRNA duplexes to ADAM10 (red bards) alongside a non-specific siRNA (black bars) at a final concentration of 10 nM in 12-well plates. Following 24 hours, HUVECs were stimulated with 100 U/ml TNFα along with 10 ng/ml IFNγ for an additional 24 hours. Freshly isolated PBLs were then added to the pre-activated HUVEC monolayer in M199+BSA and incubated for 7 minutes. Non-adherent PBLs were washed off using M199+BSA and HUVEC monolayers were fixed using 2% formaldehyde. Images of five different fields of view of the endothelial monolayer were made using phase-contrast microscopy. PBLs were classified as firmly adherent or transmigrated (A). The total number of cells classified for each of the behaviours were combined to give a total adhesion count (B). Knockdown of ADAM10 was assessed as described in the legend for Figure 3.1 (C) and (D). Error bars represent the standard error of the mean from five independent experiments. Data were normalised by arcsine transformation and statistically analysed by a one-way ANOVA and Dunnett's post-hoc comparisons test for total adhesion data and confirmation of knockdown (***$p < 0.001$ compared to the negative control siRNA transfected data) or by a two-way ANOVA and Bonferroni post-hoc comparisons test for PBL cell behaviour (**$p < 0.01$ compared to the negative control siRNA transfected data).

To determine whether an ADAM10 inhibitor (GI254023X) yields similar data to the knockdown, initial experiments were carried out to establish an appropriate concentration of inhibitor to use. For these experiments, HUVECs were plated into 12-well plates and grown until confluent. Previously published data using this pharmacological inhibitor showed a dose of 10μM was sufficient in reducing the transmigration of PHA-blast T-cells or a pre-B cell line L1.2 cells across ECV304 monolayers (Hundhausen et al., 2007; Schulz et al., 2008; Schwarz et al., 2010; Powers et al., 2012). Therefore, HUVEC monolayers were subjected to either 0.02% DMSO control or 2.5 μM, 5 μM, 10 μM, 20 μM or 40 μM GI254023X treatment alongside cytokine treatment as previously described for static adhesion assays. Phase-contrast images following 24-hour incubation with the ADAM10 inhibitor at the various doses revealed that the inhibitor did not affect HUVEC monolayer integrity (Figure 3.3 A). Inhibition of HUVEC-expressed ADAM10 mimicked the phenotype observed when HUVEC-expressed ADAM10 was knocked down under static conditions, resulting in a decrease in the ability of PBLs to transmigrate, with a concentration of 10 μM or 20 μM being significant to visualise this phenotype (Figure 3.3 B). This was supported by a dose-dependent concomitant increase in firmly adherent PBLs (Figure 3.4 B). Moreover, inhibition of endothelial ADAM10 did not alter the total adhesion of PBLs (Figure 3.3 C). These data lead to the adoption of 20 μM of the inhibitor for future experiments.

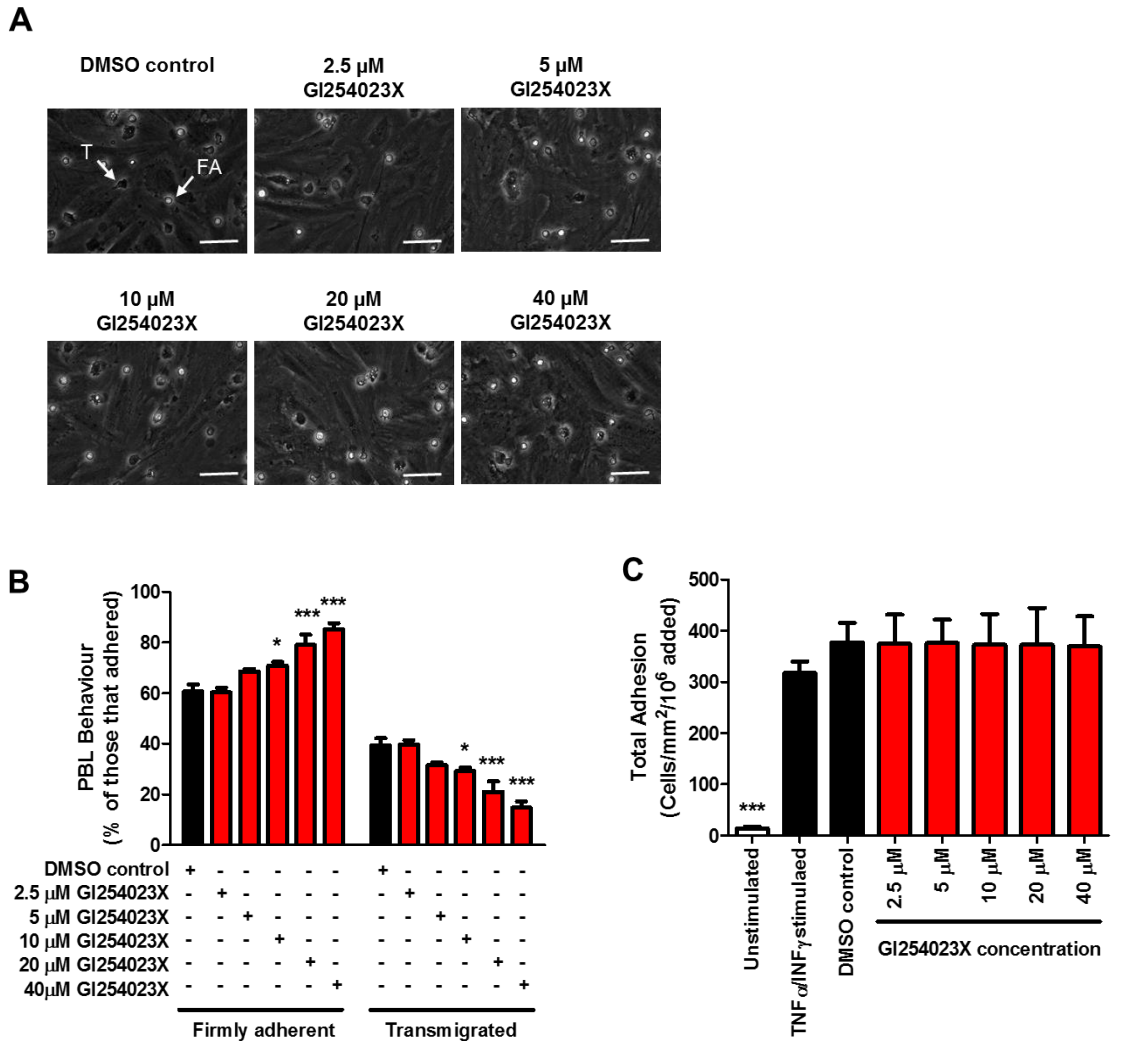

Figure 3.3 Inhibition of endothelial ADAM10 decreases lymphocyte transmigration under *in vitro* static conditions. HUVECs were plated into 12-well plates. Once confluent, the HUVECs were stimulated as previously described in the legend for Figure 3.2 along with either 0.02% DMSO (black bar) or increasing concentrations of the ADAM10 inhibitor (2.5, 5, 10, 20 or 40 µM GI254023X) (red bar) for 24 hours before being incorporated into a static adhesion assay to assess PBL adhesion and transmigration. Representative phase contrast images of PBL adhesion at 7 minutes post-incubation were made to assess HUVEC monolayer integrity (A) and analysed for PBL behaviours (B) along with total adhesion (A), as previously described in the legend for Figure 3.2. Error bars represent the standard error of the mean from four independent experiments. Data were normalised by arcsine transformation and statistically analysed by a one-way ANOVA and Dunnett's post-hoc comparisons test for total adhesion (***$p < 0.001$ compared to DMSO control data) or by a two-way ANOVA and Bonferroni post-hoc comparisons test for cell behaviours (*$p < 0.05$, ***$p < 0.01$ compared to DMSO control data). Examples of FA – firmly adherent (phase bright) or T – transmigrated (phase dark) cells are highlighted (A). Scale bar: 50µm.

To further the ADAM10 inhibitor data findings in Figure 3.3, the effects of ADAM10 inhibition on PBL transmigration under flow conditions was investigated. Confluent HUVEC monolayers were seeded into Ibidi microslides and stimulated with 100 U/ml TNFα and 10 ng/ml IFNγ for 24 hours in the presence of 0.02% DMSO or 20 μM GI254023X – a concentration that was shown to reduce PBL transmigration to similar levels to that observed following ADAM10 siRNA (Figure 3.3). PBL behaviours were analysed, as explained previously. Inhibition of HUVEC-expressed ADAM10 mimicked the phenotype observed when HUVEC-expressed ADAM10 was knocked down. Inhibition of HUVEC-expressed ADAM10 resulted in a decrease in the ability of PBLs to transmigrate (Figure 3.4 A & B). This was supported by a concomitant increase in the percentage of firmly adherent PBLs (Figure 3.4 A & B). No differences were observed between the ADAM10 inhibitor treated cells and for DMSO control cells when looking at PBL rolling behaviour (Figure 3.4 A & B) or PBL velocity behaviours (Table 3.2). In addition, no differences in total adhesion were observed following endothelial ADAM10 inhibition (Figure 3.4 C).

In summary, these data demonstrate that endothelial ADAM10 is able to regulate the transmigration of PBLs under physiological *in vitro* conditions in a model of chronic inflammation.

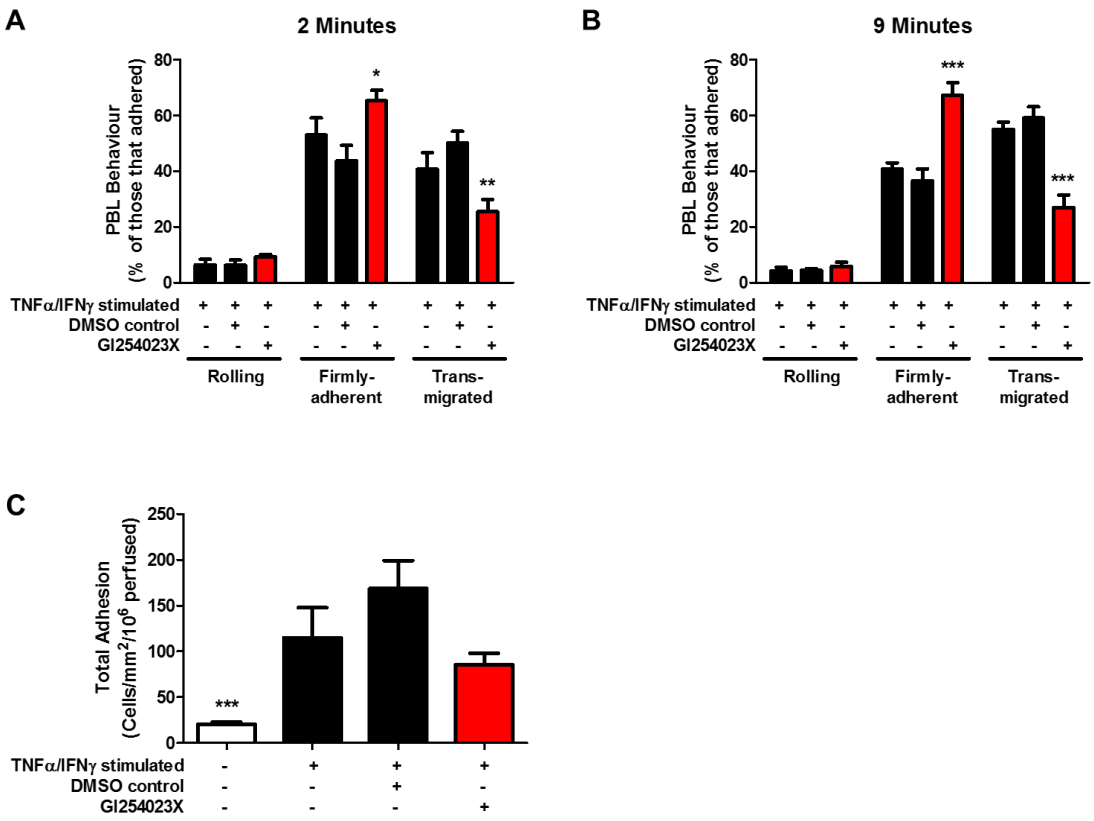

Figure 3.4 Inhibition of endothelial ADAM10 decreases the transmigration of lymphocytes under *in vitro* flow conditions. HUVECs were plated into 6-well Ibidi slides. Once confluent, the HUVECs were stimulated as previously described in the legend for Figure 3.1 along with either 0.02% DMSO (black bar) or 20 µM GI254023X (red bar) for 24 hours before being incorporated into the flow adhesion assay to assess PBL adhesion and transmigration. Video recordings of PBL adhesion at specific time-points were made and analysed for PBL behaviours (A) and (B) along with total adhesion (C), as previously described in the legend for Figure 3.1. Error bars represent the standard error of the mean from five independent experiments. Data were normalised by arcsine transformation and statistically analysed by a one-way ANOVA and Dunnett's post-hoc comparisons test for total adhesion (***$p < 0.001$ compared to DMSO control data) or by a two-way ANOVA and Bonferroni post-hoc comparisons test for cell behaviours (*$p < 0.05$, **$p < 0.01$, ***$p < 0.001$ compared to DMSO control data).

Condition		Rolling velocity (μm sec^{-1})	Firmly adherent velocity (μm min^{-1})	Transmigrated velocity (μm min^{-1})
HUVEC treatment	**-**	5.92 ± 0.28	3.51 ± 0.25	13.76 ± 1.37
	DMSO control	6.07 ± 0.17	4.23 ± 0.88	14.83 ± 1.32
	GI254023X	5.54 ± 0.26	3.41 ± 0.47	16.21 ± 0.62
PBL treatment	**DMSO control**	6.61 ± 0.33	4.27 ± 0.39	15.29 ± 0.71
	GI254023X	5.56 ± 0.38	3.86 ± 0.34	14.03 ±1.51

Table 3.2 Inhibition of endothelial or PBL-expressed ADAM10 has no effect on PBL velocities. PBL velocities were tracked using ImagePro cell tracking software and as explained in the legend to Table 3.1. Values represented are mean ± standard error of 40, 20, or 50 tracked cells for rolling, firmly adherent or transmigrated conditions over a minimum of three to five different experiments, respectively.

3.2.1.2 Inhibition of lymphocyte-expressed ADAM10 regulates does not regulate lymphocyte transmigration

To further characterise the role of ADAM10 in regulating the recruitment and transmigration of PBLs, the role of ADAM10 on PBLs was next targeted using the ADAM10 inhibitor. Similar approaches were used to those described earlier to decipher a role of PBL-expressed ADAM10 during PBL recruitment and transmigration. Initial experiments focused on the role of ADAM10 inhibited PBLs under flow adhesion conditions. For these experiments, isolated PBLs were treated with either 0.02% DMSO or with 20 µM GI254023X for 30 minutes at room temperature before being incorporated into the flow assay. In addition, 20 µM GI254023X was also added to the wash buffer to prevent dilution of the inhibitor treated PBLs during perfusion. Interestingly, inhibition of PBL-expressed ADAM10 did not alter the ability of PBLs to transmigrate under flow conditions. No differences in PBL behaviour were observed when PBL-expressed ADAM10 was inhibited (Figure 3.5 A & B). In addition, no difference in total adhesion was observed when PBL-expressed ADAM10 was inhibited (Figure 3.5 A). Moreover, no differences in PBL velocity behaviour were observed following PBL ADAM10 inhibition (Table 3.2). Similar observations were also made when PBL-expressed ADAM10 was inhibited and incorporated into a static adhesion assay (Figure 3.6).

Altogether, these findings suggest a role for endothelial ADAM10, but not PBL-expressed ADAM10 in regulating the transmigration of PBLs in models of chronic inflammation under both physiological flow conditions and static adhesion conditions.

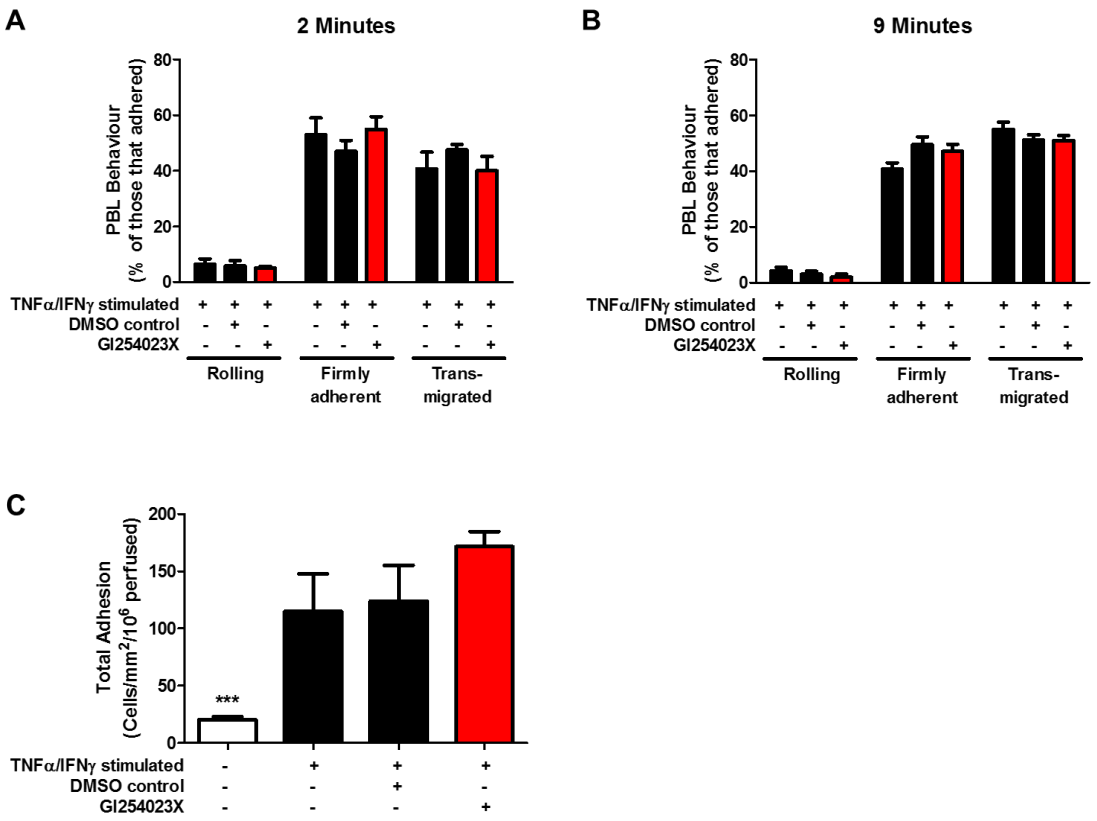

Figure 3.5 Inhibition of lymphocyte-expressed ADAM10 does not alter lymphocyte transmigration under *in vitro* flow conditions. HUVECs were plated into 6-well Ibidi slides. Once confluent, the HUVECs were stimulated as previously described in the legend for Figure 3.1 before being incorporated into the flow adhesion assay to assess PBL adhesion and transmigration. For ADAM10 inhibitor or DMSO conditions, PBLs were pre-incubated with either 20 µM GI254023X (red bar) or 0.02% DMSO (black bar) for 30 minutes prior to being incorporated into the flow adhesion assay. In addition, 20 µM GI254023X was added to the wash buffer when perfusing ADAM10 inhibited PBLs to prevent dilution of the inhibitor. Video recordings of PBL adhesion at specific time-points were made and analysed for PBL behaviours (A) and (B) along with total adhesion (C), as previously described in the legend for Figure 3.1. Error bars represent the standard error of the mean from three independent experiments. Data were normalised by arcsine transformation and statistically analysed by a one-way ANOVA and Dunnett's post-hoc comparisons test for total adhesion (***$p < 0.001$ compared to DMSO control data) or by a two-way ANOVA and Bonferroni post-hoc comparisons test for cell behaviours.

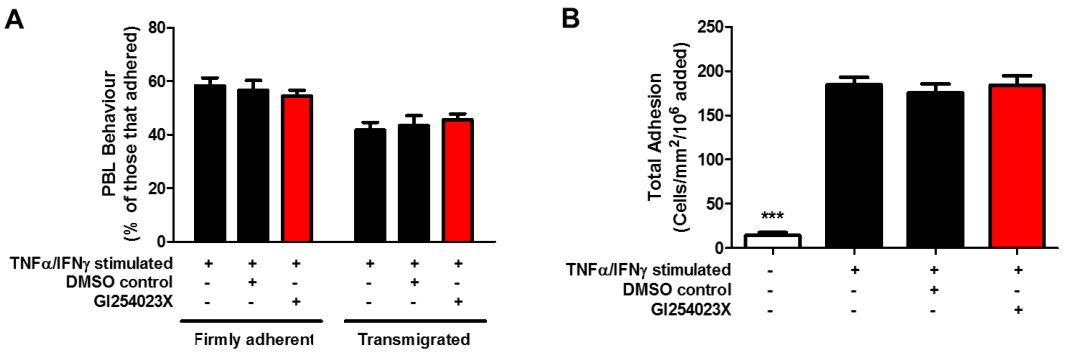

Figure 3.6 Inhibition of lymphocyte-expressed ADAM10 does not alter lymphocyte transmigration under *in vitro* static conditions. HUVECs were plated into 12-well plates. Once confluent, the HUVECs were stimulated as previously described in the legend for Figure 3.2 before being incorporated into a static adhesion assay to assess PBL adhesion and transmigration. For ADAM10 inhibitor or DMSO conditions, PBLs were pre-incubated with either 20 µM GI254023X (red bar) or 0.02% DMSO (black bar) for 30 minutes prior to being incorporated into the static adhesion assay. Phase contrast images of PBL adhesion at 7 minutes post-incubation were made and analysed for PBL behaviours (A) along with total adhesion (B), as previously described in the legend for Figure 3.2. Error bars represent the standard error of the mean from five independent experiments. Data were normalised by arcsine transformation and statistically analysed by a one-way ANOVA and Dunnett's post-hoc comparisons test for total adhesion (***$p < 0.001$ compared to DMSO control data) or by a two-way ANOVA and Bonferroni post-hoc comparisons test for cell behaviours.

3.2.2 Effects of ADAM10 knockdown/inhibition on myeloid cell recruitment and transmigration

3.2.2.1 Neutrophil recruitment and transmigration is independent of ADAM10

Neutrophils are the most abundant leukocyte subset found in the peripheral vasculature and play a fundamental role in immune surveillance and inflammation. To elucidate whether neutrophil adhesion and transmigration is regulated by ADAM10, HUVEC-expressed ADAM10 or its activity was reduced either by using siRNA or by using the pharmacological inhibitor. Initial experiments were performed to establish the optimal doses of recombinant human TNFα to be administered to maximise the chances of visualising changes in neutrophil behaviour under flow conditions. From preliminary data, treatment of HUVECs for 4 hours with a dose of 100 U/ml was deemed sufficient in seeing significant changes in neutrophil behaviour under flow conditions (data not shown) and correlated with previous cytokine stimulation data published by our group (Munir et al., 2015).

Initial experiments targeted endothelial ADAM10 using a gene knockdown approach. The flow adhesion assay was performed as previously described (Section 3.2.1.1), except isolated human neutrophils were used instead of PBLs. Respective neutrophil behaviours were counted and total adhesion values were calculated, as explained earlier. Knockdown of endothelial ADAM10 had no effect on neutrophil rolling, arrest and transmigration (Figure 3.7 A & B). In addition, neutrophil adhesion was unaffected by endothelial ADAM10 knockdown (Figure 3.7 C). ADAM10 knockdown efficiency was assessed by flow cytometry, as previously described and was ~90% reduced upon quantitation (Figure 3.7 D & E). In addition, neutrophil velocity behaviour was analysed, and found to be similar to that observed with PBLs, showing knockdown of endothelial ADAM10 did not alter neutrophil rolling, firmly adherent or transmigrated velocities (Table 3.3).

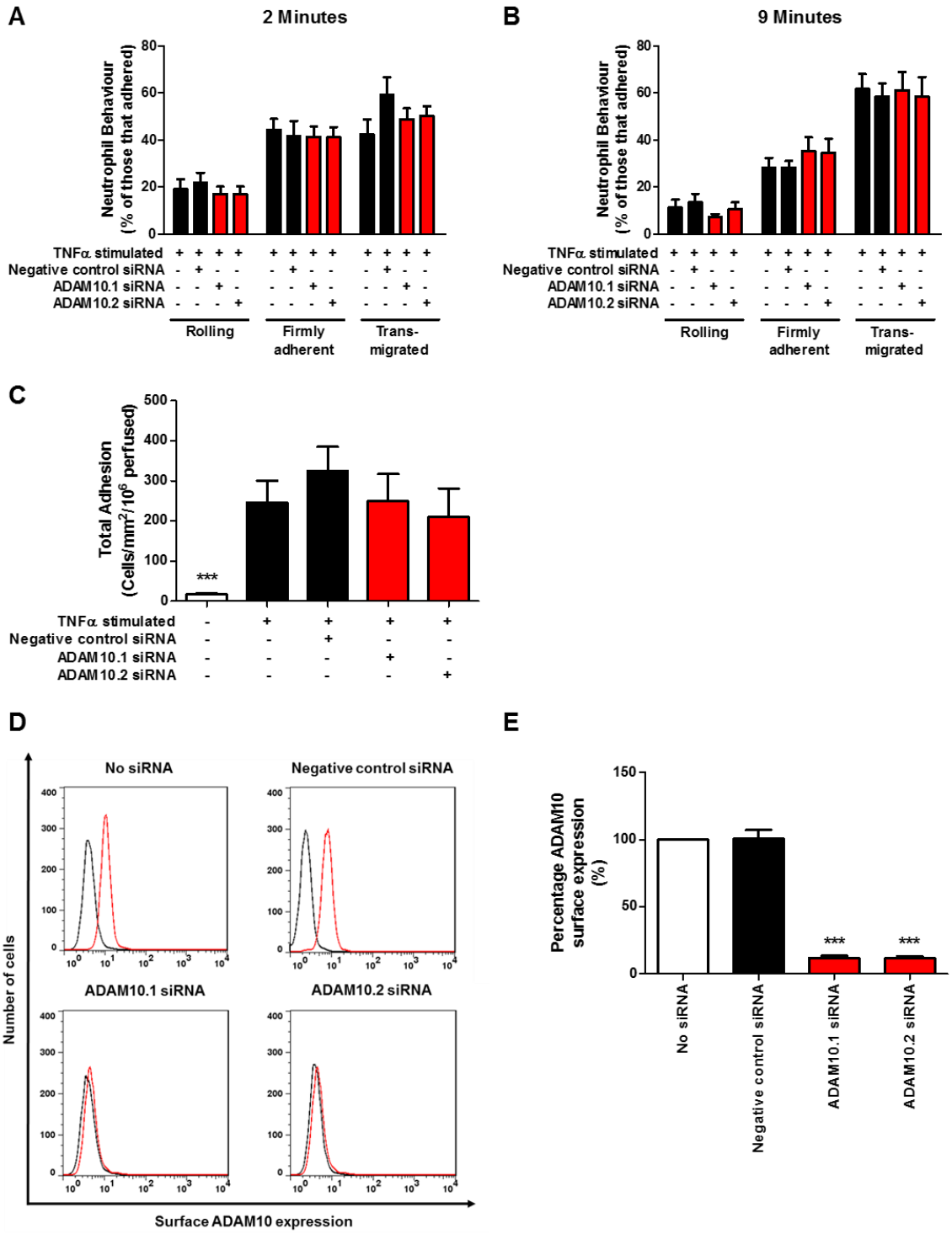
A
2 Minutes
Neutrophil Behaviour (% of those that adhered)
TNFα stimulated
Negative control siRNA
ADAM10.1 siRNA
ADAM10.2 siRNA
Rolling
Firmly adherent
Trans-migrated
B
9 Minutes
C
Total Adhesion (Cells/mm²/10⁶ perfused)
***
D
No siRNA
Negative control siRNA
ADAM10.1 siRNA
ADAM10.2 siRNA
Number of cells
Surface ADAM10 expression
E
Percentage ADAM10 surface expression (%)
No siRNA
Negative control siRNA
ADAM10.1 siRNA
ADAM10.2 siRNA

Figure 3.7 Knockdown of endothelial ADAM10 does not alter the ability of neutrophils to transmigrate under *in vitro* flow conditions. HUVECs were transfected with two different siRNA duplexes to ADAM10 (red bars) alongside a non-specific siRNA (black bars) as explained in the legend to Figure 3.1. After 24 hours, the HUVECs were stimulated with 100 U/ml TNFα along for 4 hours. Freshly isolated neutrophils were then perfused over the pre-activated HUVEC monolayer at 0.05Pa in PBSA for 4 minutes. Video recordings of five different fields of view of the endothelial monolayer were made using time-lapse video microscopy at two-minutes (A) or nine-minutes (B) post perfusion of neutrophils, respectively. Neutrophils were classified as rolling, firmly adherent or transmigrated. The total number of cells classified for each of the behaviours were combined to give a total adhesion count (C). HUVECs transfected with siRNA were analysed by flow cytometry to measure surface ADAM10 expression. The red line represents ADAM10 staining and the black line isotype control staining (D). Surface ADAM10 levels from panel E were quantitated and normalised to the 'No siRNA' treated condition (E). Error bars represent the standard error of the mean from seven independent experiments. Data were normalised by arcsine transformation and statistically analysed by a one-way ANOVA and Dunnett's post-hoc comparisons test for total adhesion and knockdown confirmation (***$p < 0.001$ compared to Negative control siRNA data) or by a two-way ANOVA and Bonferroni post-hoc comparisons test for cell behaviours.

Condition	Rolling velocity ($\mu m\ sec^{-1}$)	Firmly adherent velocity ($\mu m\ min^{-1}$)	Transmigrated velocity ($\mu m\ min^{-1}$)
No siRNA	6.17 ± 0.24	5.25 ± 0.56	15.21 ± 1.20
Negative control siRNA	6.15 ± 0.60	5.67 ± 1.15	13.56 ± 1.11
ADAM10.1 siRNA	6.39 ± 0.36	4.26 ± 0.78	16.29 ± 0.73
ADAM10.2 siRNA	6.49 ± 0.33	4.67 ± 0.92	15.22 ± 1.09

Table 3.3 Knockdown of endothelial ADAM10 has no effect on neutrophil velocities. Neutrophil velocities were tracked using ImagePro cell tracking software as described in the legend to Table 3.1. Values represented are mean ± standard error of 20, 30, or 70 tracked cells for rolling, firmly adherent or transmigrated conditions over three to seven different experiments, respectively.

The endothelial ADAM10 knockdown data findings were further confirmed by repeating the assays but this time HUVECs were treated with either 0.02% DMSO or 20 µM GI254023X for 24 hours. Neutrophils were isolated as previously described and the flow assay was carried out. Neutrophil behaviours were analysed, as explained previously. Inhibition of HUVEC-expressed ADAM10 mimicked the phenotype observed when HUVEC-expressed ADAM10 was knocked down. Inhibition of HUVEC-expressed ADAM10 did not alter the ability of neutrophils to transmigrate (Figure 3.8 A & B). Similarly, inhibition of HUVEC-expressed ADAM10 had no effect on neutrophil total adhesion (Figure 3.8 C) or neutrophil velocity behaviours (Table 3.4).

Neutrophil recruitment is regulated by multiple cytokines. To investigate if the responses observed following endothelial ADAM10 inhibition were cytokine dependent, the recruitment and transmigration of neutrophils to IL-1β stimulated HUVECs was investigated. For these assays, HUVECs were grown to confluence in Ibidi microslides as previously described. Instead of treating the cells with TNFα, the cells were treated with 5 ng/ml IL-1β for 4 hours in addition to treatment of the endothelium with either the ADAM10 inhibitor or DMSO control, as previously described. The Ibidi microslide was incorporated into a flow assay and respective neutrophil behaviours were recorded. Neutrophils underwent normal recruitment and transmigration on IL-1β stimulated HUVECs and no differences were observed when endothelial ADAM10 was inhibited (Figure 3.8 D & E). Moreover, no difference in neutrophil total adhesion was observed when endothelial ADAM10 was inhibited (Figure 3.8 F).

These data confirm, by using two different modes of targeting endothelial ADAM10 (pharmacological or siRNA knockdown), that neutrophil recruitment and transmigration in *in vitro* models of TNFα-induced or IL-1β-induced inflammation is independent of endothelial ADAM10.

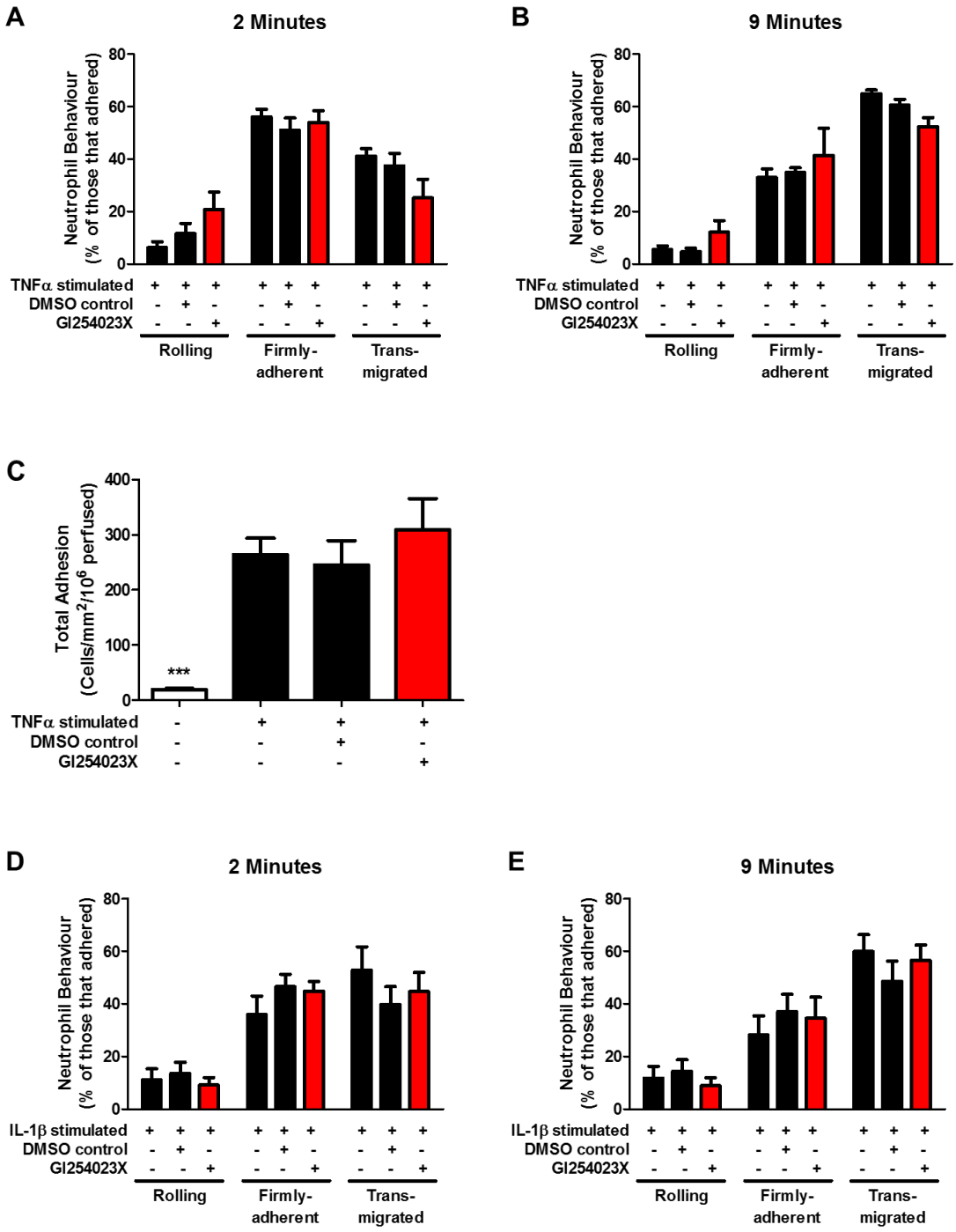
A
2 Minutes
Neutrophil Behaviour (% of those that adhered)
TNFα stimulated
DMSO control
GI254023X
Rolling
Firmly-adherent
Trans-migrated
B
9 Minutes
C
Total Adhesion (Cells/mm²/10⁶ perfused)
***
D
2 Minutes
IL-1β stimulated
E
9 Minutes

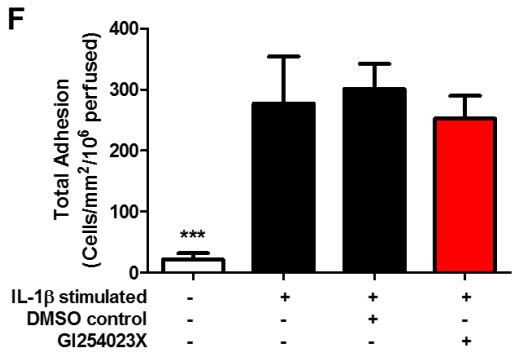

Figure 3.8 Inhibition of endothelial ADAM10 does not alter the ability of neutrophils to transmigrate under *in vitro* flow conditions. HUVECs were plated into 6-well Ibidi slides. Once confluent, the HUVECs were treated with either 0.02% DMSO (black bar) or 20 μM GI254023X (red bar) for 24 hours in addition to being stimulated for the final 4 hours with TNFα as previously described in the legend for Figure 3.7 (A – C) or with 5 ng/ml IL-1β (D – F) before being incorporated into the flow adhesion assay to assess neutrophil adhesion and transmigration. Video recordings of neutrophil adhesion at specific time-points were made and analysed for neutrophil behaviours (A & B) and (D & E) along with total adhesion (C) and (F), as previously described in the legend for Figure 3.7. Error bars represent the standard error of the mean from five independent experiments. Data were normalised by arcsine transformation and statistically analysed by a one-way ANOVA and Dunnett's post-hoc comparisons test for total adhesion (***$p < 0.001$ compared to DMSO control data) or by a two-way ANOVA and Bonferroni post-hoc comparisons test for cell behaviours.

Condition		Rolling velocity (μm sec^{-1})	Firmly adherent velocity (μm min^{-1})	Transmigrated velocity (μm min^{-1})
HUVEC treatment	**-**	5.43 ± 0.56	3.44 ± 0.44	12.75 ± 2.93
	DMSO control	4.54 ± 0.56	4.23 ± 0.84	13.94 ± 2.04
	GI254023X	5.32 ± 0.45	3.23 ± 0.21	15.98 ± 1.34
Neutrophil treatment	**DMSO control**	4.67 ± 0.23	4.12 ± 0.45	16.73 ± 0.19
	GI254023X	5.34 ± 0.94	3.20 ± 0.38	14.30 ± 1.29

Table 3.4 Inhibition of endothelial or neutrophil-expressed ADAM10 has no effect on neutrophil velocities under TNFα stimulated conditions. Neutrophil velocities were tracked using ImagePro cell tracking software and as explained in the legend to Table 3.1. Values represented are mean ± standard error of 45, 30, or 50 tracked cells for rolling, firmly adherent or transmigrated conditions over three to five different experiments, respectively.

Condition		Rolling velocity (μm sec^{-1})	Firmly adherent velocity (μm min^{-1})	Transmigrated velocity (μm min^{-1})
HUVEC treatment	**-**	7.09 ± 1.22	5.04 ± 1.06	14.63 ± 0.85
	DMSO control	6.62 ± 0.90	5.63 ± 1.04	14.98 ± 0.87
	GI254023X	6.63 ± 0.66	4.07 ± 0.40	16.00 ± 0.67
Neutrophil treatment	**DMSO control**	6.81 ± 0.54	3.73 ± 0.71	14.45 ± 1.01
	GI254023X	7.34 ± 1.83	4.45 ± 2.20	14.47 ± 2.49

Table 3.5 Inhibition of endothelial or neutrophil-expressed ADAM10 has no effect on neutrophil velocities under IL-1β stimulated conditions. Netrophil velocities were tracked using ImagePro cell tracking software and as explained in the legend to Table 3.1. Values represented are mean ± standard error of 15, 20, or 40 tracked cells for rolling, firmly adherent or transmigrated conditions over three to four different experiments, respectively.

To determine whether ADAM10 expressed on neutrophils has a role in regulating the recruitment and transmigration of neutrophils, neutrophil ADAM10 activity was targeted using the ADAM10 inhibitor. For these experiments, isolated neutrophils were treated with either 0.02% DMSO or with 20 µM GI254023X for 30 minutes at room temperature before being incorporated into the flow assay. In addition, 20 µM GI254023X was also added to the wash buffer to prevent dilution of the inhibitor treated neutrophils during perfusion. Inhibition of neutrophil-expressed ADAM10 did not alter the ability of neutrophils to transmigrate under flow conditions. No differences in neutrophil behaviour were observed when neutrophil-expressed ADAM10 was inhibited (Figure 3.9 A & B). In addition, there was no difference in total adhesion when neutrophil-expressed ADAM10 was inhibited (Figure 3.9 C). Moreover, no changes in neutrophil velocity behaviour were observed following inhibition of neutrophil-expressed ADAM10 (Table 3.4).

In addition, the recruitment and transmigration of ADAM10 inhibited neutrophils to IL-1β stimulated HUVECs was unaltered (Figure 3.9 D & E). Similarly, no differences in neutrophil total adhesion were observed (Figure 3.9 F). When looking at neutrophil velocities on IL-1β stimulated HUVECs, no differences were observed in neutrophil rolling, firmly adherent or transmigrated velocities following neutrophil ADAM10 inhibition or endothelial ADAM10 inhibition (Table 3.5).

Taken together, these results show that neutrophil recruitment and transmigration is independent of neutrophil-expressed ADAM10 under *in vitro* models of TNFα and IL-1β induced inflammation.

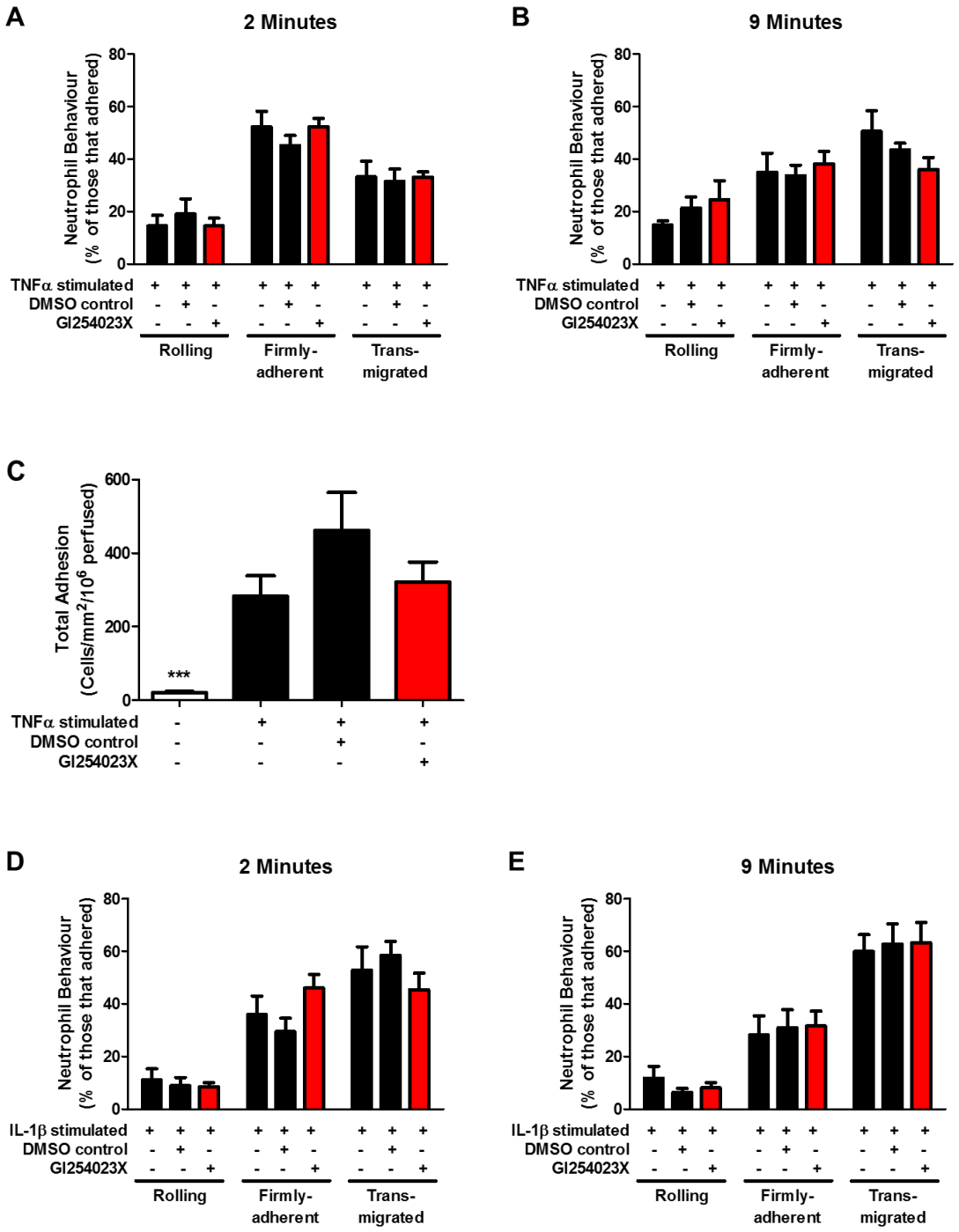
A
2 Minutes
Neutrophil Behaviour (% of those that adhered)
TNFα stimulated
DMSO control
GI254023X
Rolling
Firmly-adherent
Trans-migrated
B
9 Minutes
C
Total Adhesion (Cells/mm2/10^6 perfused)
***
D
IL-1β stimulated
E

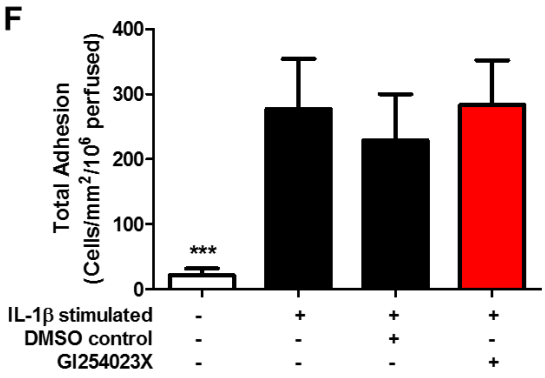

Figure 3.9 Inhibition of neutrophil-expressed ADAM10 does not alter neutrophil transmigration under *in vitro* flow conditions. HUVECs were plated into 6-well Ibidi slides. Once confluent, the HUVECs were stimulated as previously described in the legend for Figure 3.7 (A – C) or with 5 ng/ml IL-1β (D – F) before being incorporated into the flow adhesion assay to assess neutrophil adhesion and transmigration. For ADAM10 inhibitor or DMSO conditions, neutrophils were pre-incubated with either 20 µM GI254023X (red bar) or 0.02% DMSO (black bar) for 30 minutes prior to being incorporated into the flow adhesion assay. In addition, 20 µM GI254023X was added to the wash buffer when perfusing ADAM10 inhibited neutrophils to prevent dilution of the inhibitor. Video recordings of neutrophil adhesion at specific time-points were made and analysed for neutrophil behaviours (A & B) and (D & E) along with total adhesion (C) and (F), as previously described in the legend for Figure 3.7. Error bars represent the standard error of the mean from four independent experiments. Data were normalised by arcsine transformation and statistically analysed by a one-way ANOVA and Dunnett's post-hoc comparisons test for total adhesion (***$p < 0.001$ compared to DMSO control data) or by a two-way ANOVA and Bonferroni post-hoc comparisons test for cell behaviours.

The data presented in this chapter has so far shown that endothelial ADAM10 regulates the efficient transmigration of PBLs but not neutrophils. Indeed, neutrophils are known to release proteolytic enzymes upon their activation (for example, neutrophil elastase), which can act locally to degrade junctional proteins, thereby facilitating their transmigration (Pham, 2008). In order to elucidate the differences observed between neutrophil transmigration and PBL transmigration following endothelial ADAM10 inhibition, the effects of inhibiting neutrophil elastase was investigated. For these assays, HUVECs were treated with the ADAM10 inhibitor and stimulated as previously described. Either untreated neutrophils or neutrophils that had previously been treated with 100 µg/ml α_1-antitrypsin (an inhibitor to neutrophil elastase release) for 30 minutes at room temperature, were perfused over the pre-activated HUVECs and respective neutrophil behaviours were recorded and analysed. Treatment of neutrophils with α_1-antitrypsin significantly reduced the ability of neutrophils to transmigrate over TNFα stimulated HUVECs. This was accompanied by a subsequent increase in the number of firmly adherent neutrophils on the surface of HUVECs (Figure 3.10 A & B). Similar to the findings in Figure 3.9, inhibition of endothelial ADAM10 did not affect the ability of neutrophils to transmigrate (Figure 3.10 A & B). α_1-antitrypsin treatment reduced the migration of neutrophils over ADAM10 inhibited HUVECs or DMSO treated HUVECs equally (Figure 3.10 A & B). No differences in neutrophil total adhesion following α_1-antitrypsin treatment of neutrophils were observed (Figure 3.10 C). In addition, neutrophil velocities were unaltered following treatment of neutrophils with α_1-antitrypsin (Table 3.6).

These data suggest that the lack of an effect of endothelial ADAM10 inhibition on neutrophil transmigration is not because neutrophils use serine proteases such as neutrophil elastase to overcome this.

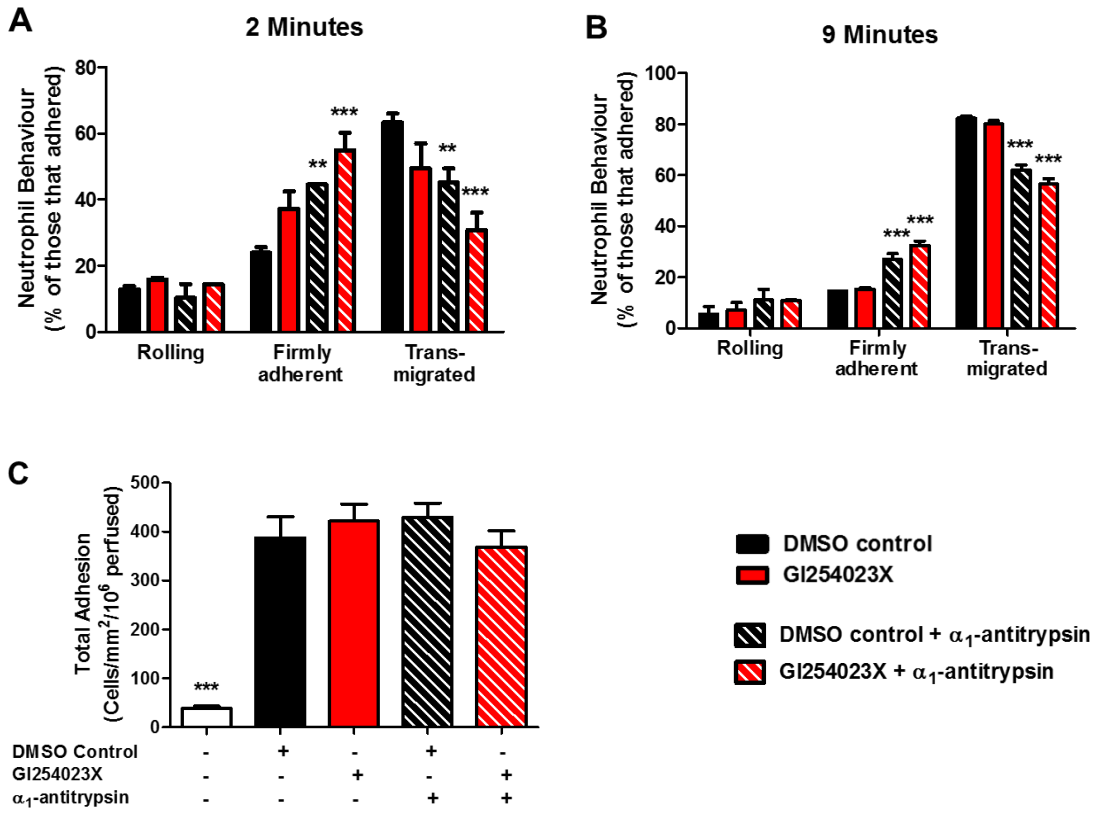

Figure 3.10 Inhibition of serine protease activity suppresses neutrophil transmigration independently of endothelial ADAM10 inhibition under *in vitro* flow conditions. HUVECs were plated into 6-well Ibidi microslides. Once confluent, the HUVECs were treated either with 20 µM GI254023X or 0.02% DMSO for 24 hours. For the remaining 4 hours, HUVECs were treated with 100U/ml TNFα before being incorporated into the flow assay. Neutrophils were isolated and purified as explained in the legend to Figure 3.7. Separately, neutrophils were incubated with 100 µg/ml α_1-antitrypsin for 30 minutes before being perfused in the flow assay. In addition, α_1-antitrypsin treated neutrophils were perfused in wash buffer containing 100 µg/ml α_1-antitrypsin to prevent dilution of the inhibitor. Video recordings of neutrophil adhesion at specific time-points were made and analysed for neutrophil behaviours (A) and (B) along with total adhesion (C), as previously described in the legend for Figure 3.7. Error bars represent the standard error of the mean from four independent experiments. Data were normalised by arcsine transformation and statistically analysed by a one-way ANOVA and Dunnett's post-hoc comparisons test for total adhesion (***$p < 0.001$ compared to DMSO control data) or by a two-way ANOVA and Bonferroni post-hoc comparisons test for cell behaviours (**$p < 0.01$, ***$p < 0.001$ compared to DMSO control data). When comparing differences between ADAM10 treated and DMSO treated endothelial cells following neutrophil α_1-antitrypsin treatments, a Students *t*-test was used.

Condition		Rolling velocity (μm sec^{-1})	Firmly adherent velocity (μm min^{-1})	Transmigrated velocity (μm min^{-1})
No treatment	**DMSO control**	5.29 ± 0.77	2.13 ± 0.30	15.61 ± 1.03
	GI254023X	5.30 ± 0.75	2.24 ± 0.41	17.15 ± 1.36
α_1-antityrpsin treatment	**DMSO control**	6.35 ± 1.01	2.14 ± 0.11	12.23 ± 1.06
	GI254023X	5.52 ± 2.05	1.92 ± 0.23	12.05 ± 1.81

Table 3.6 Inhibition of endothelial or neutrophil-expressed ADAM10 in the presence of α_1-anti-trypsin treatment has no effect on neutrophil velocities. Neutrophil velocities were tracked using ImagePro cell tracking software and as explained in the legend to Table 3.1. Values represented are mean ± standard error of 15, 20, or 40 tracked cells for rolling, firmly adherent or transmigrated conditions over three to four different experiments, respectively.

3.2.2.2 Monocyte recruitment and transmigration is independent of ADAM10

Monocytes are myeloid cells which have been implicated in driving many chronic inflammatory diseases such as atherosclerosis. To investigate the role of endothelial ADAM10 in regulating the transmigration of monocytes, an *in vitro* static adhesion assay was utilised. This assay has previously been well characterised to measure key monocyte-endothelial interactions that are important in deciphering optimal monocyte adhesion and transmigration (Woodfin et al., 2011). A HUVEC monolayer was treated with either 20µM GI254023X or 0.02% DMSO for 24 hours and stimulated with 100 U/ml TNFα for the final four hours. Monocytes were isolated from peripheral blood mononuclear cells (PBMCs) by passing through $CD14^+$ MACS columns to select for $CD14^+$ monocytes. Isolated monocytes were washed and used at $1x10^5$/ml. Monocytes were co-incubated with HUVECs for 7 minutes at 37°C. Non-adherent monocytes were washed off and HUVEC monolayers were fixed using 2% formaldehyde. Respective monocyte behaviours were counted and total adhesion values calculated, as explained for previous static adhesion assays.

Inhibition of endothelial ADAM10 had no effect on monocyte transmigration (Figure 3.11 A). In addition, monocyte adhesion was unaffected by endothelial ADAM10 inhibition (Figure 3.11 B). Inhibition of monocyte-expressed ADAM10 did not alter the ability of monocytes to transmigrate (Figure 3.12 A). Similarly, no differences in monocyte total adhesion were observed following monocyte-ADAM10 inhibition (Figure 3.12 B).

These data suggest that monocyte adhesion and transmigration is independent of endothelial or monocyte-expressed ADAM10 under conditions of TNFα induced inflammation.

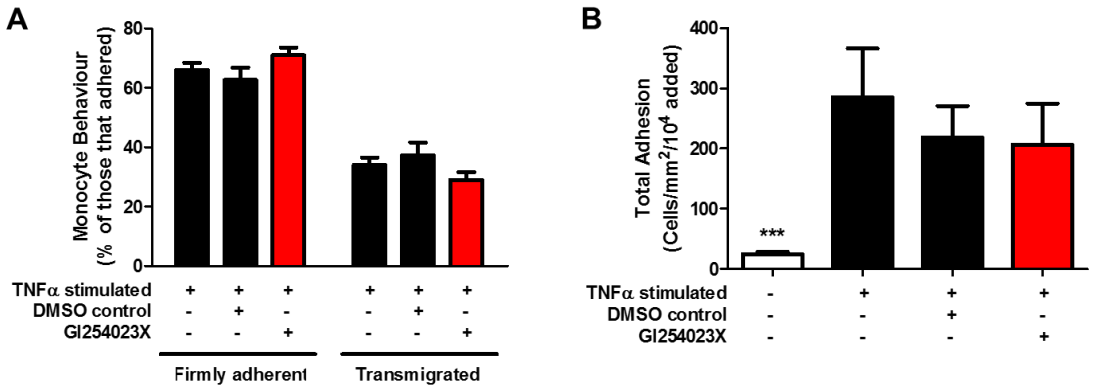

Figure 3.11 Inhibition of endothelial ADAM10 does not alter the ability of monocytes to transmigrate under *in vitro* static conditions. Confluent HUVECs were stimulated with 100U/ml TNFα along with either 0.02% DMSO (black bar) or 20µM GI254023X (red bar) for 24 hours. Freshly isolated monocytes were then added to the pre-activated HUVEC monolayer in M199+BSA and incubated at 37°C for 7 minutes. Video-recordings of five different fields of view of the endothelial monolayer were made using phase-contrast video microscopy. Monocytes were classified as firmly adherent or transmigrated (A). The total number of cells classified for each of the behaviours were combined to give a total adhesion count (B). Error bars represent the standard error of the mean from three independent experiments. Data were normalised by arcsine transformation and statistically analysed by a one-way ANOVA and Dunnett's post-hoc comparisons test for total adhesion (***$p < 0.001$ compared to DMSO control data) or by a two-way ANOVA and Bonferroni post-hoc comparisons test for cell behaviours.

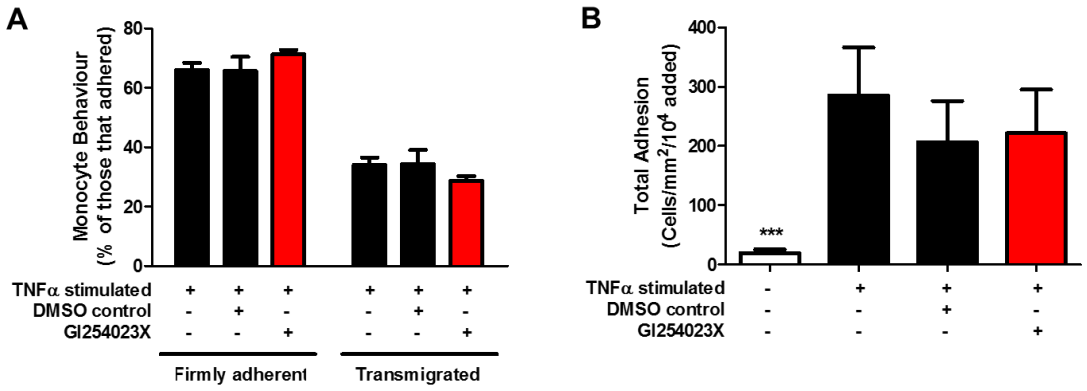

Figure 3.13 Inhibition of monocyte-expressed ADAM10 does not alter the ability of monocytes to transmigration under *in vitro* static conditions. Confluent HUVECs were stimulated with 100U/ml TNFα along for 24 hours. Freshly isolated monocytes were then added to the pre-activated HUVEC monolayer in M199+BSA and incubated at 37°C for 7 minutes. Separately, monocytes were incubated with either 0.02% DMSO (black bar) or 20µM GI254023X (red bar) for 30 minutes prior to being added to the pre-activated HUVEC monolayer. Video-recordings of five different fields of view of the endothelial monolayer were made using phase-contrast video microscopy. Monocytes were classified as firmly adherent or transmigrated (A). The total number of cells classified for each of the behaviours were combined to give a total adhesion count (B). Error bars represent the standard error of the mean from three independent experiments. Data were normalised by arcsine transformation and statistically analysed by a one-way ANOVA and Dunnett's post-hoc comparisons test for total adhesion (***$p < 0.001$ compared to DMSO control data) or by a two-way ANOVA and Bonferroni post-hoc comparisons test for cell behaviours.

3.3 DISCUSSION

Migration of leukocytes through vessel walls to sites of inflammation is an important component of the hosts' immune response against pathogens and tissue injury. The role of proteolytic shedding of key CAMs and transmembrane inserted chemokines by metalloproteases belonging to the ADAM family has been shown to potentially regulate transendothelial migration of leukocytes. However, many studies have utilised cell line models and transfected cells to overexpress specific transmembrane proteins under non-physiological static conditions to decipher the role of proteolytic shedding in leukocyte adhesion and transmigration (Hundhausen et al., 2007; Schwarz et al., 2010; Schulz et al., 2008). As such, the role of proteolytic shedding in primary cells under physiological flow conditions is still largely unknown. In this chapter, the role of one ADAM member, termed ADAM10, in supporting and facilitating leukocyte transmigration during inflammation was investigated *in vitro*.

The data presented in this chapter highlights a role of endothelial ADAM10 in regulating the efficient transmigration of lymphocytes under physiological flow conditions and static adhesion conditions. These findings are in line with previously published data that showed a role of endothelial ADAM10 in regulating the transmigration of cultured human T cells pre-activated with the mitogen phytohaemagglutinin (PHA). In these assays, the authors co-incubated PHA blast T cells with unstimulated HUVECs treated with the ADAM10 inhibitor (GI254023X) and monitored T cell migration in a static transwell assay (Schulz et al., 2008). Inhibition of endothelial ADAM10 was shown to reduce the transmigration of PHA blast T cells (Schulz et al., 2008). Furthermore, the authors also targeted endothelial ADAM10 using siRNA and showed a similar reduction in the ability of PHA blast T cells to transmigrate (Schulz et al., 2008). In addition to this study, a separate study by Schwarz et al. showed that knockdown of endothelial ADAM10 regulated the adhesion of the L1.2 pre-B cell line, stably transfected with CX3CR1, on TNFα/IFNγ stimulated HUVECs (Schwarz et al., 2010). In line with these observations,

data presented in this chapter further confirms a role of endothelial ADAM10 in lymphocyte transmigration under static conditions, in addition to under physiological flow conditions, in a well-characterised model of TNFα/IFNγ-induced inflammation.

Targeting of ADAM10 on PHA blast T cells has also been shown to reduce the ability of lymphocytes to transmigrate under static conditions (Schulz et al., 2008). To see if similar observations could be seen under physiological flow conditions, ADAM10 expressed on primary PBLs was targeted using the ADAM10 inhibitor. Inhibition of ADAM10 on PBLs did not alter the ability of PBLs to transmigrate under flow or static conditions in a model of TNFα/IFNγ-induced inflammation. It is possible to speculate that the difference observed between the data presented in this chapter and the published data by Schulz et al. could be down to nature of the adhesion assay along with the use of primary human lymphocytes versus cultured lymphocytes. Indeed, Schulz et al. showed that transmigration of the PHA blast T cells was reduced following co-incubation for 24 hours whilst the adhesion assays used in this chapter only lasted for 13 minutes. In addition, the culture condition of PHA blast T cells requires stimulation of these cells with interleukin-2, which changes the repertoire of proteins at the cell surface, compared to PBLs. For example, PHA blast T cells have been shown to upregulate the expression of the $\alpha_L\beta_2$ integrin that supports adhesion on endothelial ICAM-1 (McGettrick et al., 2009) whilst PBLs utilise $\alpha_4\beta_1$ for their optimal adhesion (Ahmed et al., 2011).

In the present study, a detailed analysis of ADAM10's role in neutrophil recruitment and transmigration was carried out. Knockdown or inhibition of endothelial ADAM10 did not affect neutrophil recruitment on TNFα or IL-1β stimulated HUVECs under flow conditions. However, previously published data by Dreymueller et al. showed that knockdown of ADAM10 expression in human lung microvascular endothelial cells decreased the transmigration of human neutrophils towards the chemokine interleukin-8, in a static transwell chemotaxis model (Dreymueller et al., 2012a). TNFα stimulation of primary HUVECs has been shown to promote the release of interleukin-8 from HUVECs, which

supports neutrophil adhesion (Luu et al., 2000). However, under physiological conditions, neutrophils also require engagement of specific CAMs, which facilitate their efficient attachment and motility, and therefore differences between chemotactic assays (e.g. IL-8 stimulation) and adhesion assays (e.g. TNFα stimulation) may overcome any differences in neutrophil transmigration that are observed following endothelial ADAM10 knockdown or inhibition. For example, chemotaxis assays largely rely on the directional movement of leukocytes towards a specific stimulus and this process takes a substantially longer time compared to neutrophil adhesion, which is a rapid response occurring within a few minutes of initiation (Nourshargh et al., 2010).

Following on from the findings that endothelial ADAM10 does not regulate the transmigration of neutrophils, the role of neutrophil-expressed ADAM10 in facilitating neutrophil transmigration was investigated. Inhibition of ADAM10 (using GI254023X) on human neutrophils reduced the transmigration of neutrophils on ECV304 cells towards intrerleukin-8. This phenotype was associated with a decrease in neutrophil adhesion to fibronectin but not ICAM-1, and a decrease in chemokine-induced upregulation of α_5-integrin (Pruessmeyer et al., 2014). It is worth noting that ECV304 cells are not endothelial cells since they lack the expression of key endothelial markers such as VE-cadherin (Kiessling et al., 1999) and therefore are regarded as poor tools for assessing leukocyte adhesion and transmigration. Furthermore, deletion of ADAM10 in the haematopoietic lineage using a *vav* promoter caused a decrease in neutrophil transmigration in the lungs following LPS challenge *in vivo*. This suppression in transmigration was associated with a reduction in Rho GTPase activation and a reduction in actin polymerisation, thereby hindering neutrophil transmigration in ADAM10-deficient cells (Dreymueller et al., 2014). The differences observed following ADAM10 inhibition in the present study and previously published data on the deletion of ADAM10 under *in vitro* and *in vivo* conditions might be best explained through the use of different inflammatory models. Indeed, previously published studies of ADAM10s role in neutrophil

transmigration have focused on acute inflammatory models in response to bacterial challenge using LPS and the data presented in this chapter has focused on the use of cytokine-induced inflammation. Many differences between *in vivo* and *in vitro* models of inflammation have been reported concerning neutrophil transmigration. In line with the inflammatory model used in the present study, *in vitro* studies have largely focussed on neutrophil interactions with cultured endothelial cell monolayers without considering the tissue stroma and other vessel wall components, which are increasingly becoming more important in modulating endothelial cell function during neutrophil transmigration (Proebstl et al., 2012). In addition, visualising neutrophil transmigration in the cremasteric tissue in response to pro-inflammatory cytokines *in* vivo has revealed that the process of neutrophil transmigration takes longer (~15-45 minutes) compared to *in vitro* models using the same pro-inflammatory cytokines (~2 minutes) (Woodfin et al., 2009). The difference between *in vitro* and *in vivo* models prompts further investigation to elucidate the role of endothelial ADAM10 in neutrophil transmigration by using mice with a specific deletion of ADAM10 in the endothelial lineage.

The data presented in the current chapter highlighted a role of endothelial ADAM10 in regulating the transmigration of PBLs but not neutrophils. To investigate the differences observed between neutrophil and lymphocyte transmigration following endothelial ADAM10 inhibition, the role of neutrophil derived proteases was investigated. Neutrophils are well documented to contain large pools of intracellular proteases that are rapidly released upon activation (Pham, 2008), whilst lymphocytes have considerably smaller pools of such proteases. Indeed, the release of neutrophil derived proteases such as neutrophil elastase upon neutrophil activation may degrade key junctional proteins, such as VE-cadherin, thereby aiding the transmigration of neutrophils (Hermant et al., 2003). As such, the aim was to determine if inhibiting neutrophil elastase release caused neutrophils to become dependent on endothelial ADAM10 to facilitate their transmigration. Pre-treatment of neutrophils with a neutrophil elastase inhibitor (α_1-antitrypsin), reduced

the transmigration of neutrophils independently of endothelial ADAM10 inhibition. This data suggests that neutrophils are able to utilise other mechanisms such as the release of neutrophil elastase to overcome the endothelial barrier during neutrophil transmigration in the presence of ADAM10 inhibition. Moreover, activation of neutrophils has been shown to release MMPs such as MMP9, which facilitates the migration of neutrophils through the endothelial and venular basement membrane barriers (Stefanidakis et al., 2004). The differences in proteolytic composition between leukocyte subsets might allow certain leukocytes, such as neutrophils, to migrate more readily, independently of changes in vascular integrity (Hermant et al., 2003; Nourshargh and Marelli-Berg, 2005).

Under pro-inflammatory conditions, monocytes also undergo recruitment and transmigration and therefore could be regulated by ADAM10. The findings in this chapter showed that human primary monocyte transmigration was independent of ADAM10. Inhibition of either ADAM10 expressed on monocytes or on HUVECs did not alter the transmigration of monocytes on TNFα stimulated HUVECs. This was not supported by data from Tsubota *et al*. which showed that knockdown of ADAM10 on HUVECs suppressed the transmigration of $CD14^+$ monocytes in a transwell static assay (Tsubota et al., 2013). Furthermore, data from Tsubota et al. highlighted a role of monocyte-expressed ADAM17, which regulated the surface expression of the leukocyte-integrin complex, Mac-1 that supports monocyte transmigration (Tsubota et al., 2013). Knockdown of ADAM17 or ADAM10 on human monocytes was associated with a reduction in the release of the Mac-1 integrin complex. This correlated with prolonged migration of ADAM17 knocked down monocytes, but not ADAM10 knocked down monocytes, on TNFα-activated HUVECs, suggesting monocyte transmigration is independent of ADAM10 (Tsubota et al., 2013).

It is worth noting that the dosage of ADAM10 inhibitor used in the experiments in the present chapter was at 20 µM and previous studies have used the inhibitor at half the concentration (10 µM), and as such there is the possibility that the ADAM10 inhibitor

could be having off target effects at such a high dose. Nevertheless, the inhibitor data are consistent with the data from knockdown studies using two different siRNA duplexes.

In summary, this chapter describes a role for endothelial ADAM10 in regulating the transmigration of lymphocytes, but not neutrophils or monocytes, using *in vitro* physiological flow and static adhesion assays with primary HUVECs and leukocytes. To try to elucidate the mechanism by which ADAM10 regulates the transmigration of PBLs, the next chapter focused on the role of ADAM10 endothelial substrates that potentially regulate PBL transmigration.

CHAPTER 4

ADAM10 REGULATES LYMPHOCYTE TRANSMIGRATION BY REGULATING CELL SURFACE EXPRESSION LEVELS OF ITS SUBSTRATE VE-CADHERIN

4.1 INTRODUCTION

The mechanism by which endothelial ADAM10 promotes leukocyte transmigration, and in particular the substrate(s) involved, is not clear. Of the many substrates identified on endothelial cells that undergo proteolytic cleavage, only a handful are proteolytically processed by ADAM10. ADAM10-mediated leukocyte transmigration under inflammatory conditions has been shown to be regulated by endothelial cell substrates such as the two transmembrane chemokines, CX3CL1 and CXCL16, which regulate THP-1 monocyte transmigration (Hundhausen et al., 2007) or the adherens junctional protein, VE-cadherin, that regulates vascular permeability (Schulz et al., 2008). The aim of the present chapter was to extend the findings in Chapter 3 by determining the mechanism by which ADAM10 promoted PBL transmigration by elucidating whether a specific substrate accounts for the ADAM10 effect.

4.2 RESULTS

4.2.1 ADAM10 surface levels on endothelial cells are not affected by pro-inflammatory cytokine stimulation

Before experiments were conducted to determine whether individual substrates could be responsible for the role of ADAM10 in PBL transmigration, the expression levels of ADAM10 itself were assessed to determine whether cytokine stimulation of HUVECs had any effect. In these experiments, ADAM10 expression was measured by flow cytometry. As a control, HUVECs were transfected with either a non-silencing control siRNA or with one of two siRNA duplexes to ADAM10 at a final concentration of 10 nM (see Section 2.2.4.2). Following 24 hours after transfection, HUVECs were then stimulated with either 100U/ml TNFα alone or in combination with 10 ng/ml IFNγ or left unstimulated for a further 24 hours. Cytokine stimulation did not alter the relative surface expression of ADAM10 (Figure 4.1 A & B). The efficacy of the cytokine treatment was confirmed by upregulation of VCAM-1 expression (Figure 4.1 C & D). Specificity of the ADAM10 staining was confirmed by the significant reduction in expression levels following knockdown (Figure 4.1 A & B). This data suggests that ADAM10 surface levels are not regulated under conditions of TNFα or TNFα/IFNγ-induced pro-inflammatory conditions.

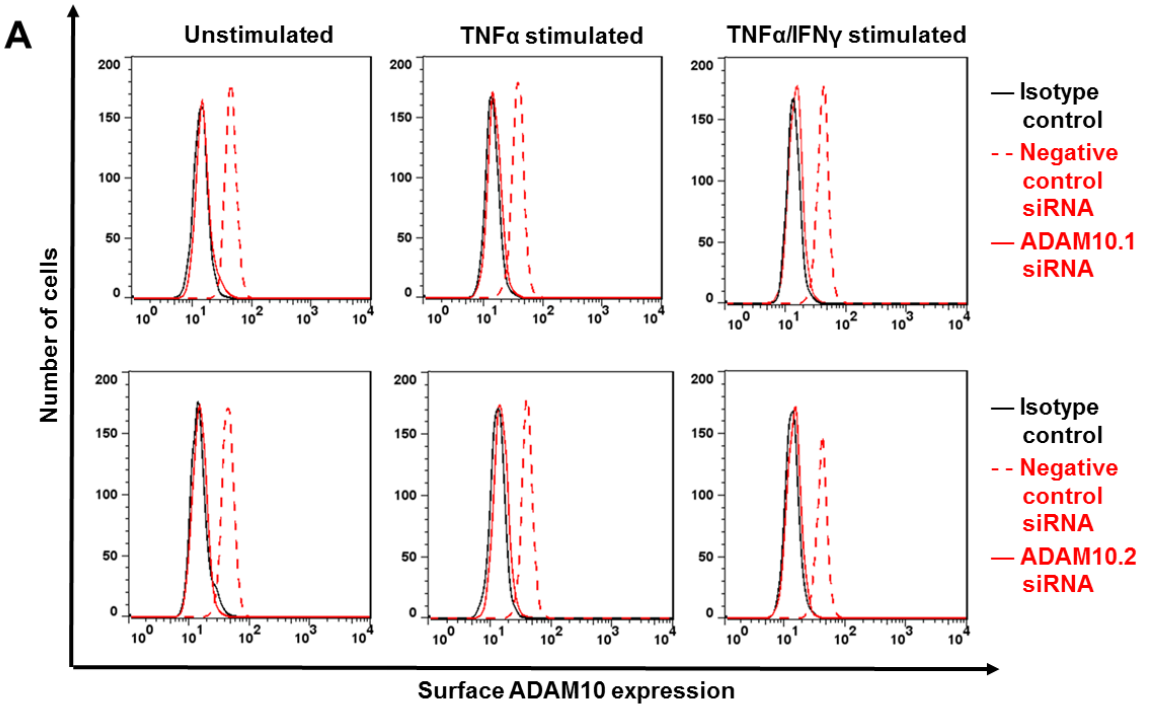
A
Unstimulated
TNFα stimulated
TNFα/IFNγ stimulated
Number of cells
Surface ADAM10 expression
— Isotype control
- - Negative control siRNA
— ADAM10.1 siRNA
— Isotype control
- - Negative control siRNA
— ADAM10.2 siRNA

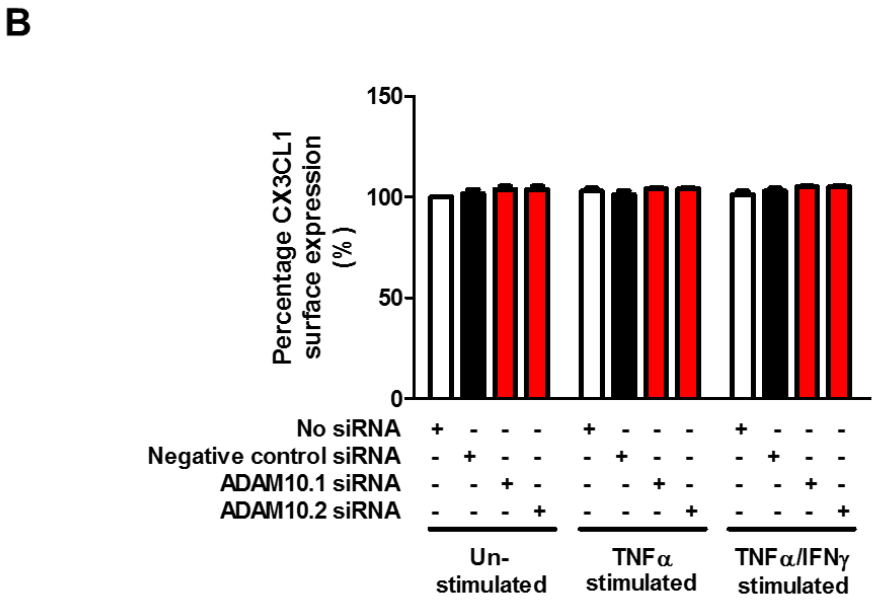
B
Percentage CX3CL1 surface expression (%)
No siRNA
Negative control siRNA
ADAM10.1 siRNA
ADAM10.2 siRNA
Un-stimulated
TNFα stimulated
TNFα/IFNγ stimulated

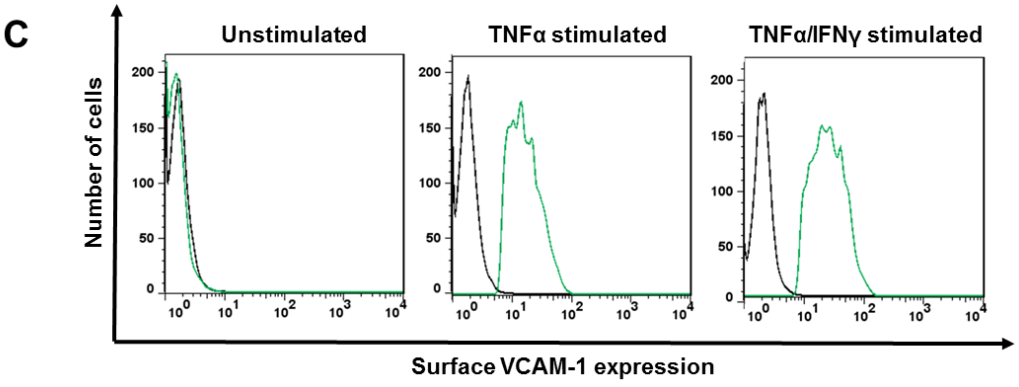
C
Unstimulated
TNFα stimulated
TNFα/IFNγ stimulated
Number of cells
Surface VCAM-1 expression

D

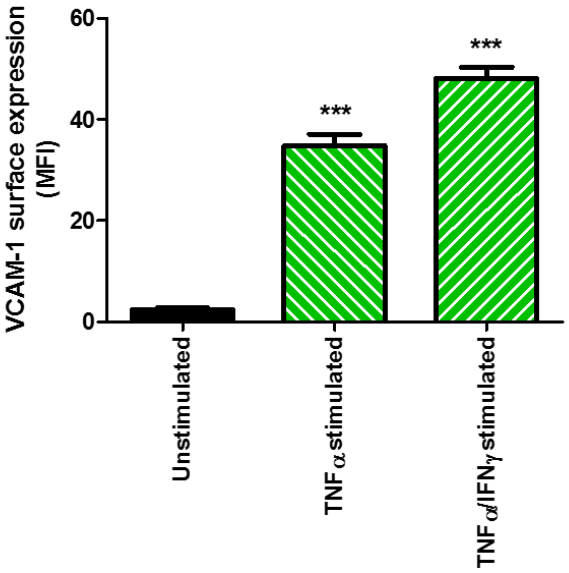

Figure 4.1 ADAM10 surface levels are not affected by cytokine stimulation. HUVECs were transfected with two different siRNA duplexes to ADAM10 alongside a non-specific siRNA at a final concentration of 10 nM. 24 hours after transfection, the HUVECs were stimulated with either 100 U/ml TNFα alone or in combination with 10 ng/ml IFNγ or left unstimulated. Following 24 hours of stimulation, HUVECs were dissociated with accutase and stained on ice for ADAM10 before being analysed by flow cytometry to measure surface ADAM10 expression. The broken red line represents ADAM10 staining of negative control siRNA transfected cells and the red line represents ADAM10 staining following ADAM10 knockdown. The black line represents isotype control staining (A). Surface ADAM10 levels from panel A were quantitated and normalised to the "No siRNA" treated condition (B). The effects of cytokine stimulation were confirmed by flow cytometry by staining for VCAM-1. The green line represents VCAM-1 staining and the black line represents isotype control staining (C). Surface VCAM-1 levels from panel C were quantitated (D). Error bars represent the standard error of the mean from five independent experiments. Data were analysed by One-way ANOVA followed by a Dunnett's multiple-comparisons post-hoc test (***$p < 0.001$).

4.2.2 The transmembrane chemokine CX3CL1 is expressed on HUVECs but CXCL16 is not

To begin to elucidate whether CX3CL1 and CXCL16 could be responsible for ADAM10's role in PBL transmigration, their expression on HUVECs was assessed by flow cytometry in the presence or absence of ADAM10 siRNA knockdown or following ADAM10 inhibition. CX3CL1 was expressed on the surface of HUVECs, but levels were not altered by ADAM10 knockdown and/or cytokine treatment (Figure 4.2 A & B). Consistent with the knockdown data findings, inhibition of ADAM10 did not alter the surface expression of CX3CL1 on HUVECs (Figure 4.2 C & D). In contrast to CX3CL1 expression, HUVECs seemed not to express CXCL16 (Figure 4.3). Moreover, the expression of CXCL16 was unaltered following ADAM10 knockdown or inhibition under the various cytokine stimulatory conditions (Figure 4.3 A & B). To rule out the possibility of the antibody not binding to CXCL16, HEK293T cells were transiently transfected with a human expression construct for CXCL16. A positive population of transfected cells was detected, indicating that the antibody detects CXCL16 (Figure 4.3 C).

Collectively, these results suggest that CX3CL1, but not CXCL16, is expressed on HUVECs. However, CX3CL1 is unlikely to be responsible for the role of ADAM10 in regulating PBL transmigration, because its levels are not affected by ADAM10 knockdown or inhibition.

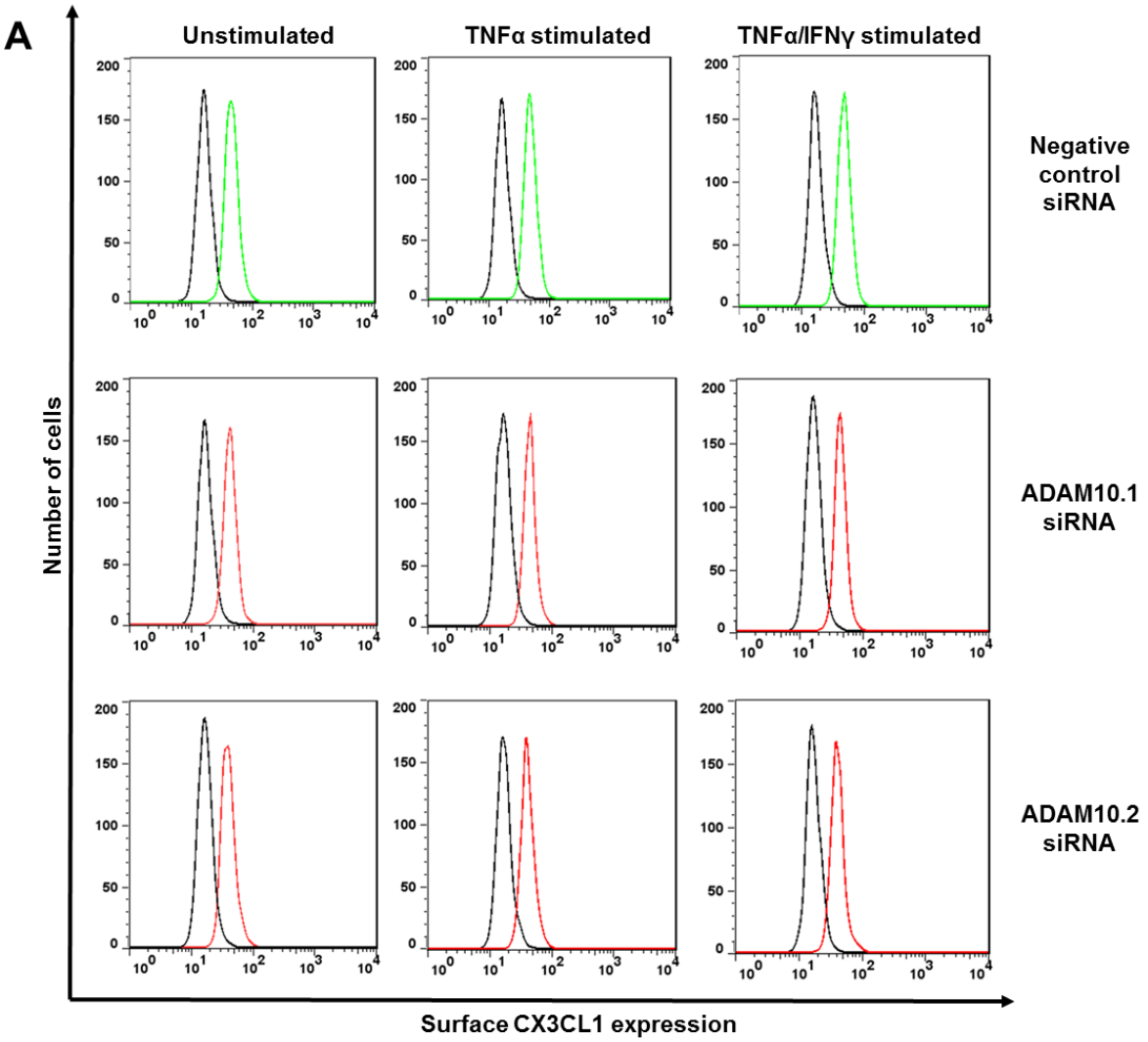
A
Unstimulated
TNFα stimulated
TNFα/IFNγ stimulated
Negative control siRNA
ADAM10.1 siRNA
ADAM10.2 siRNA
Number of cells
Surface CX3CL1 expression

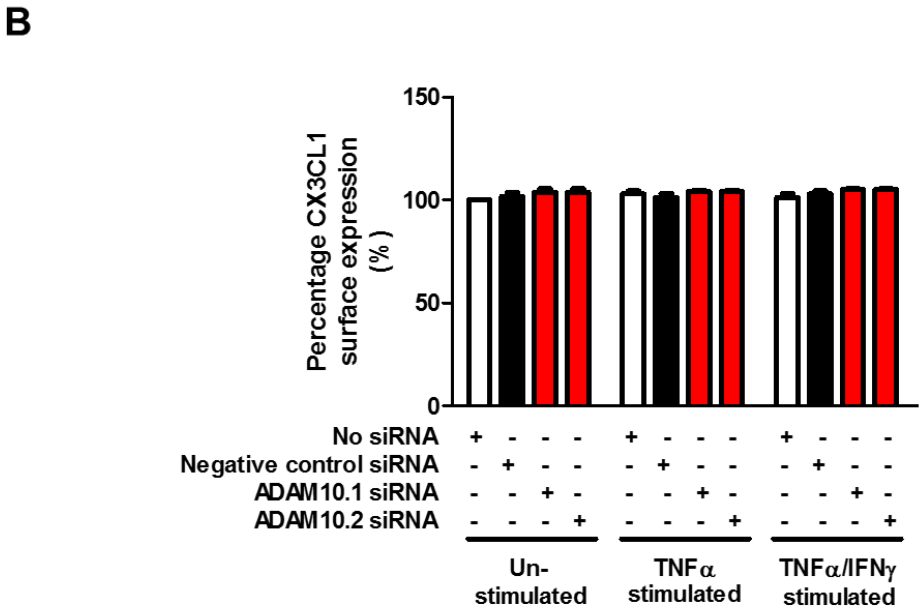
B
Percentage CX3CL1 surface expression (%)
No siRNA
Negative control siRNA
ADAM10.1 siRNA
ADAM10.2 siRNA
Un-stimulated
TNFα stimulated
TNFα/IFNγ stimulated

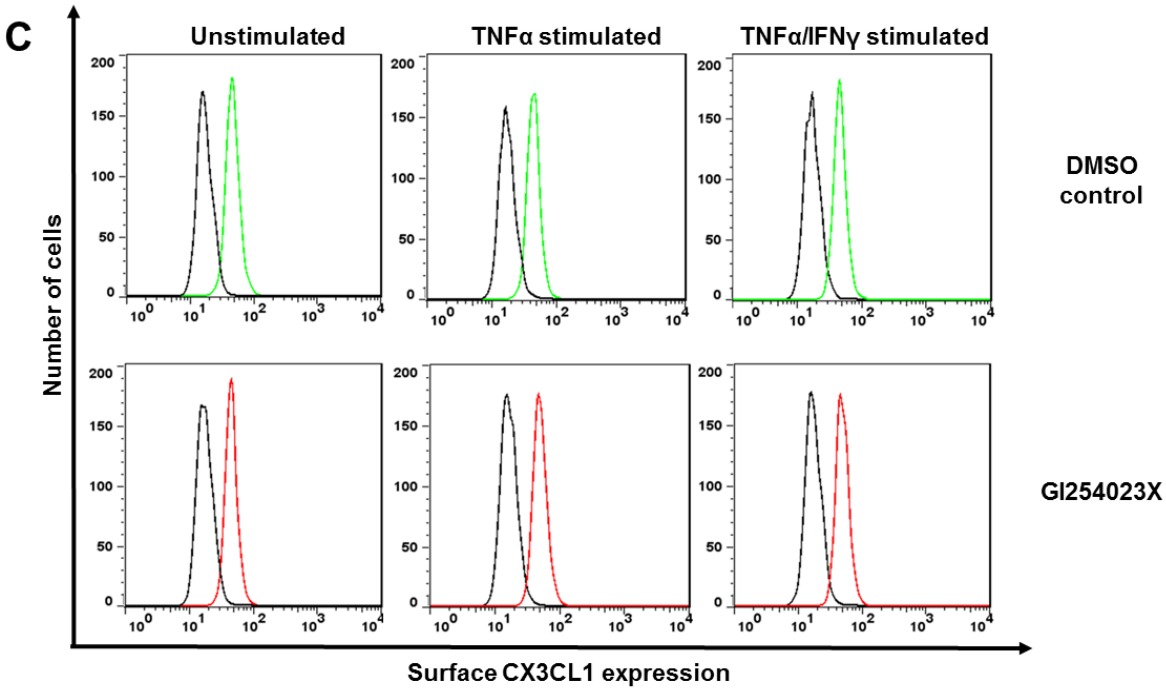
C
Unstimulated
TNFα stimulated
TNFα/IFNγ stimulated
DMSO control
GI254023X
Number of cells
Surface CX3CL1 expression

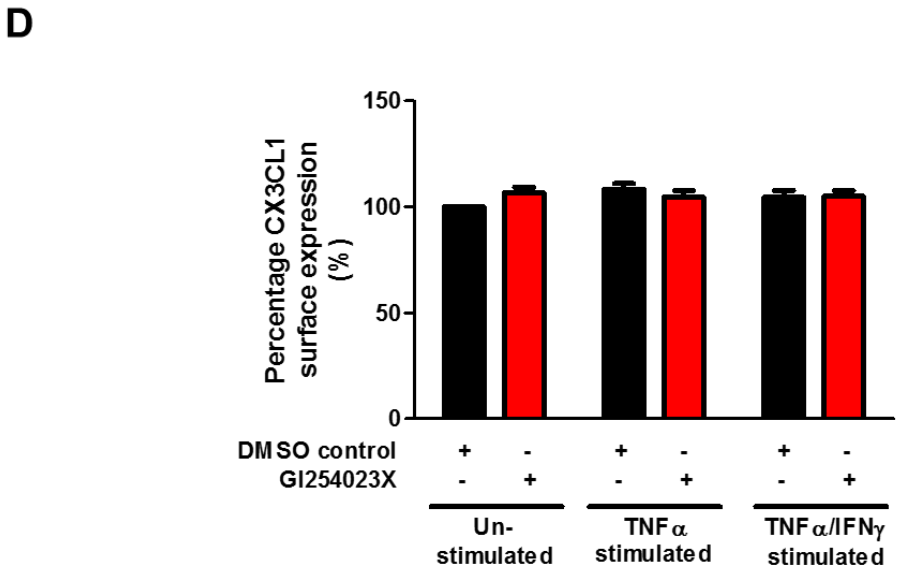
D
Percentage CX3CL1 surface expression (%)
DMSO control
GI254023X
Un-stimulated
TNFα stimulated
TNFα/IFNγ stimulated

Figure 4.2 CX3CL1 expression on HUVECs is not altered by ADAM10 knockdown or inhibition under cytokine stimulated conditions. HUVECs were transfected with siRNA duplexes to ADAM10 as explained in the legend to Figure 4.2 or underwent treatment with 20 µM GI254023X or 0.02% DMSO control. In addition, HUVECs were stimulated with either 100 U/ml TNFα alone or in combination with 10 ng/ml IFNγ or left unstimulated. Following 24 hours of stimulation, HUVECs were stained for CX3CL1. The green line represents CX3CL1 staining of negative control siRNA transfected cells and the red line represents CX3CL1 staining following ADAM10 knockdown. The black line represents isotype control staining (A). Surface CX3CL1 levels from panel A were quantitated and normalised to the "No siRNA" treated condition (B). HUVECs treated with the ADAM10 inhibitor were analysed by flow cytometry to measure surface CX3CL1 expression. The green line represents CX3CL1 staining of DMSO control treated cells and the red line represents CX3CL1 staining following GI254023X treatment. The black line represents isotype control staining (C). Surface CX3CL1 levels from panel C were quantitated and normalised to the "DMSO control" treated condition (D). Error bars represent the standard error of the mean from four independent experiments. Data were analysed by One-way ANOVA followed by a Dunnett's multiple-comparisons post-hoc test. Confirmation of ADAM10 knockdown under the various cytokine stimulatory conditions was assessed by flow cytometry as explained in the legend to Figure 4.1 and shown to be ~90% reduced upon quantitation (data not shown).

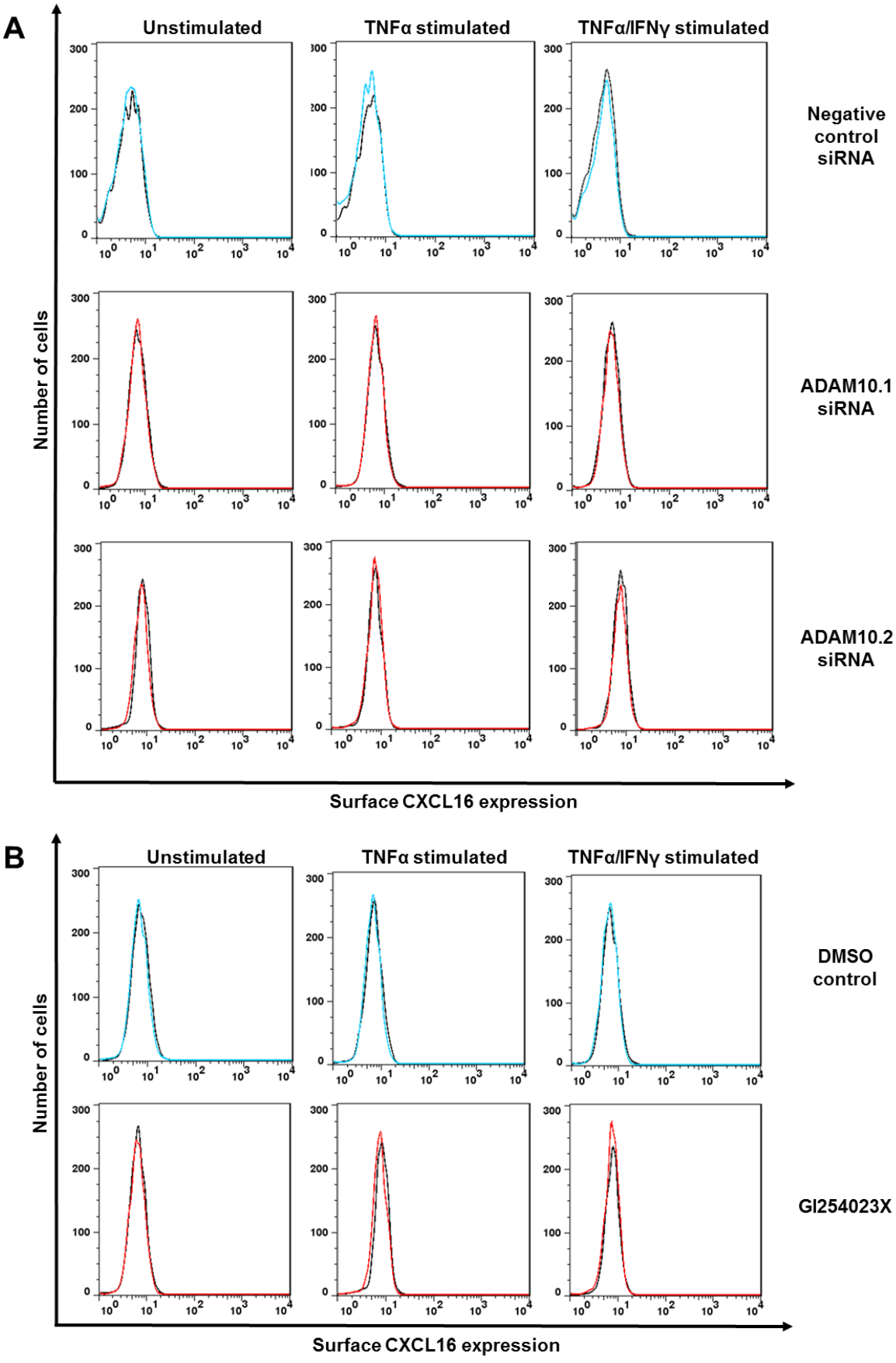
A
Unstimulated
TNFα stimulated
TNFα/IFNγ stimulated
Negative control siRNA
ADAM10.1 siRNA
ADAM10.2 siRNA
Number of cells
Surface CXCL16 expression
B
Unstimulated
TNFα stimulated
TNFα/IFNγ stimulated
DMSO control
GI254023X
Number of cells
Surface CXCL16 expression

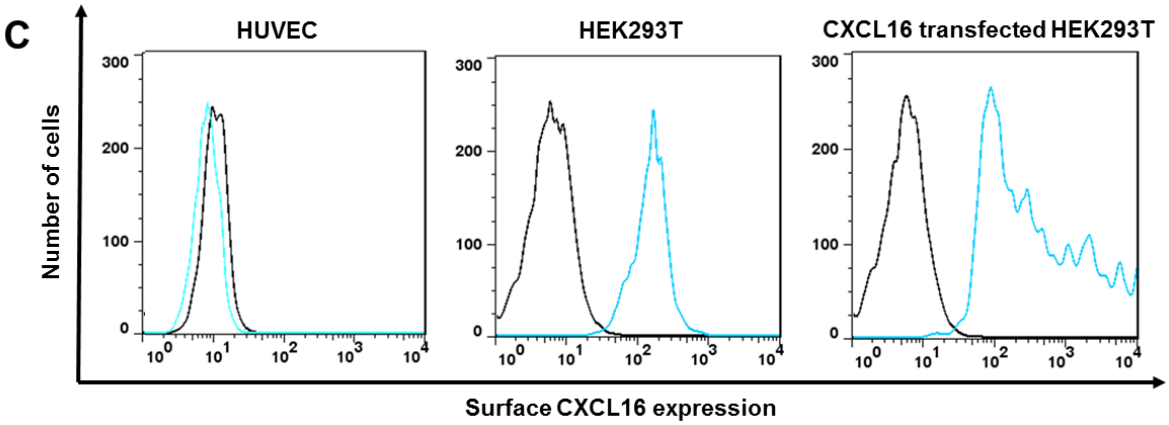

Figure 4.3 CXCL16 is not expressed on HUVECs. HUVECs were dissociated and stained for CXCL16, as explained in the figure legend to Figure 4.2. HUVECs transfected with siRNA were analysed by flow cytometry to measure surface CXCL16 expression. The cyan line represents CXCL16 staining of negative control siRNA transfected cells and the red line represents CXCL16 staining following ADAM10 knockdown. The black line represents isotype control staining (A). HUVECs treated with the ADAM10 inhibitor were analysed by flow cytometry to measure surface CXCL16 expression. The cyan line represents CXCL16 staining of DMSO control treated cells and the red line represents CXCL16 staining following GI254023X treatment. The black line represents isotype control staining (B). In addition, as a positive control, HEK293T cells were transfected with an expression vector containing CXCL16 cDNA, before being stained for CXCL16, as explained in panel A (C). Error bars represent the standard error of the mean from four independent experiments. Confirmation of ADAM10 knockdown under the various cytokine stimulatory conditions was assessed by flow cytometry as explained in the legend to Figure 4.1 and shown to be ~90% reduced upon quantitation (data not shown).

4.2.3 The chemokine receptors, CX3CR1 and CXCR6 are differentially expressed on major lymphocyte subsets

Having shown that HUVECs express CX3CL1 but not CXCL16, experiments now focused on looking at their receptors, CX3CR1 and CXCR6, on the various PBL subsets. For these experiments, PBLs were incubated with a cocktail of antibodies to define the various lymphocyte subsets (namely, CD3, CD4, CD8, CD19, and CD56) and additional antibodies to the chemokine receptors, CX3CR1 and CXCR6, were added. Lymphocyte subsets were characterised by their surface antigen expression by gating on the specific populations (as explained in Section 2.2.6) and analysed for expression of the chemokine receptors. Expression of the chemokine receptor CX3CR1 was undetectable on PBL subsets (Figure 4.4 A) as compared to $CD14^+$ monocytes that were isolated from a peripheral blood mononuclear cell (PBMC) preparation, as a positive control. CXCR6 expression was found on B cells, NK T cells and $CD56^{low}$ NK cells, with a lower expression of the chemokine receptor found on $CD4^+$ and $CD8^+$ T cells along with $CD56^{hi}$ NK cells (Figure 4.4 B). Taken together, these results suggest that PBL subsets express the chemokine receptor CXCR6, but not CX3CR1, which could differentially alter the transmigration of the distinct PBL subsets. In particular, the lack of expression of CX3CR1 indicates that its chemokine ligand on HUVECs, CX3CL1, is not responsible for the effect of ADAM10 on PBL transmigration.

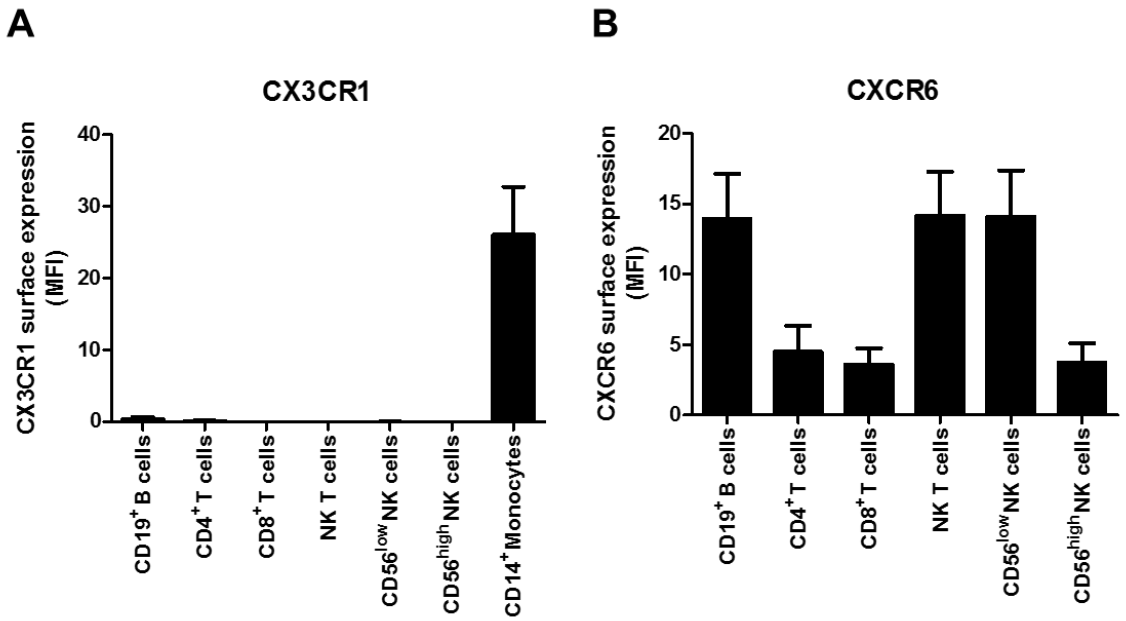

Figure 4.4 Major PBL populations differentially express the chemokine receptors CX3CR1 and CXCR6. Purified PBLs (or PBMCs for the case of $CD14^+$ monocyte staining) were stained with the panel of lymphocyte subset antibodies (CD3 $PerCy^{3.3}$, CD56 PE, CD4 Alexa Fluor 700, CD8 Pacific Blue and CD19 $PECy^7$). In addition, the PBLs were stained with 2 µl/FACS tube with the chemokine receptors, CX3CR1 (FITC) and CXCR6 (APC). The relative surface expression of CX3CR1 or CXCR6 was determined on the various lymphocyte subsets by flow cytometry and quantitated (A) and (B). In addition, CD14 Monocytes isolated from a PBMC preparation were stained for CX3CR1 as a positive control for staining (A). Data are shown as mean ± standard error of the mean and are representative of three independent experiments. Data were analysed using one-way ANOVA and Bonferroni's multiple comparisons post-test.

4.2.4 ADAM10 regulates VE-cadherin shedding

Previous data has suggested a role of ADAM10 in regulating the shedding of VE-cadherin (Schulz et al., 2008). In the absence of ADAM10 activity, VE-cadherin levels were shown to be upregulated due to a decrease in its shedding. However, it is not clear whether the elevated VE-cadherin is truly responsible for regulating the transmigratory phenotype observed in Chapter 3. As a first step to test this, experiments were performed to confirm that VE-cadherin shedding is impaired in the absence of ADAM10 in HUVECs. In these experiments, HUVECs were transfected with either two different siRNA duplexes to ADAM10 or a negative control non-specific siRNA duplex. 24 hours after transfection, 10 μM DAPT (a γ-secretase inhibitor) was added to prevent additional cleavage by γ-secretase following ADAM10 cleavage and the cells were cultured for an additional 24 hours. Cells were lysed and Western blotted with an antibody to the C-terminal tail of VE-cadherin. For control cells, bands at 100 kDa and 35 kDa were observed. The 100 kDa corresponds to full length VE-cadherin and the 35 kDa band is the cleaved C-terminal fragment. Knockdown of endothelial ADAM10 confirmed that cleavage of VE-cadherin is dependent on ADAM10 by causing a ~75% or greater decrease in VE-cadherin proteolysis (Figure 4.5 A & B). This was accompanied by the ~90% reduction in ADAM10 surface expression as analysed by flow cytometry (Figure 4.5 C & D).

In addition, the knockdown data findings were further validated using the ADAM10 inhibitor. In these assays, HUVECs were incubated either with 0.02% DMSO or 20 μM GI254023X in addition to 10 μM DAPT for 24 hours. The cells were harvested and the Western blotted with an antibody to the C-terminal tail of VE-cadherin. As shown in Figure 4.6 A, VE-cadherin C-terminal fragment generation was strongly diminished by incubation of HUVECs with the ADAM10 inhibitor compared to DMSO control treated cells, with a 90% reduction in the C-terminal fragment (Figure 4.6 A & B).

Taken together, the data in this section indicates that ADAM10 is essential for shedding of VE-cadherin.

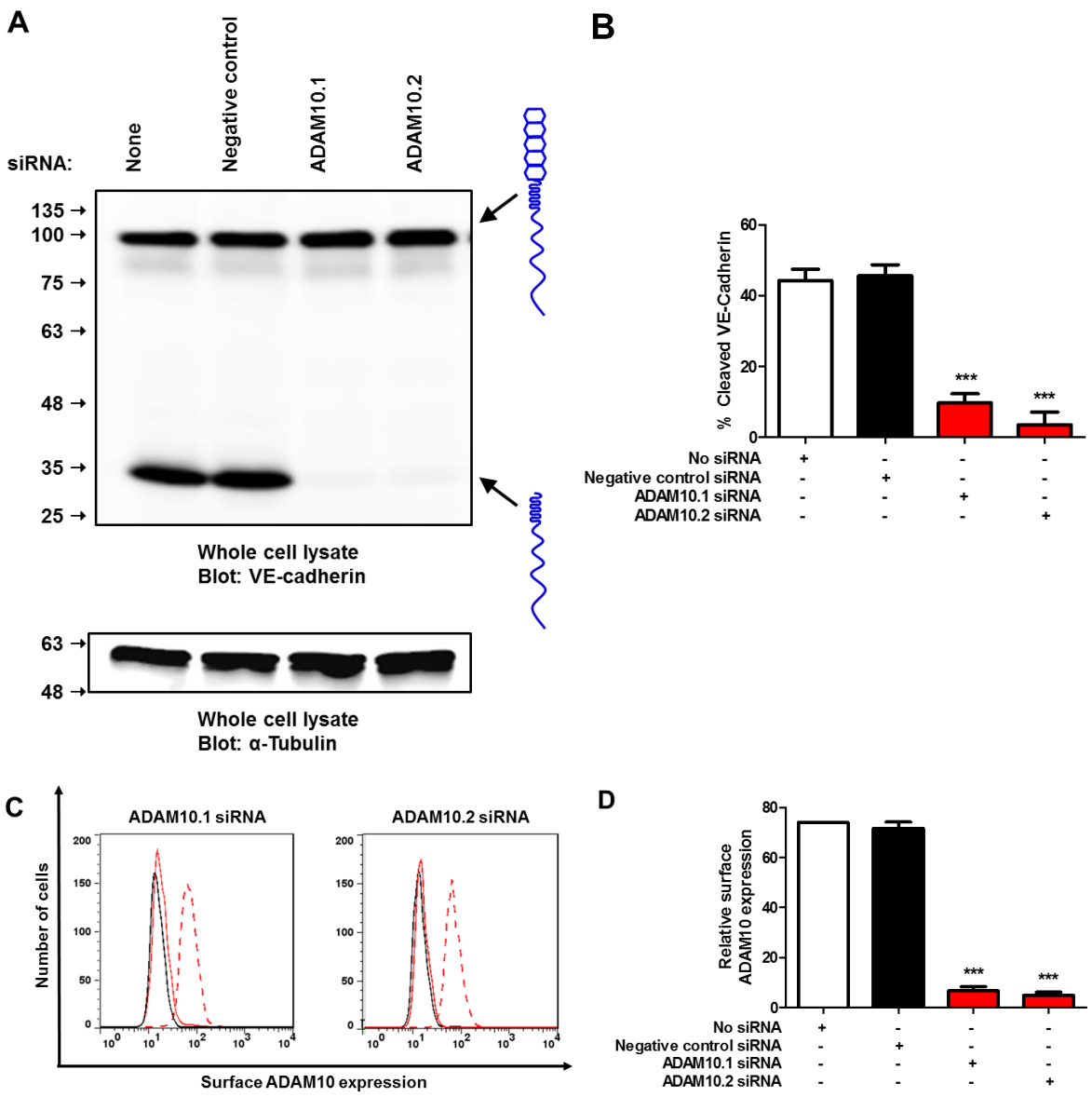
A
siRNA:
None
Negative control
ADAM10.1
ADAM10.2
135
100
75
63
48
35
25
Whole cell lysate
Blot: VE-cadherin
63
48
Whole cell lysate
Blot: α-Tubulin
B
% Cleaved VE-Cadherin
60
40
20
0
***
***
No siRNA + - - -
Negative control siRNA - + - -
ADAM10.1 siRNA - - + -
ADAM10.2 siRNA - - - +
C
ADAM10.1 siRNA
ADAM10.2 siRNA
Number of cells
200
150
100
50
0
Surface ADAM10 expression
D
Relative surface ADAM10 expression
80
60
40
20
0
***
***
No siRNA + - - -
Negative control siRNA - + - -
ADAM10.1 siRNA - - + -
ADAM10.2 siRNA - - - +

Figure 4.5 Knockdown of endothelial ADAM10 reduces VE-cadherin shedding. HUVECs were transfected with two different siRNA duplexes to ADAM10 (red) alongside a non-specific siRNA (black bar) at a final concentration of 10 nM. 24 hours after transfection, 10 μM of the γ-secretase inhibitor, DAPT was added to the culture media to prevent further proteolytic processing of VE-cadherin after ADAM10 cleavage. Following an additional 24 hours, HUVEC lysates were Western blotted with an antibody to the C-terminal tail of VE-cadherin or to tubulin as a loading control. The membrane was imaged and bands quantified on the Odyssey Infrared Imaging System (A). The percentage cleaved was calculated by dividing the cleaved VE-cadherin fragment (~35 kDa) by the total VE-cadherin (relative band intensities corresponding to full length (~100) and cleaved VE-cadherin added together) expressed as a percentage (B). Knockdown efficiency of ADAM10 was confirmed by flow cytometry. The broken red line represents ADAM10 surface expression on negative control siRNA transfected cells and the red solid line represents ADAM10 surface expression on ADAM10 siRNA transfected cells (C). Surface ADAM10 levels from panel C were quantitated and normalised to the "No siRNA" treated condition (D). Error bars represent the standard error of the mean from five independent experiments. Data were normalised by arcsine transformation and statistically analysed by a Dunnett's multiple-comparisons post-hoc test (***$p < 0.001$ compared to negative control siRNA treated cells).

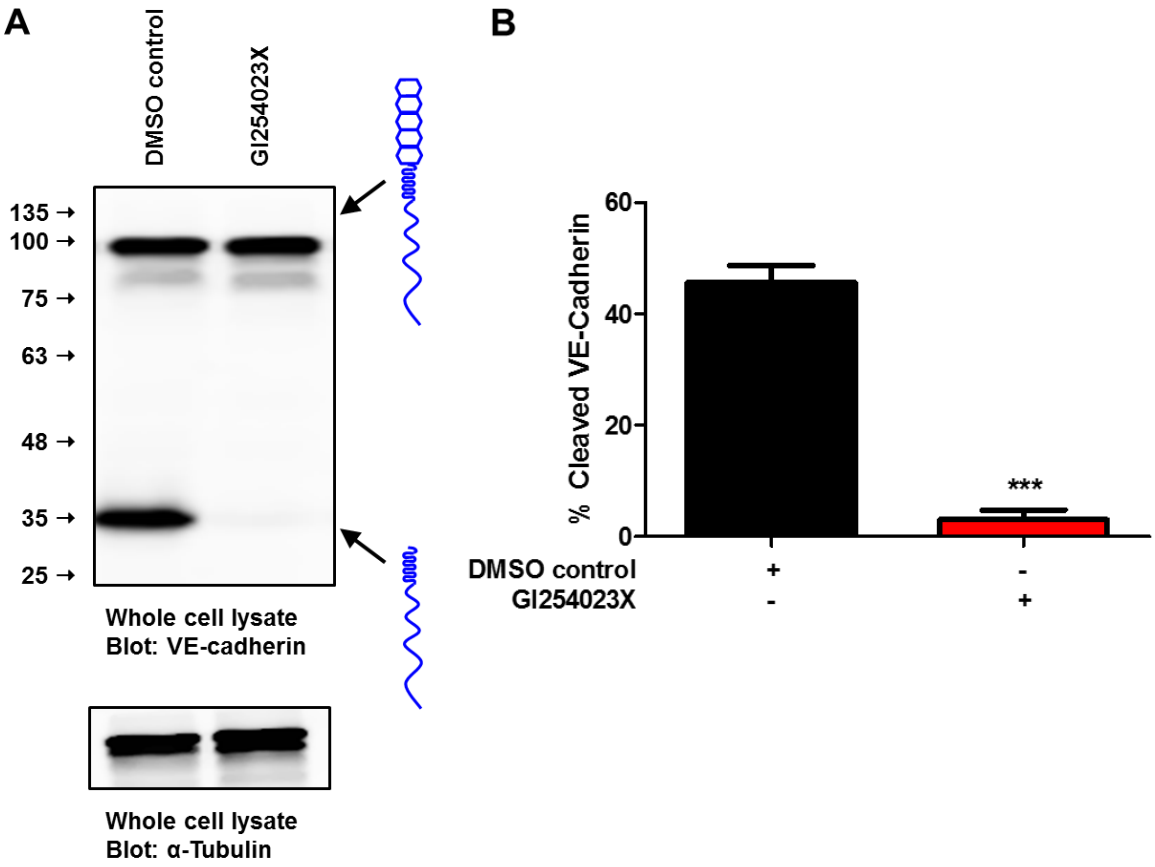

Figure 4.6 Inhibition of endothelial ADAM10 reduces VE-cadherin shedding. HUVECs were treated with either 0.02% DMSO (black bar) or 20 µM GI254023X (red bar) in combination with 10 µM DAPT and subsequently Western blotted as explained in the legend to Figure 4.5 (A). The percentage cleaved was calculated as explained in the legend to Figure 4.5 (B). Error bars represent the standard error of the mean from four independent experiments. Data were normalised by arcsine transformation and statistically analysed by Students *t*-test (***$p < 0.001$ compared to DMSO control treated cells).

4.2.5 VE-cadherin expression is regulated by endothelial ADAM10 independently of cytokine stimulation

Having shown that ADAM10 regulates the shedding of VE-cadherin, the effects of ADAM10 on VE-cadherin surface levels were next investigated. In these experiments, HUVECs were transfected with siRNA duplexes to ADAM10 and appropriate controls, as explained earlier. In addition, HUVECs were stimulated with either 100 U/ml TNFα alone or in combination with 10 ng/ml IFNγ for 24 hours. The cells were harvested and stained for VE-cadherin and analysed by flow cytometry as previously explained. Knockdown of ADAM10 increased the surface expression of VE-cadherin by approximately 40% (Figure 4.7 A & B). ADAM10 inhibition of HUVECs caused VE-cadherin surface levels to increase to a similar extent to that observed following endothelial ADAM10 knockdown (Figure 4.7 C & D). Furthermore, cytokine treatment did not affect VE-cadherin surface levels (Figure 4.7). These results indicate that endothelial ADAM10 is able to regulate the surface expression levels of VE-cadherin independently of cytokine stimulation.

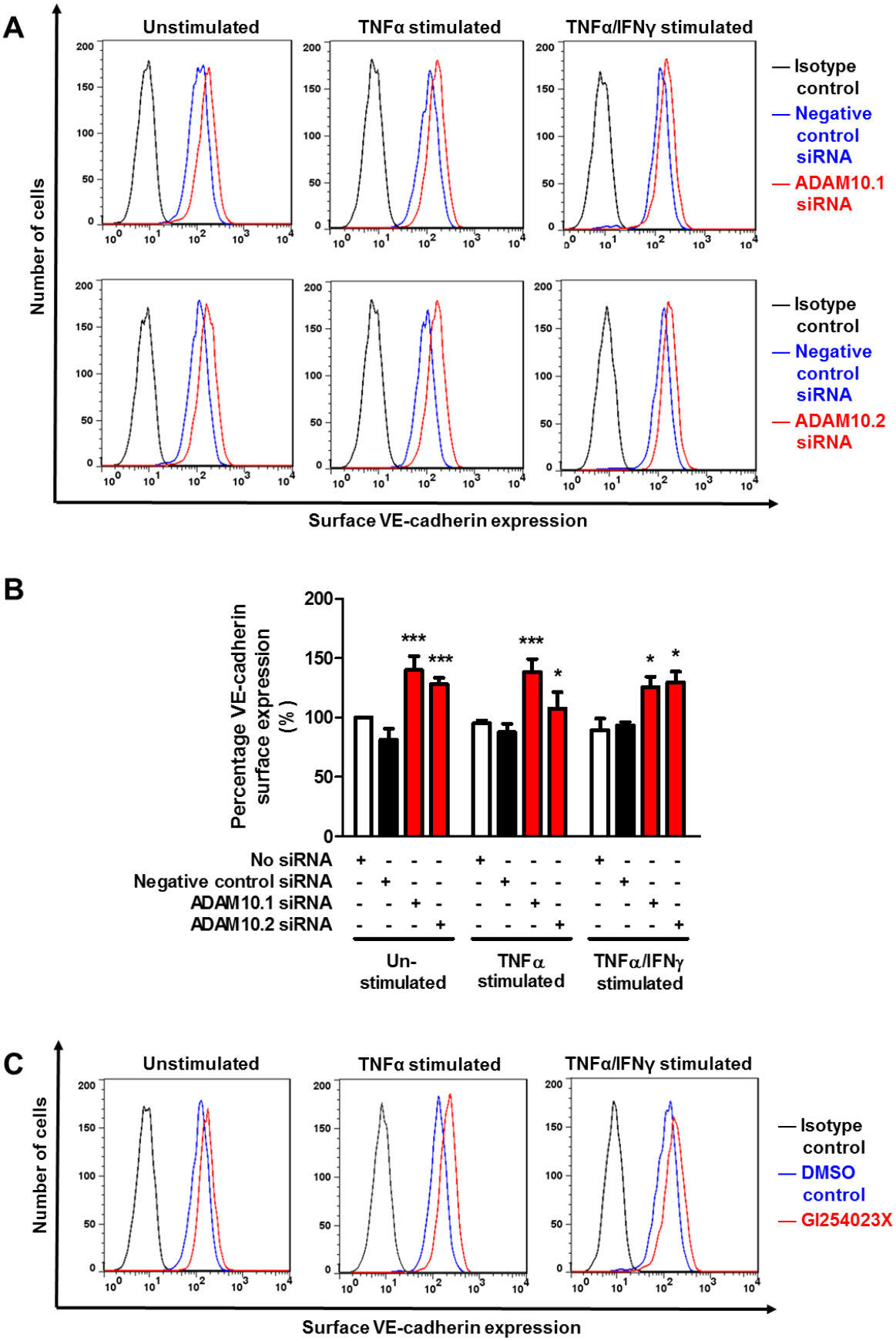
A
Unstimulated
TNFα stimulated
TNFα/IFNγ stimulated
Number of cells
Surface VE-cadherin expression
Isotype control
Negative control siRNA
ADAM10.1 siRNA
ADAM10.2 siRNA
B
Percentage VE-cadherin surface expression (%)
No siRNA
Negative control siRNA
ADAM10.1 siRNA
ADAM10.2 siRNA
Un-stimulated
TNFα stimulated
TNFα/IFNγ stimulated
C
DMSO control
GI254023X

D

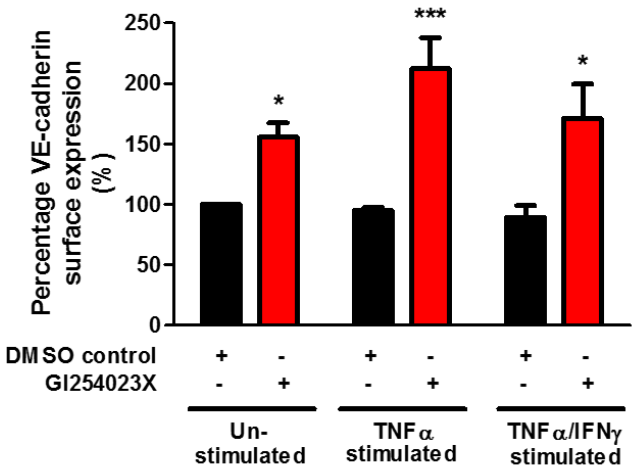

Figure 4.7 Knockdown or inhibition of endothelial ADAM10 increases VE-cadherin surface expression. HUVECs were transfected with siRNA duplexes to ADAM10 or underwent treatment with the ADAM10 inhibitor as explained in the legend to Figure 4.2. In addition, HUVECs were stimulated with either 100 U/ml TNFα alone or in combination with 10 ng/ml IFNγ or left unstimulated. Following 24 hours of stimulation, HUVECs were stained for VE-cadherin expression and processed by flow cytometry (A & C). VE-cadherin surface levels were quantitated and normalised to either 'No siRNA' treated or 'DMSO' treated conditions (B & D). Error bars represent the standard error of the mean from four independent experiments. Data were analysed by One-way ANOVA followed by a Dunnett's multiple-comparisons post-hoc test (*$p < 0.05$ and ***$p < 0.001$). Confirmation of ADAM10 knockdown under the various cytokine stimulatory conditions was assessed by flow cytometry as explained in the legend to Figure 4.2 and shown to be ~90% reduced upon quantitation (data not shown).

4.2.6 Knockdown or inhibition of ADAM10 increases endothelial barrier function

Endothelial cell-cell junctions control the intercellular permeability to plasma solutes, and their integrity depends on the structure and function of VE-cadherin (Lampugnani et al., 1995; Vestweber, 2012a; Schulz et al., 2008; Flemming et al., 2015). Since VE-cadherin levels were found to be increased in the absence of ADAM10 in the previous section, an experiment was designed to test whether this was accompanied by increased integrity of the HUVEC monolayer. In these experiments, HUVECs were seeded onto gelatine coated 0.4 µm pore filters before being transfected with either one or two different siRNA duplexes to ADAM10 or a negative control non-specific siRNA duplex. These transwell filters were placed into a previously calibrated EndOhm chamber and resistance readings were taken at 0, 4, 12, 24, and 48-hour time points. The resistance readings were converted to represent the resistance across the whole filter. Knockdown of endothelial ADAM10 results in an increase in electrical resistance when compared to negative control siRNA transfected cells (Figure 4.8 A). This was apparent 24 and 48 hours after seeding the cells (Figure 4.8 A), when the monolayers had reached confluence (Figure 4.8 B). These were also the time points at which ADAM10 knockdown had reached substantial levels (Figure 4.8 C & D).

To further validate the knockdown data findings, a similar assay was setup in which HUVECs were treated with either 0.02% DMSO or 20 µM GI254023X and resistance readings were taken at specific time points as described above. Inhibition of endothelial ADAM10 resulted in an increase in electrical resistance (Figure 4.9 A). Again, the increase in resistance was apparent when the cells had reached full confluence (24 and 48 hours after seeding) (Figure 4.9 B).

Altogether, endothelial ADAM10 seems to regulate endothelial barrier integrity by increasing resistance through a mechanism that potentially relied on the increased formation of junctional protein complexes.

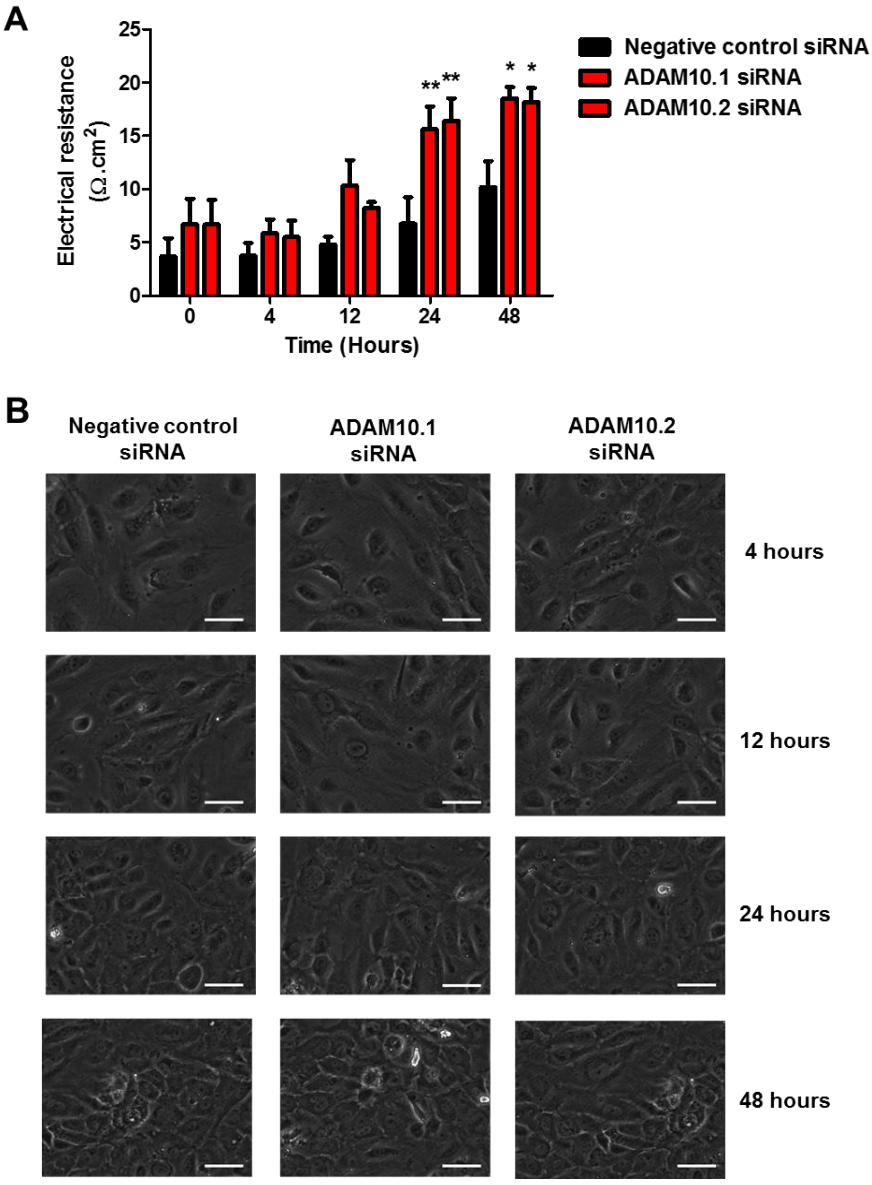
A
Electrical resistance
(Ω.cm2)
25
20
15
10
5
0
0
4
12
24
48
Time (Hours)
**
**
*
*
Negative control siRNA
ADAM10.1 siRNA
ADAM10.2 siRNA
B
Negative control siRNA
ADAM10.1 siRNA
ADAM10.2 siRNA
4 hours
12 hours
24 hours
48 hours

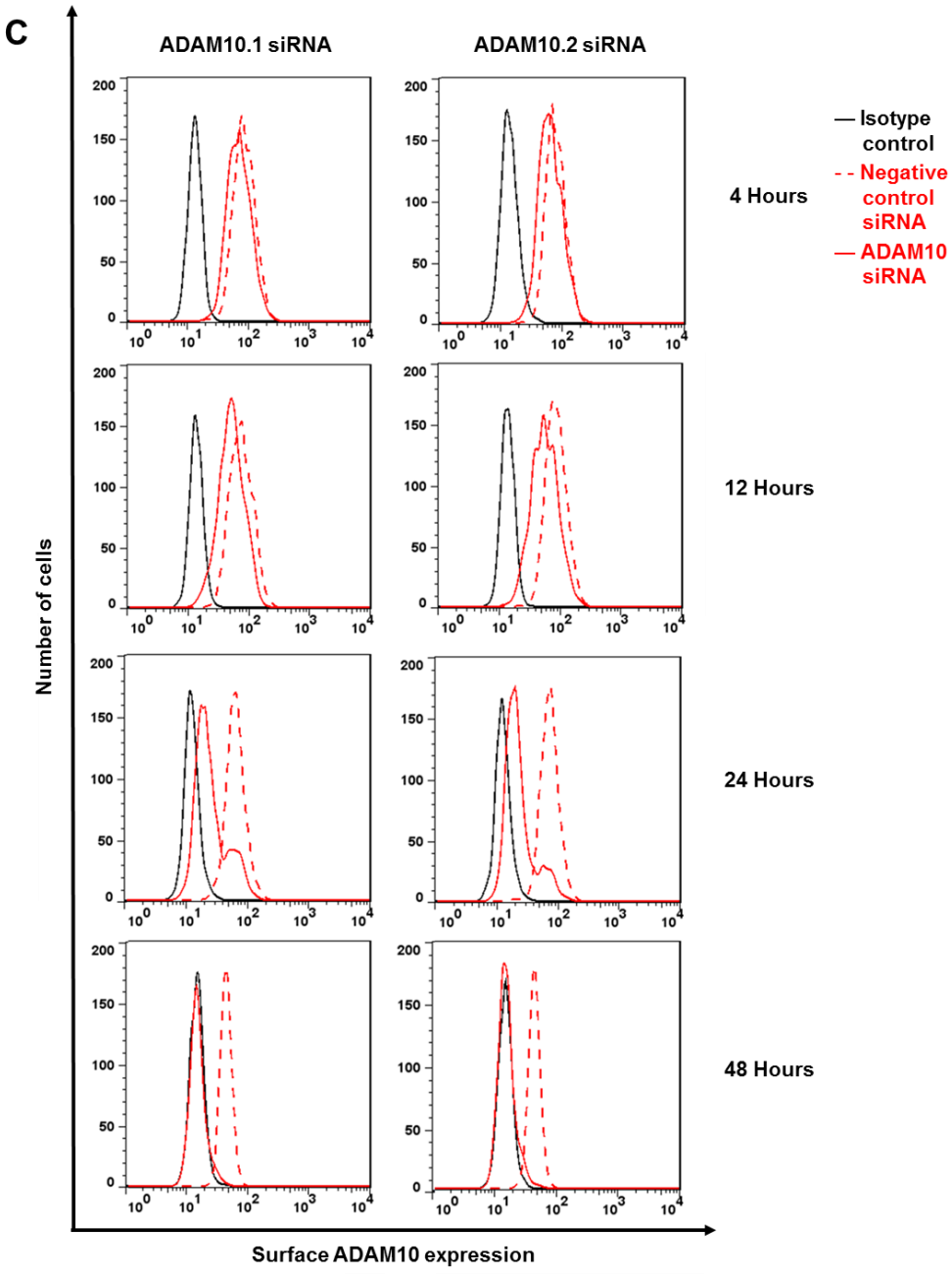
C
ADAM10.1 siRNA
ADAM10.2 siRNA
— Isotype control
- - Negative control siRNA
— ADAM10 siRNA
4 Hours
12 Hours
24 Hours
48 Hours
Number of cells
Surface ADAM10 expression

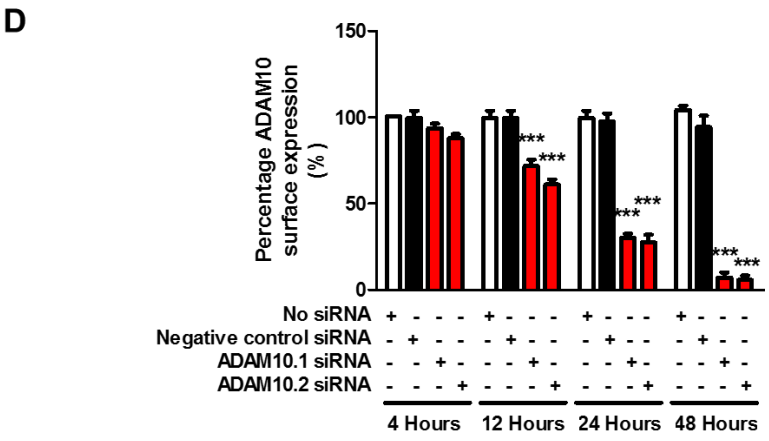
D
Percentage ADAM10 surface expression (%)
No siRNA
Negative control siRNA
ADAM10.1 siRNA
ADAM10.2 siRNA
4 Hours
12 Hours
24 Hours
48 Hours

Figure 4.8 Knockdown of endothelial ADAM10 increases transendothelial electrical resistance. HUVECs were transfected with two different siRNA duplexes to ADAM10 (red bars) alongside a non-specific siRNA (black bar) at a final concentration of 10 nM on gelatine-coated 0.4 µM pore filters. In addition, HUVECs were plated into 12 well plates and transfected with siRNA duplexes to assess knockdown efficiency as explained above. Resistance readings were then taken at respective time points post siRNA transfection following calibration of the EndOhm chamber (A). HUVEC monolayers were checked for confluency prior to taking resistance readings by taking phase contrast images at the respective time points (B). ADAM10 knockdown confirmation was confirmed by flow cytometry as explained in the legend to Figure 4.1. The broken red line represents ADAM10 expression on negative control siRNA transfected cells whilst the solid red line represents ADAM10 expression following ADAM10 knockdown at the specific time points (C). Surface ADAM10 levels from panel C were quantitated and normalised to the "No siRNA" treated condition (D). Error bars represent the standard error of the mean from four independent experiments. Data were analysed by two-way ANOVA followed by a Bonferroni multiple-comparisons post-hoc test (*$p < 0.05$, **$p < 0.01$, ***$p < 0.001$ compared to negative control siRNA treated conditions). Scale bar: 80 µM

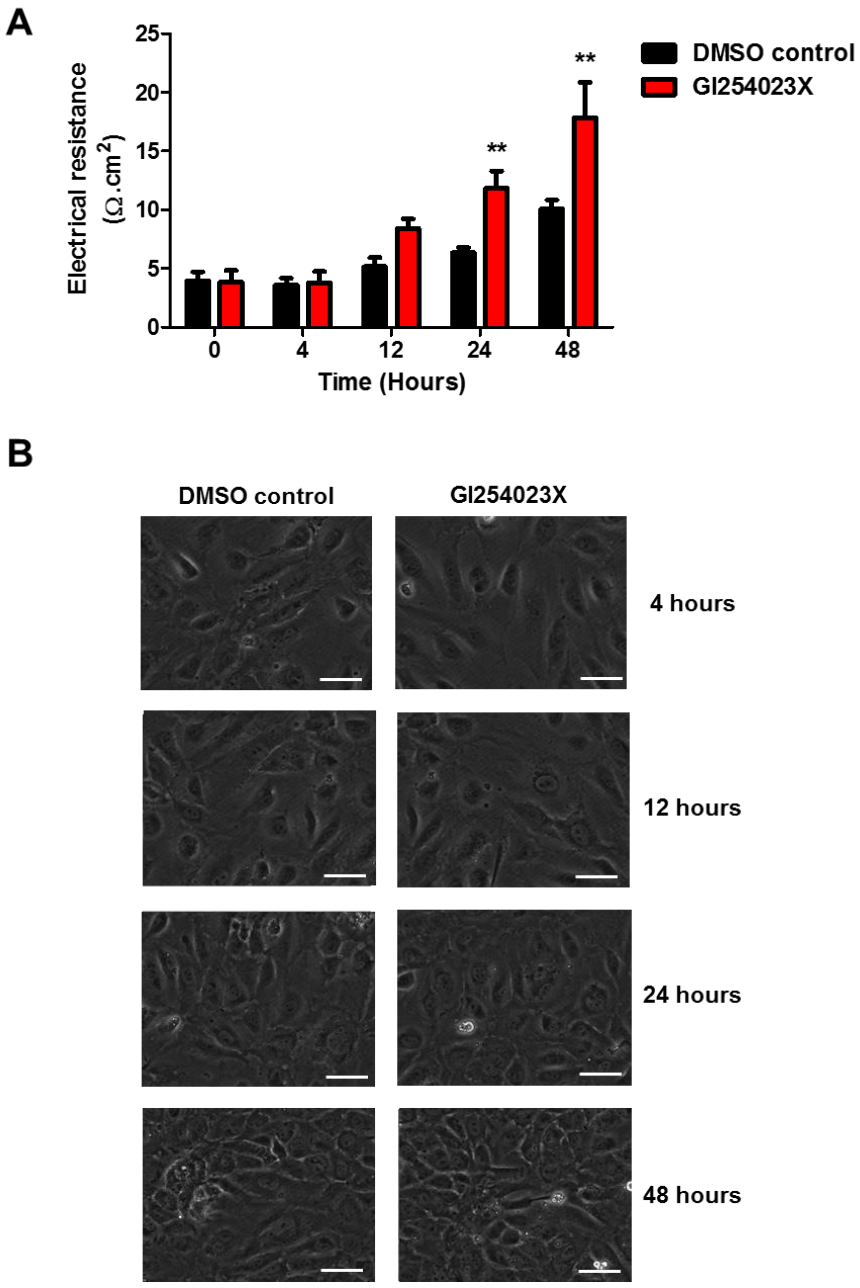

Figure 4.9 Inhibition of endothelial ADAM10 increases transendothelial electrical resistance. HUVECs were plated on transwell filters as detailed in the legend to Figure 4.8. HUVEC were then treated with media containing either 0.02% DMSO or 20 µM GI254023X and resistance readings were taken at the respective time points as explained in the legend to Figure 4.8 (A). HUVEC monolayers were checked for confluency prior to taking resistance readings by taking phase contrast images at the respective time points (B). Error bars represent the standard error of the mean from three independent experiments. Data were analysed by two-way ANOVA followed by a Bonferroni multiple-comparisons post-hoc test (*$p < 0.05$, **$p < 0.01$ compared to negative control siRNA treated conditions). Scale bar: 80 µM

4.2.7 Partial VE-cadherin knockdown to normal levels rescues the PBL transmigration defect

The increased VE-cadherin expression and monolayer integrity could explain the impaired PBL transmigration in the absence of ADAM10. To test this hypothesis, experiments were designed to partially knock down VE-cadherin back to wildtype levels, in the absence of ADAM10, and to then test whether PBL transmigration is restored. As a first step, and with the sole aim of establishing VE-cadherin knockdown, static adhesion assays were carried out in which VE-cadherin was targeted at varying final siRNA concentrations (0.01 nM, 0.1 nM, 1 nM, or 10 nM) or a non-specific control siRNA duplex. VE-cadherin knockdown efficiency by flow cytometry revealed a dose-dependent decrease in VE-cadherin surface expression with increasing concentrations of siRNA over time (Figure 4.10 A & B). Knockdown of VE-cadherin with 10 nM siRNA resulted in a ~60% reduction in VE-cadherin surface levels that was maintained 72 hours post-transfection (Figure 4.10 A & B). Phase contrast images of HUVEC monolayers confirmed that a partial loss of VE-cadherin was sufficient to maintain endothelial monolayer integrity (Figure 4.10 C). Static adhesion assays were setup with the VE-cadherin transfected HUVECs as previously described whereby HUVEC were stimulated with 100 U/ml TNFα and 10 ng/ml IFNγ for 24 hours before co-incubating the cytokine stimulated HUVECs with $1x10^6$ PBLs for 7 minutes. These assays revealed that a partial loss of VE-cadherin did not alter the ability of PBLs to transmigrate (Figure 4.10 D). Furthermore, no differences in PBL total adhesion were observed following endothelial cell VE-cadherin knockdown at the various siRNA concentrations (Figure 4.10 E).

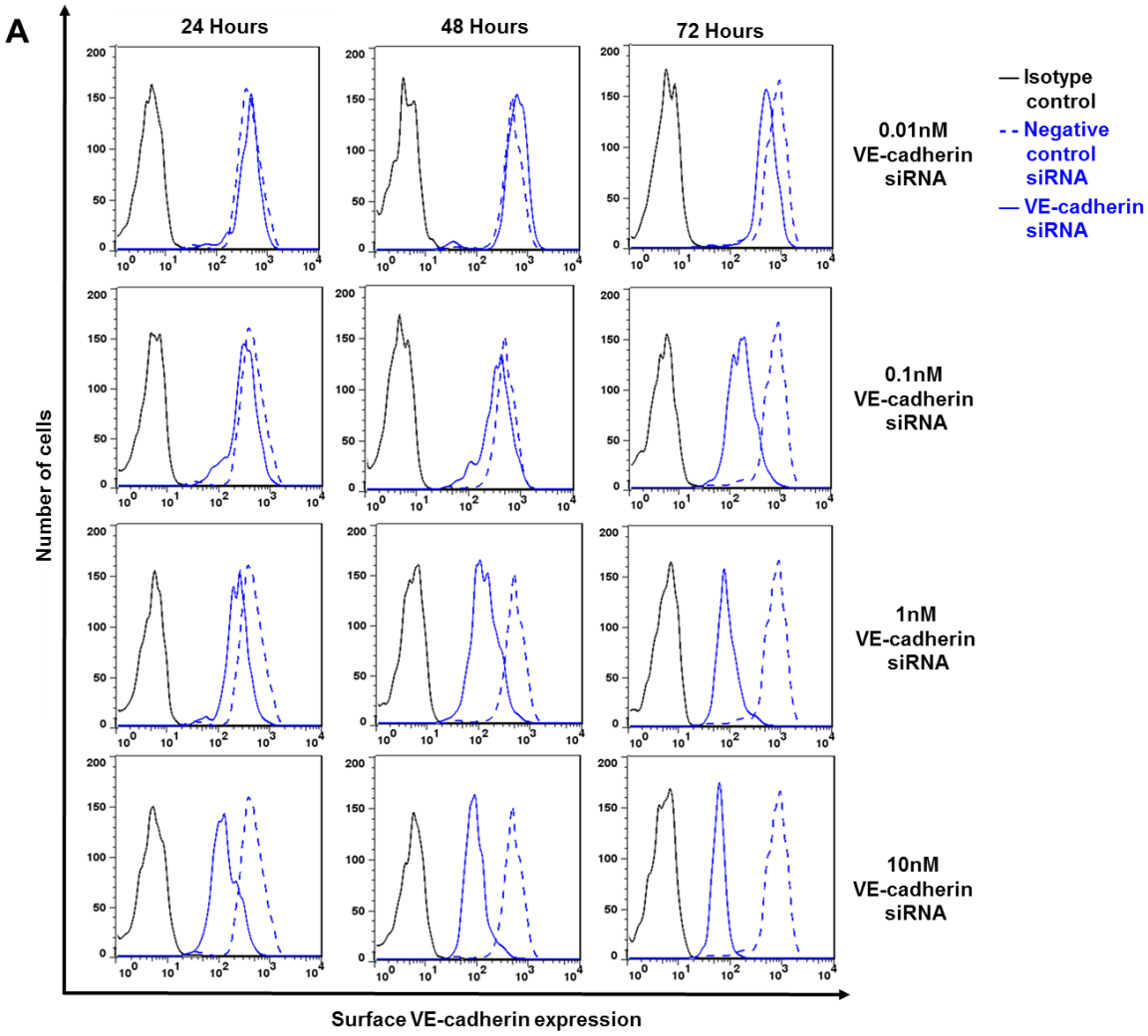
A
24 Hours
48 Hours
72 Hours
0.01nM VE-cadherin siRNA
0.1nM VE-cadherin siRNA
1nM VE-cadherin siRNA
10nM VE-cadherin siRNA
Isotype control
Negative control siRNA
VE-cadherin siRNA
Number of cells
Surface VE-cadherin expression
B
Percentage VE-cadherin surface expression (%)
No siRNA
Negative control siRNA
0.01nM VE-cadherin.1 siRNA
0.1nM VE-cadherin.1 siRNA
1nM VE-cadherin.1 siRNA
10nM VE-cadherin.1 siRNA
24 Hours
48 Hours
72 Hours

C

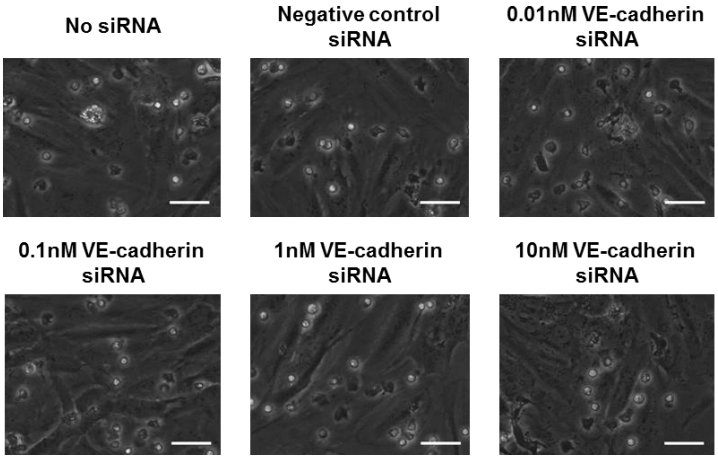
No siRNA
Negative control siRNA
0.01nM VE-cadherin siRNA
0.1nM VE-cadherin siRNA
1nM VE-cadherin siRNA
10nM VE-cadherin siRNA

D

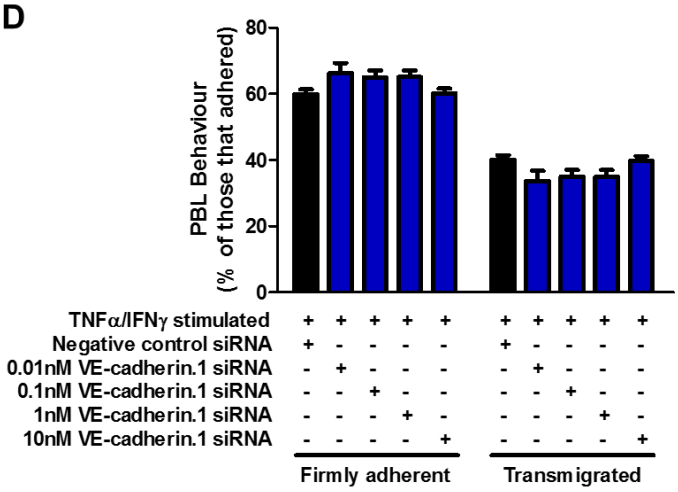
PBL Behaviour (% of those that adhered)
80
60
40
20
0
TNFα/IFNγ stimulated + + + + + + + + + +
Negative control siRNA + - - - - + - - - -
0.01nM VE-cadherin.1 siRNA - + - - - - + - - -
0.1nM VE-cadherin.1 siRNA - - + - - - - + - -
1nM VE-cadherin.1 siRNA - - - + - - - - + -
10nM VE-cadherin.1 siRNA - - - - + - - - - +
Firmly adherent
Transmigrated

E

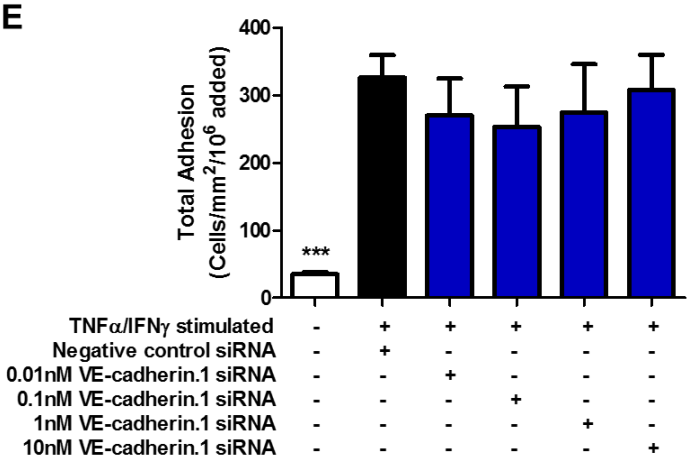
Total Adhesion (Cells/mm²/10⁶ added)
400
300
200
100
0
***
TNFα/IFNγ stimulated - + + + + +
Negative control siRNA - + - - - -
0.01nM VE-cadherin.1 siRNA - - + - - -
0.1nM VE-cadherin.1 siRNA - - - + - -
1nM VE-cadherin.1 siRNA - - - - + -
10nM VE-cadherin.1 siRNA - - - - - +

Figure 4.10 Partial knockdown of VE-cadherin does not alter lymphocyte adhesion and transmigration under *in vitro* static adhesion conditions. HUVECs were transfected with two different siRNA duplexes to VE-cadherin (blue bars) at varying final concentrations (0.01 nM, 0.1 nM, 1 nM or 10 nM) alongside a non-specific siRNA (black bar) at a final concentration of 10 nM before being analysed by flow cytometry to measure surface VE-cadherin expression. The broken blue line represents VE-cadherin staining of cells transfected with a negative control siRNA and the solid blue line represents VE-cadherin staining following VE-cadherin knockdown. The black line isotype control staining (A). Surface VE-cadherin levels from panel A were quantitated and normalised to the "No siRNA" treated condition (B). Effects of VE-cadherin knockdown on PBL transmigration were assessed. 24 hours after transfection, the HUVECs were stimulated with 100 U/ml TNFα along with 10 ng/ml IFNγ for an additional 24 hours and static adhesion assays were carried out as previously described in Section 2.3.5. Phase contrast images of five different fields of view per well were made to assess lymphocyte transmigration and monolayer integrity (C). PBLs were classified as firmly adherent or transmigrated (D). The total number of cell classified for each of the behaviours was combined to give a total adhesion count (E). Error bars represent the standard error of the mean from five independent experiments. Data were normalised by arcsine transformation and statistically analysed by one-way ANOVA and Dunnett's post-hoc comparisons test for total adhesion data and confirmation of siRNA knockdown (*$p < 0.05$, **$p < 0.01$, ***$p < 0.001$ compared to Negative control siRNA data) or by a two-way ANOVA and Bonferroni post-hoc comparisons test for PBL cell behaviour.

To determine whether the ADAM10-dependent PBL transmigration defect can be rescued by restoring elevated VE-cadherin levels back to normal, the effects of knockdown of ADAM10 in combination with a partial VE-cadherin knockdown was investigated. From the VE-cadherin siRNA titration data, a final concentration of 0.5 nM VE-cadherin siRNA was chosen due to its expected ~45% reduction in VE-cadherin surface levels (Figure 4.10). For these static adhesion assays, HUVECs were transfected with one of two siRNA duplexes to VE-cadherin either alone or in combination with one of two siRNA duplexes to ADAM10. Strikingly, reduction of VE-cadherin back to wildtype levels restored the transmigration defect in the absence of ADAM10 (Figure 4.11 A). No differences in PBL total adhesion were observed following individual or combined knockdowns of VE-cadherin and ADAM10 (Figure 4.11 B). Flow cytometry confirmed that VE-cadherin expression levels had returned to normal levels following the partial knockdown of VE-cadherin in combination with 'complete' ADAM10 knockdown; quantitation revealed that this was significant (Figure 4.11 C & D).

In addition to studies carried out using ADAM10 knockdown, the ADAM10 inhibitor was also used in combination with a partial VE-cadherin knockdown. For these static adhesion assays, HUVECs were transfected with one of two siRNA duplexes to VE-cadherin (at a final concentration of 0.5 nM) and compared to non-specific control siRNA duplex treated cells. Following 24 hours, HUVECs were stimulated and 20 μM GI254023X was added to respective conditions and the PBL static adhesion assay was carried out as previously described. In a strikingly similar manner to the ADAM10 knockdown data findings in Figure 4.11, partial knockdown of VE-cadherin in the presence of the ADAM10 inhibitor restored PBL transmigration (Figure 4.12 A). No differences in PBL total adhesion were observed following knockdown of VE-cadherin in the presence of absence of the ADAM10 inhibitor (Figure 4.12 B). Flow cytometry confirmed that VE-cadherin expression levels had returned to normal following the partial

knockdown in the presence of the ADAM10 inhibitor and quantitation revealed this was significant (Figure 4.12 C & D).

Taken together, these results strongly suggest that the elevated VE-cadherin surface expression level is responsible for impaired PBL transmigration in the absence of ADAM10.

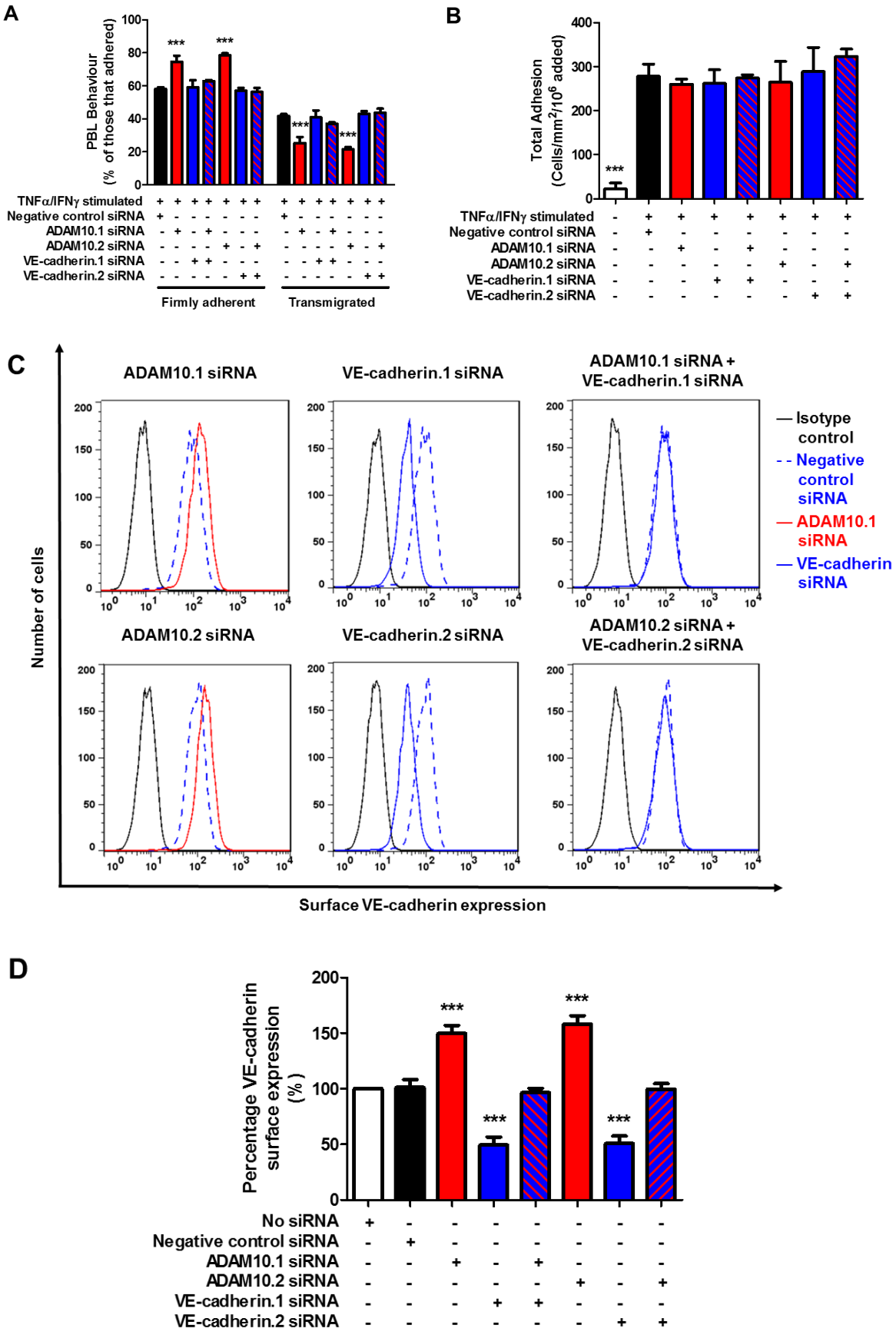
A
PBL Behaviour (% of those that adhered)
TNFα/IFNγ stimulated
Negative control siRNA
ADAM10.1 siRNA
ADAM10.2 siRNA
VE-cadherin.1 siRNA
VE-cadherin.2 siRNA
Firmly adherent
Transmigrated
B
Total Adhesion (Cells/mm²/10⁶ added)
C
ADAM10.1 siRNA
VE-cadherin.1 siRNA
ADAM10.1 siRNA + VE-cadherin.1 siRNA
ADAM10.2 siRNA
VE-cadherin.2 siRNA
ADAM10.2 siRNA + VE-cadherin.2 siRNA
Isotype control
Negative control siRNA
ADAM10.1 siRNA
VE-cadherin siRNA
Number of cells
Surface VE-cadherin expression
D
Percentage VE-cadherin surface expression (%)
No siRNA
Negative control siRNA
ADAM10.1 siRNA
ADAM10.2 siRNA
VE-cadherin.1 siRNA
VE-cadherin.2 siRNA

Figure 4.11 Partial knockdown of VE-cadherin in the presence of ADAM10 knockdown restores normal PBL transmigration under *in vitro* static adhesion conditions. HUVECs were transfected with two different siRNA duplexes to VE-cadherin (blue bars) at a final concentration of 0.5 nM either alone or in combination with two different siRNA duplexes to ADAM10 (red bars) at a final concentration of 10 nM alongside a non-specific siRNA (black bar) at a final concentration of 10 nM in 12 well plates. 24 hours after transfection, the HUVECs were stimulated and PBL adhesion and transmigration was assessed as previously described. PBLs were classified as firmly adherent or transmigrated (A). The total number of cell classified for each of the behaviours was combined to give a total adhesion count (B). HUVECs transfected with siRNA were analysed by flow cytometry to measure surface VE-cadherin expression. The broken blue line represents VE-cadherin staining of cells transfected with a negative control siRNA and the solid blue line represents VE-cadherin staining following VE-cadherin knockdown with the solid red line representing VE-cadherin staining following ADAM10 knockdown. The black line represents isotype control staining (C). Surface VE-cadherin levels from panel C were quantitated and normalised to the "No siRNA" treated condition (D). Error bars represent the standard error of the mean from five independent experiments. Data were normalised by arcsine transformation and statistically analysed by one-way ANOVA and Dunnett's post-hoc comparisons test for total adhesion data and knockdown confirmation (***$p < 0.01$ compared to Negative control siRNA transfected data) or by a two-way ANOVA and Bonferroni post-hoc comparisons test for PBL cell behaviour (***$p < 0.01$ compared to the negative control siRNA transfected data). Confirmation of ADAM10 knockdown was assessed by flow cytometry as explained in the legend to Figure 4.2 and shown to be ~90% reduced upon quantitation (data not shown).

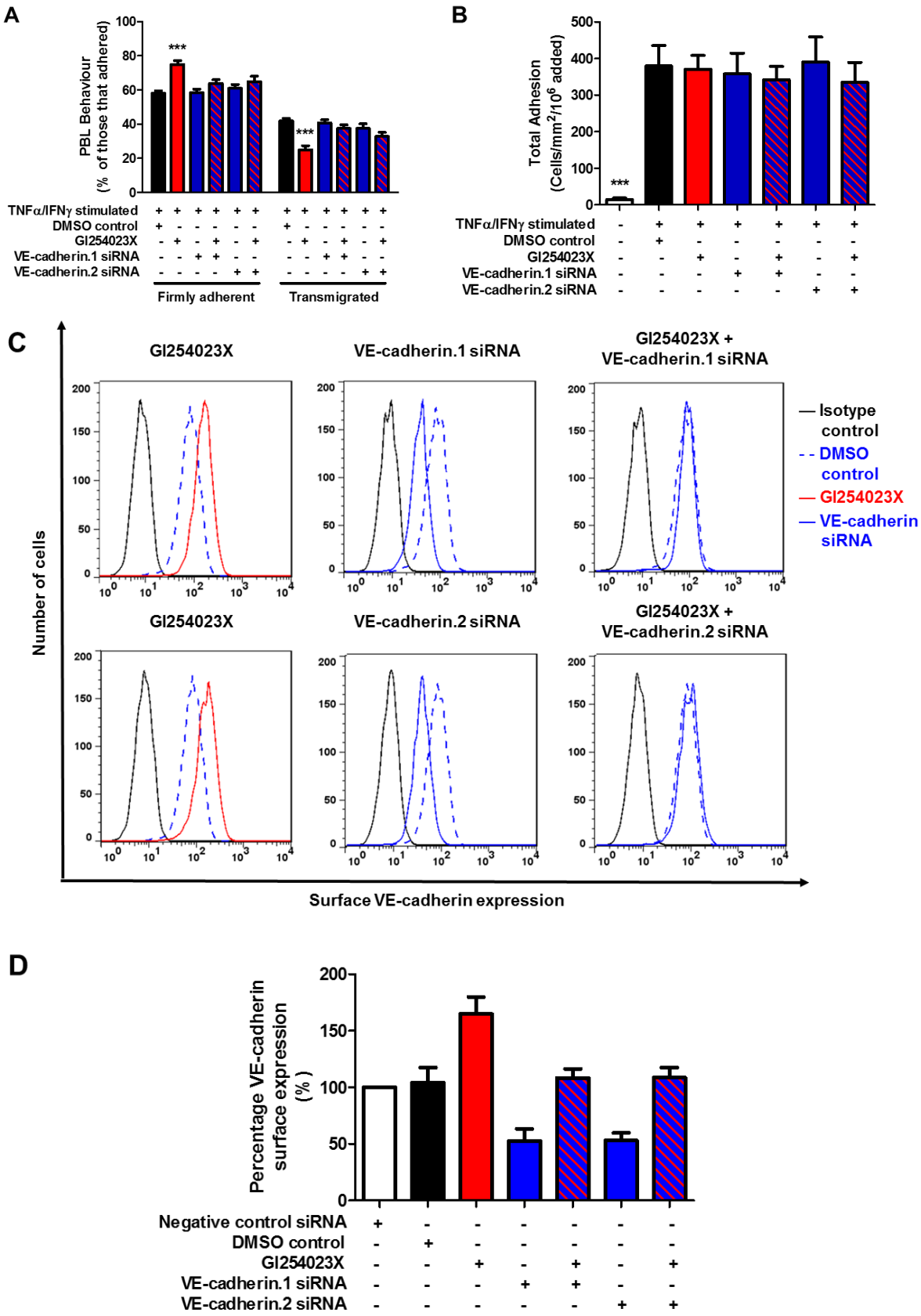
A
PBL Behaviour (% of those that adhered)
TNFα/IFNγ stimulated
DMSO control
GI254023X
VE-cadherin.1 siRNA
VE-cadherin.2 siRNA
Firmly adherent
Transmigrated
B
Total Adhesion (Cells/mm²/10⁶ added)
C
GI254023X
VE-cadherin.1 siRNA
GI254023X + VE-cadherin.1 siRNA
GI254023X
VE-cadherin.2 siRNA
GI254023X + VE-cadherin.2 siRNA
Isotype control
DMSO control
GI254023X
VE-cadherin siRNA
Number of cells
Surface VE-cadherin expression
D
Percentage VE-cadherin surface expression (%)
Negative control siRNA
DMSO control
GI254023X
VE-cadherin.1 siRNA
VE-cadherin.2 siRNA

Figure 4.12 Partial knockdown of VE-cadherin in the presence of ADAM10 inhibition restores normal PBL transmigration under *in vitro* static adhesion conditions. HUVECs were transfected with two different siRNA duplexes to VE-cadherin (blue bars) at a final concentration of 0.5 nM alongside a non-specific siRNA (black bar) at a final concentration of 10 nM. 24 hours after transfection, the HUVECs were stimulated as previously explained in the legend to Figure 4.11 in addition to treatment with 20 µM GI254023X or 0.02% DMSO control. Following 24 hours, PBL adhesion, and transmigration was assessed as previously explained in the legend to Figure 4.10. PBLs were classified as firmly adherent or transmigrated (A). The total number of cell classified for each of the behaviours was combined to give a total adhesion count (B). HUVECs transfected with siRNA were analysed by flow cytometry to measure surface VE-cadherin expression as explained in the legend to Figure 4.11 (C). Surface VE-cadherin levels from panel C were quantitated and normalised to the "Negative control siRNA" treated condition (D). Error bars represent the standard error of the mean from four independent experiments. Data were normalised by arcsine transformation and statistically analysed by one-way ANOVA and Dunnett's post-hoc comparisons test for total adhesion data and knockdown confirmation (*$p < 0.05$, **$p < 0.01$, ***$p < 0.001$ compared to DMSO control data) or by a two-way ANOVA and Bonferroni post-hoc comparisons test for PBL cell behaviour (***$p < 0.01$ compared to DMSO control data).

4.3 DISCUSSION

Paracellular transmigration of leukocytes through the endothelial cell junctions is now regarded as the primary mode through which leukocytes breach the endothelial cell barrier in the peripheral vasculature (Nourshargh and Alon, 2014; Ley et al., 2007). This requires the transient dissociation and disassembly of key endothelial cell junctional proteins, such as VE-cadherin and other homophilic interactions between adjacent endothelial cells (Turowski et al., 2008). Upon binding of leukocytes to the vessel wall, outside-in signalling events dictate endothelial cell junction protein fate by facilitating their disassembly and transient internalisation and recycling (Nottebaum et al., 2008; Vockel and Vestweber, 2013; Turowski et al., 2008; Wessel et al., 2014). The proteolytic cleavage of key junctional proteins has been shown to also facilitate leukocyte extravasation (Schulz et al., 2008; Koenen et al., 2009; Colom et al., 2015). The present study builds on the findings in Chapter 3 by identifying VE-cadherin as the key endothelial ADAM10 substrate involved in primary human PBL transmigration.

Previous studies have shown that cleavage of CX3CL1 and CXCL16 promote leukocyte transmigration, but this was based on transfection of these transmembrane chemokines into cell lines, rather than the endogenous proteins on primary endothelial cells (Hundhausen et al., 2007; Schwarz et al., 2010). By using flow cytometry screening approaches, HUVECs were found to express endogenous levels of CX3CL1, but not CXCL16. These findings are supported by previously published data showing endogenous expression of CX3CL1 on HUVECs (Garton et al., 2001) and a weak expression of CXCL16 in primary smooth muscle cells and associated HUVECs at the mRNA level (Hofnagel et al., 2002) . To determine whether CX3CL1 could be important in facilitating PBL transmigration, levels of its receptor on PBLs, CX3CR1, were measured by flow cytometry. Major peripheral blood lymphocyte subsets were shown not to express CX3CR1. Previous published data highlighted that a select population (~20%) of human peripheral blood memory $CD8^+$ T cells stain positive for CX3CR1 (Foussat et al., 2000).

However, this specific subpopulation of T cells has been shown not to be the major lymphocyte subset (memory $CD4^+$ T cells) that migrates across TNFα/IFNγ stimulated HUVECs (Ahmed et al., 2011; Chimen et al., 2015). As a positive control, $CD14^+$ monocytes stained positive for this chemokine receptor. Human monocyte subsets have been shown to differentially express CX3CR1 and the expression of this chemokine receptor has been linked to distinct migratory phenotypes of both murine and human monocytes (Geissmann et al., 2003). For example, $CD14^+CD16^{++}CX3CR1^{++}$ monocytes have previously been shown to undergo rapid adhesion to activated endothelium by binding to CX3CL1 (Ancuta et al., 2004). Furthermore, PBMCs or monocyte derived THP-1 cells have been shown to adhere to TNFα/IFNγ stimulated HUVECs via CX3CR1 mediated adhesion on endothelial CX3CL1 under static conditions (Hundhausen et al., 2007; Schwarz et al., 2010). Cleavage of CX3CL1 by ADAM10 under ionomycin-induced conditions was shown to reduce PBMC or THP-1 cell adhesion (Hundhausen et al., 2007; Schwarz et al., 2010). However, it yet remains to be shown if shedding of CX3CL1 decreases the adhesion of specific human monocyte subsets under physiological conditions, namely the non-classical ($CD14^+CD16^{++}CX3CR1^{++}$ monocytes) or intermediate ($CD14^{++}CD16^+CX3CR1^{++}$ monocytes) subsets that have important role in patrolling and local surveillance of tissue and pro-inflammatory phenotypes, respectively (Wong et al., 2011).

In addition to screening PBL populations for the chemokine receptor CX3CR1, PBL subsets were also screened for their expression of CXCR6. In line with previously published data, flow cytometry revealed PBLs differentially express CXCR6, with higher levels of the receptor expressed on B cells, $CD56^{low}$ NK cells and NK T cells, and lower expression on $CD4^+$ and $CD8^+$ T cells and $CD56^{hi}$ NK cells (Latta et al., 2007). However, a functional role for CXCR6-mediated adhesion can be ruled out due to the lack of it's ligand CXCL16 on HUVECs.

Targeting of endothelial ADAM10 using gene knockdown or through the use of the ADAM10 inhibitor upregulated the surface expression of another ADAM10 substrate, VE-cadherin. This was supported by a subsequent increase in the resistance of endothelial monolayers. In addition, a decrease in VE-cadherin shedding was observed following ADAM10 knockdown or inhibition. Indeed, a reduction in VE-cadherin shedding by inhibition of ADAM10 has been previously reported (Schulz et al., 2008). The same study also showed that inhibition of endothelial ADAM10 reduced vascular permeability as measured by increased resistance to the passage of 40 kDa FITC-dextran (Schulz et al., 2008). In addition, a separate study showed similar findings in which inhibition of ADAM10 on human dermal microvascular endothelial cells reduced the release of soluble VE-cadherin under TNFα cytokine stimulated conditions, with a subsequent increase in trans-endothelial electrical resistance (Flemming et al., 2015). Collectively, these data suggest that endothelial ADAM10 is able to regulate endothelial junctions by enhancing endothelial electrical resistance, increasing the surface expression of VE-cadherin and subsequently reducing VE-cadherin shedding.

Though previous studies have highlighted that ADAM10 inhibition or knockdown decreases the shedding of VE-cadherin and decreases endothelial monolayer permeability (Schulz et al., 2008; Donners et al., 2010; Flemming et al., 2015), it is still not clear whether this is the cause of the reduced PBL transmigration. In order to determine whether increased VE-cadherin expression levels were causing the transmigration defect, ADAM10 knockdown or inhibition was combined with partial VE-cadherin knockdown designed to return VE-cadherin levels to normal. Strikingly, this approach restored PBL transmigration under conditions of ADAM10 knockdown or inhibition. Flow cytometry confirmed that VE-cadherin expression levels had returned to normal following the partial knockdown, and quantitation revealed this was significant. Taken together, these data suggest that regulation of VE-cadherin surface levels by ADAM10, most likely due to the proteolytic cleavage of VE-cadherin, can control the transmigration efficiency of PBLs.

CHAPTER 5

ADAM10-INTERACTING ENDOTHELIAL TETRASPANINS TSPAN5 AND TSPAN17 PROMOTE LYMPHOCYTE TRANSMIGRATION

5.1 INTRODUCTION

Tetraspanins are a superfamily of 33 transmembrane proteins in mammals that regulate the intracellular trafficking and membrane localisation of the so-called 'partner' proteins with which they associate (Charrin et al., 2014; Hemler, 2014). Tetraspanin association with specific partner proteins has been shown to be important in the leukocyte adhesion cascade. Following rolling, leukocytes undergo firm adhesion by forming integrin-mediated interactions with endothelial cell CAMs, ICAM-1 and VCAM-1. Leukocyte-expressed CD81 clusters the integrin $\alpha_4\beta_1$, which has been shown to lead to increased adhesion strengthening of leukocytes to VCAM-1 (Feigelson et al., 2003). In addition, endothelial tetraspanins CD9 and CD151 cluster the IgSF members ICAM-1 and VCAM-1 into adhesive platforms that facilitate leukocyte adhesion and transmigration (Barreiro et al., 2008). Indeed, loss of CD9 or CD151 on endothelial cells impaired leukocyte adhesion and transmigration, highlighting a fundamental role of tetraspanins in these processes (Barreiro et al., 2005). Moreover, the use of *in vitro* and *in vivo* models has highlighted a role of the tetraspanin CD63 in regulating the trafficking and subsequent clustering of P-selectin, that is required for optimal leukocyte capture such that loss of CD63 in endothelial cells resulted in impaired leukocyte recruitment (Doyle et al., 2011). These data provide evidence for a role of tetraspanins in leukocyte recruitment and adhesion.

As demonstrated in chapters three and four, endothelial ADAM10 is able to regulate the transmigration of PBLs by selectively modulating the surface levels of the adherens junctional protein VE-cadherin. The Tomlinson group and another independent research group have recently published that ADAM10 associates with a subgroup of tetraspanins termed the TspanC8s that consist of six largely understudied tetraspanins, namely Tspan5, 10, 14, 15, 17 and 33, which are related by sequence (Dornier et al., 2012; Haining et al., 2012). Interaction with a TspanC8 was shown to be required for the exit of ADAM10 from the endoplasmic reticulum, enzymatic maturation and trafficking to the cell

surface (Dornier et al., 2012; Haining et al., 2012; Prox et al., 2012b). Indeed, different TspanC8s have been shown to promote the differential cleavage of various ADAM10 substrates. For example, overexpression of Tspan5 and Tspan14, but not Tspan15, has been shown to promote ADAM10 dependent shedding of Notch (Dornier et al., 2012). In addition, overexpression of Tspan15 promoted ADAM10-dependent shedding of N-cadherin in a cell line model (Prox et al., 2012b; Noy et al., 2016; Jouannet et al., 2016). Tspan15 has also been shown to both promote and inhibit ADAM10-dependent shedding of APP in a cell line model (Prox et al., 2012b; Jouannet et al., 2016). The difference in shedding highlighted by these two studies is most likely due to the different cells that were used (HEK293T cells by Prox *et al*. or U2OS cells by Jouannet *et al*.) to assess a role of Tspan15 mediated ADAM10 shedding. However, a role for a specific endothelial TspanC8 in ADAM10-mediated VE-cadherin shedding and PBL transmigration, has not been reported. The aim of this chapter was to investigate this possibility.

5.2 RESULTS

5.2.1 HUVECs express the TspanC8 tetraspanins Tspan5, 14, 15 and 17

Previous studies in the Tomlinson group have shown that HUVECs express four of the TspanC8s, namely Tspan5, 14, 15 and 17, by serial analysis of gene expression (SAGE) (Bailey et al., 2011) and five TspanC8s by RT-PCR, namely Tspan5, 10, 14, 15 and 17 (Haining et al., 2012). However, the effects of cytokine-stimulation on the expression of these TspanC8s has not previously been investigated and so formed the basis of initial investigations in this chapter. Since antibodies were not available to the TspanC8 tetraspanins, RT-PCR was used to determine the relative mRNA expression of the TspanC8s in HUVECs. HUVECs expressed four of the six TspanC8s with greatest expression for Tspan14 (Figure 5.1 A). Tspan5 was also expressed at ~50% of the level of Tspan14, along with Tspan15 and Tspan17 which were expressed at ~25% and ~10% of the level of Tspan14, respectively (Figure 5.1 A). Tspan10 and Tspan33 were undetectable in HUVECs (Figure 5.1 A). To determine whether HUVEC TspanC8 expression is altered upon cytokine stimulation, HUVECs were stimulated with 100 U/ml TNFα and 10 ng/ml IFNγ. RT-PCR confirmed that the TspanC8 expression profile was not significantly affected by the cytokine stimulation (Figure 5.1 B). To summarise, at least at the mRNA level, HUVECs express Tspan5, 15 and 17, with Tspan14 being the most prominently expressed, but lack the expression of Tspan10 or 33.

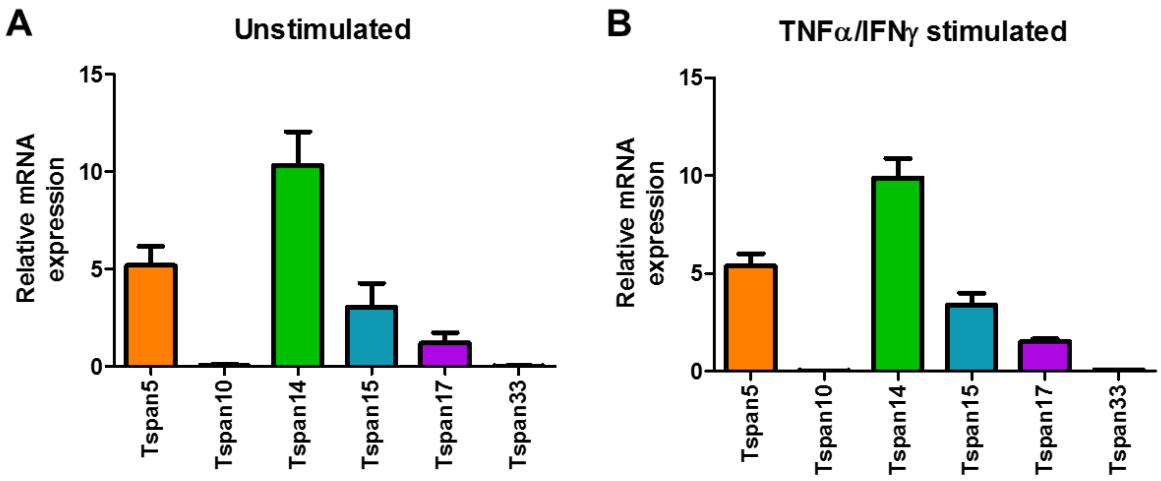

Figure 5.1 HUVECs express endogenous Tspan5, 14, 15 and 17 at the mRNA level. HUVECs were harvested and RNA was isolated as previously described in Section 2.4.3. Isolated RNA was converted into cDNA before carrying out RT-PCR to assess the endogenous expression of the six TspanC8s. Relative Ct values, as calculated as the point at which the threshold meets the amplification curve in the exponential phase of the PCR reaction, were converted into $2^{\Delta\Delta Ct}$ corresponding to the relative fold change in expression and plotted as the relative mRNA expression taking into account GAPDH expression as a housekeeping gene. Endogenous expression levels corresponding to unstimulated HUVECs (A) or HUVECs stimulated with 100 U/ml TNFα and 10 ng/ml IFNγ for 24 hours (B) are shown. Error bars represent the standard error of the mean from four individual experiments.

5.2.2 Overexpression of TspanC8s in HUVECs does not affect PBL transmigration, but alters ADAM10 surface expression and VE-cadherin proteolysis

To investigate whether overexpression of each of the TspanC8s in HUVECs effects PBL transmigration, HUVECs were transduced with lentivirus that expressed the various TspanC8s and a puromycin resistance marker. Puromycin-resistant cells were incorporated into static adhesion assays to assess PBL transmigration, as performed previously. Lentiviral overexpression of each of the TspanC8s in HUVECs did not significantly alter the percentage of PBLs that were firmly adhered or had transmigrated (Figure 5.2 A). In addition, there were no changes in the total number of PBLs that adhered (Figure 5.2 B).

Lentivirally transduced HUVECs were also monitored for their expression of ADAM10 and VE-cadherin by flow cytometry. Overexpression of Tspan15 and Tspan33 doubled ADAM10 surface expression compared to control conditions (Figure 5.3 A & B). Overexpression of the other TspanC8s had no effect on surface ADAM10 levels (Figure 5.3 A & B). In addition, no changes in VE-cadherin surface expression were observed in HUVECs overexpressing any of the TspanC8s (Figure 5.4 A & B).

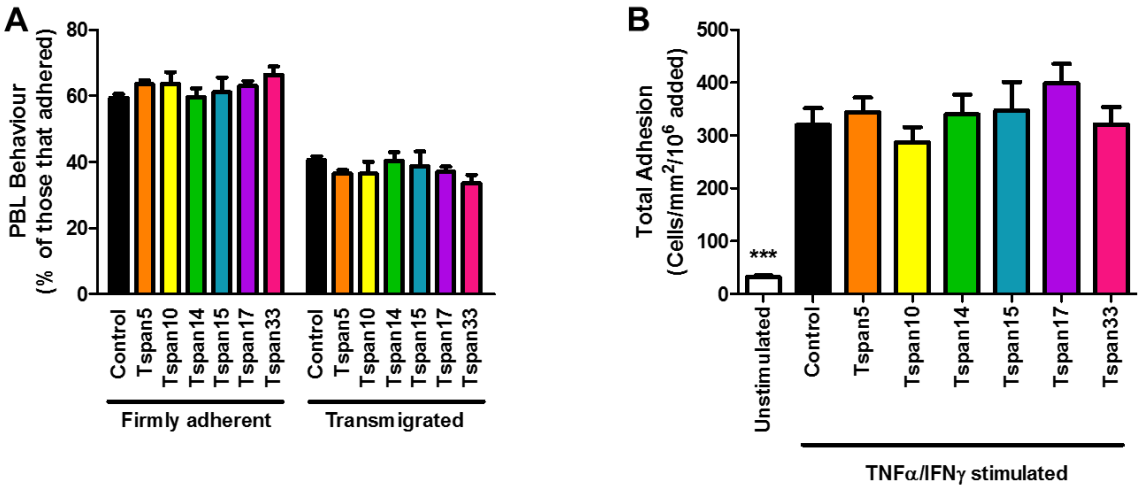

Figure 5.2 Lentiviral overexpression of TspanC8s does not affect lymphocyte transmigration under *in vitro* static conditions. HUVECs were lentivirally transduced with virus-containing media from HEK293T cells transfected individually with the various TspanC8s (Tspan5 – orange bars, Tspan10 – yellow bars, Tspan14 – green bars, Tspan15 – blue bars, Tspan17 – purple bars, Tspan33 – pink bars) or with a mock control vector (black bar). 48 hours after transduction, HUVECs were selected for positive infection by treatment with 2 µg/ml puromycin for an additional 48 hours. Positively selected HUVECs were incorporated into a static adhesion assay to assess PBL adhesion and transmigration as previously explained. PBLs were classified as firmly adherent or transmigrated (A). The total number of cell classified for each of the behaviours was combined to give a total adhesion count (B). Error bars represent the standard error of the mean from four independent experiments. Data were normalised by arcsine transformation and statistically analysed by one-way ANOVA and Dunnett's post-hoc comparisons test for total adhesion data (***$p < 0.001$ compared to 'control' overexpressing cell data) or by a two-way ANOVA and Bonferroni post-hoc comparisons test for PBL cell behaviour.

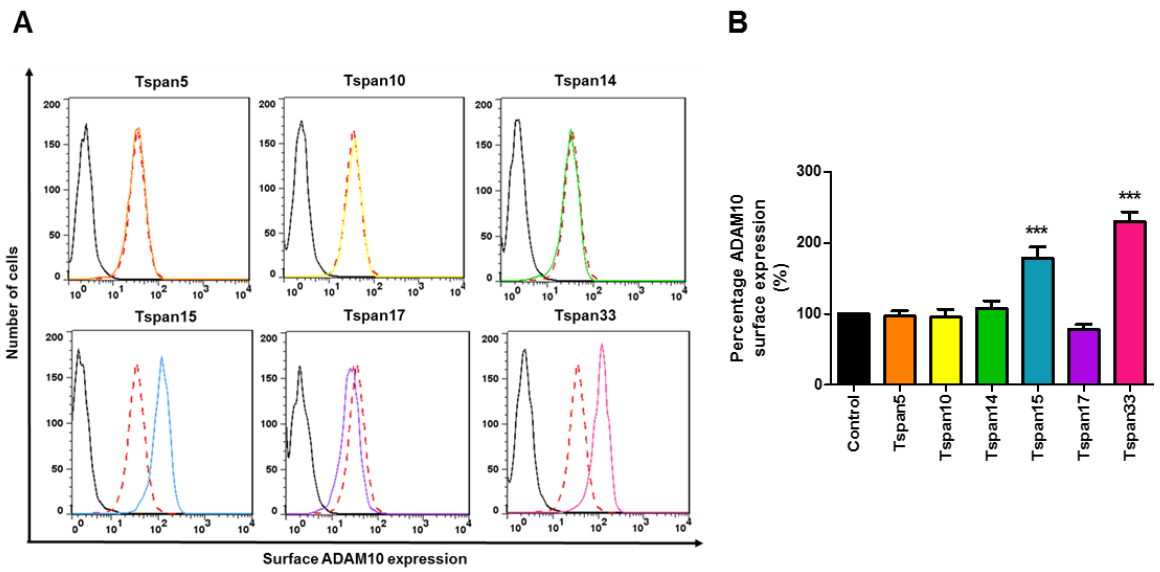

Figure 5.3 Lentiviral overexpression of Tspan15 and Tspan33 increases surface ADAM10 expression on HUVECs. HUVECs were lentivirally transduced and selected as explained in the legend to Figure 5.2 before undergoing flow cytometry to measure surface ADAM10 expression. The orange, yellow, green, blue, purple, and pink solid lines represent ADAM10 expression in the TspanC8 transduced HUVECs. The broken red line represents basal ADAM10 expression in the mock control vector transduced HUVECs. The black line represents isotype control staining (A). Surface ADAM10 levels from panel A were quantitated and geometric mean values are shown in (B). Error bars represent the standard error or the mean from four independent experiments. Data were statistically analysed by One-way ANOVA followed by a Dunnett's multiple-comparisons post-hoc test (***$p < 0.001$ compared to 'mock control vector' transduced HUVECs).

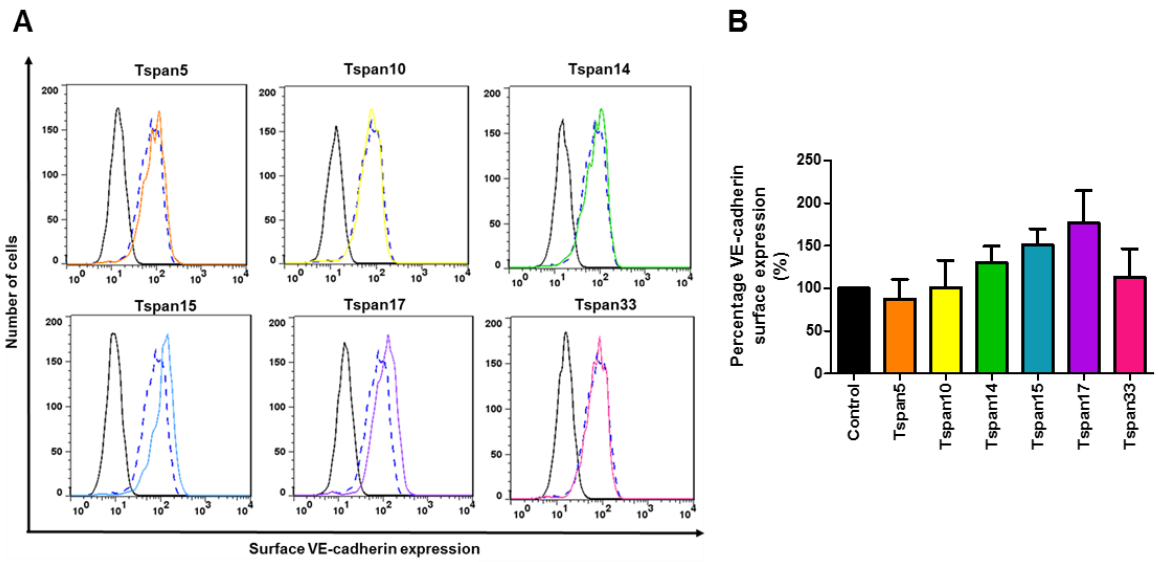

Figure 5.4 Lentiviral overexpression of TspanC8s does not alter VE-cadherin expression on HUVECs. Lentivirally transduced HUVECs were stained for the expression of VE-cadherin and data is presented as explained in the legend to Figure 5.3. Error bars represent the standard error or the mean from four independent experiments. Data were statistically analysed by One-way ANOVA followed by a Dunnett's multiple-comparisons post-hoc test.

Although the surface levels of VE-cadherin were not effected by overexpression of the TspanC8s, cleavage of VE-cadherin may have been altered. To evaluate this possibility, lentivirally transduced HUVECs were assessed for their ability to cleave VE-cadherin using Western blotting. The cells were treated with 10 μM DAPT (a γ-secretase inhibitor) to prevent cleavage of the C-terminal fragment and the cells were cultured for an additional 24 hours. Western blotting of cell lysates, using an antibody which binds to the cytoplasmic tail of VE-cadherin, showed that overexpression of Tspan15 or 33 reduced VE-cadherin shedding from ~60% of VE-cadherin shed in the control lane to ~30% shed for either Tspan15 or 33 overexpressing cells (Figure 5.5 A & B). Overexpression of Tspan5, 10, 14 or 17 did not alter cleavage of VE-cadherin (Figure 5.5 A & B). FLAG blotting showed that each of the TspanC8s were overexpressed to varying levels. It was noted that Tspan10, 15 and 33 had considerably stronger expression levels than the other TspanC8s (Figure 5.5 C).

Taken together, the data indicated that overexpression of any individual TspanC8 does not regulate PBL transmigration, yet overexpression of Tspan15 or Tspan33 resulted in increased ADAM10 surface expression and reduced VE-cadherin shedding. The latter is the opposite of what might have been expected if VE-cadherin shedding was simply determined by levels of ADAM10. Since Tspan15 and Tspan33 were particularly strongly expressed, compared with most of the other TspanC8s, it is possible that these were sequestering ADAM10 away from VE-cadherin. To speculate further, it is possible that one of the other TspanC8s might promote VE-cadherin shedding, but that its lentiviral expression level was too low in the experiments for any significant shedding increase to be observed. To test these ideas, TspanC8 knockdown approached were employed in the experiments that follow.

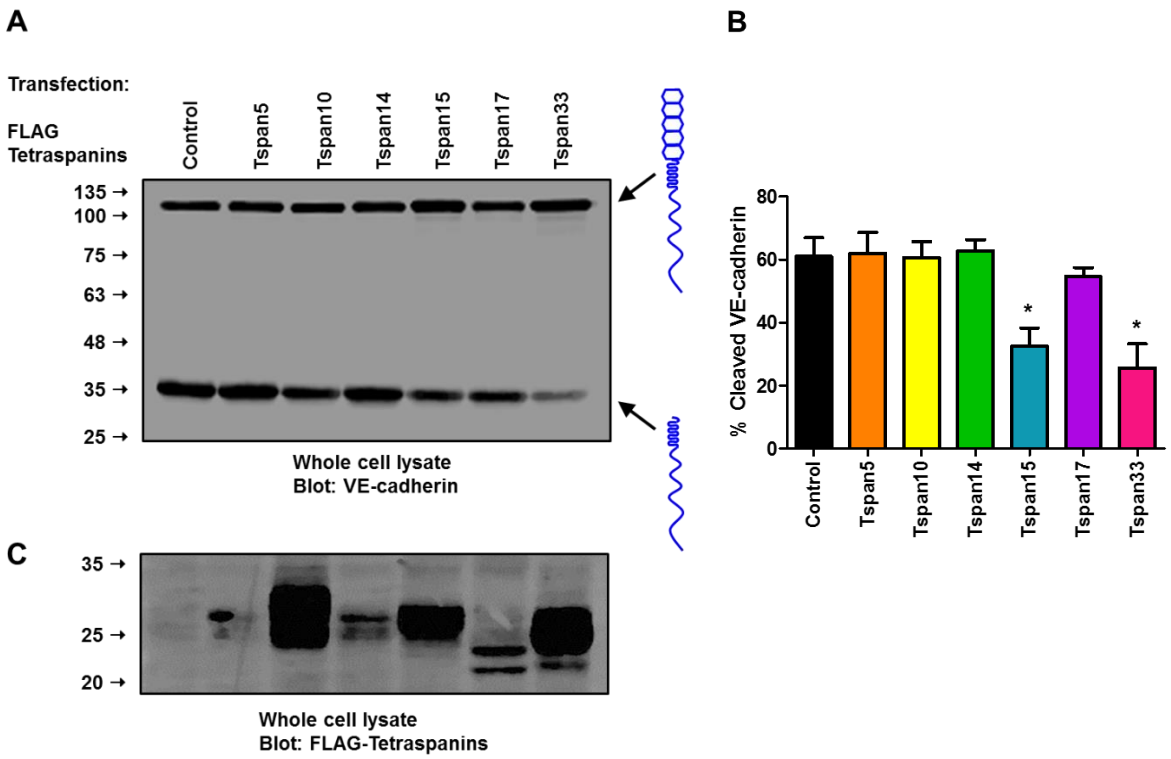

Figure 5.5 Lentiviral overexpression of Tspan15 and Tspan33 reduce VE-cadherin cleavage. HUVECs were lentivirally transduced and selected as explained in the legend to Figure 5.2. HUVECs were treated with 10 μM DAPT for 24 hours to prevent further proteolytic processing of VE-cadherin after ADAM10 cleavage. HUVECs were then harvested and subjected to Western blotting for VE-cadherin. The membrane was imaged and bands quantified on the Odyssey Infrared Imaging System (A). The percentage cleaved was calculated by dividing the cleaved VE-cadherin fragment (~35 kDa) by the total VE-cadherin (relative band intensities corresponding to full length (~100) and cleaved VE-cadherin added together) (B). The membrane was stripped and re-probed with mouse anti-FLAG to assess TspanC8 tetraspanin expression (C). Error bars represent the standard error of the mean from four independent experiments. Data were analysed by One-way ANOVA followed by a Dunnett's multiple-comparisons post-hoc test (*$p < 0.05$ compared to mock 'control' vector transduced cells).

5.2.3 Knockdown of individual TspanC8s in HUVECs does not affect PBL transmigration or ADAM10-dependent changes in VE-cadherin shedding

A siRNA-mediated gene knockdown approach of endogenous TspanC8s was utilised to elucidate a possible role of different TspanC8s in regulating the role of ADAM10 during PBL transmigration. HUVECs were transfected with one of two siRNA duplexes that target each of the six TspanC8s or with a non-specific control siRNA duplex. All duplexes were used at a final concentration of 10 nM. 24 hours after transfection, HUVECs were stimulated with 100 U/ml TNFα and 10 ng/ml IFNγ for an additional 24 hours, and the static adhesion assay was carried out as previously explained. Knockdown of any one TspanC8 did not alter the ability of PBLs to transmigrate or firmly adhere (Figure 5.6 A & C). In addition, no differences in total adhesion of PBLs were observed following individual TspanC8 tetraspanin knockdown (Figure 5.6 B & D). To confirm that each of the individual TspanC8 tetraspanin knockdowns had worked, cDNA was produced from extracted RNA and quantitative PCR was performed, as previously explained. Knockdown of TspanC8s expressed in HUVECs resulted in ~75%, ~52%, ~80% and ~80% reduction in mRNA expression for Tspan5, 14, 15 and 17, respectively (Figure 5.6 E). Since Tspan10 and Tspan33 were not detected at endogenous levels in resting HUVECs, the knockdown efficiency could not be calculated and these 'knockdowns' served as additional negative controls.

To determine whether knockdown of each of the individual TspanC8s affects ADAM10 or VE-cadherin surface levels, HUVECs were transfected with one of two siRNA duplexes that target each of the six TspanC8s or with a non-specific control siRNA duplex, as explained above. Flow cytometry analysis revealed that the knockdown of Tspan14 or Tspan15 resulted in a ~12% reduction in ADAM10 surface levels (Figure 5.7). Knockdown of the other TspanC8s (Tspan5, 10, 17 or 33) did not affect basal ADAM10 surface levels (Figure 5.7). Similarly, knockdown of individual TspanC8s in HUVECs did not affect basal VE-cadherin surface levels (Figure 5.8).

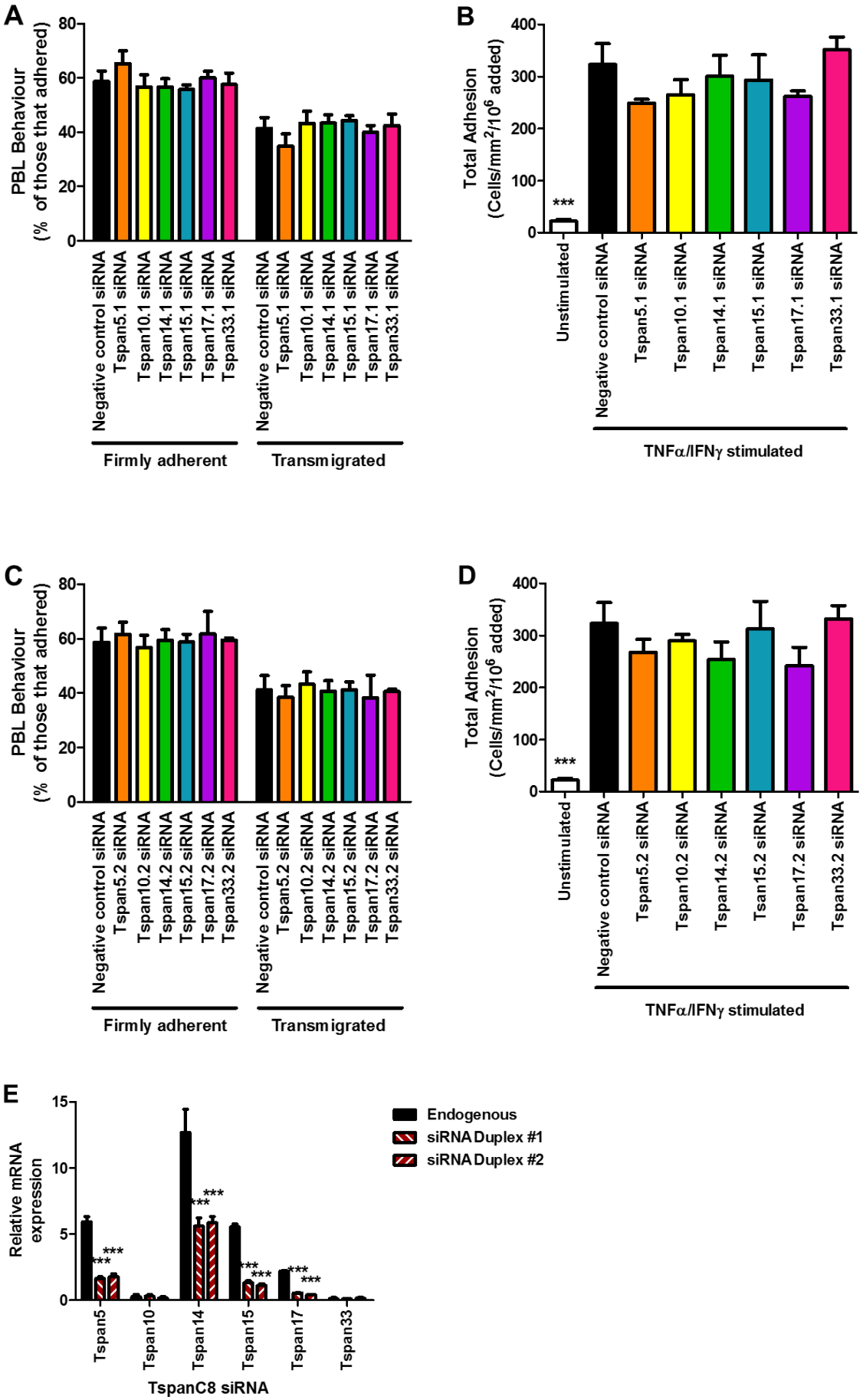
A
PBL Behaviour (% of those that adhered)
Negative control siRNA
Tspan5.1 siRNA
Tspan10.1 siRNA
Tspan14.1 siRNA
Tspan15.1 siRNA
Tspan17.1 siRNA
Tspan33.1 siRNA
Firmly adherent
Transmigrated
B
Total Adhesion (Cells/mm2/10^6 added)
***
Unstimulated
TNFα/IFNγ stimulated
C
Tspan5.2 siRNA
Tspan10.2 siRNA
Tspan14.2 siRNA
Tspan15.2 siRNA
Tspan17.2 siRNA
Tspan33.2 siRNA
D
Tsan15.2 siRNA
E
Relative mRNA expression
Endogenous
siRNA Duplex #1
siRNA Duplex #2
Tspan5
Tspan10
Tspan14
Tspan15
Tspan17
Tspan33
TspanC8 siRNA

Figure 5.6 Knockdown of individual tetraspanins does not alter the ability of PBLs to transmigrate under *in vitro* static conditions. HUVECs were transfected with two different siRNA duplexes to the various TspanC8s at a final concentration of 10 nM. 24 hours after transfection, the HUVECs were stimulated and PBL adhesion and transmigration was assessed as previously explained for static adhesion assays. PBLs were classified as firmly adherent or transmigrated (A & C). The total number of cell classified for each of the behaviours was combined to give a total adhesion count (B & D). HUVECs transfected with siRNA were analysed by RT-PCR to measure the relative knockdown efficiency of the various TspanC8s at the mRNA level, as explained in the legend to Figure 5.1 (E). Error bars represent the standard error of the mean from four independent experiments. Data were normalised by arcsine transformation and statistically analysed by one-way ANOVA and Dunnett's post-hoc comparisons test for total adhesion data and knockdown confirmation (***$p < 0.001$ compared to negative control siRNA transfected data) or by a two-way ANOVA and Bonferroni post-hoc comparisons test for PBL cell behaviour.

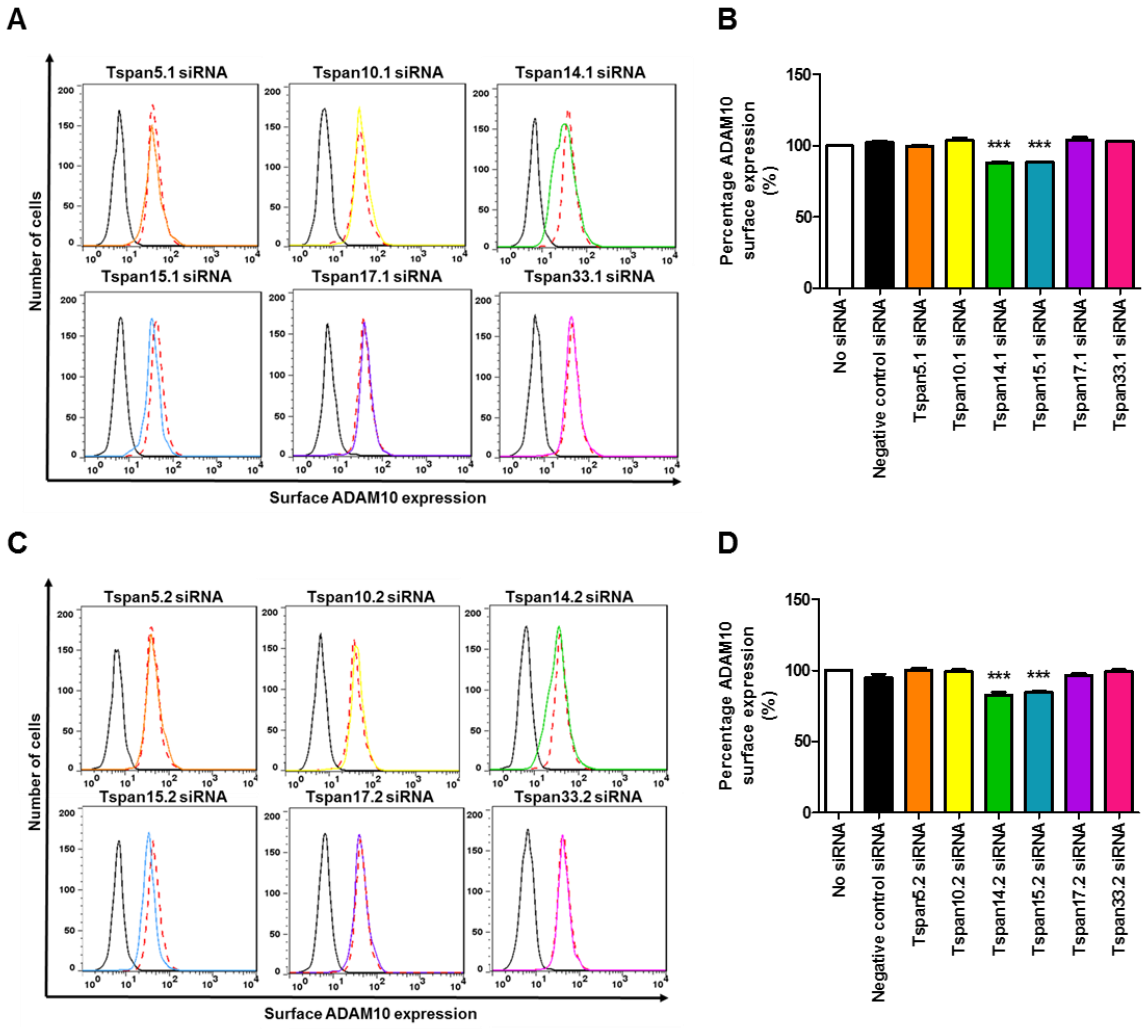

Figure 5.7 Knockdown of Tspan14 or Tspan15 reduces ADAM10 surface expression. HUVECs were transfected with one of two siRNA duplexes to the various TspanC8s or with a negative control siRNA as explained in the legend to Figure 5.6. Following 48 hours, HUVECs were harvested processed by flow cytometry to measure surface ADAM10 expression as explained in the legend to Figure 5.3 (A & C). Surface ADAM10 levels from panel A & C were quantitated and normalised to the average ADAM10 surface expression in the 'no siRNA' condition (B & D). Confirmation of individual TspanC8 knockdowns were assessed by RT-PCR as explained in the legend to Figure 5.1 and shown to be 50-90% reduced upon quantitation and in line with mRNA levels shown in Figure 5.6 (data not shown). Error bars represent the standard error or the mean from four independent experiments. Data were statistically analysed by One-way ANOVA followed by a Dunnett's multiple-comparisons post-hoc test (***$p < 0.01$ compared to 'negative control siRNA' transfected HUVECs).

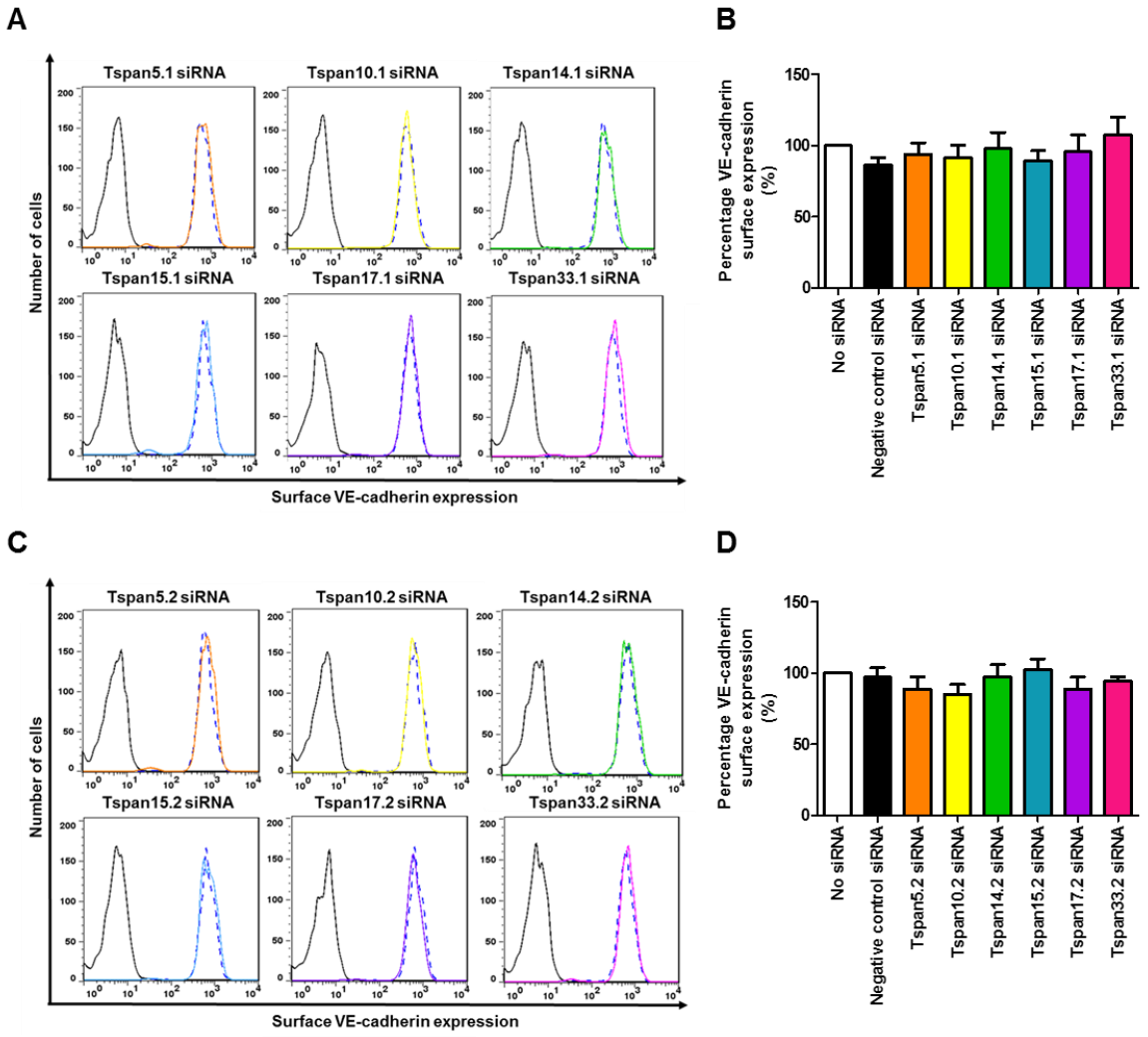

Figure 5.8 Knockdown of TspanC8s do not affect VE-cadherin surface expression. Individual TspanC8 knocked down HUVECs were stained for the expression of VE-cadherin and data is presented as explained in the legend to Figure 5.7. Error bars represent the standard error or the mean from four independent experiments. Data were statistically analysed by One-way ANOVA followed by a Dunnett's multiple-comparisons post-hoc test.

To determine the effects of individual TspanC8 knockdowns on ADAM10 activity towards VE-cadherin, HUVECs were transfected with one of two siRNA duplexes to the six TspanC8s, as explained above. 24 hours after transfection, 10 μM DAPT was added and the cells were cultured for an additional 24 hours. The cells were harvested, lysed, and subjected to SDS-PAGE Western blotting for VE-cadherin, as previously described. Knockdown of individual TspanC8s did not alter the shedding of VE-cadherin (Figure 5.9).

Collectively, these data suggest that knockdown of each individual TspanC8 in HUVECs does not affect PBL transmigration, VE-cadherin shedding or VE-cadherin surface levels. Furthermore, only a partial reduction in ADAM10 surface levels is observed following Tspan14 or Tspan15 knockdown, but ADAM10 surface levels remain unaltered in cells with reduced Tspan5 or Tspan17.

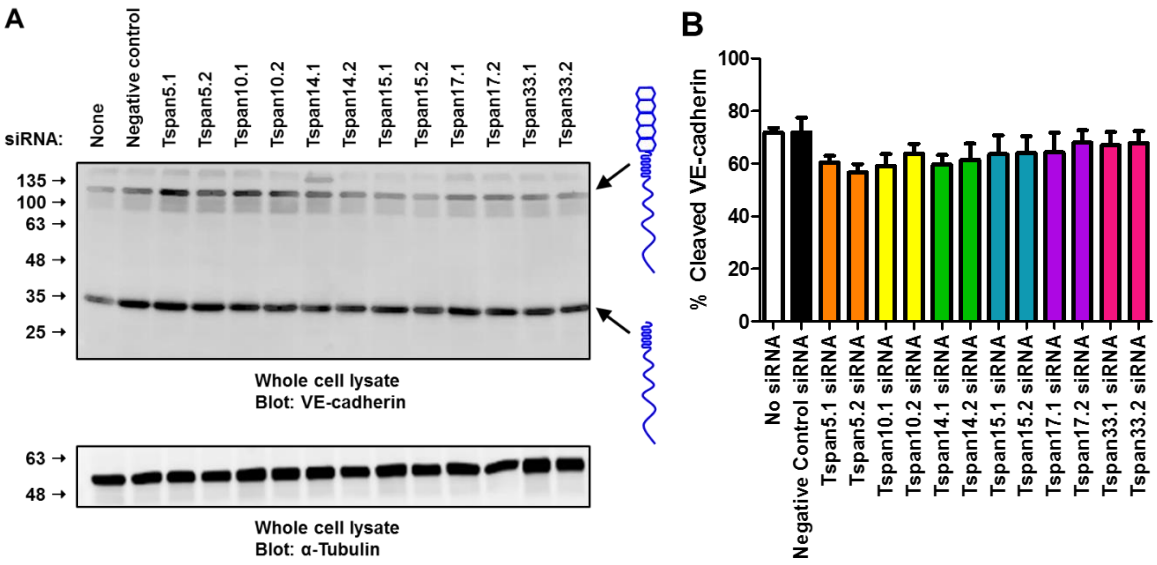

Figure 5.9 Knockdown of TspanC8s does not affect VE-cadherin cleavage. HUVECs were transfected with siRNA duplexes to the various TspanC8s as explained in the legend to Figure 5.6. Following 24 hours, HUVECs were treated with 10 µM DAPT for an additional 24 hours to prevent further proteolytic processing of VE-cadherin after ADAM10 cleavage. HUVECs were then harvested, lysed and Western blotting was carried out for VE-cadherin as explained in the legend to Figure 5.5. α-Tubulin was used as a loading control. The membrane was imaged and bands quantified on the Odyssey Infrared Imaging System (A). The percentage cleaved was calculated as previously explained in the legend to Figure 5.5 (B). Confirmation of individual TspanC8 knockdowns were assessed by RT-PCR as explained in the legend to Figure 5.1 and shown to be 50-90% reduced upon quantitation and in line with mRNA levels shown in Figure 5.6 (data not shown). Error bars represent the standard error of the mean from four independent experiments. Data were analysed by One-way ANOVA followed by a Dunnett's multiple-comparisons post-hoc test.

5.2.4 The presence of Tspan5 or Tspan17 is sufficient to maintain PBL transmigration under cytokine stimulatory conditions

Since individual TspanC8 knockdowns did not affect the ability of PBLs to transmigrate, it was speculated that the TspanC8s could be compensating for each other since all the TspanC8s expressed in HUVECs can promote ADAM10 maturation (Haining et al., 2012). Therefore, a combination knockdown approach was undertaken to investigate the role of individual TspanC8s in regulating PBL transmigration. In these set of experiments, HUVECs were transfected with siRNA duplexes corresponding to all six of the TspanC8s (30 nM siRNA in total) or five of the six TspanC8s (25 nM siRNA in total) or with a non-specific siRNA duplex (30 nM). This approach allowed the function of each individual TspanC8 tetraspanin to be investigated without compensation from another family member. 24 hours after transfection, HUVECs were stimulated with 100 U/ml TNFα and 10 ng/ml IFNγ for an additional 24 hours and a static adhesion assay was carried out as previously explained. Interestingly, knockdown of all TspanC8s in HUVECs suppressed the transmigration of PBLs to ~45% of the control transfected HUVECs (Figure 5.10 A & C). Knockdown of five of the six TspanC8s also suppressed PBL transmigration, with the exceptions of HUVECs that retained the expression of Tspan5 or Tspan17, which maintained PBL transmigration equivalent to control transfected HUVECs (Figure 5.10 A & C). No significant differences in PBL total adhesion were observed following combination TspanC8 knockdown (Figure 5.10 B & D). Interestingly, CLUSTAL Omega protein sequence analysis showed that Tspan5 and 17 are the two most highly related TspanC8s, sharing 78% identity in human (Figure 5.11), which is consistent with their common role in regulating PBL transmigration. Confirmation of TspanC8s knockdown efficiency under the various combination knockdown conditions was assessed by RT-PCR as previously described. Knockdown of Tspan5, Tspan14, Tspan15 or Tspan17 resulted in 60%, 50% 70% or 60% reduction in expression, respectively (Figure 5.12). Combination knockdown of HUVECs transfected with siRNA duplexes corresponding to

five of the six TspanC8s did not alter mRNA expression of the individual TspanC8 not targeted by siRNA (Figure 5.12 B – G).

To determine whether knockdown of multiple TspanC8s affects ADAM10 and VE-cadherin surface levels on HUVECs, cells with the above siRNA knockdown combinations were stained with ADAM10 and VE-cadherin as explained previously. Flow cytometry for ADAM10 revealed a partial reduction in ADAM10 surface levels in knockdown combinations that either targeted all of the TspanC8s or retained the expression of Tspan5, 10, 15, 17 or 33 (Figure 5.13). Knockdown combinations that retained the expression of Tspan14 maintained normal surface expression of ADAM10 (Figure 5.13). Flow cytometry analysis of VE-cadherin surface levels in TspanC8 knockdown combinations revealed that the knockdown combinations that retained the expression of Tspan5 or Tspan17 reduced VE-cadherin surface levels when compared to control transfected conditions (Figure 5.14). Furthermore, the other knockdown combinations, in addition to the knockdown of all TspanC8s in HUVECs, maintained basal VE-cadherin levels (Figure 5.14). Therefore, Tspan5 and Tspan17 are important for PBL transmigration and the maintenance of normal VE-cadherin expression levels at the cell surface. This is not because these TspanC8s are critical for ADAM10 surface expression, since Tspan14 is the important TspanC8 in this regard.

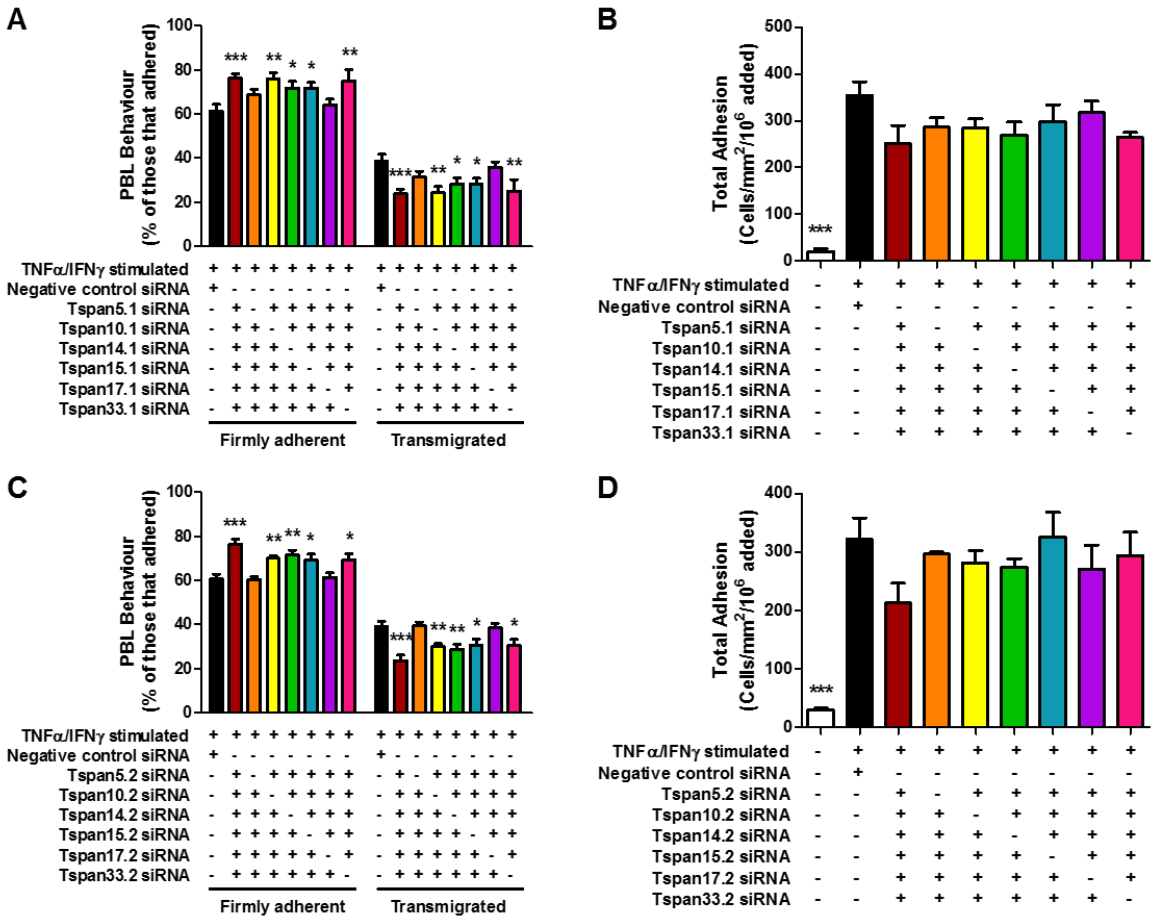

Figure 5.10 The presence of Tspan5 or Tspan17 is sufficient to maintain basal PBL transmigration under *in vitro* static conditions. HUVECs were transfected with one of two siRNA duplexes corresponding to the various TspanC8 tetraspanins at 5 nM (red bars) or transfected with 5 nM negative control siRNA duplex (black bars) for 48 hours. To evaluate the single role of a tetraspanin, all TspanC8s were knocked down using siRNA apart from a single tetraspanin hereby revealing the presence of the single tetraspanin. 24 hours after transfection, the HUVECs were stimulated and PBL adhesion and transmigration was assessed as previously explained for static adhesion assays. PBLs were classified as firmly adherent or transmigrated (A & C). The total number of cell classified for each of the behaviours was combined to give a total adhesion count (B & D). Error bars represent the standard error of the mean from at least five independent experiments. Data were normalised by arcsine transformation and statistically analysed by one-way ANOVA and Dunnett's post-hoc comparisons test for total adhesion data (***p < 0.01 compared to Negative control siRNA transfected HUVECs) or by a two-way ANOVA and Bonferroni post-hoc comparisons test for PBL cell behaviour (*p < 0.05, **p < 0.01, ***p < 0.001 compared to negative control siRNA transfected HUVECs).

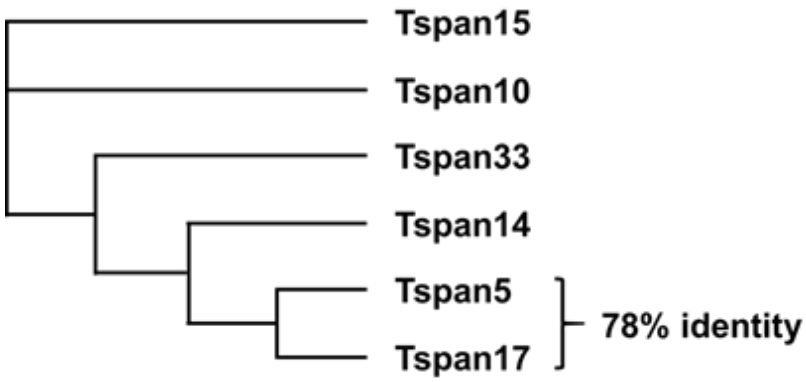

Figure 5.11 Phylogenetic tree of TspanC8 tetraspanins. TspanC8s expressed in humans were analysed for sequence similarity using Clustal OMEGA protein sequence alignment software. The high level of sequence similarity between Tspan5 and Tspan17 is highlighted.

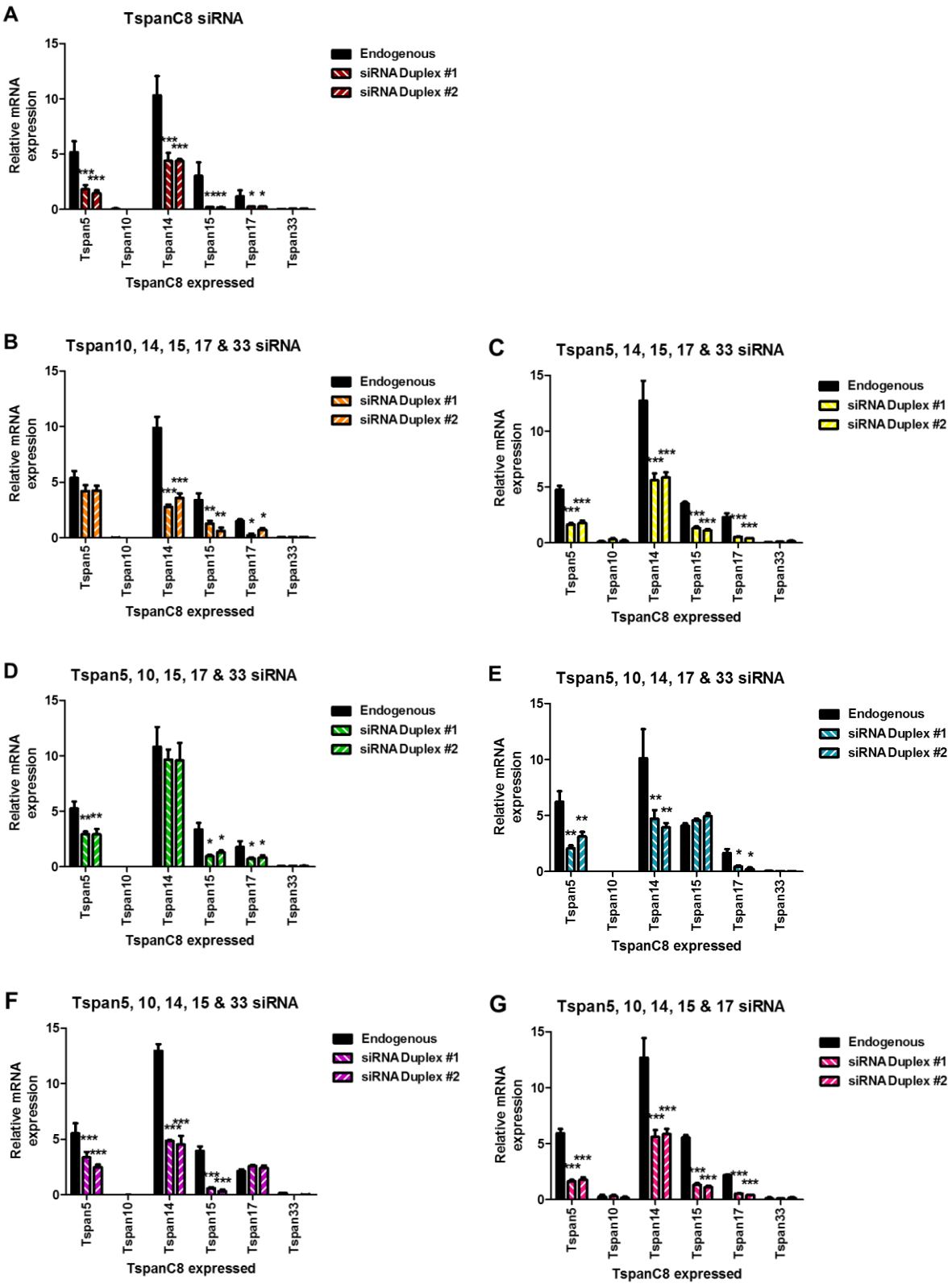
A
TspanC8 siRNA
Relative mRNA expression
Endogenous
siRNA Duplex #1
siRNA Duplex #2
Tspan5
Tspan10
Tspan14
Tspan15
Tspan17
Tspan33
TspanC8 expressed
B
Tspan10, 14, 15, 17 & 33 siRNA
C
Tspan5, 14, 15, 17 & 33 siRNA
D
Tspan5, 10, 15, 17 & 33 siRNA
E
Tspan5, 10, 14, 17 & 33 siRNA
F
Tspan5, 10, 14, 15 & 33 siRNA
G
Tspan5, 10, 14, 15 & 17 siRNA

Figure 5.12 Confirmation of TspanC8 knockdown. HUVECs transfected with combined TspanC8 siRNAs were analysed by RT-PCR to measure the relative knockdown efficiency of the various TspanC8s at the mRNA level as explained in the legend to Figure 5.1. ΔCt values were analysed as explained in the legend to Figure 5.1 and the relative fold change in expression is plotted as the relative mRNA expression (A - G). The various TspanC8 siRNA knockdown combinations are shown (B – G) along with TspanC8 siRNA where all TspanC8s have been targeted using siRNA (A). Error bars represent the standard error of the mean from five independent experiments. Data were analysed by one-way ANOVA followed by Dunnett's multiple comparisons test (*$p < 0.05$, p**< 0.01, ***$p < 0.001$ compared to endogenous TspanC8 tetraspanin expression).

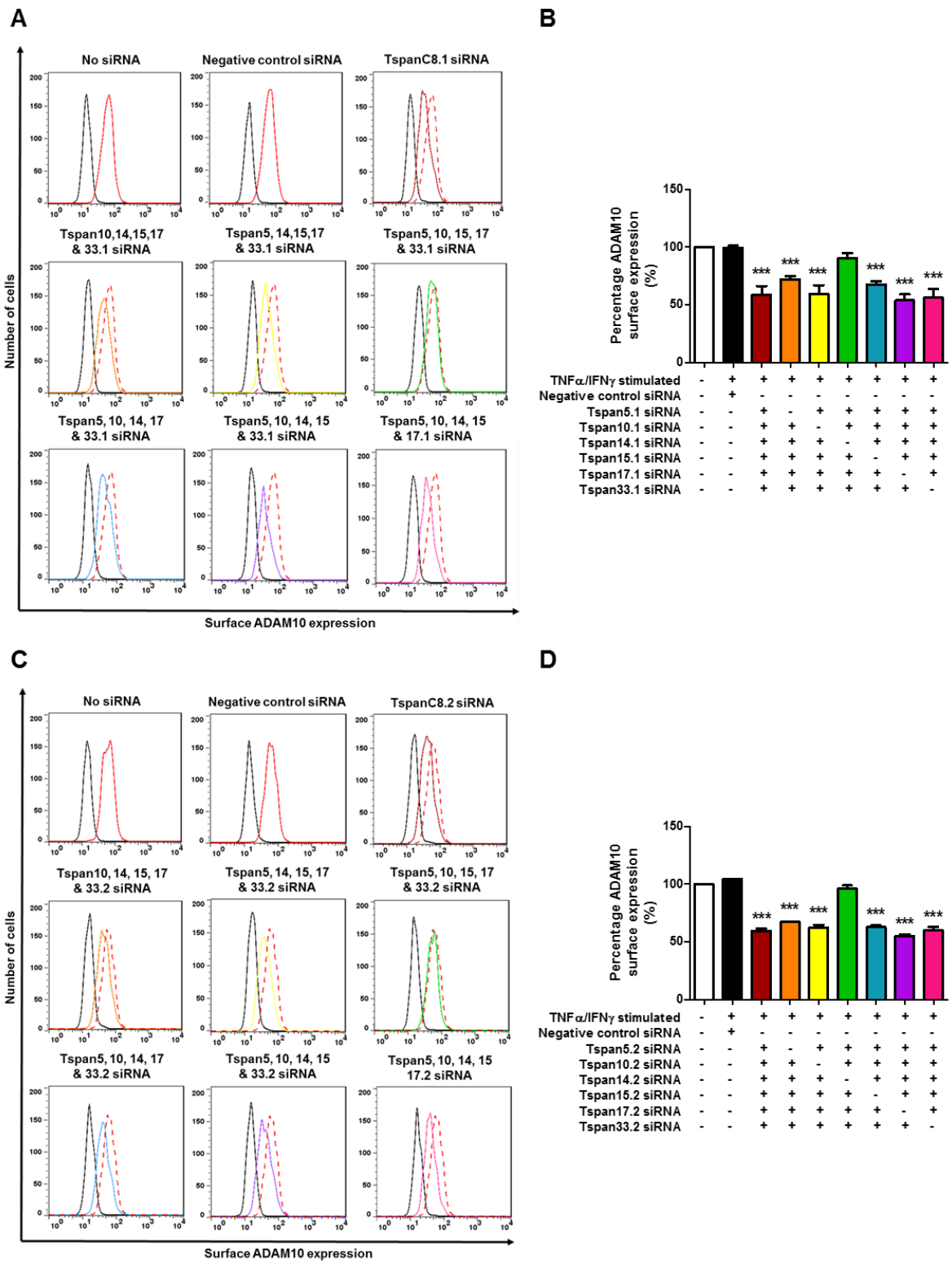
A
No siRNA
Negative control siRNA
TspanC8.1 siRNA
Tspan10,14,15,17 & 33.1 siRNA
Tspan5, 14,15,17 & 33.1 siRNA
Tspan5, 10, 15, 17 & 33.1 siRNA
Tspan5, 10, 14, 17 & 33.1 siRNA
Tspan5, 10, 14, 15 & 33.1 siRNA
Tspan5, 10, 14, 15 & 17.1 siRNA
Number of cells
Surface ADAM10 expression
B
Percentage ADAM10 surface expression (%)
TNFα/IFNγ stimulated
Negative control siRNA
Tspan5.1 siRNA
Tspan10.1 siRNA
Tspan14.1 siRNA
Tspan15.1 siRNA
Tspan17.1 siRNA
Tspan33.1 siRNA
C
No siRNA
Negative control siRNA
TspanC8.2 siRNA
Tspan10, 14, 15, 17 & 33.2 siRNA
Tspan5, 14, 15, 17 & 33.2 siRNA
Tspan5, 10, 15, 17 & 33.2 siRNA
Tspan5, 10, 14, 17 & 33.2 siRNA
Tspan5, 10, 14, 15 & 33.2 siRNA
Tspan5, 10, 14, 15 17.2 siRNA
Number of cells
Surface ADAM10 expression
D
Percentage ADAM10 surface expression (%)
TNFα/IFNγ stimulated
Negative control siRNA
Tspan5.2 siRNA
Tspan10.2 siRNA
Tspan14.2 siRNA
Tspan15.2 siRNA
Tspan17.2 siRNA
Tspan33.2 siRNA

Figure 5.13 The presence of Tspan14 is sufficient to maintain basal ADAM10 surface expression. HUVECs were transfected with one of two siRNA duplexes corresponding to the various TspanC8 tetraspanins at 5 nM (red bars) or transfected with 5 nM negative control siRNA duplex (black bars) for 48 hours. To evaluate the single role of a tetraspanin, all TspanC8s were knocked down using siRNA apart from a single tetraspanin hereby revealing the presence of the single tetraspanin not targeted using siRNA as explained in the legend to Figure 5.10. HUVECs were processed by flow cytometry to measure surface ADAM10 expression as explained in the legend to Figure 5.3 (A & C). Surface ADAM10 levels from panel A were quantitated and normalised to the average ADAM10 surface expression in the 'no siRNA' condition (B & D). Confirmation of individual TspanC8 knockdowns in the various conditions were assessed by RT-PCR as explained in the legend to Figure 5.1 and shown to be 50% or more reduced upon quantitation and in line with mRNA levels shown in Figure 5.12 (data not shown). Error bars represent the standard error or the mean from five independent experiments. Data were statistically analysed by One-way ANOVA followed by a Dunnett's multiple-comparisons post-hoc test (**$p < 0.01$, ***$p < 0.001$ compared to 'negative control siRNA' transfected HUVECs).

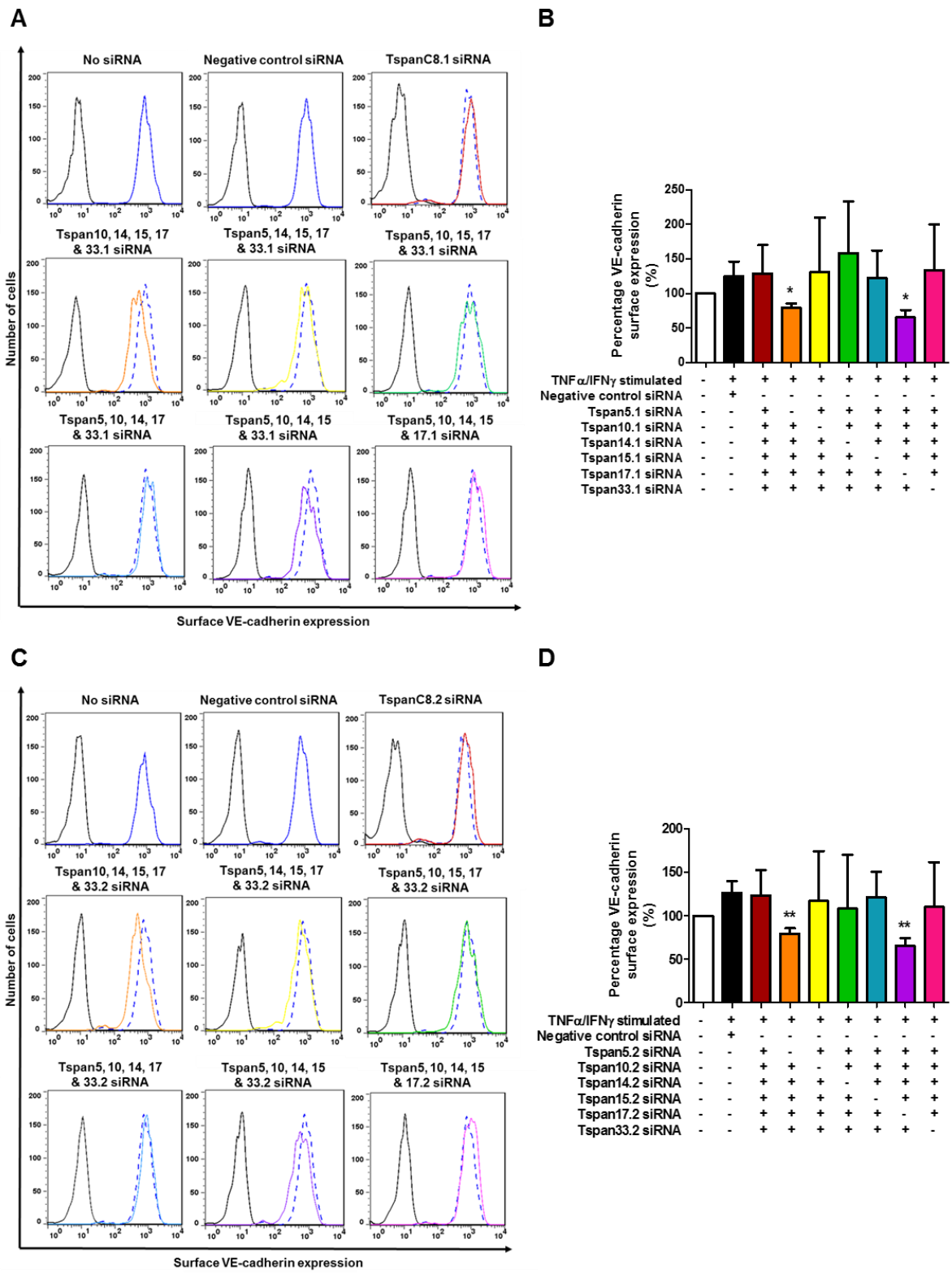
A
No siRNA
Negative control siRNA
TspanC8.1 siRNA
Tspan10, 14, 15, 17 & 33.1 siRNA
Tspan5, 14, 15, 17 & 33.1 siRNA
Tspan5, 10, 15, 17 & 33.1 siRNA
Tspan5, 10, 14, 17 & 33.1 siRNA
Tspan5, 10, 14, 15 & 33.1 siRNA
Tspan5, 10, 14, 15 & 17.1 siRNA
Number of cells
Surface VE-cadherin expression
B
Percentage VE-cadherin surface expression (%)
TNFα/IFNγ stimulated
Negative control siRNA
Tspan5.1 siRNA
Tspan10.1 siRNA
Tspan14.1 siRNA
Tspan15.1 siRNA
Tspan17.1 siRNA
Tspan33.1 siRNA
C
No siRNA
Negative control siRNA
TspanC8.2 siRNA
Tspan10, 14, 15, 17 & 33.2 siRNA
Tspan5, 14, 15, 17 & 33.2 siRNA
Tspan5, 10, 15, 17 & 33.2 siRNA
Tspan5, 10, 14, 17 & 33.2 siRNA
Tspan5, 10, 14, 15 & 33.2 siRNA
Tspan5, 10, 14, 15 & 17.2 siRNA
Number of cells
Surface VE-cadherin expression
D
Percentage VE-cadherin surface expression (%)
TNFα/IFNγ stimulated
Negative control siRNA
Tspan5.2 siRNA
Tspan10.2 siRNA
Tspan14.2 siRNA
Tspan15.2 siRNA
Tspan17.2 siRNA
Tspan33.2 siRNA

Figure 5.14 Surface VE-cadherin levels are reduced upon combination knockdowns that leave either Tspan5 or Tspan17 as the only HUVEC TspanC8. HUVECs were transfected with one of two siRNA duplexes corresponding to the various TspanC8 tetraspanins at 5 nM (red bars) or transfected with 5 nM negative control siRNA duplex (black bars) for 48 hours. To evaluate the single role of a tetraspanin, all TspanC8s were knocked down using siRNA apart from a single tetraspanin hereby revealing the presence of the single tetraspanin not targeted using siRNA as explained in the legend to Figure 5.10. HUVECs were processed by flow cytometry to measure surface VE-cadherin expression (A & C). Surface VE-cadherin levels from panel A were quantitated and normalised to the average VE-cadherin surface expression in the 'no siRNA' condition (B & D). Confirmation of individual TspanC8 knockdowns in the various conditions were assessed by RT-PCR as explained in the legend to Figure 5.1 and shown to be 50% or more reduced upon quantitation and in line with mRNA levels shown in Figure 5.12 (data not shown). Error bars represent the standard error or the mean from five independent experiments. Data were statistically analysed by One-way ANOVA followed by a Dunnett's multiple-comparisons post-hoc test (**$p < 0.01$, ***$p < 0.001$ compared to 'negative control siRNA' transfected HUVECs).

In addition to the static adhesion assay data and flow cytometry findings, the effects of combined siRNA knockdown of TspanC8s on VE-cadherin shedding was assessed. In these assays, HUVECs were transfected with siRNA duplex combinations (25 or 30 nM siRNA in total) as described previously or a non-specific siRNA duplex at a final concentration of 30 nM. 24 hours after transfection, 10 μM DAPT was added and the cells were cultured for an additional 24 hours. The cells were harvested and subjected to Western blotting for VE-cadherin as described previously. Knockdown of all TspanC8s or the various combinational knockdowns revealed no differences in VE-cadherin shedding (Figure 5.15). This result was somewhat surprising, given the previously observed effects on VE-cadherin surface expression. Nevertheless, these data suggest that endothelial Tspan5 and Tspan17 are novel facilitators of PBL transmigration through their regulation of ADAM10 and VE-cadherin surface levels. In addition, the effect of Tspan5 or Tspan17 was not due to differential changes in ADAM10 surface levels.

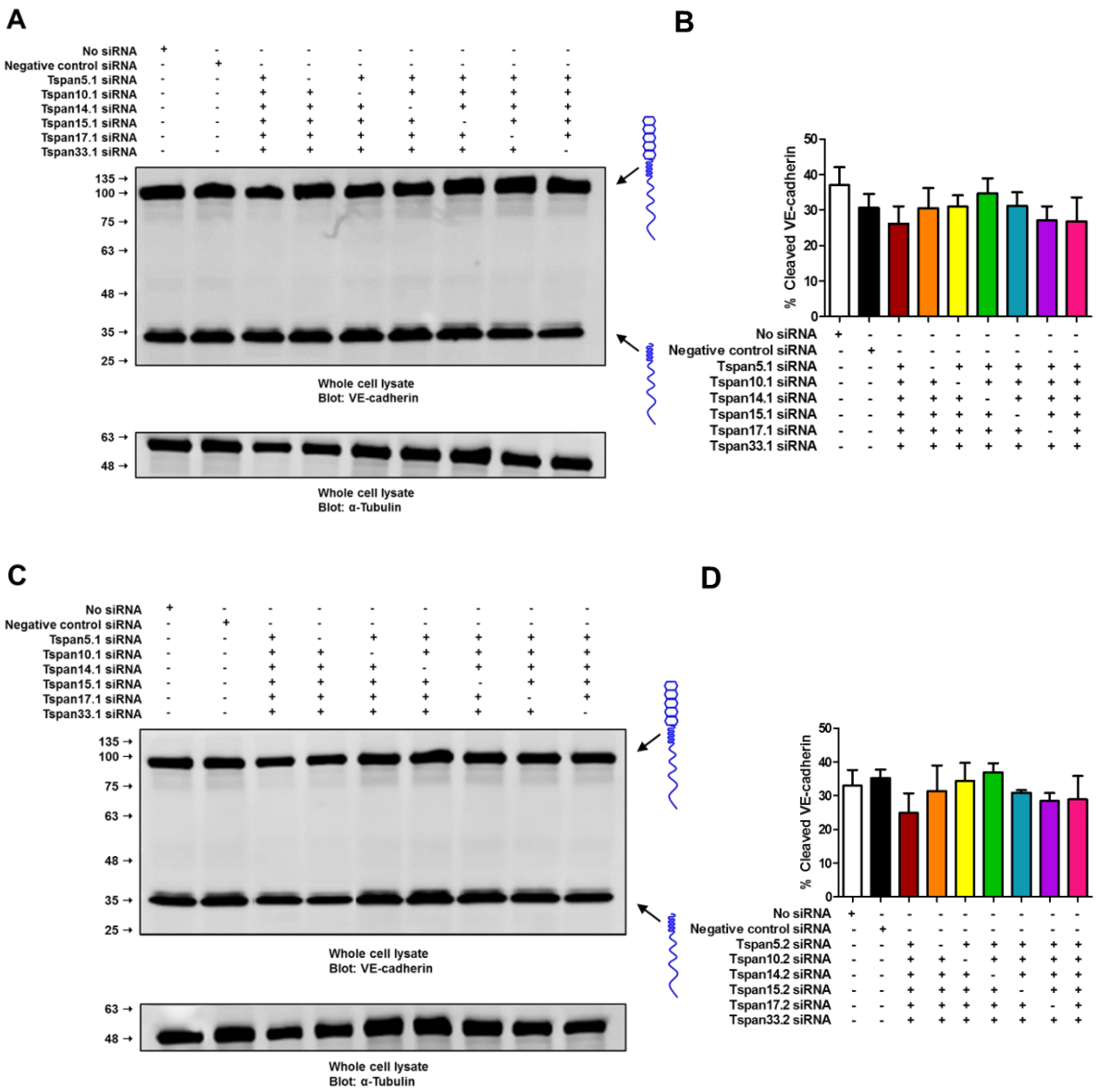

Figure 5.15 Neither knockdown of all TspanC8s nor the presence of an individual TspanC8 does not affect VE-cadherin cleavage. HUVECs were transfected with siRNA duplexes corresponding to the various TspanC8s as explained in the legend to Figure 5.10. Following 24 hours, HUVECs were treated with 10 µM DAPT for an additional 24 hours to prevent further proteolytic processing of VE-cadherin after ADAM10 cleavage. HUVECs were then harvested, lysed and converted into cell lysates prior to carrying out Western blotting for VE-cadherin as explained in the legend to Figure 5.5. α-Tubulin was used as a loading control. The membrane was imaged and bands quantified on the Odyssey Infrared Imaging System (A & C). The percentage cleaved was calculated as previously explained in the legend to Figure 5.5 (B & D). Confirmation of individual TspanC8 knockdowns in the various conditions were assessed by RT-PCR as explained in the legend to Figure 5.1 and shown to be 50% or more reduced upon quantitation and in line with mRNA levels shown in Figure 5.12 (data not shown). Error bars represent the standard error of the mean from four independent experiments. Data were analysed by One-way ANOVA followed by a Dunnett's multiple-comparisons post-hoc test.

5.2.5 Knockdown of Tspan5 and Tspan17 does not alter PBL transmigration or changes in VE-cadherin shedding and surface expression levels

Having shown that the presence of Tspan5 or Tspan17 are sufficient in maintaining basal PBL transmigration, the opposite approach of knocking down Tspan5 and Tspan17 simultaneously was investigated. HUVECs were transfected with two siRNA duplexes, one targeting Tspan5 and the other targeting Tspan17 (5 nM of each siRNA duplex), or a non-specific siRNA duplex as a control. 24 hours after transfection, HUVECs were stimulated with 100 U/ml TNFα and 10 ng/ml IFNγ for an additional 24 hours and a static adhesion assay was carried out as previously explained. Knockdown of Tspan5 and Tspan17 did not alter the ability of PBLs to transmigrate when compared to control transfected cells (Figure 5.16 A). In addition, no differences in PBL total adhesion were observed following the combined knockdown of Tspan5 and Tspan17 (Figure 5.16 B). To confirm the siRNA knockdown of Tspan5 and Tspan17, RNA was extracted from cell pellets and cDNA was produced as previously explained. Tspan5 and Tspan17 mRNA levels were assessed by real-time PCR as previously described. A ~70% reduction in Tspan5 expression and a ~75% reduction in Tspan17 expression was observed following Tspan5 and Tspan17 knockdown when compared to control transfected cells (Figure 5.16 C).

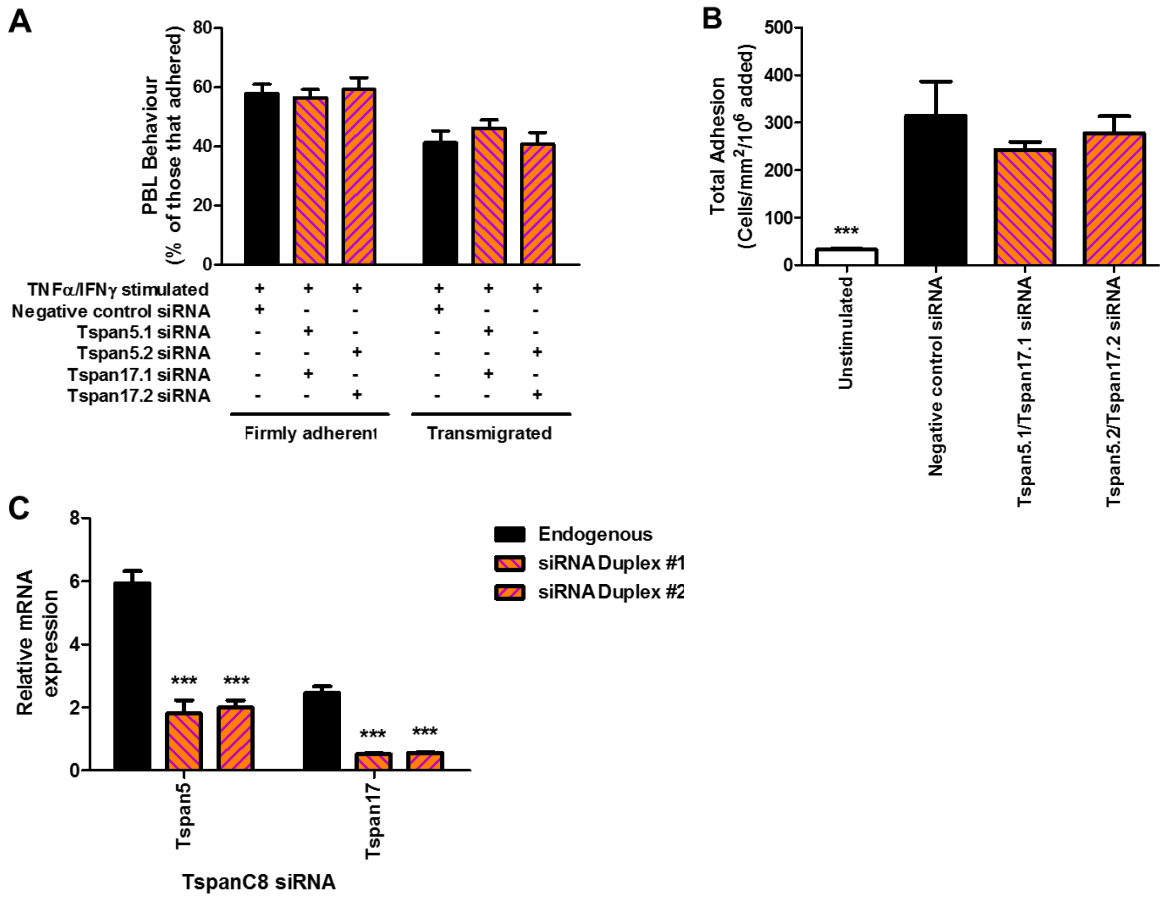

Figure 5.16 Knockdown of Tspan5 and Tspan17 does not affect PBL transmigration under *in vitro* static conditions. HUVECs were transfected with two different siRNA duplexes to Tspan5 in combination with two different siRNA duplexes to Tpan17 (orange bars with purple dashes) alongside a non-specific siRNA (black bar) at a final concentration of 10 nM. The HUVECs were then incorporated into a static adhesion assay. PBLs were classified as firmly adherent or transmigrated (A). The total number of cell classified for each of the behaviours was combined to give a total adhesion count (A) HUVECs transfected with siRNA were analysed by RT-PCR to measure the relative knockdown efficiency of the various TspanC8s at the mRNA level as previously explained in the legend to Figure 5.1 (C). Error bars represent the standard error of the mean from three independent experiments. Data were normalised by arcsine transformation and statistically analysed by one-way ANOVA and Dunnett's post-hoc comparisons test for total adhesion data and knockdown confirmation data (***$p < 0.001$ compared to negative control siRNA transfected cells) or by a two-way ANOVA and Bonferroni post-hoc comparisons test for PBL cell behaviour.

In addition to the static adhesion assay data, the effects of combined Tspan5 and Tspan17 knockdown on VE-cadherin shedding were assessed. In these assays, HUVECs were transfected with siRNA duplexes targeting Tspan5 and Tspan17. 24 hours after transfection, 10 µM DAPT was added and the cells cultured for an additional 24 hours. The cells were harvested and cell lysates were Western blotted for VE-cadherin as described previously. Knockdown of Tspan5 and Tspan15 did not alter VE-cadherin shedding when compared to control transfected cells (Figure 5.17 A & B).

Tspan5 and Tspan17 combined knockdown HUVECs were analysed for their expression of ADAM10 and VE-cadherin as explained previously. Flow cytometry analysis of surface ADAM10 levels revealed no changes in ADAM10 expression levels following combined knockdown of Tspan5 and Tspan17 when compared to control transfected cells (Figure 5.17 C & D). In addition, no differences in VE-cadherin surface expression levels were revealed following the combined knockdown of Tspan5 and Tspan17 when compared to control transfected cells (Figure 5.17 E & F).

Taken together, these data show that combined knockdown of Tspan5 and Tspan17 does not suppress PBL transmigration, suggesting the possible compensatory involvement of other TspanC8s, namely Tspan14 or Tspan15, and residual Tspan5 and Tspan17 expression due to the incomplete knockdown, in regulating PBL transmigration.

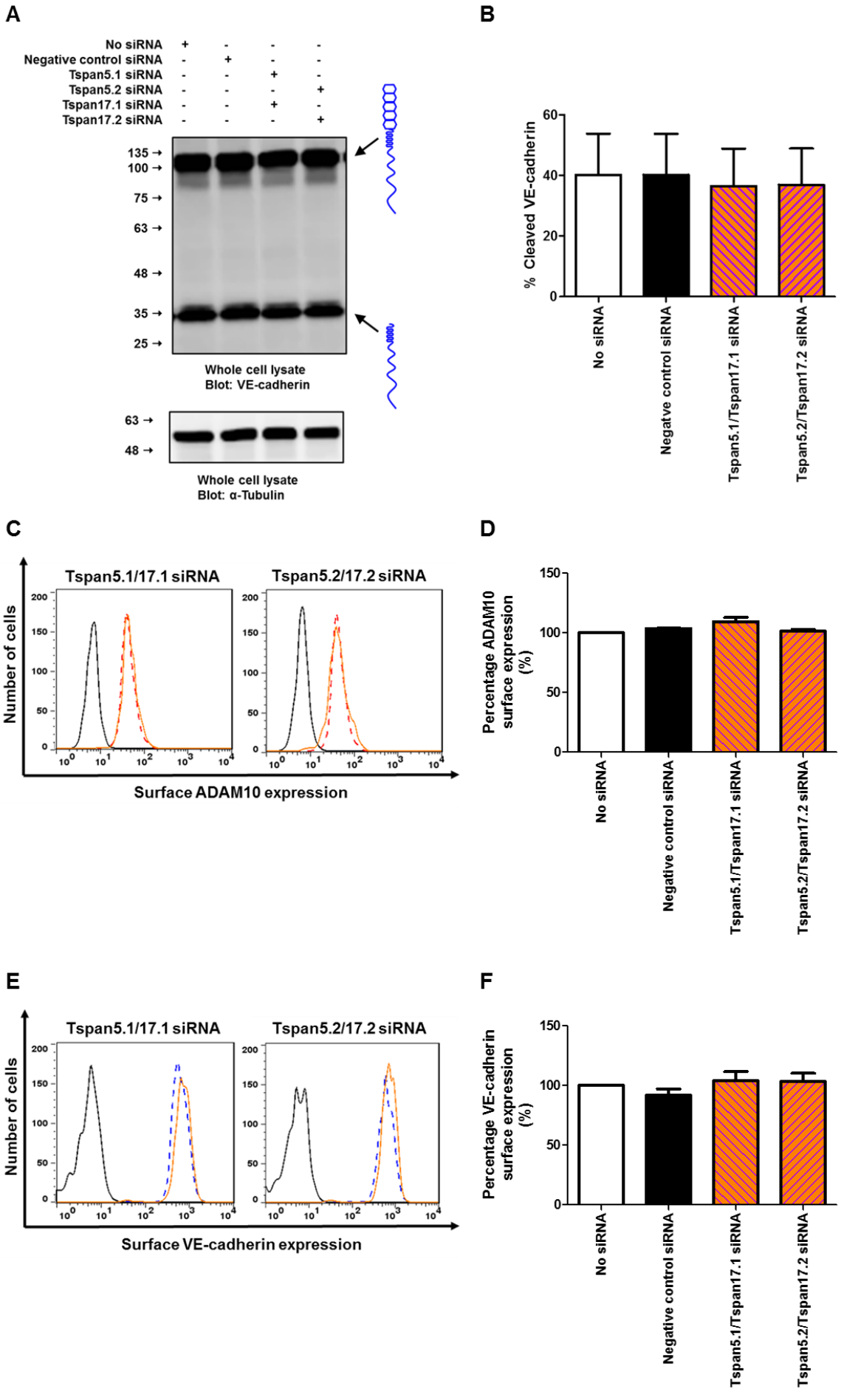
A
No siRNA + - - -
Negative control siRNA - + - -
Tspan5.1 siRNA - - + -
Tspan5.2 siRNA - - - +
Tspan17.1 siRNA - - + -
Tspan17.2 siRNA - - - +
135 →
100 →
75 →
63 →
48 →
35 →
25 →
Whole cell lysate
Blot: VE-cadherin
63 →
48 →
Whole cell lysate
Blot: α-Tubulin
B
% Cleaved VE-cadherin
60
40
20
0
No siRNA
Negatve control siRNA
Tspan5.1/Tspan17.1 siRNA
Tspan5.2/Tspan17.2 siRNA
C
Tspan5.1/17.1 siRNA
Tspan5.2/17.2 siRNA
Number of cells
Surface ADAM10 expression
D
Percentage ADAM10 surface expression (%)
150
100
50
0
No siRNA
Negative control siRNA
Tspan5.1/Tspan17.1 siRNA
Tspan5.2/Tspan17.2 siRNA
E
Tspan5.1/17.1 siRNA
Tspan5.2/17.2 siRNA
Number of cells
Surface VE-cadherin expression
F
Percentage VE-cadherin surface expression (%)
150
100
50
0
No siRNA
Negative control siRNA
Tspan5.1/Tspan17.1 siRNA
Tspan5.2/Tspan17.2 siRNA

Figure 5.17 Knockdown of Tspan5 and Tspan17 does not alter ADAM10 and VE-cadherin expression levels nor VE-cadherin shedding. HUVECs were transfected with two different siRNA duplexes to Tspan5 in combination with two different siRNA duplexes to Tspan17 (orange with purple dashes) alongside a non-specific siRNA (black bar) at a final concentration of 10 nM. 24 hours after transfection, 10 μM of the γ-secretase inhibitor, DAPT was added to the culture media to prevent further proteolytic processing VE-cadherin after ADAM10 cleavage. HUVECs were then harvested, lysed and converted into cell lysates prior to carrying out Western blotting for VE-cadherin as explained in the legend to Figure 5.5. α-Tubulin was used as a loading control. The membrane was imaged and bands quantified on the Odyssey Infrared Imaging System (A). The percentage cleaved was calculated as previously described in the legend to Figure 5.5 (B). Transfected HUVECs stained for the surface expression of ADAM10 (C & D) and VE-cadherin (E & F) as explained in the legend to Figure 5.3 (C & E). Surface ADAM10 levels or VE-cadherin levels from panels C and E were quantitated and normalised to the "No siRNA" treated condition (D & F). Confirmation of Tspan5 and Tspan17 knockdown was assessed by RT-PCR as explained in the legend to Figure 5.1 and shown to be 65-80% reduced upon quantitation and in line with mRNA levels shown in Figure 5.16 (data not shown). Error bars represent the standard error of the mean from three independent experiments. Data were analysed by One-way ANOVA followed by a Dunnett's multiple-comparisons post-hoc test.

5.3 DISCUSSION

Inflammation induced by injury or infection is characterised by changes in vascular morphology, plasma protein and fluid leakage and leukocyte transmigration. The localised proteolytic cleavage of various cell surface adhesion molecules has been implicated in the efficient transmigration of leukocytes as well as limiting leukocyte transmigration through a process known as de-adhesion (Dreymueller et al., 2012b, 2015). The metalloprotease ADAM10 has been suggested to regulate vascular permeability and PHA-blast T cell transmigration under static conditions (Schulz et al., 2008; Donners et al., 2010). Although ADAM10's function as an ectodomain sheddase has been well documented, little is known about the role of binding partner proteins in regulating the function of ADAM10. All the members of the subgroup of TspanC8 tetraspanins have been shown to all associate with ADAM10 and facilitate its enzymatic maturation (Dornier et al., 2012; Haining et al., 2012). Emerging evidence now suggests that specific TspanC8s regulate substrate cleavage of the ADAM10 substrates Notch, N-cadherin, APP, CD44 and GPVI (Jouannet et al., 2016; Noy et al., 2016). However, the role of TspanC8s in leukocyte transmigration, and their effects on VE-cadherin shedding by ADAM10, have not previously been investigated. Here the role of endothelial TspanC8s in regulating this function of ADAM10 was investigated using *in vitro* static adhesion assays. In addition, changes in VE-cadherin surface expression and shedding were monitored by flow cytometry and Western blotting techniques.

To analyse the role of TspanC8s in regulating PBL transmigration, initial experiments were performed in which HUVECs were lentivirally transduced to overexpress the individual TspanC8s before monitoring the effect of TspanC8 overexpression on PBL transmigration under *in vitro* static adhesion assay conditions. Overexpression of TspanC8s in HUVECs did not alter the ability of PBLs to transmigrate under conditions of TNFα/IFNγ induced inflammation. Furthermore, of the TspanC8s endogenously expressed in HUVECs, overexpression of Tspan5, 14 or 17 did not alter VE-cadherin

shedding nor VE-cadherin cell surface expression. Surprisingly, overexpression of Tspan15 and Tspan33 significantly reduced VE-cadherin shedding. This phenomenon was accompanied by a paradoxical increase in ADAM10 surface levels when Tspan15 or 33 were overexpressed. However, overexpression of Tspan15 or 33 did not alter VE-cadherin surface expression. It is worth noting that the three most highly expressed TspanC8s following lentiviral transduction in HUVECs were Tspan10, 15, and 33. Previously published data using overexpression models has shown Tspan10 has a largely intracellular localisation in HeLa cells (Dornier et al., 2012) and in HEk293T cells (Tomlinson, unpublished data), whilst Tspan15 and Tspan33 promoted ADAM10 membrane localisation. Although overexpression of Tspan15 and Tspan33 increased ADAM10 surface expression, a paradoxical reduction in VE-cadherin shedding was observed. It is possible to speculate that Tspan15 and Tspan33 could be sequestering ADAM10 away from an endogenous TspanC8 (such as Tspan5, 14 or 17), the function of which is to promote VE-cadherin shedding. Furthermore, the decrease in VE-cadherin shedding observed following overexpression of Tspan15 or Tspan33 did not affect surface levels of VE-cadherin. This was a surprising result, suggesting that VE-cadherin shedding does not necessarily correlate with surface expression. Certainly, there are differences in the basis of the models used to look at VE-cadherin expression. FACS only measures surface levels of VE-cadherin and so does not take into consideration internal pools of VE-cadherin that are measured by Western blot, which may encompass newly synthesised protein or protein that is passing through the endocytic pathway. In addition, it could be speculated that during the Western blotting lysis procedure a particular pool of VE-cadherin may remain attached to the cytoskeleton and therefore be resistant to solubilisation (Guo et al., 2004). Taken together, it may be possible that a significant decrease in shedding could be happening to a substantial pool of VE-cadherin that is not at the cell surface. In addition, it is worth noting that overexpression is prone to artefacts of abnormally high expression levels, and could in part be responsible for the apparently paradoxical data in this section.

Since overexpression of TspanC8s yielded data that was difficult to interpret, the focus changed to look at endogenous TspanC8s and their role in regulating PBL transmigration using a siRNA knockdown approach. Individual knockdown of TspanC8s in HUVECs did not alter the ability of PBLs to transmigrate under *in vitro* static adhesion assay conditions. Moreover, TspanC8 knockdown resulted in no changes in VE-cadherin shedding or VE-cadherin surface levels. However, knockdown of Tspan14 and 15 resulted in a small, but nevertheless significant reduction in ADAM10 surface levels. Previously, Haining et al. showed that knockdown of Tspan14 in HUVECs resulted in a ~50% reduction in ADAM10 surface levels which correlated with a reduction in VE-cadherin shedding (Haining et al., 2012). The variability in Tspan14 knockdown efficiency, namely ~75% reduced observed by Haining *et al*. and ~50% reduced in the present study, might explain the differences observed between the data presented in this chapter and that published by Haining *et al*. Indeed, the effects of prolonged knockdown (for example 48-hour knockdown used in the present study vs 72-hour knockdown used by Haining *et al*.) could differentially alter ADAM10 surface expression.

Since redundancy amongst the TspanC8s could have explained the lack of phenotype observed following individual knockdown of the TspanC8s during PBL transmigration, the focus changed to utilise a method to investigate the individual function of the TspanC8s by ruling out the function of the other TspanC8s. For these experiments, a combination knockdown approach of the TspanC8s proved pivotal in deducing a function of single TspanC8s in PBL transmigration. Knockdown of all TspanC8s in HUVECs resulted in a decrease in the ability of PBLs to transmigrate. This correlated with a reduction in ADAM10 surface levels. However, no changes in VE-cadherin shedding nor VE-cadherin surface levels were observed, suggesting that ~50% reduction in ADAM10 surface pools is sufficient to maintain basal VE-cadherin shedding, but nevertheless suppresses PBL transmigration. It could be speculated that surface levels of VE-cadherin only form part of the total VE-cadherin pool in endothelial cells and subtle changes in VE-cadherin

localisation, such as its recycling at the plasma membrane, could ultimately be facilitating the functional response in regulating lymphocyte transmigration. In addition, complete loss of TspanC8s expression was not observed, and the remaining expression of the various TspanC8s (~50% or less) could still be facilitating leukocyte transmigration.

Following on from the findings that a ~50% or greater reduction in endogenous TspanC8s is sufficient to reduce PBL transmigration, the focus changed to evaluate the individual role of specific TspanC8s in maintaining basal PBL transmigration. For this set of experiments, a combinational siRNA knockdown approach was undertaken in which HUVECs were transfected with siRNA duplexes corresponding to five of the six TspanC8s, to decipher the individual role of the TspanC8 not targeted by siRNA. Interestingly, knockdown combinations that retained the expression of Tspan5 (100% Tspan5, 50% Tspan14, 25% Tspan15 and 25% Tspan17 expression) or Tspan17 (50% Tspan5, 50% Tspan14, 25% Tspan15 and 100% Tspan17 expression) maintained basal PBL transmigration. This was supported by a reduction in VE-cadherin surface levels. This capacity of Tspan5 or Tspan17 was not due to increased ADAM10 surface levels, because a partial reduction in ADAM10 surface levels was observed and only the presence of Tspan14 was sufficient to maintain basal ADAM10 levels. This is most likely due to its relatively high expression levels on HUVECs in comparison to the other TspanC8s (Haining et al., 2012). Interestingly, Tspan5 and Tspan17 share 78% sequence homology at the protein level in humans and this might explain the common role of these TspanC8s in PBL transmigration. It is possible to speculate that Tspan5 and Tspan17 could be promoting ADAM10s trafficking to sites of VE-cadherin localisation. However, it has to be noted that VE-cadherin has been reported to be absent from endothelial adhesive platforms that are enriched with tetraspanins CD151 and CD9 that promote leukocyte adhesion and subsequent transmigration (Barreiro et al., 2008) and was shown to be absent from HUVEC tetraspanin proteomics (Tomlinson, unpublished data). Therefore, it is unlikely that VE-cadherin is tetraspanin associated. With the

emergence of TspanC8s having different interaction profiles with ADAM10, recent data from the Tomlinson group showed evidence for TspanC8s having distinct mechanisms of ADAM10 binding (Noy et al., 2016). In particular Tspan5 was shown to bind to the cysteine and stalk regions of ADAM10 whilst Tspan17 interaction with the stalk and cysteine regions was inhibited by the presence of the disintegrin domain of ADAM10 (Noy et al., 2016). Therefore, Tspan5 and Tspan17 could promote a particular ADAM10 conformation that is favourable to VE-cadherin cleavage. A reduction in VE-cadherin surface expression in the presence of Tspan5 or Tspan17 did not correlate with a reduction in VE-cadherin cleavage. As mentioned before, this rather paradoxical result might be explained by the disparity between surface expression, only accounting for a small proportion of the total VE-cadherin in the cells, and Western blotting which takes into account internal pools of VE-cadherin including newly synthesised protein and protein in that has entered the endocytic pathway.

Surprisingly, knockdown of Tspan5 and Tspan17 in combination resulted in no changes in the ability of PBLs to transmigrate. This was associated with no changes in ADAM10 and VE-cadherin surface levels nor VE-cadherin shedding. The RT-PCR confirmed that there was 100% expression of Tspan14 and 15, 30% expression of Tspan5 and 25% expression of Tspan17 following the double knockdown. Since a reasonable amount of Tspan5 and Tspan17 is still expressed following the double knockdown, it is possible to speculate that a greater knockdown of the two TspanC8s is required to see a phenotype.

Overall, the findings in this chapter highlight endothelial Tspan5 and Tspan17 as novel facilitators of lymphocyte transmigration through their regulation of ADAM10 and VE-cadherin.

CHAPTER 6

GENERAL DISCUSSION

6.1 PROJECT OVERVIEW

The primary barrier which leukocytes or macromolecules have to overcome during an inflammatory response is the venular wall, which acts as a semi-permeable barrier at the interface between circulating blood and the interstitial tissue. The process by which leukocytes exit the bloodstream involves a sequence of well-orchestrated signalling and adhesive events that occur between leukocytes and the inflamed vessel wall (Nourshargh et al., 2010; Nourshargh and Alon, 2014). Most of the initial interactions that facilitate this process occur at the leukocyte-endothelial interface. Lack of regulation of leukocyte recruitment or the inappropriate trigger of this reaction, however, can lead to severe pathological inflammatory conditions such as asthma, stroke, atherosclerosis, and cancer (Krishnamoorthy and Honn, 2006).

Proteolytic shedding of key CAMs and membrane-inserted chemokines that regulate the distinct stages of leukocyte rolling, activation-induced arrest and transmigration have offered hope in further understanding the molecular dynamics of the complex regulation of leukocyte transmigration in health and disease (Garton et al., 2006; Dreymueller et al., 2012b). Previously published data has largely focused on the use of transfected cells and cell lines to reveal an effect of proteolytic shedding during inflammation. However, mechanisms of proteolytic shedding in primary endothelial cells and in physiological flow *in vitro* models of inflammation remain largely unknown. This PhD thesis aimed to investigate the role of the metalloprotease ADAM10 in regulating leukocyte transmigration by targeting specific known ADAM10 substrates such as the adhesion molecule VE-cadherin and the transmembrane chemokines CX3CL1/CXCL16 using primary endothelial cells under physiological *in vitro* flow conditions in a model of chronic inflammation. In addition, the role of six tetraspanin transmembrane proteins, termed TspanC8s, as key regulators of ADAM10 function was investigated with the possibility that each of the TspanC8s could traffic ADAM10 to distinct substrates, thereby regulating leukocyte transmigration.

The present data demonstrates the capacity of endothelial ADAM10 to promote the transmigration of PBLs, but not other inflammatory leukocyte subsets such as neutrophils or monocytes. These findings were dependent on the regulation of VE-cadherin shedding and surface levels through ADAM10 activity. In addition, the TspanC8 tetraspanins Tspan5 and Tspan17 were shown to be novel regulators of ADAM10 during PBL transmigration. Thus, the findings of the present study contribute to our understanding of ADAM10 regulation by the TspanC8s in inflammation and have opened novel avenues for future research. The following discussion gives an overview of the possible functional consequences of ADAM10 regulation in inflammation and discusses the potential role of the TspanC8s in directing ADAM10 responses during PBL transmigration.

6.1.1 Endothelial ADAM10 is a regulator of lymphocyte transmigration during inflammation

The recruitment and activation of leukocytes into inflamed tissue involves a tightly regulated and complex process of interactions of leukocytes with different components of the venular wall (Nourshargh et al., 2010; Nourshargh and Alon, 2014). Proteolytic cleavage or 'ectodomain shedding' by metalloproteases belonging to the ADAM family have recently emerged as a possible molecular mechanism that could govern leukocyte-endothelial cell interactions by proteolytically shedding key CAMs and transmembrane chemokines (Garton et al., 2006; Dreymueller et al., 2012b). However, many studies have utilised cell line models and transfected cells to overexpress specific transmembrane proteins under non-physiological models to decipher the role of proteolytic shedding in leukocyte adhesion and transmigration (Hundhausen et al., 2007; Schwarz et al., 2010; Schulz et al., 2008). As such, the role of proteolytic shedding in primary cells and under physiological flow conditions is still largely unknown.

In this study, endothelial ADAM10, targeted on primary HUVECs using siRNA or a preferential pharmacological inhibitor, was shown to promote the efficient transmigration of human PBLs, but not neutrophils or monocytes in physiological flow and static adhesion assays. These findings are in line with previously published data that showed a role of endothelial ADAM10 in regulating the transmigration of PHA-blast T cells in a static transwell assay model (Schulz et al., 2008). A separate study by Schwarz *et al*. showed the migration of the pre B cell line L1.2 was significantly reduced on TNFα/IFNγ stimulated HUVECs in a static transwell adhesion assay (Schwarz et al., 2010). Two additional studies have highlighted a role of ADAM10 expressed on human microvascular endothelial cells (HMVEC) in regulating the transmigration of the monocytic cell line, THP-1 cells under static transwell conditions in response to TNFα/IFNγ or CCL2 (Hundhausen et al., 2007; Pruessmeyer et al., 2014). A common feature of many of these studies has been the use of leukocytic and endothelial cell lines in basic models of adhesion. In the studies that have used primary endothelium (HUVEC or HMVEC), the isolation methods have not been documented, and the cells have been outsourced from external companies, which do not disclose the previous culture methods or passage of these cells prior to their dispatch. Furthermore, unpublished data from our group has shown that subculture of HUVECs in the presence of growth factors, such as hydrocortisone, significantly reduces the response of TNFα-mediated neutrophil recruitment and adhesion (Nash/Rainger, unpublished data). In addition to the use of primary endothelium, many of the studies also used ECV-304 cells derived from epithelial bladder carcinoma cells. However, these cells do not behave like primary endothelial cells and lack the expression of key endothelial markers, such as VE-cadherin (Kiessling et al., 1999). Another difference between the data presented in the present study, compared to previously published data is the use of primary leukocytes over leukocytic cell lines. For example, Schulz *et al*. showed that inhibition of endothelial ADAM10 reduced the transmigration of PHA-blast T cells in a static transwell assay (Schulz et al., 2008). However, the culture of PHA-blast T cells requires stimulation of these cells with interleukin-2, which changes the

repertoire of proteins at the cell surface, compared to primary PBLs. For example, PHA-blast T cells upregulate the expression of $\alpha_L\beta_2$ that supports adhesion to ICAM-1 (McGettrick et al., 2009) whilst PBLs use $\alpha_4\beta_1$ for their optimal adhesion (Ahmed et al., 2011).

In addition to the use of cell type, there are also differences in the type of experimental *in vitro* model that has been used to decipher a function of endothelial ADAM10 in leukocyte transmigration. Previous studies have relied on the use of chemotaxis assays and transwell assays, which heavily rely on sedimentation and do not take into account the initial capture events that occur during leukocyte adhesion. Boyden chamber and transwell assays rely on similar principles, namely leukocytes are made to migrate across a transwell filter towards a stimulus (e.g. cytokine or chemokine) either in the presence of absence of a barrier (e.g. endothelial cells). These assays typically require a longer period of incubation to visualise leukocyte transmigration, compared to physiological flow assays or static adhesion assays with primary endothelial cells and human leukocytes (McGettrick et al., 2009). Furthermore, the basis of the static adhesion assays and flow adhesion assays used in the present study have been extensively studied and characterised in terms of the regulation of CAM expression in response to various cytokines. For example, the combined treatment of HUVECs with TNFα/IFNγ has been shown to upregulate the interferon-inducible chemokines that selectively regulate the recruitment and transmigration of memory $CD4^+$ T cells (Ahmed et al., 2011). Another difference between data presented in the present study and previously published data is the use of an *in vitro* flow adhesion assay. It is well documented that many of the CAMs that regulate leukocyte recruitment and transmigration are modulated by shear stress. In the present study, a physiological shear stress of 0.05 Pa was used, which is within the range found in post-capillary venules, the major site of leukocyte recruitment during inflammation (Sheikh et al., 2003). The use of primary endothelial cells and primary leukocytes in physiological flow adhesion and static adhesion assays may account for the

differences observed in endothelial ADAM10s role in regulating the transmigration of lymphocytes, but not neutrophils or monocytes, when compared to previously published data that has relied on the use of cell line models and transwell assays.

6.1.2 Regulation of VE-cadherin surface levels is important in mediating paracellular transmigration of lymphocytes

Following adhesion of leukocytes to the apical surface of the venular wall, leukocytes then have to breach the endothelial barrier before migrating into the tissue parenchyma towards the site of inflammation (Nourshargh et al., 2010). Since paracellular transmigration (migration of leukocytes at endothelial junctions) is the preferred route of transmigration, the role of junctional proteins and their surface regulation has been studied in quite some depth (Vestweber, 2015). One of the junctional molecules that has been shown to mediate efficient leukocyte transmigration is VE-cadherin. Targeting of VE-cadherin through the generation of genetically modified mice that contained VE-cadherin fused to α-catenin was shown to stabilise the VE-cadherin/VE-PTP complex hereby maintaining barrier integrity. Trafficking of leukocytes in a model of cremasteric inflammation in these mice revealed leukocyte transmigration into the surrounding tissue was significantly compromised (Schulte et al., 2011). In addition, co-incubation of human lymphocytes with endothelial cells resulted in a rapid dissociation of VE-cadherin from the endothelial junctions as visualised by the introduction of a VE-cadherin-GFP fusion protein (Shaw et al., 2001).

Data in this thesis highlighted that VE-cadherin regulated lymphocyte transmigration through its surface regulation. Inhibition or knockdown of endothelial ADAM10 enhanced VE-cadherin surface expression (~1.5 fold increase in surface expression), reduced VE-cadhrerin shedding and increased transendothelial electrical resistance. These findings were in line with previous studies that have shown inhibition or knockdown of ADAM10

decreases the shedding of VE-cadherin and decreases endothelial permeability (Schulz et al., 2008; Flemming et al., 2015). Following on from these publications, data presented in this thesis showed that PBL transmigration could be restored by reducing VE-cadherin surface levels back to normal in the presence of ADAM10 inhibition or knockdown combined with a partial VE-cadherin knockdown. This data suggests that the regulation of VE-cadherin surface levels by ADAM10 can control the transmigration efficiency of PBLs. In line with these obervations, recent data has highlighted that VE-cadherin surface levels can dictate the passage of lmphocytes across brain microvascular endothelial cells. Martinelli *et al*. recently reported that increased VE-cadherin expression in brain microvascular endothelial cells correlated with a decrease in the ability of lymphocytes to undergo transmigration at endothelial junctions (Martinelli et al., 2014). As such, vascular beds which generally have high endothelial resistance, such as the brain microvasculature, correlated with lymphocytes preferring transcellular modes of transmigration as opposed to migrating at cell-cell junctions. This was accomplished by lymphocytes producing invadosome-like protrusions that extend into the endothelium and migrate through the body of the endothelial cell (Martinelli et al., 2014). It remains to be shown if under conditions of increased barrier resistance lymphocytes seek other methods of transmigration in other endothelial cell vascular beds. It has been previoulsy documented that heterogeneity between endothelial cells in various vascular beds exists and as such preferable regions or ‘hot spots’ of lymphocyte transmigration may dictate the mode of lymphocyte transmigration (paracellular over transcellular and *vice versa*).

6.1.3 Potential roles for the TspanC8 tetraspanins in regulating ADAM10 activity during lymphocyte transmigration

The recent identification of six tetraspanin transmembrane proteins, termed TspanC8s, that could all interact with ADAM10 and support its enzymatic maturation highlighted a

mechanism by which ADAM10 activity could possibly be regulated (Dornier et al., 2012; Haining et al., 2012). Recent evidence now suggests that specific TspanC8s regulate substrate cleavage of the ADAM10 substrates Notch, N-cadherin, APP, CD44, and GPVI (Jouannet et al., 2016; Noy et al., 2016). However, the role of TspanC8s in facilitating lymphocyte transmigration, and their effects on VE-cadherin shedding by ADAM10 had not previously been demonstrated, and so formed the basis of investigations undertaken in the final results chapter of this thesis. A systematic knockdown approach was used to target endogenous TspanC8 expression using siRNA by investigating the individual function of the TspanC8s by ruling out the function of the other TspanC8s. Knockdown of all TspanC8s reduced the ability of PBLs to transmigrate, to a similar extent (~50% reduced) as when ADAM10 was knocked down or inhibited. However, no changes in VE-cadherin shedding nor VE-cadherin surface levels were observed, suggesting that a ~50% reduction in ADAM10 surface pools is sufficient to maintain basal VE-cadherin shedding, but nevertheless suppress PBL transmigration. As mentioned previously in the discussion to Chapter 5, surface levels only account for part of the total VE-cadherin pool in endothelial cells without taking into consideration internal pools of the protein which includes newly synthesised protein being trafficked to the cell surface and protein entering the endocytosis pathway. It also has to be noted that in these experiments, complete knockdown of all the TspanC8s was not achieved, and the possible involvement of the remaining TspanC8s (~50% or less) in regulating lymphocyte transmigration cannot be ruled out.

Further experiments into the role of individual TspanC8s in lymphocyte transmigration revealed that knockdown combinations that retained the expression of Tspan5 (100% Tspan5, 50% Tspan14, 25% Tspan15 and 25% Tspan17 expression) or Tspan17 (50% Tspan5, 50% Tspan14, 25% Tspan15 and 100% Tspan17 expression) maintained basal PBL transmigration. These knockdown combinations were also shown to reduce VE-cadherin surface expression. This capacity of Tspan5 or Tspan17 was not due to

increased ADAM10 surface levels. In fact, a partial reduction in ADAM10 surface levels was observed, and only knockdown combinations that retained the expression of Tspan14 were shown to maintain basal ADAM10 surface levels. This is most likely due to the relatively high expression levels of Tspan14 on HUVECs (Haining et al., 2012). Interestingly, Clustal OMEGA protein sequence analysis revealed that Tspan5 and Tspan17 are the most highly related TspanC8s sharing 78% sequence homology, and this might explain the common role of these TspanC8s highlighted in Chapter 5. One possible mode of action for Tspan5 and Tspan17 could be by promoting ADAM10 trafficking to endothelial junctions at sites of VE-cadherin localisation. Previously unpublished data from the Tomlinson group has shown, in a cell line model, that TspanC8/ADAM10 complexes have distinct subcellular localisation patterns. The technique used to show these subcellular localisations was bimolecular fluorescence complementation (BiFC), which has emerged in the last decade as a technique that allows a dimer of two different proteins to be visualised within a living cells (Kodama and Hu, 2012). The most striking differences were between Tspan15-ADAM10 dimers, which appeared predominantly localised to the plasma membrane, and Tspan10-ADAM10 dimers, which were largely intracellular. Of interest, Tspan5-ADAM10 dimers and Tspan17-ADAM10 dimers had varied localisations (some plasma membrane and some intracellular) (Tomlinson, unpublished data). The Rubinstein group recently published evidence for junctional localisation of Tspan5 as well as predominant membrane localisation in U20S cells through the use of confocal microscopy and single particle tracking (Jouannet et al., 2016). Tspan5 and Tspan17 have also been shown to co-localise with the late endosomal marker CD63 (Dornier et al., 2012), although ADAM10 localisation in such compartments was found to be largely absent (Jouannet et al., 2016). It may be speculated that Tspan5 or Tspan17 might couple to different Rab GTPases or Rab effectors, which orchestrate the trafficking of membrane proteins. Indeed, Rab14 knockdown has been shown to prevent ADAM10 trafficking from the endoplasmic reticulum to the cell surface in an epithelial cell line (Linford et al., 2012), similar to

TspanC8 knockdown (Dornier et al., 2012; Haining et al., 2012; Prox et al., 2012a). The mechanism by which Tspan5 and Tspan17 regulate ADAM10 trafficking and localisation in HUVECs remains to be elucidated. Additionally, it has to be noted that VE-cadherin appears not to be tetraspanin associated due to its absence in endothelial adhesive platforms (Barreiro et al., 2008) and its absence in HUVEC tetraspanin proteomics (Tomlinson, unpublished data). Recent data from the Tomlinson group has shown that the TspanC8s have distinct mechanisms of ADAM10 binding (Noy et al., 2016). In particular, Tspan5 was shown to bind to the cysteine and stalk regions of ADAM10 whilst the Tspan17 interaction with the stalk and cysteine regions was inhibited by the presence of the disintegrin domain of ADAM10 in HEK293T cells (Noy et al., 2016). It is possible to suggest that Tspan5 and Tspan17 could hold ADAM10 in a particular conformation that is favourable for VE-cadherin cleavage. Further investigations using targeted interaction-disrupting antibodies to Tspan5 or Tspan17 could be potentially beneficial in understanding the importance of the Tspan5/17-ADAM10 interaction in inflammation. The reduction in VE-cadherin surface levels observed in the presence of Tspan5 or Tspan17 was found not to correlate with an increase in VE-cadherin shedding. As explained previously, this rather paradoxical result might be explained by the fact that the pool of VE-cadherin recognised by flow cytometry surface staining only forms a small proportion of the total VE-cadherin pools in these cells. In addition, it could be speculated that during the Western blot lysis procedure a particular pool of VE-cadherin may remain attached to the cytoskeleton and therefore be resistant to solubilisation. Further investigations into the dynamics of Tspan5 and Tspan17 trafficking of ADAM10 are required to confirm if these two TspanC8s favourably take ADAM10 to endothelial cell junctions.

Surprisingly, knockdown of Tspan5 or 17 individually or in combination did not alter the ability of PBLs to transmigrate. This was associated with no changes in ADAM10 and VE-cadherin surface levels nor VE-cadherin shedding. It was noted in these experiments

that a complete loss of Tspan5 or Tspan17 individually or in combination was not observed and it is possible to speculate that a phenotype with Tspan5 or Tspan17 would only be visualised with a greater knockdown. By using this individual knockdown approach, there is also the possibility of redundancy between the TspanC8s, since all the TspanC8s have been shown to promote ADAM10 trafficking (Dornier et al., 2012; Haining et al., 2012).

Lentiviral overexpression of the individual TspanC8s in HUVECs yielded data that was difficult to interpret. Overexpression of TspanC8s in HUVECs did not alter the abilities of PBLs to transmigrate. Furthermore, of the TspanC8s endogenously expressed in HUVECs, overexpression of Tspan5, 14, 15 and 17, did not alter VE-cadherin surface levels. Surprisingly, overexpression of Tspan15 and Tspan33 significantly reduced VE-cadherin shedding which was associated with a paradoxical increase in ADAM10 surface levels. It is worth noting that the dominant effect of Tspan15 and Tspan33 was probably more likely due to relatively higher expression levels of these TspanC8s compared to Tspan5, 14 and 17 following lentiviral transduction. In addition, Tspan10 has shown to have a largely intracellular localisation in HeLa cells (Dornier et al., 2012) and in HEK293T cells (Tomlinson, unpublished data) and this may account for the reason why Tspan10 does not promote ADAM10 surface expression in the lentivirally transduced HUVECs. It is worth noting that overexpression is prone to artefacts of abnormally high expression levels, and could in part be responsible for the apparently paradoxical data observed in the lentiviral overexpression studies.

Nevertheless, the data findings highlight a novel role of the relatively uncharacterised tetraspanins, Tspan5 and Tspan17, in regulating ADAM10s activity during lymphocyte transmigration (Figure 6.1). These findings offer a starting point for future studies to explore the specific role of these TspanC8s on endothelial cells.

Thus, further experimental models are required to decipher the exact mechanisms of Tspan5 and Tspan17's action. The recent advances in gene editing techniques, such as CRISPR/Cas9, would allow the production of Tspan5/17 double knockout HUVECs that could be tested for their ability to cleave VE-cadherin and regulate PBL transmigration. An alternative mechanism could be to use human induced pluripotent stem cells and knock out Tspan5 and Tspan17 in these cells prior to their differentiation into endothelial cells. Protocols for differentiating human induced pluripotent stem cells into endothelial cells are already well characterised with the differentiated cells expressing key endothelial markers such as, VE-cadherin, PECAM-1 and VEGF (Adams et al., 2013; Rufaihah et al., 2013). To date, the functional consequence of deleting Tspan5 or Tspan17 in knockout mice has not previously been reported. Therefore, it would be interesting to genetically engineer mice with Tspan5 and Tspan17 deletions, particularly in the endothelial lineage. These mice could then be used to investigate lymphocyte recruitment and transmigration into the cremasteric tissue following induction of an inflammatory response using intravital microscopy. The use of these definitive methods will allow a more in depth analysis of the roles of Tspan5 and Tspan17 in regulating ADAM10 activity during lymphocyte transmigration.

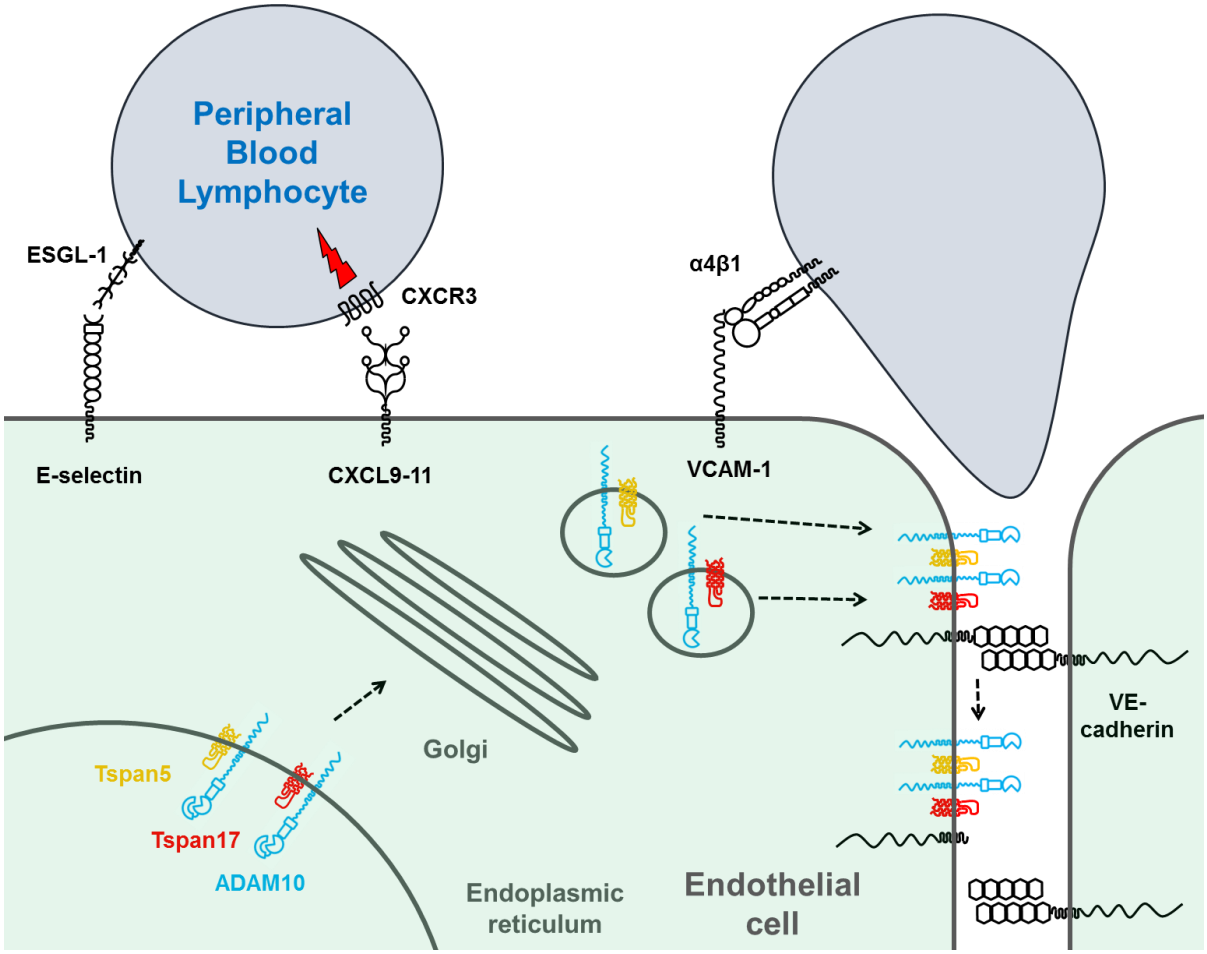

6.1 Proposed model of ADAM10 action and regulation during lymphocyte transmigration. Tspan5 and Tspan17 associate with ADAM10 and may direct ADAM10 cleavage of VE-cadherin via a mechanism that is not understood. Upon localisation of ADAM10 to endothelial cell junctions, ADAM10 is able to cleave the adhesion molecule VE-cadherin, thereby regulating normal lymphocyte transmigration.

6.2 OPEN QUESTIONS AND FUTURE PERSPECTIVES

6.2.1 What is the role of ADAM10 in regulating leukocyte transmigration *in vivo*?

Previous *in vitro* studies along with the data presented in this thesis showed a strong association between ADAM10 and lymphocyte transmigration (Schulz et al., 2008; Schwarz et al., 2010). The mechanisms by which endothelial ADAM10 regulates the transmigration of lymphocytes *in vivo* have not yet been shown. Since ADAM10 deletion

in mice results in embryonic lethality, the generation of the endothelial specific ADAM10 knockout mice (A10ΔEC) offers a possibility to investigate the role of lymphocyte transmigration *in vivo* (Glomski et al., 2011). These mice have some vasculature abnormalities, but a number of tissues, including muscle, have normal vasculature (Glomski et al., 2011). The role of endothelial ADAM10 *in vivo* could be assessed by using a well characterised *in vivo* assay of leukocyte transmigration such as visualising leukocyte arrest, rolling and transmigration across post-capillary venules in the cremaster muscle using video-intravital microscopy following intrascrotal injection of inflammatory stimuli such as TNFα. These studies would further validate the role of endothelial ADAM10 in supporting normal lymphocyte transmigration *in vivo*.

The role of ADAM10 on macrophages has been shown to be important in regulating the progression of atherosclerosis. Transplantation of bone marrow from conditional knockout mice lacking ADAM10 in the myeloid lineage (ADAM10-LysMcre) into lethally irradiated atherogenic mice ($LDLR^{-/-}$ knockout mice) resulted in an increase in atherosclerotic plaque stability (van der Vorst et al., 2015). This was associated with increased fibrosis and a reduction in the relative macrophage content in the plaque, although no difference in total plaque size was observed (van der Vorst et al., 2015). *In vitro* assays using cultured bone-marrow derived macrophages revealed ADAM10 deficiency promotes an anti-inflammatory phenotype by dampening the response of macrophages to pro-inflammatory stimuli and decreased matrix degrading properties and migration of the macrophages (van der Vorst et al., 2015). These data strongly suggest that myeloid ADAM10 may diminish atherosclerotic plaque stability by directing the balance from fibrosis to inflammation (van der Vorst et al., 2015). In chronic inflammation, such as atherosclerosis, the regulation of ADAM10 activity by TspanC8s in the various different immune cells involved remains unknown. It is possible to speculate that deletion of ADAM10 in immune cells would result in reduced lymphocyte infiltration into atherosclerotic plaques, which could reduce the pro-inflammatory composition of plaques

thereby hindering atherosclerosis progression, although this remains to be investigated. The cross talk between sentinel cells, such as mast cells, macrophages and DCs, and the endothelium is critical in supporting the efficient regulation of leukocyte recruitment. Due to the ubiquitous nature of ADAM10, isolated functions of ADAM10 in specific cells may only form part of the mechanism by which ADAM10 regulates the complex cascade of events of leukocyte transmigration during inflammation.

6.2.2 What is the role of ADAM10 in intracellular signalling pathways that are involved in leukocyte transmigration?

The data in this thesis highlighted an important role of ADAM10 in regulating VE-cadherin surface levels during lymphocyte transmigration. Recent advances in the understanding of VE-cadherin's role during leukocyte extravasation have shown an important role in the signalling mechanisms that act upon VE-cadherin during the process of lymphocyte transmigration. VE-cadherin has been shown to have a critical role in paracellular transmigration of leukocytes in which the dynamic opening and closing of endothelial junctions has to be tightly regulated so that it is sufficient to allow leukocytes to transmigrate but avoid vessel leakage (Nourshargh et al., 2010; Vestweber, 2015). In particular, disruption of endothelial junctions using a VE-cadherin antibody has been shown to promote leukocyte extravasation into inflamed tissue (Corada et al., 1999; Gotsch et al., 1997) suggesting that the adhesive strength of VE-cadherin is important in the passage of circulating leukocytes (Schulte et al., 2011).

Tyrosine phosphorylation of the VE-cadherin-catenin complex has shown promise in understanding how VE-cadherin's adhesive properties can become compromised during lymphocyte transmigration (Figure 6.2). A critical component of VE-cadherin is its intracellular association with α-, β-, and γ-catenins that aid its stability within the plasma membrane by binding to the cytoskeleton and mediate its association with VE-PTP

(Nottebaum et al., 2008). Adhesion of leukocytes to vascular endothelium has been shown to induce tyrosine phosphorylation of the VE-cadherin-catenin complex at specific tyrosine residues, namely Tyr645, Tyr658, Tyr731 and Tyr733 located on the cytoplasmic tail of VE-cadherin (Allingham et al., 2007; Nottebaum et al., 2008; Turowski et al., 2008). Furthermore, the introduction of tyrosine mutants in the VE-cadherin cytoplasmic tail has been shown to decrease the passage of both neutrophils and lymphocytes *in vitro* (Allingham et al., 2007; Turowski et al., 2008). Wessel et al. reported a critical role of VE-cadherin phosphorylation status through the use of knock-in mice that express a Y731F VE-cadherin mutant (Figure 6.2). These mice exhibited reduced lymphocyte transmigration (Wessel et al., 2014). Wessel et al. proposed that lymphocytes bind to the endothelium through an unknown receptor that then triggers the activity of the SRC homology 2-contaning protein-tyrosine phosphatase 2 (SHP2) leading to the dephosphorylation of VE-cadherin at Y731. This then leads to the transient endocytosis of VE-cadherin thereby weakening the cell-cell junctions and promoting lymphocyte transmigration (Wessel et al., 2014) (Figure 6.2). Tyrosine phosphorylation of the γ-catenin complex that forms intracellularly between VE-cadherin and its associated tyrosine phosphatase, VE-PTP, has been shown to be crucial in mediating the weakening of cell-cell adhesion. Binding of lymphocytes to inflamed endothelium induces an intracellular signalling cascade within endothelial cells that lead to the production of reactive oxygen species and enhanced Pyk2 kinase activity. Through an unknown mechanism, this leads to weakening of VE-cadherin-dependent adhesion via the dissociation of VE-PTP that is dependent on tyrosine phosphorylation of γ-catenin (Broermann et al., 2011) (Figure 6.2). Although the role of VE-cadherin phosphorylation has been extensively studied, the role of VE-cadherin shedding in such models of lymphocyte extravasation has been overlooked in these studies (Figure 6.2). It would, therefore, be interesting to investigate the link between VE-cadherin dephosphorylation at Tyr731 and ADAM10-mediated VE-cadherin shedding, which increasingly seems to be relevant to various inflammatory diseases (Sidibé et al., 2012).

It is as yet unknown what happens to the shed ectodomain fragment of VE-cadherin. Flemming *et al.* recently showed that reconstitution of endothelial cells with soluble VE-cadherin containing media caused disruption of endothelial cell-cell junctions as measured by a decrease in transendothelial electrical resistance (Flemming et al., 2015). It is also unknown if shedding of VE-cadherin on one endothelial cell promotes the shedding of VE-cadherin on the adjacent cell, thereby completely disrupting VE-cadherin homotypic interactions between adjacent cells.

Since the proteolytic shedding of VE-cadherin is irreversible, and the complete loss of VE-cadherin could be detrimental in causing vessel leakage, it could be speculated that efficient lymphocyte transmigration requires both proteolytic shedding and transient endocytosis mechanisms (Figure 6.2). Certainly, it could be considered that upon engagement of lymphocytes to endothelial cells, a small pool of apically located VE-cadherin could undergo shedding which then allows the transient dissociation of a larger pool of VE-cadherin that maintains vessel integrity once the lymphocyte has breached the endothelial barrier (Figure 6.2). Since evidence for such a paradigm is lacking, future experiments utilising shedding-resistant mutant VE-cadherin constructs, whereby the known ADAM10 shedding site has been mutated, could be used to assess this possibility. Mass spectrometry on soluble VE-cadherin ectodomain fragments have highlighted 3 regions within the juxtamembrane region of VE-cadherin that are prone to ADAM10 mediated shedding (Flemming et al., 2015) and, therefore, such ‘shedding resistant’ mutants could be generated for VE-cadherin by utilising this information.

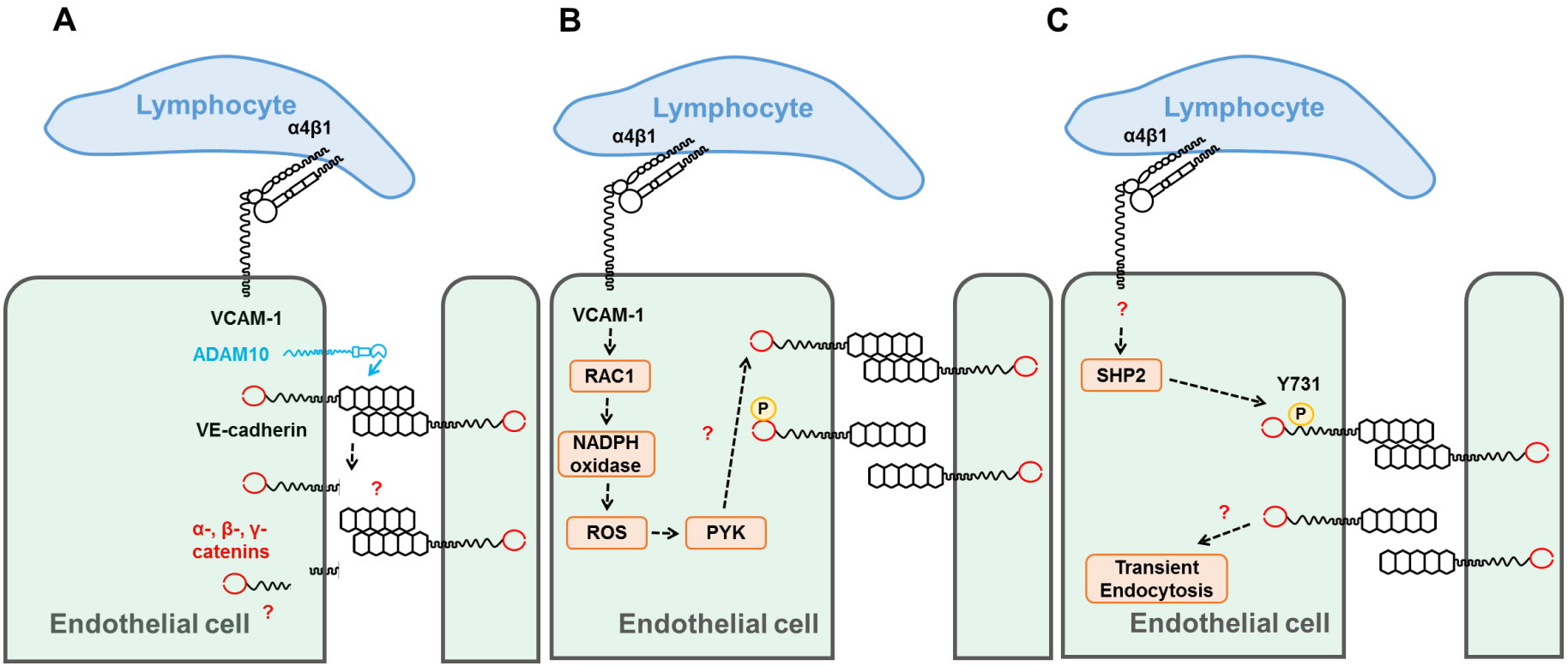

Figure 6.2. VE-cadherin acts as a master regulator of lymphocyte transmigration through its shedding and intracellular phosphorylation events. The VE-cadherin-dependent opening of cell-cell junctions can be controlled by different signalling or proteolytic shedding events thereby regulating the transmigration of lymphocytes. (A) ADAM10 has been documented as the primary sheddase that cleaves VE-cadherin releasing a soluble ectodomain fragment thereby weakening cell junctions allowing lymphocytes to transmigrate. Following removal of the soluble ectodomain, the cell-associated fragment of VE-cadherin is further processed by intramembrane proteases (namely the γ-secretase complex) releasing the intracellular domain that can exert possible intracellular signalling properties or undergo degradation. (B) Binding of lymphocytes to activated endothelial cells via $\alpha_4\beta_1$/VCAM-1 induces an intracellular signalling cascade that leads to the production of reactive oxygen species (ROS) downstream of NADPH-oxidase activity. Subsequent changes in PYK activity enhances phosphorylation of the catenin complex, by an unknown mechanism that leads to weakening of VE-cadherin-mediated adhesion. (C) Separately, through a largely unknown mechanism, activation of SRC homology 2-containing protein-tyrosine phosphatase-2 (SHP2) leads to a tyrosine dephosphorylation event on Y731, leading to rapid endocytosis of VE-cadherin, thereby weakening cell junctions and facilitating lymphocyte transmigration (Schulz *et al.* 2008; Nottebaum *et al.* 2008; Vockel and Vestweber 2013; Turowski *et al.* 2008; Wessel *et al.* 2014).

6.2.3 Could additional known or unknown ADAM10 targets be involved?

VE-cadherin forms part of an array of junctional proteins that are expressed at endothelial junctions. VE-cadherin has been shown to play an important role in lymphocyte transmigration but the involvement of other transmembrane proteins that undergo proteolytic cleavage may also be important. ADAM10 has been shown to be involved in the shedding of JAM-A in primary HUVECs (Koenen et al., 2009), although a more predominant role of ADAM17 is concluded by the authors of this study. Other junctional proteins such as CD99 and other members of the JAM family are interesting candidate molecules for ADAM10-mediated cleavage and further experimental evidence is required to conclude such possibility.

6.3 CONCLUDING REMARKS

The expression of the metalloprotease ADAM10 on endothelial cells is essential in normal transmigration of lymphocytes *in vitro*. This process is reliant on the shedding of the adhesion molecule, VE-cadherin. Endothelial tetraspanins Tspan5 and Tspan17 can facilitate the role of ADAM10 in lymphocyte transmigration *in vitro*. These findings open up the possibility of ADAM10 therapeutic targeting at the level of Tspan5 and Tspan17-ADAM10 complexes in the context of lymphocyte transmigration. This could allow ADAM10 targeting in a substrate-specific manner, so reducing the toxic side effects of globally inhibiting ADAM10. With a strong literature of ADAM10's role in chronic inflammatory diseases such as atherosclerosis emerging, targeting of ADAM10 by utilising this strategy could prove promising, given the potential role of endothelial ADAM10 in promoting lymphocyte transmigration.

REFERENCES

Abbas, Abdul K; Lichtmann, A.H. (2011) **Cellular and Molecular Immunology**. 8th ed. Oxford: Elsevier

Abel, S., Hundhausen, C., Mentlein, R., et al. (2004) The transmembrane CXC-chemokine ligand 16 is induced by IFN-gamma and TNF-alpha and shed by the activity of the disintegrin-like metalloproteinase. **Journal of Immunology**, 172 (10): 6362–6372

Adams, W.J., Zhang, Y., Cloutier, J., et al. (2013) Functional vascular endothelium derived from human induced pluripotent stem cells. **Stem Cell Reports**, 1 (2): 105–13

Ahmed, S.R., McGettrick, H.M.H., Yates, C.M., et al. (2011) Prostaglandin D2 Regulates CD4+ Memory T Cell Trafficking across Blood Vascular Endothelium and Primes These Cells for Clearance across Lymphatic. **Journal of Immunology**, 187 (3): 1432–1439

Allingham, M.J., van Buul, J.D. and Burridge, K. (2007) ICAM-1-mediated, Src- and Pyk2-dependent vascular endothelial cadherin tyrosine phosphorylation is required for leukocyte transendothelial migration. **Journal of Immunology**, 179: 4053–4064

Alon, R. and Dustin, M.L. (2007) Force as a facilitator of integrin conformational changes during leukocyte arrest on blood vessels and antigen-presenting cells. **Immunity**, 26 (1): 17–27

Alon, R., Hammer, D.A. and Springer, T.A. (1995) Lifetime of the P-selectin-carbohydrate bond and its response to tensile force in hydrodynamic flow. **Nature**. 374 (6522) pp. 539–542

Ancuta, P., Moses, A. and Gabuzda, D. (2004) Transendothelial migration of CD16+ monocytes in response to fractalkine under constitutive and inflammatory conditions. **Immunobiology**, 209 (1-2): 11–20

Anders, A., Gilbert, S., Garten, W., et al. (2001) Regulation of the alpha-secretase ADAM10 by its prodomain and proprotein convertases. **FASEB Journal**, 15 (10): 1837–9

Andreini, C., Banci, L., Bertini, I., et al. (2005) Comparative analysis of the ADAM and ADAMTS families. **Journal of Proteome Research**, 4 (3): 881–8

Arduise, C., Abache, T., Li, L., et al. (2008) Tetraspanins regulate ADAM10-mediated cleavage of TNF-alpha and epidermal growth factor. **Journal of Immunology**, 181 (10): 7002–13

Azcutia, V., Stefanidakis, M., Tsuboi, N., et al. (2012) Endothelial CD47 promotes vascular endothelial-cadherin tyrosine phosphorylation and participates in T cell recruitment at sites of inflammation in vivo. **Journal of Immunology**, 189 (5): 2553–62

Bailey, R., Herbert, J., Khan, K., et al. (2011) The emerging role of tetraspanin microdomains on endothelial cells. **Biochemical Society Transactions**, 39 (6): 1667–73

Baldwin, G., Novitskaya, V., Sadej, R., et al. (2008) Tetraspanin CD151 regulates glycosylation of (alpha)3(beta)1 integrin. **Journal of Biological Chemistry**, 283 (51): 35445–54

Barreiro, O., Vicente-Manzanares, M., Urzainqui, A., et al. (2004) Interactive protrusive structures during leukocyte adhesion and transendothelial migration. **Frontiers in Bioscience**, 9: 1849–1863

Barreiro, O., Yáñez-Mó, M., Sala-Valdés, M., et al. (2005) Endothelial tetraspanin

microdomains regulate leukocyte firm adhesion during extravasation. **Blood**, 105 (7): 2852–2861

Barreiro, O., Zamai, M., Yáñez-Mó, M., et al. (2008) Endothelial adhesion receptors are recruited to adherent leukocytes by inclusion in preformed tetraspanin nanoplatforms. **Journal of Cell Biology**, 183 (3): 527–542

Berditchevski, F., Zutter, M.M. and Hemler, M.E. (1996) Characterization of novel complexes on the cell surface between integrins and proteins with 4 transmembrane domains (TM4 proteins). **Molecular Biology of the Cell**, 7 (2): 193–207

Bianchi, M.E. (2007) DAMPs, PAMPs and alarmins: all we need to know about danger. **Journal of Leukocyte Biology**, 81 (1): 1–5

Bode, W., Gomis-Rüth, F.X. and Stöckler, W. (1993) Astacins, serralysins, snake venom and matrix metalloproteinases exhibit identical zinc-binding environments (HEXXHXXGXXH and Met-turn) and topologies and should be grouped into a common family, the “metzincins”. **FEBS Letters**, 331 (1-2): 134–40

Bozkulak, E.C. and Weinmaster, G. (2009) Selective Use of ADAM10 and ADAM17 in Activation of Notch1 Signaling. **Molecular and Cellular Biology**, 29 (21): 5679–5695

Bradbury, L.E., Kansas, G.S., Levy, S., et al. (1992) The CD19/CD21 signal transducing complex of human B lymphocytes includes the target of antiproliferative antibody-1 and Leu-13 molecules. **Journal of Immunology**, 149 (9): 2841–50

Bridges, L. and Bowditch, R. (2005) ADAM-Integrin Interactions: Potential Integrin Regulated Ectodomain Shedding Activity. **Current Pharmaceutical Design**, 11 (7): 837–847

Broermann, A., Winderlich, M., Block, H., et al. (2011) Dissociation of VE-PTP from VE-cadherin is required for leukocyte extravasation and for VEGF-induced vascular permeability in vivo. **Journal of Experimental Medicine**, 208 (12): 2393–401

Butler, L.M., McGettrick, H.M. and Nash, G.B. (2009) Static and dynamic assays of cell adhesion relevant to the vasculature. **Methods in Molecular Biology**, 467: 211–28

Caescu, C.I., Jeschke, G.R. and Turk, B.E. (2009) Active-site determinants of substrate recognition by the metalloproteinases TACE and ADAM10. **Biochemical Journal**, 424 (1): 79–88

Campbell, J.J., Qin, S., Bacon, K.B., et al. (1996) Biology of chemokine and classical chemoattractant receptors: Differential requirements for adhesion-triggering versus chemotactic responses in lymphoid cells. **Journal of Cell Biology**, 134 (1): 255–266

Carlin, L.M., Stamatiades, E.G., Auffray, C., et al. (2013) Nr4a1-dependent Ly6C(low) monocytes monitor endothelial cells and orchestrate their disposal. **Cell**, 153 (2): 362–75

Carman, C. V, Sage, P.T., Sciuto, T.E., et al. (2007) Transcellular diapedesis is initiated by invasive podosomes. **Immunity**, 26 (6): 784–97

Carman, C. V and Springer, T.A. (2004) A transmigratory cup in leukocyte diapedesis both through individual vascular endothelial cells and between them. **Journal of Cell Biology**, 167 (2): 377–88

Carman, C. V. and Springer, T. a. (2003) Integrin avidity regulation: Are changes in affinity and conformation underemphasized? **Current Opinion in Cell Biology**, 15 (5): 547–556

Charrin, S., Jouannet, S., Boucheix, C., et al. (2014) Tetraspanins at a glance. **Journal of Cell Science**, (August): 1–8

Charrin, S., Manié, S., Oualid, M., et al. (2002) Differential stability of tetraspanin/tetraspanin interactions: role of palmitoylation. **FEBS Letters**, 516 (1-3): 139–144

Charrin, S., Manié, S., Thiele, C., et al. (2003) A physical and functional link between cholesterol and tetraspanins. **European Journal of Immunology**, 33 (9): 2479–89

Charrin, S., Le Naour, F., Oualid, M., et al. (2001) The Major CD9 and CD81 Molecular Partner: Identification and Characterisation of the Complexes. **Journal of Biological Chemistry**, 276 (17): 14329–14337

Charrin, S., Naour, F. le, Silvie, O., et al. (2009a) Lateral organization of membrane proteins: tetraspanins spin their web. **Biochemical Journal**, 420 (2): 133–154

Charrin, S., Yalaoui, S., Bartosch, B., et al. (2009b) The Ig domain protein CD9P-1 down-regulates CD81 ability to support Plasmodium yoelii infection. **Journal of Biological Chemistry**, 284 (46): 31572–8

Chimen, M., McGettrick, H.M., Apta, B., et al. (2015) Homeostatic regulation of T cell trafficking by a B cell–derived peptide is impaired in autoimmune and chronic inflammatory disease. **Nature Medicine**, 21 (5): 467–475

Colom, B., Bodkin, J. V, Beyrau, M., et al. (2015) Leukotriene B4-Neutrophil Elastase Axis Drives Neutrophil Reverse Transendothelial Cell Migration In Vivo. **Immunity**, 42 (6): 1075–86

Conlon, R.A., Reaume, A.G. and Rossant, J. (1995) Notch1 is required for the coordinate segmentation of somites. **Development**, 121 (5): 1533–45

Cooke, B.M., Shunichi, U., Perry, I., et al. (1993) A Simplified Method for Culture of Endothelial Cells and Analysis of Adhesion of Blood Cells under Conditions of Flow. **Microvascular Research**, 45 (1): 33–45

Corada, M., Mariotti, M., Thurston, G., et al. (1999) Vascular endothelial-cadherin is an important determinant of microvascular integrity in vivo. **Proceedings of the National Academy of Sciences of the United States of America**, 96 (17): 9815–20

Coulthard, M.G., Morgan, M., Woodruff, T.M., et al. (2012) Eph/Ephrin signaling in injury and inflammation. **The American Journal of pathology**, 181 (5): 1493–503

Deem, T.L., Abdala-Valencia, H. and Cook-Mills, J.M. (2007) VCAM-1 activation of endothelial cell protein tyrosine phosphatase 1B. **Journal of immunology**, 178 (6): 3865–3873

Dejana, E. (2004) Endothelial cell-cell junctions: happy together. **Nature reviews. Molecular cell biology**, 5 (4): 261–70

Delandre, C., Penabaz, T.R., Passarelli, A.L., et al. (2009) Mutation of juxtamembrane cysteines in the tetraspanin CD81 affects palmitoylation and alters interaction with other proteins at the cell surface. **Experimental cell research**, 315 (11): 1953–63

Deng, W., Cho, S., Su, P.-C., et al. (2014) Membrane-enabled dimerization of the intrinsically disordered cytoplasmic domain of ADAM10. **Proceedings of the National Academy of Sciences of the United States of America**, 111 (45): 15987–92

Donners, M., Wolfs, I., Olieslagers, S., et al. (2010) A Disintegrin and Metalloprotease 10 Is a Novel Mediator of Vascular Endothelial Growth Factor–Induced Endothelial Cell Function in Angiogenesis and Is Associated with Atherosclerosis. **Arteriosclerosis, Thrombosis, and Vascular Biology**, 30 (11): 2188–95

Dornier, E., Coumailleau, F., Ottavi, J.-F., et al. (2012) TspanC8 tetraspanins regulate

ADAM10/Kuzbanian trafficking and promote Notch activation in flies and mammals. **Journal of cell biology**, 199 (3): 481–96

Doyle, E., Ridger, V., Ferraro, F., et al. (2011) CD63 is an essential cofactor to leukocyte recruitment by endothelial P-selectin. **Blood**, 118 (15): 4265–73

Dreymueller, D., Martin, C., Kogel, T., et al. (2012a) Lung endothelial ADAM17 regulates the acute inflammatory response to lipopolysaccharide. **EMBO molecular medicine**, 4 (5): 412–23

Dreymueller, D., Pruessmeyer, J., Groth, E., et al. (2012b) The role of ADAM-mediated shedding in vascular biology. **European journal of cell biology**, 91 (6-7): 472–85

Dreymueller, D., Uhlig, S. and Ludwig, A. (2015) ADAM-family metalloproteinases in lung inflammation: potential therapeutic targets. **American journal of physiology. Lung cellular and molecular physiology**, 308 (4): L325–43

Düsterhöft, S., Höbel, K., Oldefest, M., et al. (2014) A Disintegrin and Metalloprotease 17 Dynamic Interaction Sequence, the Sweet Tooth for the Human Interleukin 6 Receptor. **Journal of Biological Chemistry**, 289 (23): 16336–16348

Ebsen, H., Lettau, M., Kabelitz, D., et al. (2014) Identification of SH3 Domain Proteins Interacting with the Cytoplasmic Tail of the A Disintegrin and Metalloprotease 10 (ADAM10). **PloS one**, 9 (7): e102899

Edwards, D.R., Handsley, M.M. and Pennington, C.J. (2008) The ADAM metalloproteinases. **Molecular aspects of medicine**, 29 (5): 258–289

Engelhardt, B. and Ransohoff, R.M. (2012) Capture, crawl, cross: The T cell code to breach the blood-brain barriers. **Trends in Immunology**, 33 (12): 579–589

Espenel, C., Margeat, E., Dosset, P., et al. (2008) Single-molecule analysis of CD9 dynamics and partitioning reveals multiple modes of interaction in the tetraspanin web. **Journal of cell biology**, 182 (4): 765–76

Feigelson, S.W., Grabovsky, V., Shamri, R., et al. (2003) The CD81 Tetraspanin Facilitates Instantaneous Leukocyte VLA-4 Adhesion Strengthening to Vascular Cell Adhesion Molecule 1 (VCAM-1) under Shear Flow. **Journal of Biological Chemistry**, 278 (51): 51203–51212

Feng, D., Nagy, J.A., Pyne, K., et al. (1998) Neutrophils emigrate from venules by a transendothelial cell pathway in response to FMLP. **Journal of experimental medicine**, 187 (6): 903–15

Finger, E.B., Puri, K.D., Alon, R., et al. (1996) Adhesion through L-selectin requires a threshold hydrodynamic shear. **Nature**. 379 (6562) pp. 266–269

Finlay, B.B. and Hancock, R.E.W. (2004) Can innate immunity be enhanced to treat microbial infections? **Nature reviews. Microbiology**, 2 (6): 497–504

Flemming, S., Burkard, N., Renschler, M., et al. (2015) Soluble VE-cadherin is involved in endothelial barrier breakdown in systemic inflammation and sepsis. **Cardiovascular Research**, 107 (1): 32–44

Foussat, A., Coulomb-L'Hermine, A., Gosling, J., et al. (2000) Fractalkine receptor expression by T lymphocyte subpopulations and in vivo production of fractalkine in human. **European journal of immunology**, 30 (1): 87–97

Galkina, E., Tanousis, K., Preece, G., et al. (2003) L-selectin shedding does not regulate constitutive T cell trafficking but controls the migration pathways of antigen-activated T lymphocytes. **Journal of experimental medicine**, 198 (9): 1323–35

Garcia-España, A., Chung, P.-J., Sarkar, I.N., et al. (2008) Appearance of new tetraspanin genes during vertebrate evolution. **Genomics**, 91 (4): 326–34

Garton, K.J., Gough, P.J., Blobel, C.P., et al. (2001) Tumor necrosis factor-alpha-converting enzyme (ADAM17) mediates the cleavage and shedding of fractalkine (CX3CL1). **Journal of biological chemistry**, 276 (41): 37993–8001

Garton, K.J., Gough, P.J. and Raines, E.W. (2006) Emerging roles for ectodomain shedding in the regulation of inflammatory responses. **Journal of leukocyte biology**, 79 (6): 1105–16

Geissmann, F., Jung, S. and Littman, D.R. (2003) Blood monocytes consist of two principal subsets with distinct migratory properties. **Immunity**, 19 (1): 71–82

Glomski, K., Monette, S., Manova, K., et al. (2011) Deletion of Adam10 in endothelial cells leads to defects in organ-specific vascular structures. **Blood**, 118 (4): 1163–74

Gonzales, P.E., Solomon, A., Miller, A.B., et al. (2004) Inhibition of the tumor necrosis factor-alpha-converting enzyme by its pro domain. **Journal of biological chemistry**, 279 (30): 31638–45

Gotsch, U., Borges, E., Bosse, R., et al. (1997) VE-cadherin antibody accelerates neutrophil recruitment in vivo. **Journal of cell science**, 110 (Pt 5: 583–8

Guo, M., Wu, M.H., Granger, H.J., et al. (2004) Transference of recombinant VE-cadherin cytoplasmic domain alters endothelial junctional integrity and porcine microvascular permeability. **Journal of physiology**, 554 (Pt 1): 78–88

Hafezi-Moghadam, a, Thomas, K.L., Prorock, a J., et al. (2001) L-selectin shedding regulates leukocyte recruitment. **Journal of experimental medicine**, 193 (7): 863–72

Haining, E., Yang, J., Bailey, R., et al. (2012) The TspanC8 subgroup of tetraspanins interacts with a disintegrin and metalloprotease 10 (ADAM10) and regulates its maturation and cell surface expression. **Journal of Biological Chemistry**, 10: 1–26

Hall, K.C. and Blobel, C.P. (2012) Interleukin-1 stimulates ADAM17 through a mechanism independent of its cytoplasmic domain or phosphorylation at threonine 735. **PloS one**, 7 (2): e31600

Hartmann, D., de Strooper, B., Serneels, L., et al. (2002) The disintegrin/metalloprotease ADAM 10 is essential for Notch signalling but not for alpha-secretase activity in fibroblasts. **Human molecular genetics**, 11 (21): 2615–24

Hemler, M.E. (2014) Tetraspanin proteins promote multiple cancer stages. **Nature Reviews Cancer**, 14 (1): 49–60

Hermant, B., Bibert, S., Concord, E., et al. (2003) Identification of proteases involved in the proteolysis of vascular endothelium cadherin during neutrophil transmigration. **Journal of biological chemistry**, 278 (16): 14002–12

Herter, J. and Zarbock, A. (2013) Integrin Regulation during Leukocyte Recruitment. **Journal of immunology**, 190 (9): 4451–7

Hofnagel, O., Luechtenborg, B., Plenz, G., et al. (2002) Expression of the Novel Scavenger Receptor SR-PSOX in Cultured Aortic Smooth Muscle Cells and Umbilical Endothelial Cells. **Arteriosclerosis, Thrombosis, and Vascular Biology**, 22 (4): 710–711

Hu, Y., Kiely, J.M., Szente, B.E., et al. (2000) E-selectin-dependent signaling via the mitogen-activated protein kinase pathway in vascular endothelial cells. **Journal of immunology**, 165 (4): 2142–8

Huang, A.J., Manning, J.E., Bandak, T.M., et al. (1993) Endothelial cell cytosolic free calcium regulates neutrophil migration across monolayers of endothelial cells. **Journal of cell biology**, 120 (6): 1371–80

Huang, S., Yuan, S., Dong, M., et al. (2005) The phylogenetic analysis of tetraspanins projects the evolution of cell–cell interactions from unicellular to multicellular organisms. **Genomics**, 86 (6): 674–684

Hundhausen, C., Misztela, D., Berkhout, T.A., et al. (2003) The disintegrin-like metalloproteinase ADAM10 is involved in constitutive cleavage of CX3CL1 (fractalkine) and regulates CX3CL1-mediated cell-cell adhesion. **Blood**, 102 (4): 1186–95

Hundhausen, C., Schulte, A., Schulz, B., et al. (2007) Regulated shedding of transmembrane chemokines by the disintegrin and metalloproteinase 10 facilitates detachment of adherent leukocytes. **Journal of Immunology**, 178 (12): 8064–72

Hyun, Y.-M., Sumagin, R., Sarangi, P.P., et al. (2012) Uropod elongation is a common final step in leukocyte extravasation through inflamed vessels. **Journal of Experimental Medicine**, 209 (7): 1349–1362

Igarashi, T., Araki, S., Mori, H., et al. (2007) Crystal structures of catrocollastatin/VAP2B reveal a dynamic, modular architecture of ADAM/adamalysin/reprolysin family proteins. **FEBS Letters**, 581 (13): 2416–22

Israels, S.J. and McMillan-Ward, E.M. (2010) Palmitoylation supports the association of tetraspanin CD63 with CD9 and integrin alphaIIbbeta3 in activated platelets. **Thrombosis Research**, 125 (2): 152–8

Jackson, L.F. (2003) Defective valvulogenesis in HB-EGF and TACE-null mice is associated with aberrant BMP signaling. **EMBO Journal**, 22 (11): 2704–2716

Janes, P.W., Saha, N., Barton, W.A., et al. (2005) Adam meets Eph: an ADAM substrate recognition module acts as a molecular switch for ephrin cleavage in trans. **Cell**, 123 (2): 291–304

Johnston, B. (1996) The alpha 4-integrin supports leukocyte rolling and adhesion in chronically inflamed postcapillary venules in vivo. **Journal of Experimental Medicine**, 183 (5): 1995–2006

Jouannet, S., Saint-Pol, J., Fernandez, L., et al. (2016) TspanC8 tetraspanins differentially regulate the cleavage of ADAM10 substrates, Notch activation and ADAM10 membrane compartmentalization. **Cellular and Molecular Life Sciences**, 73 (9): 1895–915

Junge, H.J., Yang, S., Burton, J.B., et al. (2009) TSPAN12 regulates retinal vascular development by promoting Norrin- but not Wnt-induced FZD4/beta-catenin signaling. **Cell**, 139 (2): 299–311

Kanwar, S., Bullard, D.C., Hickey, M.J., et al. (1997) The association between alpha4-integrin, P-selectin, and E-selectin in an allergic model of inflammation. **Journal of Experimental Medicine**, 185 (6): 1077–1087

Kaur, S., Leszczynska, K., Abraham, S., et al. (2011) RhoJ/TCL regulates endothelial motility and tube formation and modulates actomyosin contractility and focal adhesion numbers. **Arteriosclerosis, Thrombosis, and Vascular Biology and Vascular Biology**, 31 (3): 657–664

Khokha, R., Murthy, A. and Weiss, A. (2013) Metalloproteinases and their natural inhibitors in inflammation and immunity. **Nature reviews. Immunology**, 13 (9): 649–65

Kiessling, F., Kartenbeck, J. and Haller, C. (1999) Cell-cell contacts in the human cell line ECV304 exhibit both endothelial and epithelial characteristics. **Cell and Tissue Research**, 297 (1): 131–140

Kinashi, T. (2005) Intracellular signalling controlling integrin activation in lymphocytes. **Nature reviews. Immunology**, 5 (7): 546–59

Kitadokoro, K., Bordo, D., Galli, G., et al. (2001) CD81 extracellular domain 3D structure: insight into the tetraspanin superfamily structural motifs. **EMBO Journal**, 20 (1-2): 12–8

Klein, T. and Bischoff, R. (2011) Active metalloproteases of the A Disintegrin and Metalloprotease (ADAM) family: biological function and structure. **Journal of Proteome Research**, 10 (1): 17–33

Kodama, Y. and Hu, C.-D. (2012) Bimolecular fluorescence complementation (BiFC): A 5-year update and future perspectives. **BioTechniques**, 53 (5): 285–98

Koenen, R.R., Pruessmeyer, J., Soehnlein, O., et al. (2009) Regulated release and functional modulation of junctional adhesion molecule A by disintegrin metalloproteinases. **Blood**, 113 (19): 4799–809

Krishnamoorthy, S. and Honn, K. V (2006) Inflammation and disease progression. **Cancer Metastasis Reviews**, 25 (3): 481–91

Lammich, S., Kojro, E., Postina, R., et al. (1999) Constitutive and regulated alpha-secretase cleavage of Alzheimer's amyloid precursor protein by a disintegrin metalloprotease. **Proceedings of the National Academy of Sciences of the United States of America**, 96 (7): 3922–7

Lampugnani, M.G., Corada, M., Caveda, L., et al. (1995) The molecular organization of endothelial cell to cell junctions: differential association of plakoglobin, beta-catenin, and alpha-catenin with vascular endothelial cadherin (VE-cadherin). **Journal of Cell Biology**, 129 (1): 203–17

Latta, M., Mohan, K. and Issekutz, T.B. (2007) CXCR6 is expressed on T cells in both T helper type 1 (Th1) inflammation and allergen-induced Th2 lung inflammation but is only a weak mediator of chemotaxis. **Immunology**, 121 (4): 555–64

Lawrence, M.B., Kansas, G.S., Kunkel, E.J., et al. (1997) Threshold levels of fluid shear promote leukocyte adhesion through selectins (CD62L,P,E). **Journal of Cell Biology**, 136 (3): 717–27

Lefort, C.T., Rossaint, J., Moser, M., et al. (2012) Distinct roles for talin-1 and kindlin-3 in LFA-1 extension and affinity regulation. **Blood**, 119 (18): 4275–4282

Levy, S. and Shoham, T. (2005) The tetraspanin web modulates immune-signalling complexes. **Nature reviews. Immunology**, 5 (2): 136–48

Ley, K., Laudanna, C., Cybulsky, M.I., et al. (2007) Getting to the site of inflammation: the leukocyte adhesion cascade updated. **Nature reviews. Immunology**, 7 (9): 678–89

Ley, K. and Zhang, H. (2008) Dances with leukocytes: How tetraspanin-enriched microdomains assemble to form endothelial adhesive platforms. **Journal of Cell Biology**, 183 (3): 375–376

Linford, A., Yoshimura, S., Nunes Bastos, R., et al. (2012) Rab14 and its exchange factor FAM116 link endocytic recycling and adherens junction stability in migrating cells. **Developmental Cell**, 22 (5): 952–66

Long, C., Wang, Y., Herrera, A.H., et al. (2010) In vivo role of leukocyte ADAM17 in the inflammatory and host responses during E. coli-mediated peritonitis. **Journal of**

Leukocyte Biology, 87 (June): 1097–1101

Ludwig, A. and Weber, C. (2007) Transmembrane chemokines: Versatile 'special agents' in vascular inflammation. **Thrombosis and Haemostasis**, 97 (5): 694–703

Luu, N.T., Rainger, G.E. and Nash, G.B. (2000) Differential ability of exogenous chemotactic agents to disrupt transendothelial migration of flowing neutrophils. **Journal of Immunology**, 164 (11): 5961–9

Majno, G. and Joris, I. (2008) **Cells, Tissues, and Disease: Principles of General Pathology**

Maretzky, T., Evers, A., Le Gall, S., et al. (2015) The cytoplasmic domain of a disintegrin and metalloproteinase 10 (ADAM10) regulates its constitutive activity but is dispensable for stimulated ADAM10-dependent shedding. **Journal of Biological Chemistry**, 290 (12): 7416–25

Maretzky, T., Reiss, K., Ludwig, A., et al. (2005) ADAM10 mediates E-cadherin shedding and regulates epithelial cell-cell adhesion, migration, and beta-catenin translocation. **Proceedings of the National Academy of Sciences of the United States of America**, 102 (26): 9182–7

Marmon, S., Hinchey, J., Oh, P., et al. (2009) Caveolin-1 expression determines the route of neutrophil extravasation through skin microvasculature. **The American Journal of Pathology**, 174 (2): 684–92

Martinelli, R., Gegg, M., Longbottom, R., et al. (2009) ICAM-1-mediated endothelial nitric oxide synthase activation via calcium and AMP-activated protein kinase is required for transendothelial lymphocyte migration. **Molecular Biology of the Cell**, 20 (3): 995–1005

Martinelli, R., Zeiger, A.S., Whitfield, M., et al. (2014) Probing the biomechanical contribution of the endothelium to lymphocyte migration: diapedesis by the path of least resistance. **Journal of Cell Science**, 127 (Pt 17): 3720–3734

Matsumoto, A.K., Martin, D.R., Carter, R.H., et al. (1993) Functional dissection of the CD21/CD19/TAPA-1/Leu-13 complex of B lymphocytes. **Journal of Experimental Medicine**, 178 (4): 1407–17

McDonald, B., Pittman, K., Menezes, G.B., et al. (2010) Intravascular danger signals guide neutrophils to sites of sterile inflammation. **Science**, 330 (6002): 362–366

McEver, R.P. (2002) Selectins: Lectins that initiate cell adhesion under flow. **Current Opinion in Cell Biology**, 14 (5): 581–586

McEver, R.P. and Zhu, C. (2010) Rolling cell adhesion. **Annual review of Cell and Developmental Biology**, 26: 363–96

McGettrick, H.M., Hunter, K., Moss, P.A., et al. (2009) Direct observations of the kinetics of migrating T cells suggest active retention by endothelial cells with continual bidirectional migration. **Journal of Leukocyte Biology**, 85 (1): 98–107

Medzhitov, R. (2008) Origin and physiological roles of inflammation. **Nature**, 454 (7203): 428–435

Millán, J., Hewlett, L., Glyn, M., et al. (2006) Lymphocyte transcellular migration occurs through recruitment of endothelial ICAM-1 to caveola- and F-actin-rich domains. **Nature Cell Biology**, 8 (2): 113–123

Min, G., Wang, H., Sun, T.-T., et al. (2006) Structural basis for tetraspanin functions as revealed by the cryo-EM structure of uroplakin complexes at 6-A resolution. **Journal of Cell Biology**, 173 (6): 975–83

Montpellier, C., Tews, B.A., Poitrimole, J., et al. (2011) Interacting regions of CD81 and two of its partners, EWI-2 and EWI-2wint, and their effect on hepatitis C virus infection. **Journal of Biological Chemistry**, 286 (16): 13954–13965

Moser, M., Legate, K.R., Zent, R., et al. (2009) The tail of integrins, talin, and kindlins. **Science**, 324 (5929): 895–899

Muller, W. a (2011) Mechanisms of leukocyte transendothelial migration. **Annual Review of Pathology**, 6: 323–344

Munir, H., Rainger, G.E., Nash, G.B., et al. (2015) Analyzing the effects of stromal cells on the recruitment of leukocytes from flow. **Journal of Visualized Experiments : JoVE**, (95): e52480

Nath, D., Slocombe, P.M., Stephens, P.E., et al. (1999) Interaction of metargidin (ADAM-15) with alphavbeta3 and alpha5beta1 integrins on different haemopoietic cells. **Journal of Cell Science**, 112 (Pt 4: 579–87

Nath, D., Slocombe, P.M., Webster, A., et al. (2000) Meltrin gamma(ADAM-9) mediates cellular adhesion through alpha(6)beta(1)integrin, leading to a marked induction of fibroblast cell motility. **Journal of Cell Science**, 113 (Pt 1: 2319–28

Nikopoulos, K., Gilissen, C., Hoischen, A., et al. (2010) Next-Generation Sequencing of a 40 Mb Linkage Interval Reveals TSPAN12 Mutations in Patients with Familial Exudative Vitreoretinopathy. **American Journal of Human Genetics**, 86 (2): 240–247

Nottebaum, A.F., Cagna, G., Winderlich, M., et al. (2008) VE-PTP maintains the endothelial barrier via plakoglobin and becomes dissociated from VE-cadherin by leukocytes and by VEGF. **Journal of Experimental Medicine**, 205 (12): 2929–2945

Nourshargh, S. and Alon, R. (2014) Leukocyte Migration into Inflamed Tissues. **Immunity**, 41 (5): 694–707

Nourshargh, S., Hordijk, P.P.L. and Sixt, M. (2010) Breaching multiple barriers: leukocyte motility through venular walls and the interstitium. **Nature reviews. Molecular Cell Biology**, 11 (5): 366–378

Nourshargh, S. and Marelli-Berg, F.M. (2005) Transmigration through venular walls: a key regulator of leukocyte phenotype and function. **Trends in Immunology**, 26 (3): 157–65

Noy, P.J., Yang, J., Reyat, J.S., et al. (2016) TspanC8 Tetraspanins and A Disintegrin and Metalloprotease 10 (ADAM10) Interact Via Their Extracellular Regions: Evidence For Distinct Binding Mechanisms For Different TspanC8s. **Journal of Biological Chemistry**, 291 (7): 3145–57

Odintsova, E., Butters, T.D., Monti, E., et al. (2006) Gangliosides play an important role in the organization of CD82-enriched microdomains. **Biochemical Journal**, 400 (2): 315–25

Orth, P., Reichert, P., Wang, W., et al. (2004) Crystal structure of the catalytic domain of human ADAM33. **Journal of Molecular Biology**, 335 (1): 129–37

Peschon, J.J., Slack, J.L., Reddy, P., et al. (1998) An Essential Role for Ectodomain Shedding in Mammalian Development. **Science**, 282 (5392): 1281–1284

Petri, B., Kaur, J., Long, E.M., et al. (2011) Endothelial LSP1 is involved in endothelial dome formation, minimizing vascular permeability changes during neutrophil transmigration in vivo. **Blood**, 117 (3): 942–952

Pfau, S., Leitenberg, D., Rinder, H., et al. (1995) Lymphocyte adhesion-dependent calcium signaling in human endothelial cells. **Journal of Cell Biology**, 128 (5): 969–978

Pham, C.T.N. (2008) Neutrophil serine proteases fine-tune the inflammatory response. **The International Journal of Biochemistry & Cell Biology**, 40 (6-7): 1317–33

Phillipson, M., Heit, B., Colarusso, P., et al. (2006) Intraluminal crawling of neutrophils to emigration sites: a molecularly distinct process from adhesion in the recruitment cascade. **Journal of Experimental Medicine**, 203 (12): 2569–75

Phillipson, M., Kaur, J., Colarusso, P., et al. (2008) Endothelial domes encapsulate adherent neutrophils and minimize increases in vascular permeability in paracellular and transcellular emigration. **PloS one**, 3 (1932-6203 (Electronic)): e1649

Phillipson, M. and Kubes, P. (2011) The neutrophil in vascular inflammation. **Nature Medicine**, 17 (11): 1381–90

Ponnuchamy, B. and Khalil, R.A. (2008) Role of ADAMs in Endothelial Cell Permeability Cadherin Shedding and Leukocyte Rolling. **Circulation Research**, 102 (10): 1139–42

Postina, R., Schroeder, A., Dewachter, I., et al. (2004) A disintegrin-metalloproteinase prevents amyloid plaque formation and hippocampal defects in an Alzheimer disease mouse model. **Journal of Clinical Investigation**, 113 (10): 1456–64

Poulter, J. a., Ali, M., Gilmour, D.F., et al. (2010) Mutations in TSPAN12 Cause Autosomal-Dominant Familial Exudative Vitreoretinopathy. **American Journal of Human Genetics**, 86 (2): 248–253

Powers, M.E., Kim, H.K., Wang, Y., et al. (2012) ADAM10 mediates vascular injury induced by Staphylococcus aureus α-hemolysin. **Journal of Infectious Diseases**, 206 (3): 352–6

Proebstl, D., Voisin, M.-B., Woodfin, A., et al. (2012) Pericytes support neutrophil subendothelial cell crawling and breaching of venular walls in vivo. **Journal of Experimental Medicine**, 209 (6): 1219–34

Prox, J., Rittger, A. and Saftig, P. (2012a) Physiological functions of the amyloid precursor protein secretases ADAM10, BACE1, and presenilin. **Experimental Brain Research**, 217 (3-4): 331–41

Prox, J., Willenbrock, M., Weber, S., et al. (2012b) Tetraspanin15 regulates cellular trafficking and activity of the ectodomain sheddase ADAM10. **Cellular and Molecular Life Sciences**, 69 (17): 2919–2932

Pruessmeyer, J., Hess, F.M., Ahlert, H., et al. (2014) Leukocytes require the metalloproteinase ADAM10 but not ADAM17 for cell migration and for inflammatory leukocyte recruitment into the alveolar space. **Blood**, 123 (26): 4077–4088

Pruessmeyer, J. and Ludwig, A. (2009) The good, the bad and the ugly substrates for ADAM10 and ADAM17 in brain pathology, inflammation and cancer. **Seminars in Cell & Developmental Biology**, 20 (2): 164–74

Puri, K.D., Doggett, T.A., Huang, C., et al. (2005) The role of endothelial PI3Kgamma activity in neutrophil trafficking. **Blood**, 106 (1): 150–7

Rainger, G.E., Stone, P., Morland, C.M., et al. (2001) A novel system for investigating the ability of smooth muscle cells and fibroblasts to regulate adhesion of flowing leukocytes to endothelial cells. **Journal of Immunological Methods**, 255 (1-2): 73–82

Rajesh, S., Sridhar, P., Tews, B.A., et al. (2012) Structural basis of ligand interactions of the large extracellular domain of tetraspanin CD81. **Journal of Virology**, 86 (18): 9606–16

Raucci, A., Cugusi, S., Antonelli, A., et al. (2008) A soluble form of the receptor for

advanced glycation endproducts (RAGE) is produced by proteolytic cleavage of the membrane-bound form by the sheddase a disintegrin and metalloprotease 10 (ADAM10). **FASEB Journal**, 22 (10): 3716–27

Reiss, K. and Saftig, P. (2009) The “a disintegrin and metalloprotease” (ADAM) family of sheddases: physiological and cellular functions. **Seminars in Cell & Developmental Biology**, 20 (2): 126–37

Reyes, R., Monjas, A., Yánez-Mó, M., et al. (2015) Different states of integrin LFA-1 aggregation are controlled through its association with tetraspanin CD9. **Biochimica et Biophysica Acta**, 1853 (10): 2464–2480

Rose-John, S. (2013) ADAM17, shedding, TACE as therapeutic targets. **Pharmacological Research**, 71: 19–22

Rot, A. (2010) Chemokine patterning by glycosaminoglycans and interceptors. **Frontiers in Bioscience**, 15: 645–660

Rufaihah, A.J., Huang, N.F., Kim, J., et al. (2013) Human induced pluripotent stem cell-derived endothelial cells exhibit functional heterogeneity. **American Journal of Translational Research**, 5 (1): 21–35

Sadik, C.D., Kim, N.D. and Luster, A.D. (2011) Neutrophils cascading their way to inflammation. **Trends in Immunology**, 32 (10): 452–460

Saftig, P. and Lichtenthaler, S.F. (2015) The alpha secretase ADAM10: A metalloprotease with multiple functions in the brain. **Progress in Neurobiology**, 135: 1–20

Saftig, P. and Reiss, K. (2011) The “A Disintegrin And Metalloproteases” ADAM10 and ADAM17: novel drug targets with therapeutic potential? **European Journal of Cell Biology**, 90 (6-7): 527–535

San Lek, H., Morrison, V.L., Conneely, M., et al. (2013) The spontaneously adhesive leukocyte function-associated antigen-1 (LFA-1) integrin in effector T cells mediates rapid actin- and calmodulin-dependent adhesion strengthening to ligand under shear flow. **Journal of Biological Chemistry**, 288 (21): 14698–14708

Schenkel, A.R., Mamdouh, Z. and Muller, W. a (2004) Locomotion of monocytes on endothelium is a critical step during extravasation. **Nature Immunology**, 5 (4): 393–400

Schlöndorff, J., Becherer, J.D. and Blobel, C.P. (2000) Intracellular maturation and localization of the tumour necrosis factor alpha convertase (TACE). **Biochemical Journal**, 347 Pt 1: 131–8

Schmidt, S., Moser, M. and Sperandio, M. (2013) The molecular basis of leukocyte recruitment and its deficiencies. **Molecular Immunology**, 55 (1): 49–58

Schulte, D., Küppers, V., Dartsch, N., et al. (2011) Stabilizing the VE-cadherin–catenin complex blocks leukocyte extravasation and vascular permeability. **EMBO Journal**, 30 (20): 4157–4170

Schulz, B., Pruessmeyer, J., Maretzky, T., et al. (2008) ADAM10 regulates endothelial permeability and T-cell transmigration by proteolysis of vascular endothelial cadherin. **Circulation Research**, 102 (10): 1192–1201

Schwarz, N., Pruessmeyer, J., Hess, F.M., et al. (2010) Requirements for leukocyte transmigration via the transmembrane chemokine CX3CL1. **Cellular and Molecular Life Sciences**, 67 (24): 4233–4248

Seigneuret, M. (2006) Complete predicted three-dimensional structure of the facilitator transmembrane protein and hepatitis C virus receptor CD81: conserved and variable

structural domains in the tetraspanin superfamily. **Biophysical Journal**, 90 (1): 212–27

Seigneuret, M., Delaguillaumie, A., Lagaudrière-Gesbert, C., et al. (2001) Structure of the tetraspanin main extracellular domain. A partially conserved fold with a structurally variable domain insertion. **Journal of Biological Chemistry**, 276: 40055–40064

Serhan, C.N., Chiang, N. and Van Dyke, T.E. (2008) Resolving inflammation: dual anti-inflammatory and pro-resolution lipid mediators. **Nature reviews. Immunology**, 8 (5): 349–61

Serru, V., Le Naour, F., Billard, M., et al. (1999) Selective tetraspan-integrin complexes (CD81/alpha4beta1, CD151/alpha3beta1, CD151/alpha6beta1) under conditions disrupting tetraspan interactions. **Biochemical Journal**, 340 (Pt 1 (Pt 1): 103–111

Shamri, R., Grabovsky, V., Gauguet, J.-M., et al. (2005) Lymphocyte arrest requires instantaneous induction of an extended LFA-1 conformation mediated by endothelium-bound chemokines. **Nature Immunology**, 6 (5): 497–506

Sharma, C., Yang, X.H. and Hemler, M.E. (2008) DHHC2 affects palmitoylation, stability, and functions of tetraspanins CD9 and CD151. **Molecular Biology of the Cell**, 19 (8): 3415–25

Shaw, S.K., Bamba, P.S., Perkins, B.N., et al. (2001) Real-time imaging of vascular endothelial-cadherin during leukocyte transmigration across endothelium. **Journal of Immunology**, 167 (4): 2323–30

Sheikh, S., Rainger, G.E., Gale, Z., et al. (2003) Exposure to fluid shear stress modulates the ability of endothelial cells to recruit neutrophils in response to tumor necrosis factor-alpha: a basis for local variations in vascular sensitivity to inflammation. **Blood**, 102 (8): 2828–34

Shoham, T., Rajapaksa, R., Boucheix, C., et al. (2003) The tetraspanin CD81 regulates the expression of CD19 during B cell development in a postendoplasmic reticulum compartment. **Journal of Immunology**, 171 (8): 4062–4072

Shulman, Z., Cohen, S.J., Roediger, B., et al. (2012) Transendothelial migration of lymphocytes mediated by intraendothelial vesicle stores rather than by extracellular chemokine depots. **Nature Immunology**, 13 (1529-2916 (Electronic)): 67–76

Sidibé, A., Mannic, T., Arboleas, M., et al. (2012) Soluble VE-cadherin in rheumatoid arthritis patients correlates with disease activity: Evidence for tumor necrosis factor α-induced VE-cadherin cleavage. **Arthritis and Rheumatism**, 64 (1): 77–87

Simon, S.I., Hu, Y., Vestweber, D., et al. (2000) Neutrophil tethering on E-selectin activates beta 2 integrin binding to ICAM-1 through a mitogen-activated protein kinase signal transduction pathway. **Journal of Immunology**, 164 (8): 4348–58

Singh, R.J.R., Mason, J.C., Lidington, E. a, et al. (2005) Cytokine stimulated vascular cell adhesion molecule-1 (VCAM-1) ectodomain release is regulated by TIMP-3. **Cardiovascular Research**, 67 (1): 39–49

Smalley, D.M. and Ley, K. (2005) L-selectin: mechanisms and physiological significance of ectodomain cleavage. **Journal of Cellular and Molecular Medicine**, 9 (2): 255–66

Sperandio, M., Smith, M.L., Forlow, S.B., et al. (2003) P-selectin glycoprotein ligand-1 mediates L-selectin-dependent leukocyte rolling in venules. **Journal of Experimental Medicine**, 197 (10): 1355–63

Stawikowska, R., Cudic, M., Giulianotti, M., et al. (2013) Activity of ADAM17 (a disintegrin and metalloprotease 17) is regulated by its noncatalytic domains and secondary structure

of its substrates. **Journal of Biological Chemistry**, 288 (31): 22871–9

Stefanidakis, M., Ruohtula, T., Borregaard, N., et al. (2004) Intracellular and cell surface localization of a complex between alphaMbeta2 integrin and promatrix metalloproteinase-9 progelatinase in neutrophils. **Journal of Immunology**, 172 (11): 7060–8

Sterk, L.M.T., Geuijen, C.A.W., van den Berg, J.G., et al. (2002) Association of the tetraspanin CD151 with the laminin-binding integrins alpha3beta1, alpha6beta1, alpha6beta4 and alpha7beta1 in cells in culture and in vivo. **Journal of Cell Science**, 115 (Pt 6): 1161–73

Sundd, P., Gutierrez, E., Koltsova, E.K., et al. (2012) 'Slings' enable neutrophil rolling at high shear. **Nature**, 488 (7411): 399–403

Takeda, S., Igarashi, T., Mori, H., et al. (2006) Crystal structures of VAP1 reveal ADAMs' MDC domain architecture and its unique C-shaped scaffold. **EMBO Journal**, 25 (11): 2388–96

Takeuchi, O. and Akira, S. (2010) Pattern Recognition Receptors and Inflammation. **Cell**, 140 (6): 805–820

Tang, J., Zarbock, A., Gomez, I., et al. (2011) Adam17-dependent shedding limits early neutrophil influx but does not alter early monocyte recruitment to inflammatory sites. **Blood**, 118 (3): 786–94

Termini, C.M., Cotter, M.L., Marjon, K.D., et al. (2014) The membrane scaffold CD82 regulates cell adhesion by altering α4 integrin stability and molecular density. **Molecular Biology of the Cell**, 25 (10): 1560–73

Thompson, R.D., Noble, K.E., Larbi, K.Y., et al. (2001) Platelet-endothelial cell adhesion molecule-1 (PECAM-1)-deficient mice demonstrate a transient and cytokine-specific role for PECAM-1 in leukocyte migration through the perivascular basement membrane. **Blood**, 97 (6): 1854–60

Tousseyn, T., Thathiah, A., Jorissen, E., et al. (2009) ADAM10, the rate-limiting protease of regulated intramembrane proteolysis of Notch and other proteins, is processed by ADAMS-9, ADAMS-15, and the gamma-secretase. **Journal of Biological Chemistry**, 284 (17): 11738–47

Tsakadze, N.L., Sithu, S.D., Sen, U., et al. (2006) Tumor necrosis factor-alpha-converting enzyme (TACE/ADAM-17) mediates the ectodomain cleavage of intercellular adhesion molecule-1 (ICAM-1). **Journal of Biological Chemistry**, 281 (6): 3157–64

Tsubota, Y., Frey, J.M., Tai, P.W.L., et al. (2013) Monocyte ADAM17 Promotes Diapedesis during Transendothelial Migration: Identification of Steps and Substrates Targeted by Metalloproteinases. **Journal of Immunology**, 190: 4236–4244

Turowski, P., Martinelli, R., Crawford, R., et al. (2008) Phosphorylation of vascular endothelial cadherin controls lymphocyte emigration. **Journal of Cell Science**, 121: 29–37

Vandenbroucke, R.E., Dejonckheere, E. and Libert, C. (2011) A therapeutic role for matrix metalloproteinase inhibitors in lung diseases? **The European Respiratory Journal**, 38 (5): 1200–14

Vestweber, D. (2012a) Novel insights into leukocyte extravasation. **Current Opinion in Hematology**. 19 (3) pp. 212–217

Vestweber, D. (2012b) Relevance of endothelial junctions in leukocyte extravasation and vascular permeability. **Annals of the New York Academy of Sciences**. 1257 (1) pp.

184–192

Vestweber, D. (2015) How leukocytes cross the vascular endothelium. **Nature Reviews Immunology**, 15 (11): 692–704

Vestweber, D. and Blanks, J.E. (1999) Mechanisms that regulate the function of the selectins and their ligands. **Physiological Reviews**, 79 (1): 181–213

Vockel, M. and Vestweber, D. (2013) How T cells trigger the dissociation of the endothelial receptor phosphatase VE-PTP from VE-cadherin. **Blood**, 122 (14): 2512–2522

Voisin, M.B. and Nourshargh, S. (2013) Neutrophil transmigration: Emergence of an adhesive cascade within venular walls. **Journal of Innate Immunity**. 5 (4) pp. 336–347

van der Vorst, E.P.C., Jeurissen, M., Wolfs, I.M.J., et al. (2015) Myeloid A disintegrin and metalloproteinase domain 10 deficiency modulates atherosclerotic plaque composition by shifting the balance from inflammation toward fibrosis. **The American Journal of Pathology**, 185 (4): 1145–55

van der Vorst, E.P.C., Keijbeck, A.A., de Winther, M.P.J., et al. (2012) A disintegrin and metalloproteases: molecular scissors in angiogenesis, inflammation and atherosclerosis. **Atherosclerosis**, 224 (2): 302–8

Walcheck, B., Moore, K.L., Mcever, R.P., et al. (1996) Neutrophil-neutrophil interactions under hydrodynamic shear stress involve L-selectin and PSGL-1 - A mechanism that amplifies initial leukocyte accumulation on P-selectin in vitro. **Jounral of Clinical Investigation**, 98 (5): 1081–1087

Weber, S., Niessen, M.T., Prox, J., et al. (2011) The disintegrin/metalloproteinase Adam10 is essential for epidermal integrity and Notch-mediated signaling. **Development**, 138 (3): 495–505

Wegmann, F., Petri, B., Khandoga, A.G., et al. (2006) ESAM supports neutrophil extravasation, activation of Rho, and VEGF-induced vascular permeability. **Journal of Experimental Medicine**, 203 (7): 1671–1677

Weskamp, G., Ford, J.W., Sturgill, J., et al. (2006) ADAM10 is a principal “sheddase” of the low-affinity immunoglobulin E receptor CD23. **Nature Immunology**, 7 (12): 1293–8

Wessel, F., Winderlich, M., Holm, M., et al. (2014) Leukocyte extravasation and vascular permeability are each controlled in vivo by different tyrosine residues of VE-cadherin. **Nature Immunology**, 15 (3): 223–30

Winterwood, N.E., Varzavand, A., Meland, M.N., et al. (2006) A Critical Role for Tetraspanin CD151 in α3β1 and α6β4 Integrin – dependent Tumor Cell Functions on Laminin-5. **Molecular Biology of the Cell**, 17 (June): 2707–2721

Wong, E., Maretzky, T., Peleg, Y., et al. (2015) The Functional Maturation of A Disintegrin and Metalloproteinase (ADAM) 9, 10, and 17 Requires Processing at a Newly Identified Proprotein Convertase (PC) Cleavage Site. **Journal of Biological Chemistry**, 290 (19): 12135–46

Wong, H.S., Jaumouillé, V., Heit, B., et al. (2014) Cytoskeletal confinement of CX3CL1 limits its susceptibility to proteolytic cleavage by ADAM10. **Molecular Biology of the Cell**, 25 (24): 3884–99

Wong, K.L., Tai, J.J.-Y., Wong, W.-C., et al. (2011) Gene expression profiling reveals the defining features of the classical, intermediate, and nonclassical human monocyte subsets. **Blood**, 118 (5): e16–31

Woodfin, A., Reichel, C.A., Khandoga, A., et al. (2007) JAM-A mediates neutrophil transmigration in a stimulus-specific manner in vivo: evidence for sequential roles for JAM-A and PECAM-1 in neutrophil transmigration. **Blood**, 110 (6): 1848–56

Woodfin, A., Voisin, M.-B., Beyrau, M., et al. (2011) The junctional adhesion molecule JAM-C regulates polarized transendothelial migration of neutrophils in vivo. **Nature Immunology**, 12 (8): 761–9

Woodfin, A., Voisin, M.-B., Imhof, B. a, et al. (2009) Endothelial cell activation leads to neutrophil transmigration as supported by the sequential roles of ICAM-2, JAM-A, and PECAM-1. **Blood**, 113 (24): 6246–57

Xu, D., Sharma, C. and Hemler, M. (2009) Tetraspanin12 regulates ADAM10-dependent cleavage of amyloid precursor protein. **FASEB Journal**, 23 (11): 3674–3681

Xu, P., Liu, J., Sakaki-Yumoto, M., et al. (2012) TACE activation by MAPK-mediated regulation of cell surface dimerization and TIMP3 association. **Science Signaling**, 5 (222): ra34

Yan, Y., Shirakabe, K. and Werb, Z. (2002) The metalloprotease Kuzbanian (ADAM10) mediates the transactivation of EGF receptor by G protein-coupled receptors. **Journal of Cell Biology**, 158 (2): 221–6

Yang, X.H., Mirchev, R., Deng, X., et al. (2012) CD151 restricts the alpha 6 integrin diffusion mode. **Journal of Cell Science**, 125 (6): 1478–1487

Yang, X.H., Richardson, A.L., Torres-Arzayus, M.I., et al. (2008) CD151 accelerates breast cancer by regulating alpha 6 integrin function, signaling, and molecular organization. **Cancer Research**, 68 (9): 3204–3213

Yauch, R.L., Berditchevski, F., Harler, M.B., et al. (1998) Highly stoichiometric, stable, and specific association of integrin alpha3beta1 with CD151 provides a major link to phosphatidylinositol 4-kinase, and may regulate cell migration. **Molecular Biology of the Cell**, 9 (10): 2751–65

Ye, F., Petrich, B.G., Anekal, P., et al. (2013) The mechanism of kindlin-mediated activation of integrin αIIbβ3. **Current Biology**, 23 (22): 2288–2295

Yoda, M., Kimura, T., Tohmonda, T., et al. (2011) Dual functions of cell-autonomous and non-cell-autonomous ADAM10 activity in granulopoiesis. **Blood**, 118 (26): 6939–42

Zarbock, A., Ley, K., McEver, R.P., et al. (2011) Leukocyte ligands for endothelial selectins: Specialized glycoconjugates that mediate rolling and signaling under flow. **Blood**, 118 (26): 6743–6751

Van Zelm, M.C., Smet, J., Adams, B., et al. (2010) CD81 gene defect in humans disrupts CD19 complex formation and leads to antibody deficiency. **Journal of Clinical Investigation**, 120 (4): 1265–1274

Zhang, C., Tian, L., Chi, C., et al. (2010) Adam10 is essential for early embryonic cardiovascular development. **Developmental Dynamics**, 239 (10): 2594–602

Zhao, R., Wang, A., Hall, K.C., et al. (2014) Lack of ADAM10 in endothelial cells affects osteoclasts at the chondro-osseus junction. **Journal of Orthopaedic Research**, 32 (2): 224–30

Zhu, Y.-Z., Luo, Y., Cao, M.-M., et al. (2012) Significance of palmitoylation of CD81 on its association with tetraspanin-enriched microdomains and mediating hepatitis C virus cell entry. **Virology**, 429 (2): 112–23

Zuidscherwoude, M., Göttfert, F., Dunlock, V.M.E., et al. (2015) The tetraspanin web

revisited by super-resolution microscopy. **Scientific Reports**, 5: 12201